[redacted]

Z65-12065

Copy No. 36

SID 63-1460

DATA REPORT FOR APOLLO MODEL FSJ-3 WIND TUNNEL TESTS IN TUNNEL A OF THE VON KARMAN GAS DYNAMICS FACILITY, AEDC

(First Series) [U]

NAS9-150

Volume 1 (of 2)

December 1963

Apollo

N79-76084

(NASA-CR-116672) APOLLO MODEL FSJ-3 WIND TUNNEL TESTS IN TUNNEL A OF THE VON KARMAN GAS DYNAMICS FACILITY, AEDC, VOLUME 1 (North American Aviation, Inc.) 204 p

Unclas
00/02 11287

FF No. 6 (NASA CR OR TMX OR AD NUMBER) (CATEGORY)

[redacted]

[redacted]

[redacted]

Z65·12065

Accession No. 00114

Copy No. 36

SID 63-1460

DATA REPORT FOR APOLLO MODEL FSJ-3 WIND TUNNEL TESTS IN TUNNEL A OF THE VON KARMAN GAS DYNAMICS FACILITY, AEDC

(First Series)

NAS9-150

Volume 1 (of 2)

[U]

December 1963

Exhibit I, Paragraph 5.5

CLASSIFICATION CHANGE

To UNCLASSIFIED

By authority of GDS-E011652 Date 12/31/72

Changed by L. Shirley

Classified Document Master Control Station, NASA

Scientific and Technical Information Facility

This document contains information affecting the national defense of the United States within the meaning of the Espionage Laws, Title 18 U.S.C. Section 793 and 794. Its transmission or revelation of its contents in any manner to an unauthorized person is prohibited by law.

NORTH AMERICAN AVIATION, INC.

SPACE and INFORMATION SYSTEMS DIVISION

[redacted]

[redacted] ONLY

FOREWORD

The FSJ-3 jet-effects model tests were conducted under NASA Apollo contract NAS9-150 in tunnel A of the von Karman Gas Dynamics Facility at the Arnold Engineering Development Center, Tullahoma, Tennessee, during the week of 29 July 1963.

This report was prepared by J. D. Moote of the Apollo Aerodynamic Engineering Section in accordance with paragraph 5.5, Exhibit I of the NASA Apollo contract NAS9-150.

CO[redacted]

ABSTRACT

An investigation was conducted to determine the aerodynamic characteristics and launch escape system (LES) jet impingement characteristics of the Apollo launch escape vehicle (LEV) at various LES rocket motor thrust levels. A 0.045-scale model of the LEV with unheated air jets for LES exhaust jet simulation was used for the tests. Force, moment, and pressure distribution data were obtained in the Mach number range from 1.5 to 6.0 at angles of attack from 0 to 50 degrees. Data were also obtained at the uncalibrated Mach number of 0.70 for comparison with other jet-effects data.

The data indicate considerable and variable effects of the LES jets on the LEV aerodynamics characteristics; particularly on axial force and pitching moment coefficients. The stability of the LEV due to aerodynamic forces is always reduced by the effects of the jets. The magnitude and sign of the difference between jet-on and jet-off drag coefficients is dependent on LES thrust coefficient, angle of attack, and Mach number. Jet impingement on the command module is primarily dependent on thrust coefficient and angle of attack; increasing with increasing angle of attack and decreasing thrust coefficient.

[redacted]

CO[redacted]

CONTENTS

Section		Page
	INTRODUCTION	1
I	MODEL DESCRIPTION	3
	Air System	3
	Model Configuration	7
II	INSTRUMENTATION	13
	Force Measurement	13
	Pressure Instrumentation	13
	Photographic Instrumentation	15
III	TEST INSTALLATION AND PROCEDURES	
	Installation	17
	Test Procedure	20
	Test Conditions	20
IV	LES JET SIMULATION TECHNIQUE	23
V	DISCUSSION	31
	Force and Moment Data	31
	Pressure Data	33
	Schlieren Photographs	33
	Data Reduction	33
	Data Accuracy	33
	APPENDIXES	
	A. Plotted Data	A-1
	B. Tabulated Data (Volume 2)	B-2

[redacted]

~~CONFIDENTIAL~~

ILLUSTRATIONS

Figure		Page
1	FSJ-3 Model Parts	4
2	FSJ-3 Model Assemble ($\theta = 0$)	5
3	FSJ-3 Air System	6
4	Escape Motor E_{65}	8
5	Tower Structure T_{28}	9
6	Command Module C_{40}	10
7	Nozzle Configuration N_8	11
8	Pressure Tap Locations	14
9	FSJ-3 (Configuration 1) Installation in AEDC-VKF Tunnel A	18
10	FSJ-3 (Configuration 3) Installation in AEDC-VKF Tunnel A	19
11	$Pcm/P\infty$ m and $Pcp/P\infty$ p Versus $\frac{\gamma j\ M^2 j\ Aj}{S\pi}$	25
12	Boundary Streamline Flow Direction Versus $\frac{\gamma j\ Mj^2\ Aj}{S\pi}$	27
13	Computed Plume Shape Comparisons	28
14	Airflow and Theoretical Chamber Pressure Versus Indicated Chamber Pressure, P_{c1}	29
15	Schlieren Photographs at $M\infty = 1.48$	35
16	Schlieren Photographs at $M\infty = 1.98$	36
17	Schlieren Photographs at $M\infty = 2.99$	38
18	Schlieren Photographs at $M\infty = 3.99$	40
19	Schlieren Photographs at $M\infty = 4.99$	42
20	Schlieren Photographs at $M\infty = 5.97$	43

~~CONFIDENTIAL~~

NOMENCLATURE

The following symbols are used throughout this report and in the appendixes.

Symbol	Definition
A	Axial force, lbs
A_j	Flow area of isentropically expanded jet, sq in.
A_t	Nozzle throat area, sq in.
C_A	Axial force coefficient, $A/q_\infty S\pi$
C_N	Normal force coefficient, $N/q_\infty S\pi$
C_Y	Side force coefficient, $Y/q_\infty S\pi$
C_m	Pitching moment coefficient, $m/q_\infty S\pi d$
C_n	Yawing moment coefficient, $n/q_\infty S\pi d$
C_ℓ	Rolling moment coefficient, $\ell/q_\infty S\pi d$
C_P	Pressure coefficient, $P-P_\infty/q_\infty$
C_L	Lift coefficient, $L/q_\infty S\pi$
C_D	Drag coefficient, $D/q_\infty S\pi$
C_T	Thrust coefficient, $T/q_\infty S\pi$
C_{T_i}	Ideal thrust coefficient, $\mathring{M}_j V_j/q_\infty S\pi$
D	Drag, lbs
d	Reference length, in.
L	Lift, lbs
ℓ	Rolling moment, in. - lbs

~~CONFIDENTIAL~~

Symbol	Definition
M	Mach number
$\mathring{M}$	Mass flow rate, lb-sec/ft
m	Pitching moment, in.-lbs
N	Normal force, lbs
n	Yawing moment, in.-lbs
P	Pressure, psia
q	Dynamic pressure, psi
Re	Reynolds number
r	Command module radius
$S\pi$	Reference area, in.^{2}
S/r	Surface distance from CM nose divided by CM radius
S.F.	Model scale factor
T_T	Total temperature, °R
V	Velocity, ft/sec
W_a	Air flow rate, lbs/sec
Y	Side force, lbs
X	Axial distance from CM apex (negative towards heat shield face), in.
$\overline{X}$	Axial distance to reference center of gravity
X_{CP}	Axial distance to center of pressure
Z	Vertical distance from model axis, in. (positive downward)
$\overline{Z}$	Vertical distance to reference center of gravity
α	Angle of attack, deg

~~CONFIDENTIAL~~

Symbol	Definition
β	Angle of sideslip, deg
γ	Ratio of specific heats
θ	Model-balance offset angle, deg
δ	Jet boundary streamline direction, deg

Subscripts

A	Refers to CM apex axis system
a	Refers to model air system
B	Refers to balance
C	Refers to nozzle chamber
i	Refers to ideal conditions
j	Refers to isentropically expanded jet conditions
m	Refers to FSJ-3 model
P	Refers to prototype LES
V	Refers to vent instrumentation on CM
0	Refers to stagnation conditions
1	Refers to balance in C_{40} command module when used with force or moment coefficients
2	Refers to balance in E_{65} rocket motor case when used with force or moment coefficients
1-47	Refers to pressure tap location when used with P
∞	Refers to ambient flight or tunnel conditions (M_0 and M_∞ are synonomous)
c. g.	Refers to reference center-of-gravity axis system

~~CONFIDENTIAL~~

Constants

$S_{\pi\ m}$	37.7186 in.^{2}
$S_{\pi\ p}$	18,617 in.^{2}
d_m	6.93 in.
d_p	154 in.
$\bar{x}/d$	-0.31564
$\bar{z}/d$	0.0440
γ_{jm}	1.40
γ_{jp}	1.23
γ_∞	1.40

~~CONFIDENTIAL~~

CONFIDENTIAL

INTRODUCTION

The 0.045 FSJ-3 jet-effects model of the Apollo launch escape vehicle (LEV) was tested in the 40 x 40 inch supersonic wind tunnel at the Arnold Engineering Development Center (AEDC) to investigate the aerodynamic characteristics and escape rocket exhaust impingement pressures on the module during operation of the launch escape system (LES).

Force, moment, and pressure data were obtained from the command module plus tower component of the model. Force and moment data were obtained from the model rocket motor component. Total LEV characteristics were obtained by the summation of component data. The tests were conducted in the angle-of-attack range from 0 to 50 degrees and the Mach number range from 1.48 to 6.0. Data were also obtained at 0.7 Mach number, with the wind tunnel operating at an uncalibrated off-design condition. These data were obtained primarily for comparison with other jet-effects data from the FSJ-1 hydrogen peroxide model, which was tested in a transonic wind tunnel.

Tabulated and plotted data are presented in the appendixes, and a discussion of the data, the test, and the model is presented in subsequent sections. A complete description of the model is presented in the pretest report.[1]

[1] Pretest Report for the 0.045-Scale Apollo Force Model FSJ-3 Wind Tunnel Test in the AEDC von Karman Gas Dynamics Facility Tunnel A. SID 63-352 (10 April 1963).

CONFIDENTIAL

CON[redacted]

I. MODEL DESCRIPTION

The FSJ-3 is a 0.045-scale stainless steel model of the Apollo launch escape vehicle (LEV) with provisions for exhausting unheated air through simulated launch escape system (LES) rocket nozzles. Figure 1 shows all model parts completely disassembled. The command module (CM) and escape tower are installed on the AEDC 4.01-Y-36-012 balance. The model air system extends from the sting through the CM and tower without touching either and contains the simulated LES nozzles. The model rocket motor, excluding the nozzles, is installed on the AEDC 401-Y-36-003 balance which is attached to the forward end of the air system. Figure 2 shows the assembled model. (The strakes shown on the CM were removed before testing.)

AIR SYSTEM

The high pressure air from the AEDC 4000 psi supply is brought to the model installation in two flexible lines which are manifolded at the aft model support structure (Figure 3). From this manifold the air is ducted through two solid pipes located on either side of the -012 balance to another manifold in the CM. A single pipe, concentric with the model centerline, extends from the forward manifold through the tower to the nozzle adapter which contains the simulated LES nozzles and the attachment for the -003 balance. The air system is physically isolated from the -012 balance, the CM, and the tower. The nozzle description is presented in the following tabulation:

Configuration Designation	Exit Div. Angle (deg)	Area Ratio	Throat Diam. (in.)	Exit Diam. (in.)	Placement
N_8	13.5	3.19	0.4003	0.7155	Top Pitch
		2.75	0.4313	0.7155	Yaw (2)
		2.41	0.4601	0.7155	Bottom Pitch

These nozzles are not to scale except for the exit area, the exit location, and the centerline inclination to the model centerline.

[redacted]

~~CONFIDENTIAL~~

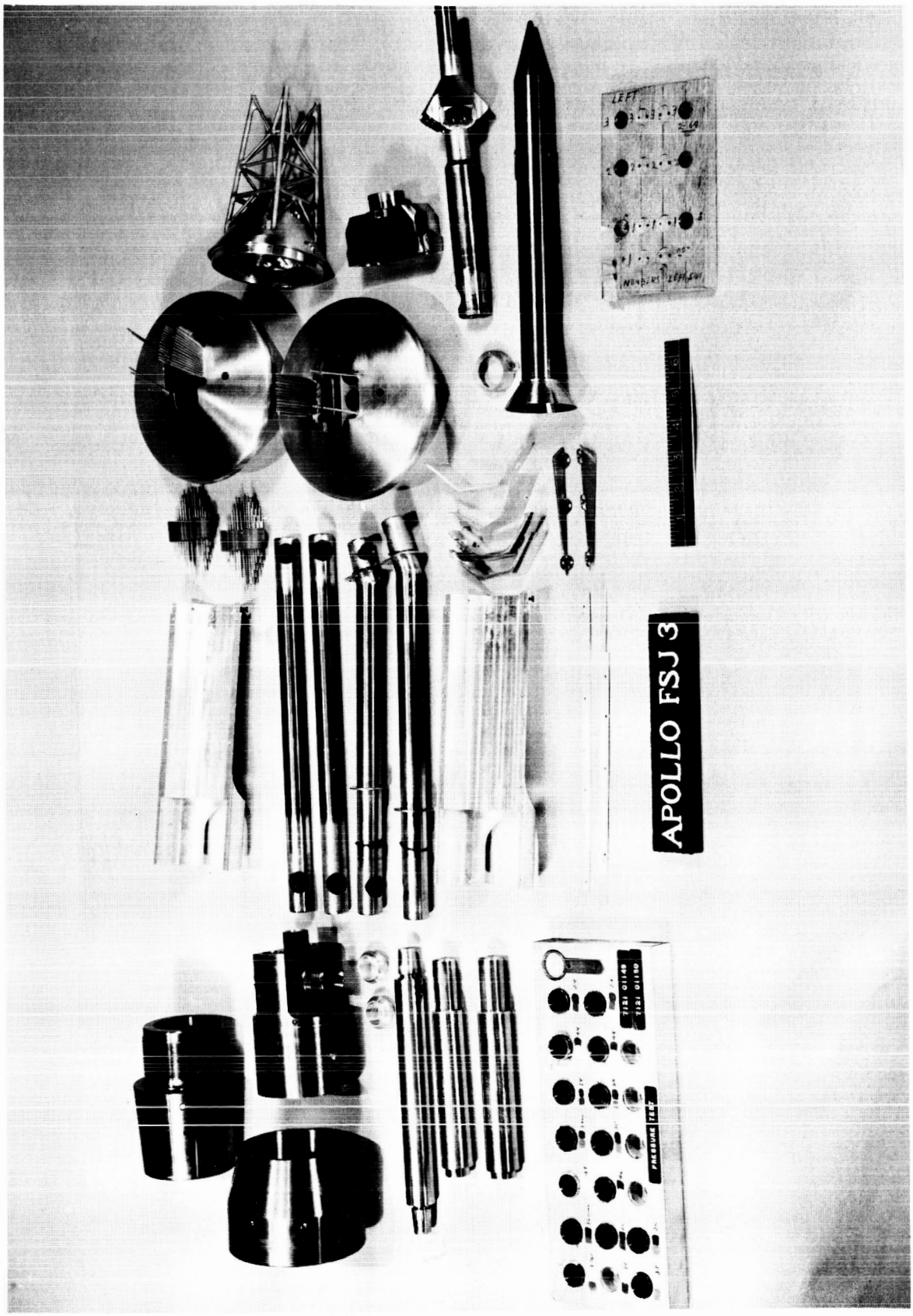

Figure 1. FSJ-3 Model Parts

~~CONFIDENTIAL~~

CON~~FIDENTIAL~~

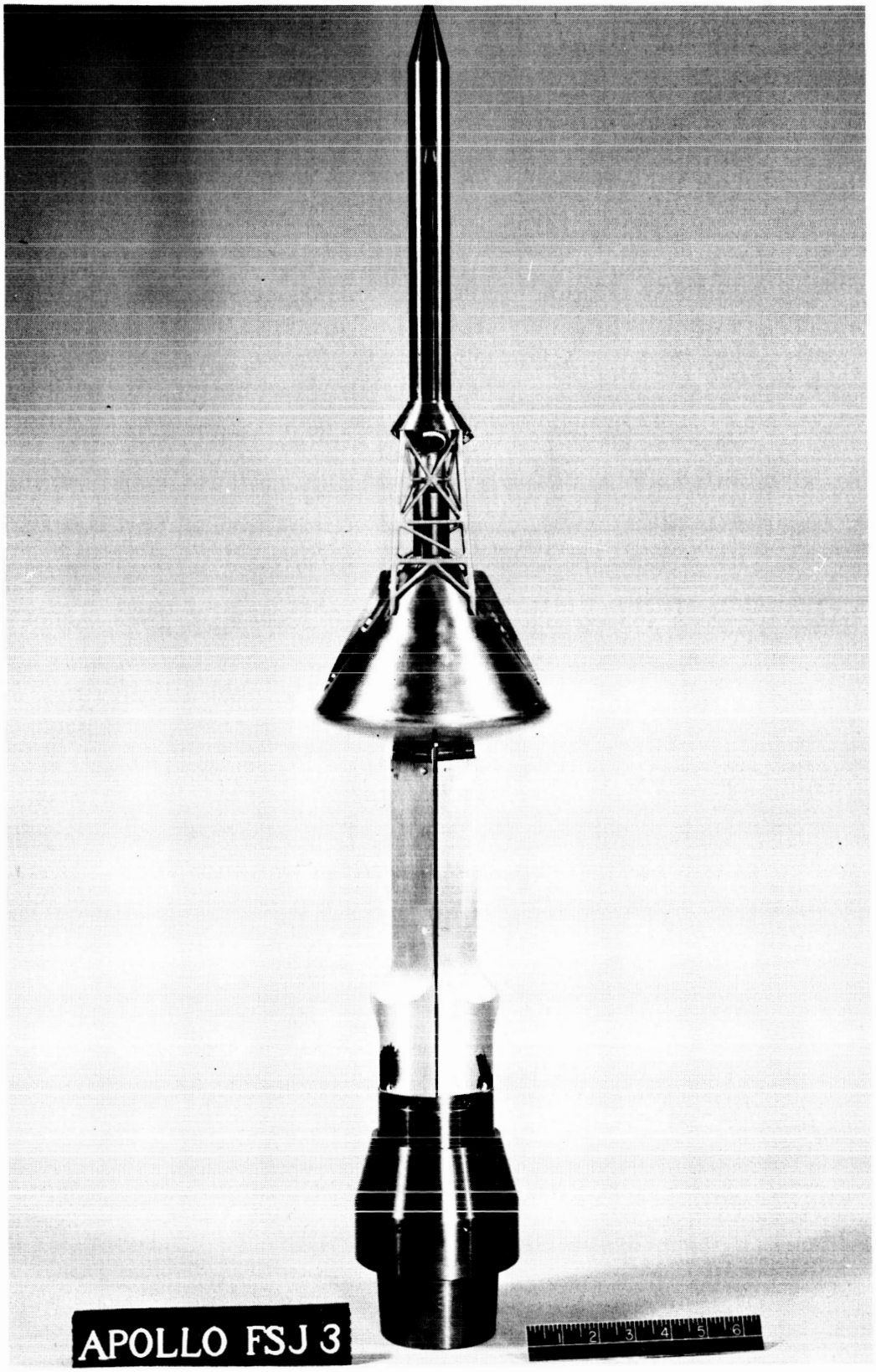

Figure 2. FSJ-3 Model Assemble ($\theta = 0$)

~~CONFIDENTIAL~~

~~CONFIDENTIAL~~

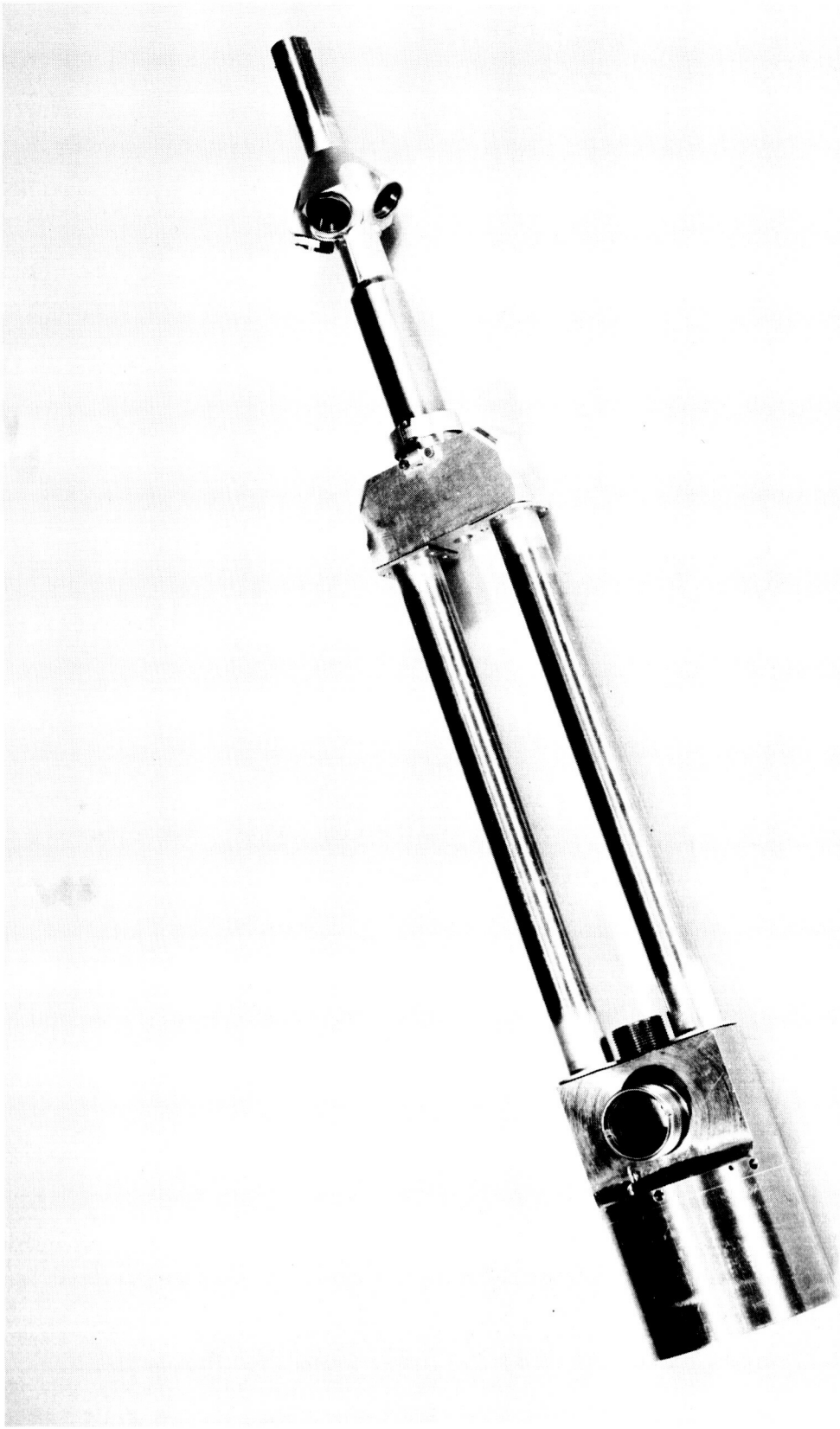

Figure 3. FSJ-3 Air System

~~CONFIDENTIAL~~

CON[redacted]

MODEL CONFIGURATION

Full-scale dimensions of the components of the LEV configuration used during the test are given in the following listing.

Escape Motor, E_{65} (Figure 4)

Total length	269.67 in.
Diameter	26.00 in.
Nose Radius	2.00 in.
Nose included angle	30.00 deg.
Skirt base diameter	52.73 in.
Skirt flare angle	34.00 deg

Tower Structure, T_{28} (Figure 5)

Total length	113.45 in.
Number of longitudinal members	4
Number of cross braces	8
Number of diagonal braces	28
Diameter of longitudinal members	4.16 in.
Diameter of braces	2.78 in.
Distance from top of tower to support ring	32.13 in.
Diameter of ring	23.00 in.
Distance between attack points at the command module	
Horizontal plane	50.67 in.
Vertical plane	46.84 in.
Distance between attack points at the rocket motor base	36.04 in.

Command Module, C_{40} (Figure 6)

Maximum diameter	154.00 in.
Radius of spherical blunt end	184.80 in.
Corner radius	7.7 in.
Conical surface half angle	33.00 deg
Distance from apex to truncation station	20.31 in.

Rocket Nozzle Configuration, N_8 (Figure 7)

(Not to scale, description given in preceding section)

[redacted]

~~CONFIDENTIAL~~

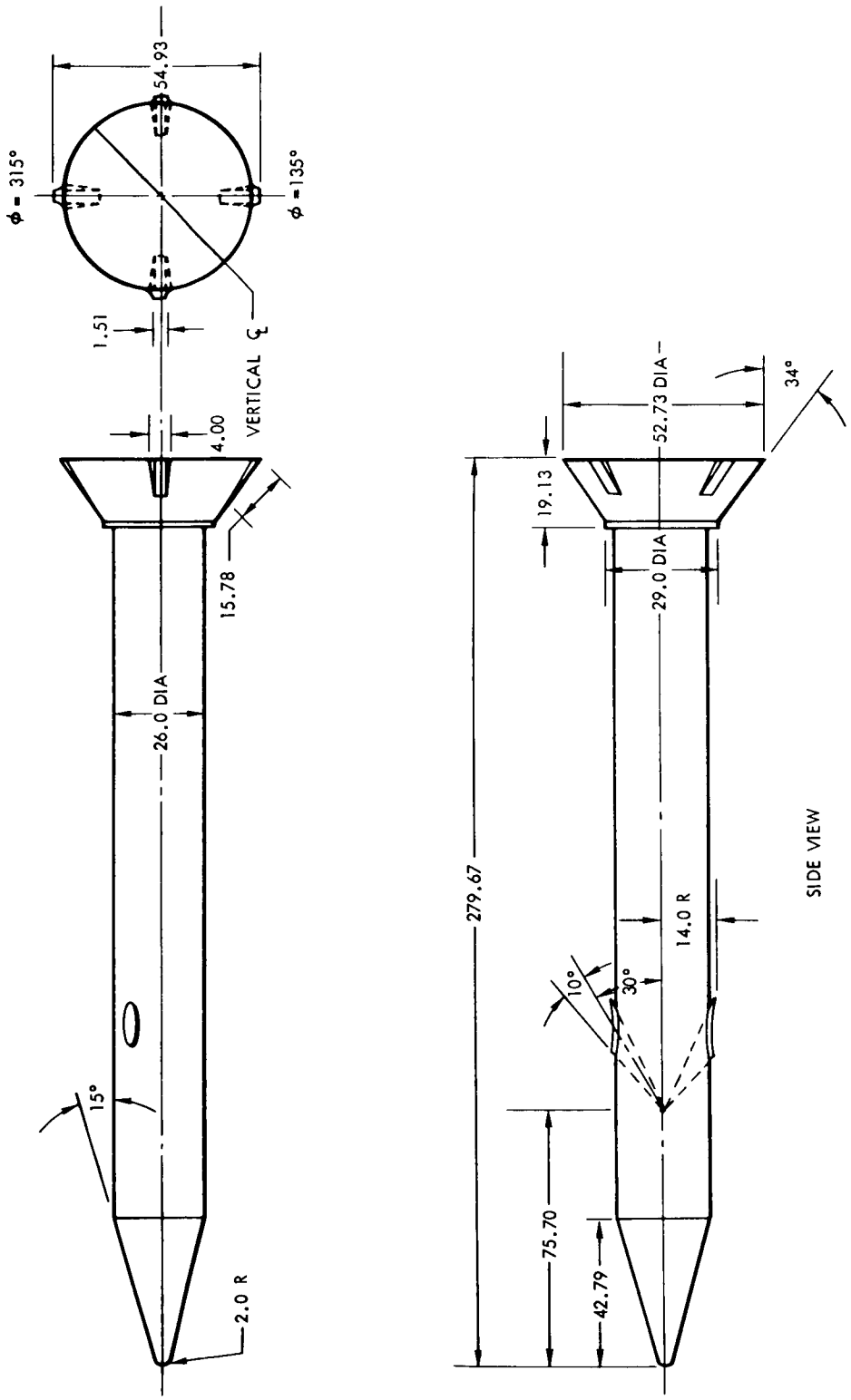

ESCAPE ROCKET E_{65}

DRAWING NOT TO SCALE

FULL-SCALE DIMENSIONS IN INCHES

Figure 4. Escape Motor E_{65}

~~CONFIDENTIAL~~

CON[redacted]

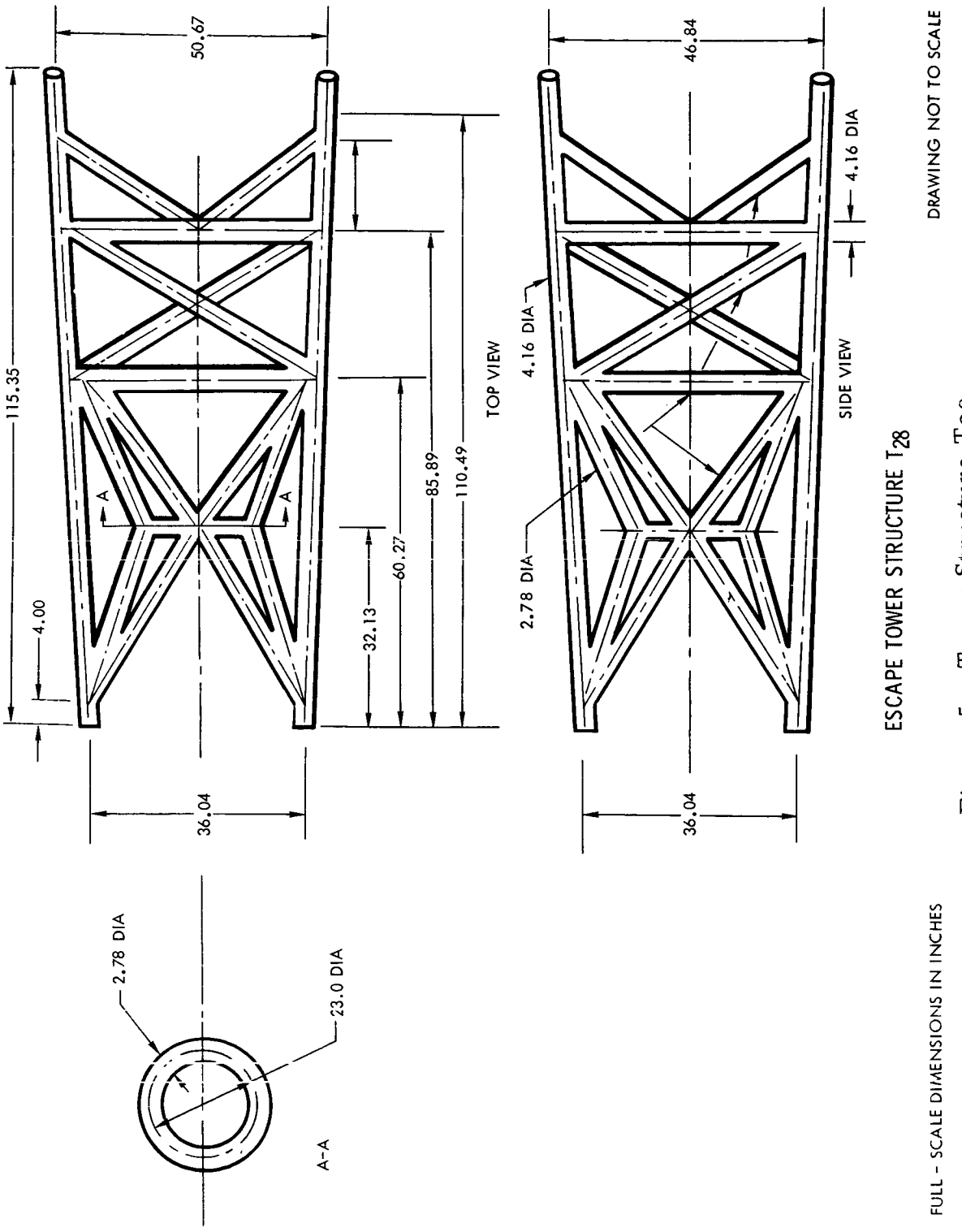

Figure 5. Tower Structure T_{28}

[redacted]

~~CONFIDENTIAL~~

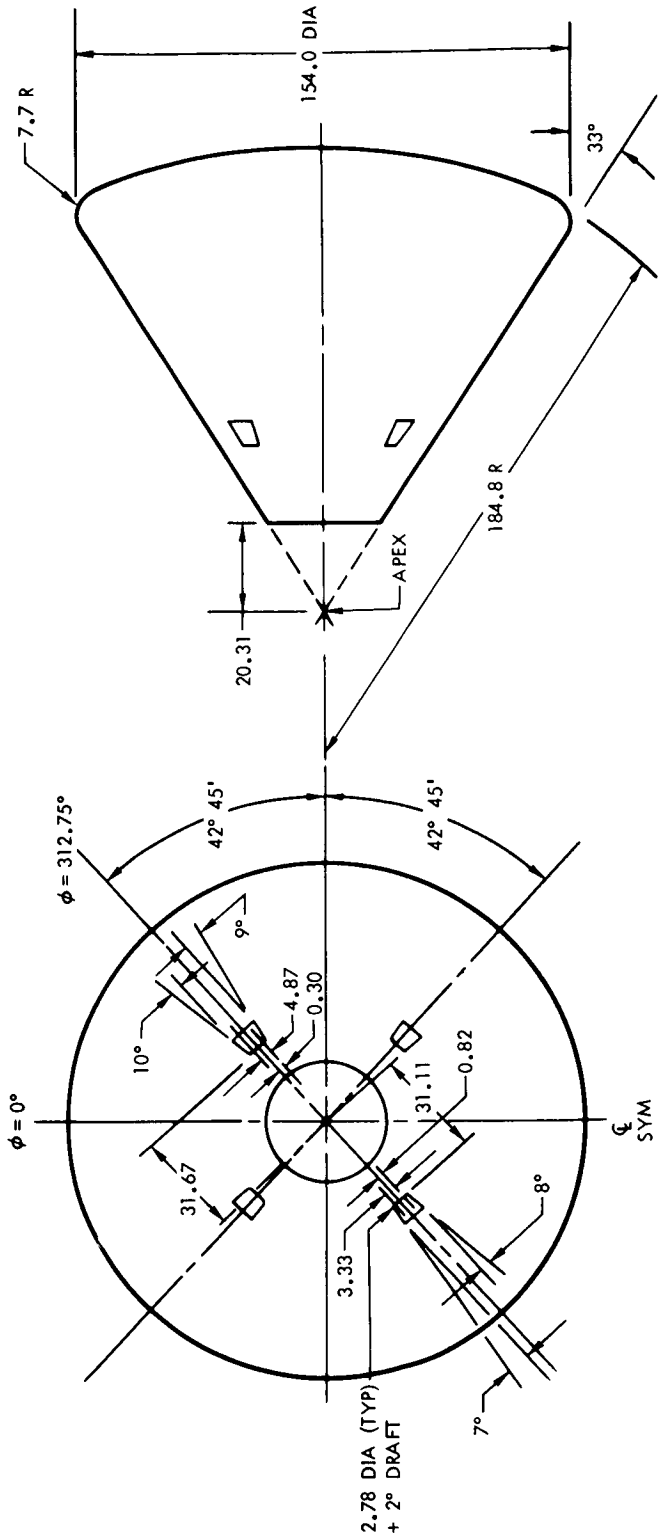

DRAWING NOT TO SCALE

COMMAND MODULE C40

FULL-SCALE DIMENSIONS IN INCHES

Figure 6. Command Module C_{40}

~~CONFIDENTIAL~~

CON[redacted]

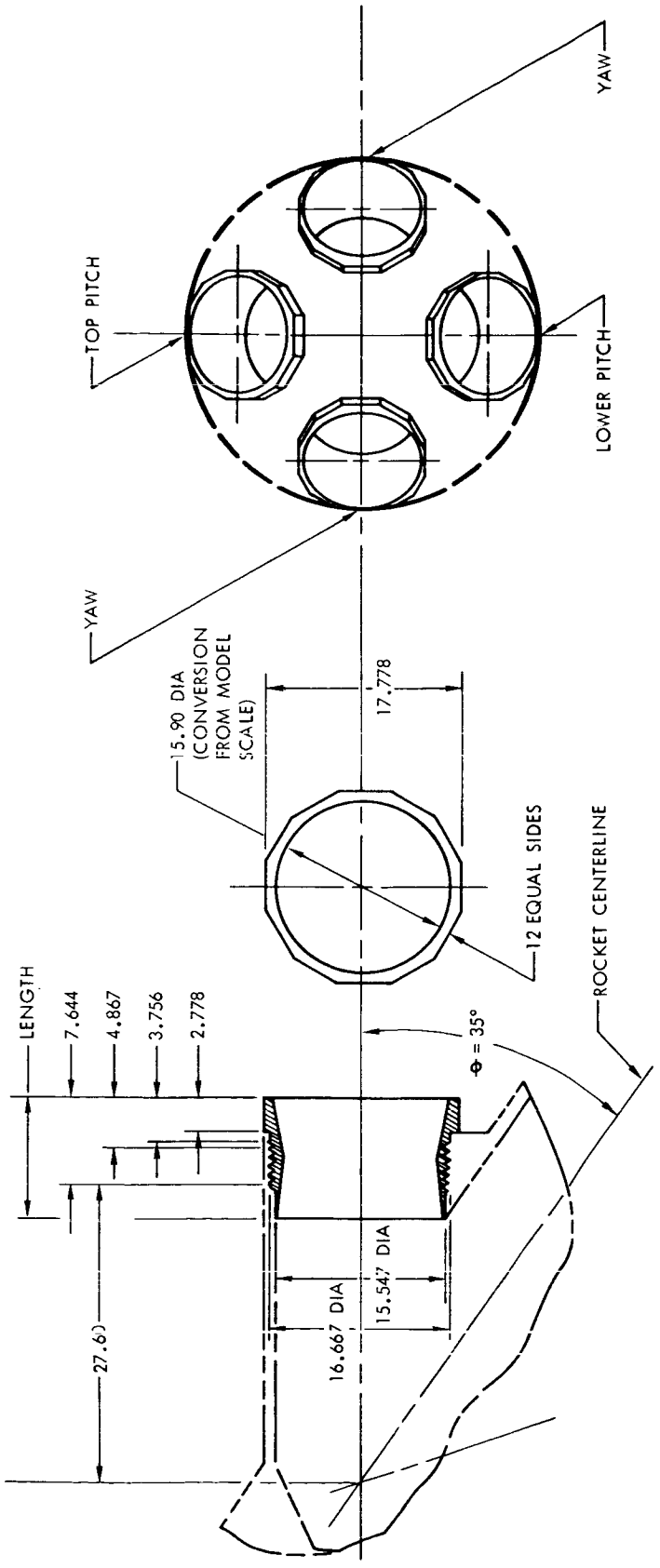

ESCAPE ROCKET NOZZLES N_6, N_7, N_8, AND N_9

SET 1	NOZZLE	TOP PITCH	YAW	LOWER PITCH
N_6	THROAT DIA LENGTH	12.229 8.880	13.173 8.880	14.056 8.880
SET 2				
N_7	THROAT DIA LENGTH	10.393 11.073	11.198 10.671	11.947 10.307
SET 3				
N_8	THROAT DIA LENGTH	8.896 13.627	9.584 13.333	10.224 13.076
SET 4				
N_9	THROAT DIA LENGTH	7.727 13.462	8.324 13.400	8.880 13.271

FULL-SCALE DIMENSIONS IN INCHES

DRAWING NOT TO SCALE

Figure 7. Nozzle Configuration N_8

[redacted]

II. INSTRUMENTATION

FORCE MEASUREMENT

Forces and moments on the CM and tower were measured by means of the AEDC 4.01-Y-36-012 six-component balance which has the following capacity ratings.

Component	Rated Load
Normal Force	500 lbs
Side Force	250 lbs
Chord Force	125 lbs
Rolling Moment	400 in. - lbs
Pitching Moment	1000 in. - lbs
Yawing Moment	500 in. - lbs

Forces and moments on the rocket motor body were measured by means of the AEDC 4.06-Y-36-003 six-component balance which has the following capacity ratings.

Component	Rated Loads
Normal Force	100 lbs
Side Force	100 lbs
Chord Force	30 lbs
Rolling Moment	350 in. - lbs
Pitching Moment	350 in. - lbs
Yawing Moment	25 in. - lbs

PRESSURE INSTRUMENTATION

Pressure taps are installed on the left side of the command module at the locations shown in Figure 8 and tabulated below. The tubing for these taps is routed through the base of the command module and inside the windshield. A short length of soft tubing in each line prevents excessive transmittal of forces and moments by the pressure lines.

~~CONFIDENTIAL~~

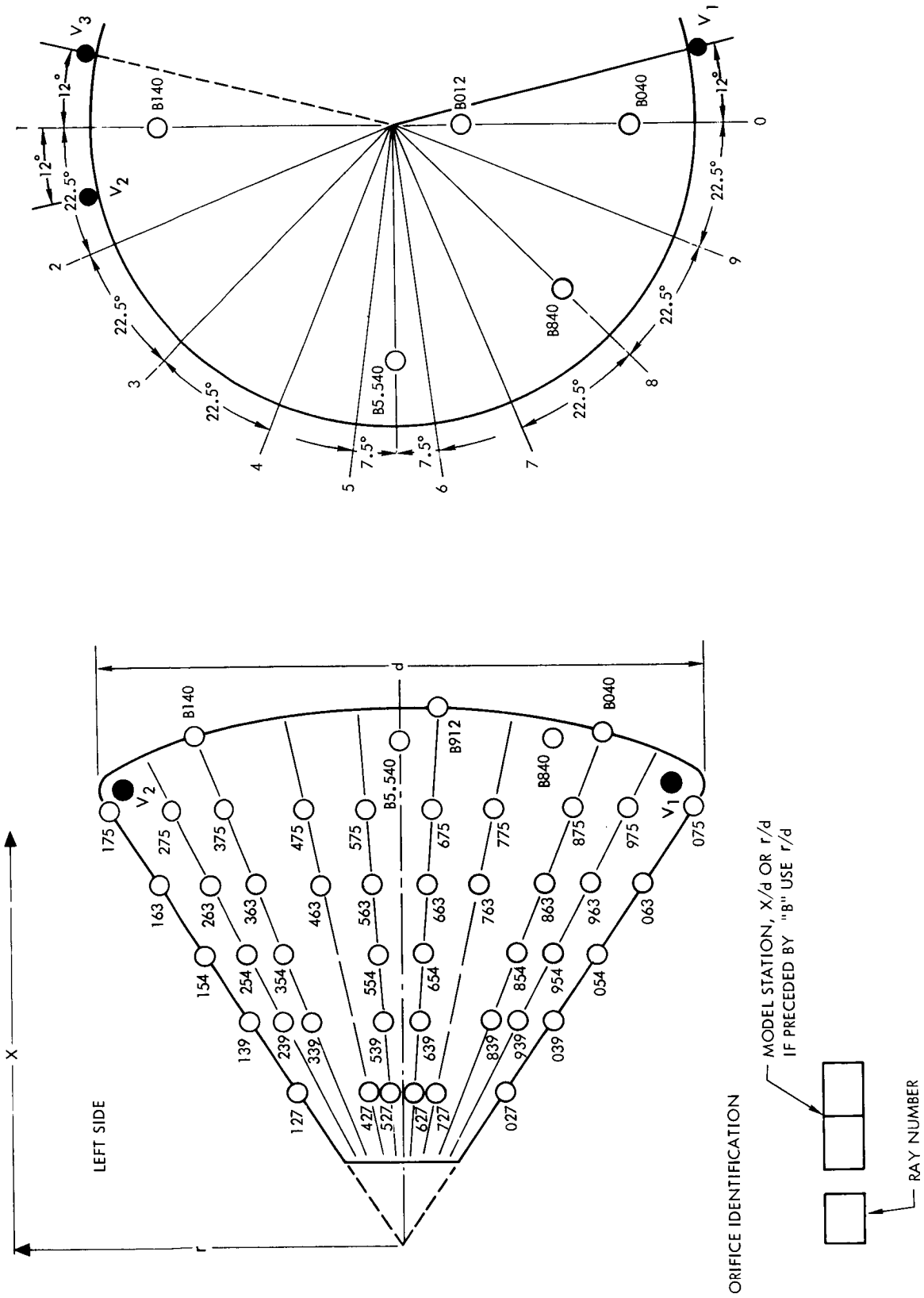

Figure 8. Pressure Tap Locations

~~CONFIDENTIAL~~

CON[redacted]

	Tap Identification	s/r
NAA	127 427 527 627 727 027	0.57909
AEDC	(6) (5) (4) (3) (2) (1)	
Data Column-Row	6-11 5-11 4-11 3-11 2-11 1-11	
NAA	139 239 339 539 639 839 939 039	0.86526
AEDC	(14) (13) (12) (11) (10) (9) (8) (7)	
Data Column-Row	5-14 4-14 3-14 2-14 1-14 9-11 8-11 7-11	
NAA	154 254 354 554 654 854 954 054	1.20143
AEDC	(22) (21) (20) (19) (18) (17) (16) (15)	
Data Column-Row	4-17 3-17 2-17 1-17 9-14 8-14 7-14 6-14	
NAA	163 263 363 463 563 663 763 863 963 063	1.43759
AEDC	(32) (31) (30) (29) (28) (27) (26) (25) (24) (23)	
Data Column-Row	5-20 4-20 3-20 2-20 1-20 9-17 8-17 7-17 6-17 5-17	
NAA	175 275 375 475 575 675 775 875 975 075	1.72376
AEDC	(42) (41) (40) (39) (38) (37) (36) (35) (34) (33)	
Data Column-Row	6-23 5-23 4-23 3-23 2-23 1-23 9-20 8-20 7-20 6-20	
NAA	B140 B5. 540 B840 B040	2.07753
AEDC	(46) (45) (44) (43)	
Data Column-Row	4-26 3-26 2-26 1-26	
NAA	B012	2.65262
AEDC	(47)	
Data Column-Row	5-26	
NAA	V1 V2 V3	1.75
AEDC	(48) (49) (50)	
Data Column-Row	7-26 8-26 9-26	

Three taps are installed in the nozzle adapter to measure chamber pressure. These pressure measurements were used to set the desired thrust simulation. Motor base pressures, skirt base pressures, command module cavity pressure, and windshield internal pressure were also measured.

PHOTOGRAPHIC INSTRUMENTATION

The VKF tunnel A Schlieren system was utilized during the test. Still and motion pictures were taken to document the flow conditions. A ground glass screen was available for Schlieren observation during the test.

III. TEST INSTALLATION AND PROCEDURES

INSTALLATION

Figure 9 shows the FSJ-3 installed in the VKF tunnel A on the yaw actuator. (The strakes shown on the CM were removed before testing.) The model and actuator were oriented such that movement of the actuator pitched the model in the vertical plane. This orientation provided an angle-of-attack range of 0 to 60 degrees in the plane perpendicular to the Schlieren system centerline. Installation of the 20 degrees offset model (θ = 20 degrees) changed this range to 20 to 80 degrees. A linkage change in the actuator is required to change its range from 0-30 degrees to 30-60 degrees.

The yaw actuator is mounted on the tunnel sector which provided approximately 20 degrees of model rotation in the horizontal plane. With the FSJ-3 installation this provided a sideslip angle range from -15 to +5 degrees.

The high pressure air for LES jet simulation was piped into the tunnel aft of the diffuser and brought forward to the sector through two 1.5 inch diameter pipes. From the sector to model the air was ducted through flexible lines to provide for movement of the yaw actuator. Control of the airflow and pressure was accomplished at a control station outside the tunnel which was remotely operated from the tunnel A control room.

The stainless steel pressure instrumentation lines are in the air stream from the model to the sector which has provisions for routing them out of the tunnel, where they are attached to the Gianinni valving system. The balance leads are also routed through the sector and connected at a junction box outside the tunnel.

Three installation configurations were used to cover the desired angle-of-attack range. Configuration 1 consisted of the 0-30 degree actuator range and the straight (θ = 0 degree) model; configuration 2, consisted of the 0-30 degree actuator range and the offset (θ = 20 degrees) model; and configuration 3 consisted of the 30-60 degree actuator range and the offset model. Configuration 3 is shown in Figure 10. The nose cone was removed to avoid interferrence with the tunnel ceiling. (The strakes shown on the CM would have been removed before testing if time for testing this configuration had been available.) The angle-of-attack ranges for these configurations were 0-30 degrees, 20-50 degrees, and 50-80 degrees, respectively.

~~CONFIDENTIAL~~

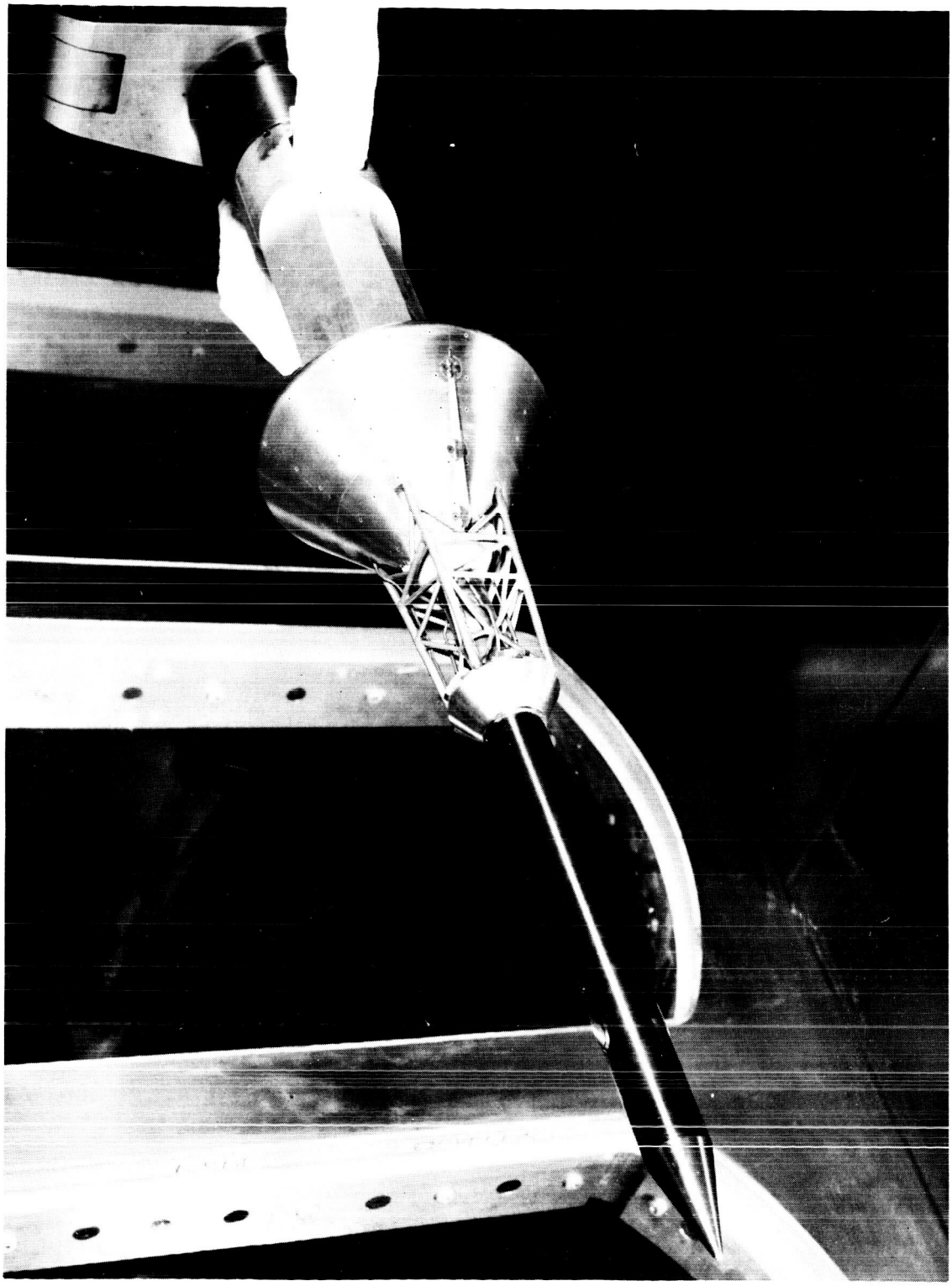

Figure 9. FSJ-3 (Configuration 1) Installation in AEDC-VKF Tunnel A

~~CONFIDENTIAL~~

CONFIDENTIAL

Figure 10. FSJ-3 (Configuration 3) Installation in AEDC-VKF Tunnel A

CONFIDENTIAL

TEST PROCEDURE

The test procedure followed during the testing of the FSJ-3 model consisted generally of the following steps.

1. Reduce test section pressure for starting
2. Start tunnel
3. Set desired tunnel pressure conditions and null nozzle actuators at proper positions
4. Starting at minimum angle of attack, record force data only at α intervals (5 degrees or less) through the α range of the configuration with the jets off
5. Starting at maximum α, record force and pressure data at α intervals (5 degrees or more) as the actuator is returned to the minimum position
6. Repeat steps 4 and 5 at three selected jet pressure levels
7. Repeat steps 4 through 6 for selected sideslip angles
8. Repeat steps 3 through 7 for desired Mach numbers. (Can be obtained without shutting tunnel down.) Shut tunnel down
9. Repeat steps 1 through 8 for other tunnel Mach number ranges
10. Change installation configuration and repeat steps 1 through 9.

TEST CONDITIONS

The tunnel flow conditions were selected to simulate altitude and dynamic pressure conditions within the trajectory envelope of the prototype launch escape vehicle. The Reynolds number simulation was therefore not close because of the model scale and the lack of ambient temperature simulation.

The following list presents the nominal wind tunnel conditions for the test.

M_∞	P_o	P_∞	q_∞	T_o	R_e
0.7	13.80 psia	9.95 psia	3.42 psi	546°R	2.05×10^6
1.48	8.21	2.30	3.53	549	1.42
1.98	9.69	1.28	3.50	550	1.42
2.99	19.56	0.54	3.38	550	1.70
3.99	25.13	0.168	1.87	556	1.29
4.99	22.15	0.044	0.738	556	0.695
5.97	31.90	0.020	0.52	546	0.659

IV. LES JET SIMULATION TECHNIQUE

The subject testing of the FSJ-3 jet-effects model utilizes unheated air as the fluid for simulation of the LES solid propellant exhaust products. Since the two fluids are considerably different it is appropriate to briefly describe the analysis which supports the simulation technique. The simulation parameters which were determined to be most important from the jet-effects simulation point of view are jet momentum ratio and jet plume shape. For the sake of expediency and also because actual values would be difficult to obtain, the nozzle efficiencies of the prototype and the model were assumed equal. Simulation of ideal momentum ratio and plume shapes were therefore pursued.

The ideal momentum ratio is defined as ideal thrust coefficient, C_{T_i} where

$$C_{T_i} = \left(\frac{\mathring{M}_j V_j}{q_\infty S_\pi}\right)_{proto} = \left(\frac{\mathring{M}_j V_j}{q_\infty S_\pi}\right)_{model} \tag{1}$$

for correct simulation. This is expanded to

$$2\,\frac{\gamma_{j_p} M_{j_p}^2 P_{j_p} A_{j_p}}{\gamma_{\infty_p} M_{\infty_p}^2 P_{\infty_p} S_{\pi_p}} = 2\,\frac{\gamma_{j_m} M_{j_m}^2 P_{j_m} A_{j_m}}{\gamma_{\infty_m} M_{\infty_m}^2 P_{\infty_m} S_{\pi_m}} \tag{2}$$

Since M_{∞_m} and γ_{∞_m} are set equal to M_{∞_p} and γ_{∞_p} in the tunnel and P_∞ equals P_j for an isentropically (ideally) expanded jet this equation reduces to

$$\frac{\gamma_{j_p} M_{j_p}^2 A_{j_p}}{S_{\pi_p}} = \frac{\gamma_{j_m} M_{j_m}^2 A_{j_m}}{S_{\pi_m}} \tag{3}$$

since

$$M_{j_p} = f\,(P_{c_p}/P_{\infty_p} \text{ and } \gamma_{j_p}), \tag{4}$$

~~CONFIDENTIAL~~

$$A_{j_p} = f\,(P_{c_p}/P_{\infty p},\ \gamma_{j_p} \text{ and } A_{t_p}), \tag{5}$$

$$M_{j_m} = f\,(P_{c_m}/P_{\infty m} \text{ and } \gamma_{j_m}), \tag{6}$$

and

$$A_{j_m} = f\,(P_{c_m}/P_{\infty m},\ \gamma_{j_m},\ \text{and } A_{t_m}); \tag{7}$$

$$P_{c_m}/P_{\infty m} = f\,(P_{c_p}/P_{\infty p},\ \gamma_{j_p},\ A_{t_p},\ \gamma_{j_m},\ A_{t_m},\ \text{S.F.}) \text{ for jet} \tag{8}$$

momentum simulation. The value of A_{t_m} was selected to maintain $P_{c_m}/P_{\infty m}$ within the capabilities of the AEDC facility. Figure 11 shows the relationship between $P_{c_m}/P_{\infty m}$ and $P_{c_p}/P_{\infty p}$. The values of C_T appearing on the plots in Appendix A were computed from the following equation.

$$C_T = \frac{2\gamma_{j_m} M_{j_m}^2 P_{j_m} A_{j_m}}{\gamma_{\infty_m} M_{\infty_m}^2 P_{\infty m} S_{\pi m}} \times \eta_N \times \frac{\text{Cos } 35°}{\text{Cos } 2.75°} \tag{9}$$

where η_N is a computed prototype nozzle efficiency based on static LES motor firings.

The primary parameter considered for plume shape simulation was the flow direction, δ, of the boundary streamline as it leaves the nozzle exit. Figure 12 shows this comparison between the prototype and the FSJ-3 model. Figure 13 shows comparisons of plume shapes which were defined by means of a modified method of characteristics computer program.

Because of the space restriction in the model rocket motor base areas, it was not possible to design a plenum chamber upstream of the nozzles to stagnate the air. It is therefore necessary to turn the airflow 145 degrees at high velocities which incurs high pressure losses and makes it impossible to measure nozzle stagnation pressure by means of a wall tap. An airflow rate calibration of the chamber pressure tap on the model centerline, P_{c_1}, was accomplished to provide a means for setting the simulated LES thrust level.

$$\text{Thrust} \sim P_c = \frac{W_a \sqrt{T_{T_a}}}{0.5318\ A_{t_m}} \sim P_{c_1} \tag{10}$$

Figure 14 is the calibration curve for P_c vs P_{c_1}.

CON[redacted]

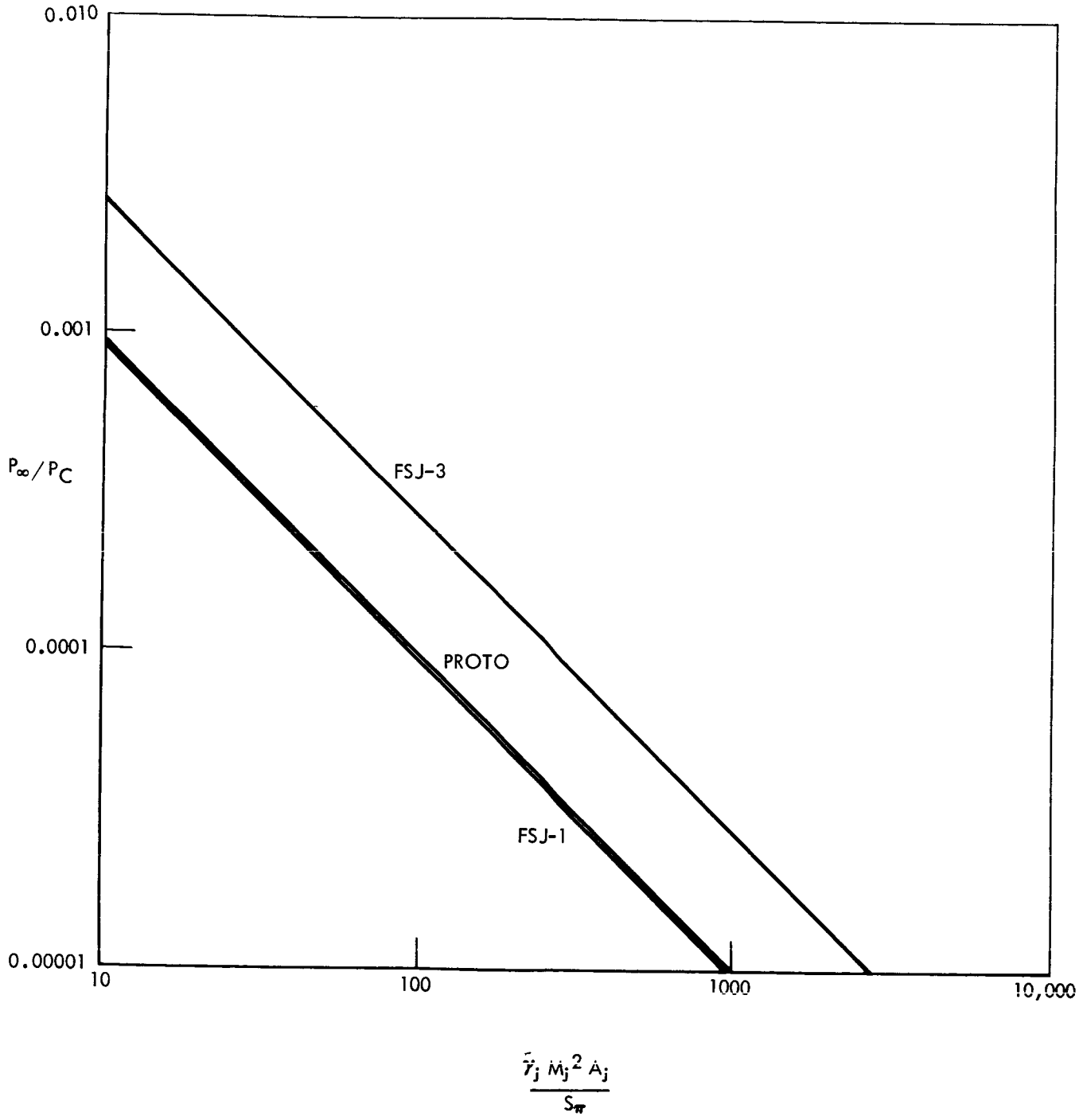

Figure 11. Pcm/P∞ m and Pcp/P∞ p Versus $\frac{\gamma j\ M^2 j\ Aj}{S\pi}$ (Sheet 1 of 2)

[redacted]

~~CONFIDENTIAL~~

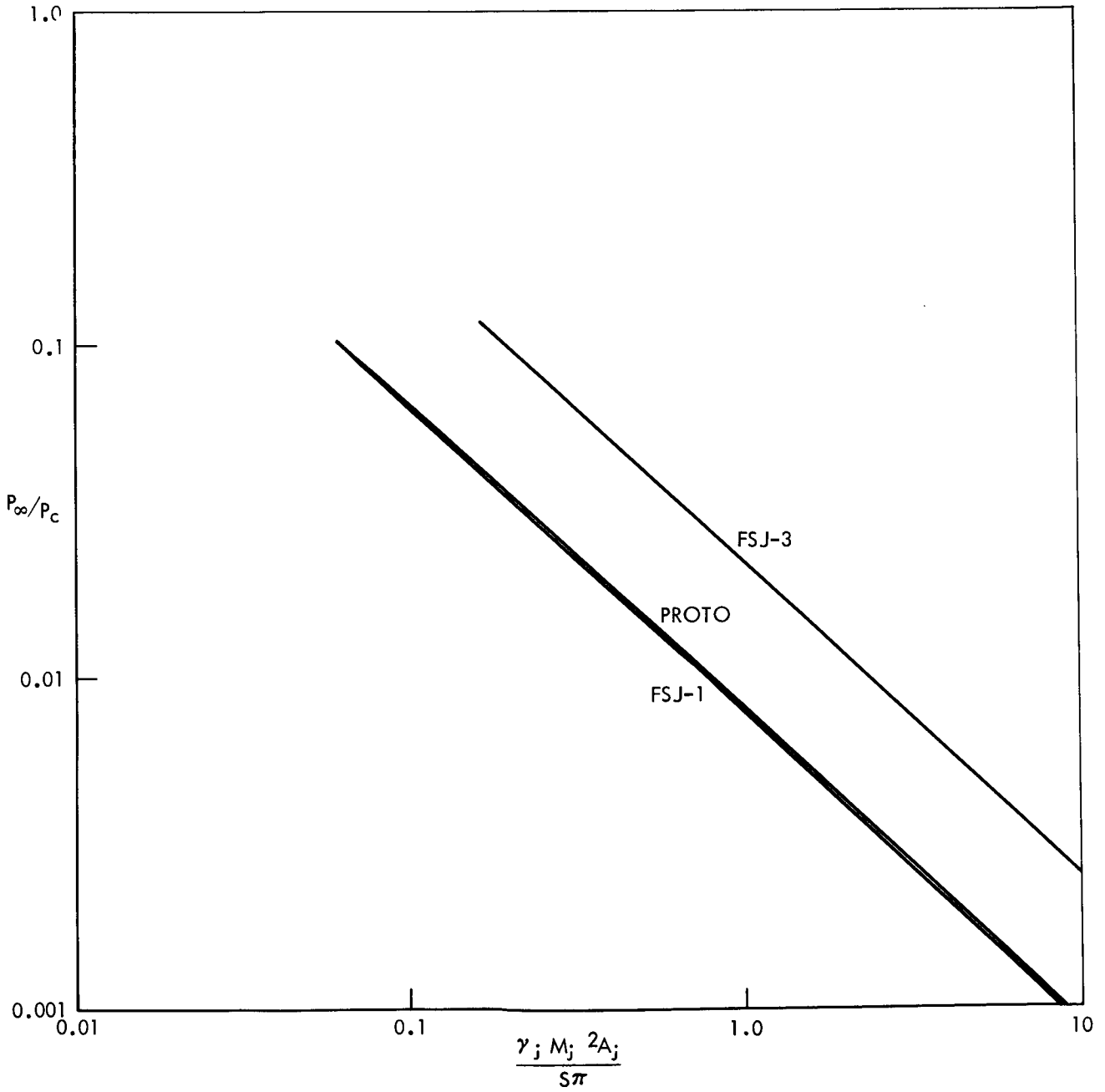

Figure 11. Pcm/P∞ m and Pcp/P∞ p Versus $\frac{\gamma_j M^2_j A_j}{S\pi}$ (Sheet 2 of 2)

~~CONFIDENTIAL~~

CON[redacted]

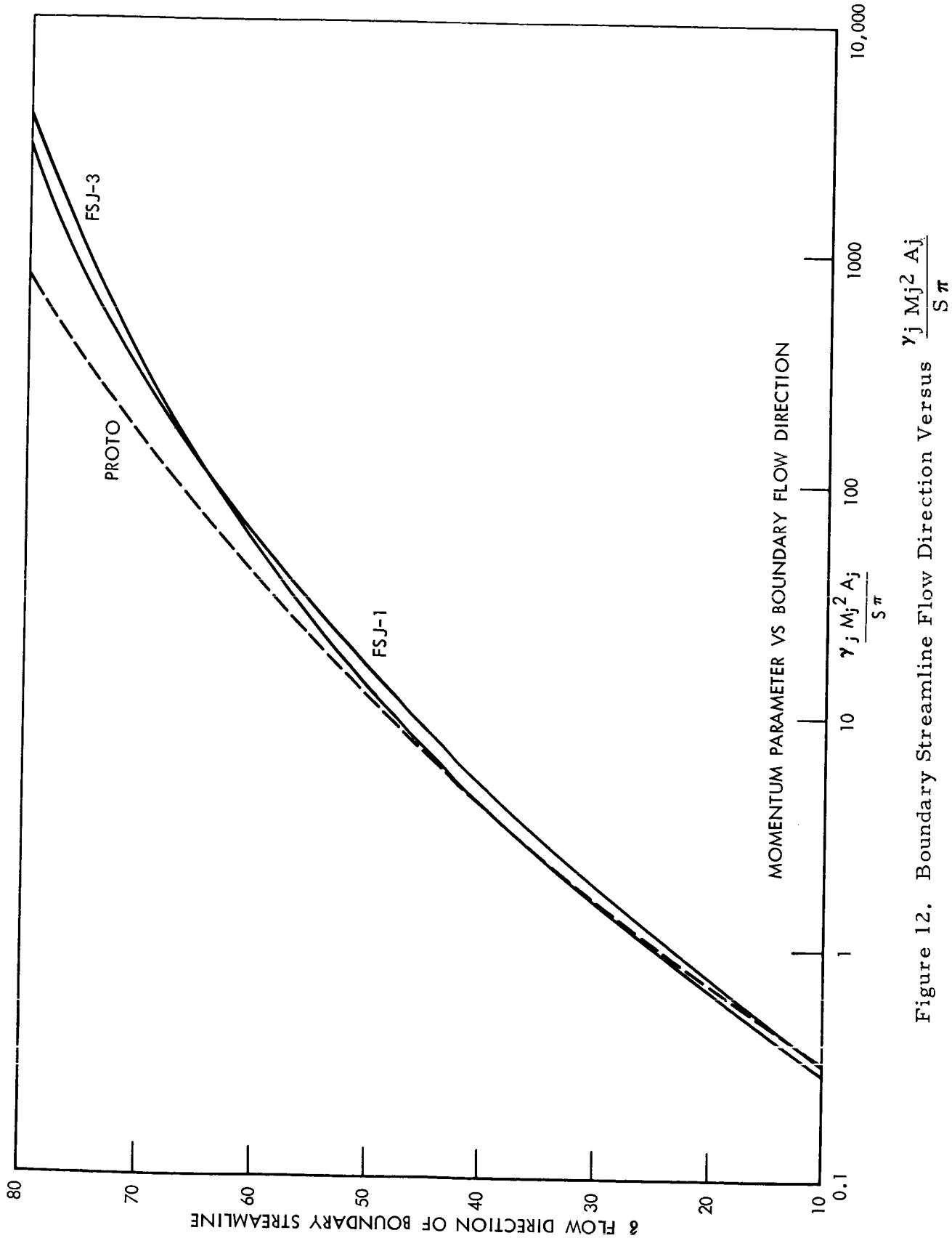

Figure 12. Boundary Streamline Flow Direction Versus $\frac{\gamma_j M_j^2 A_j}{S \pi}$

[redacted]

~~CONFIDENTIAL~~

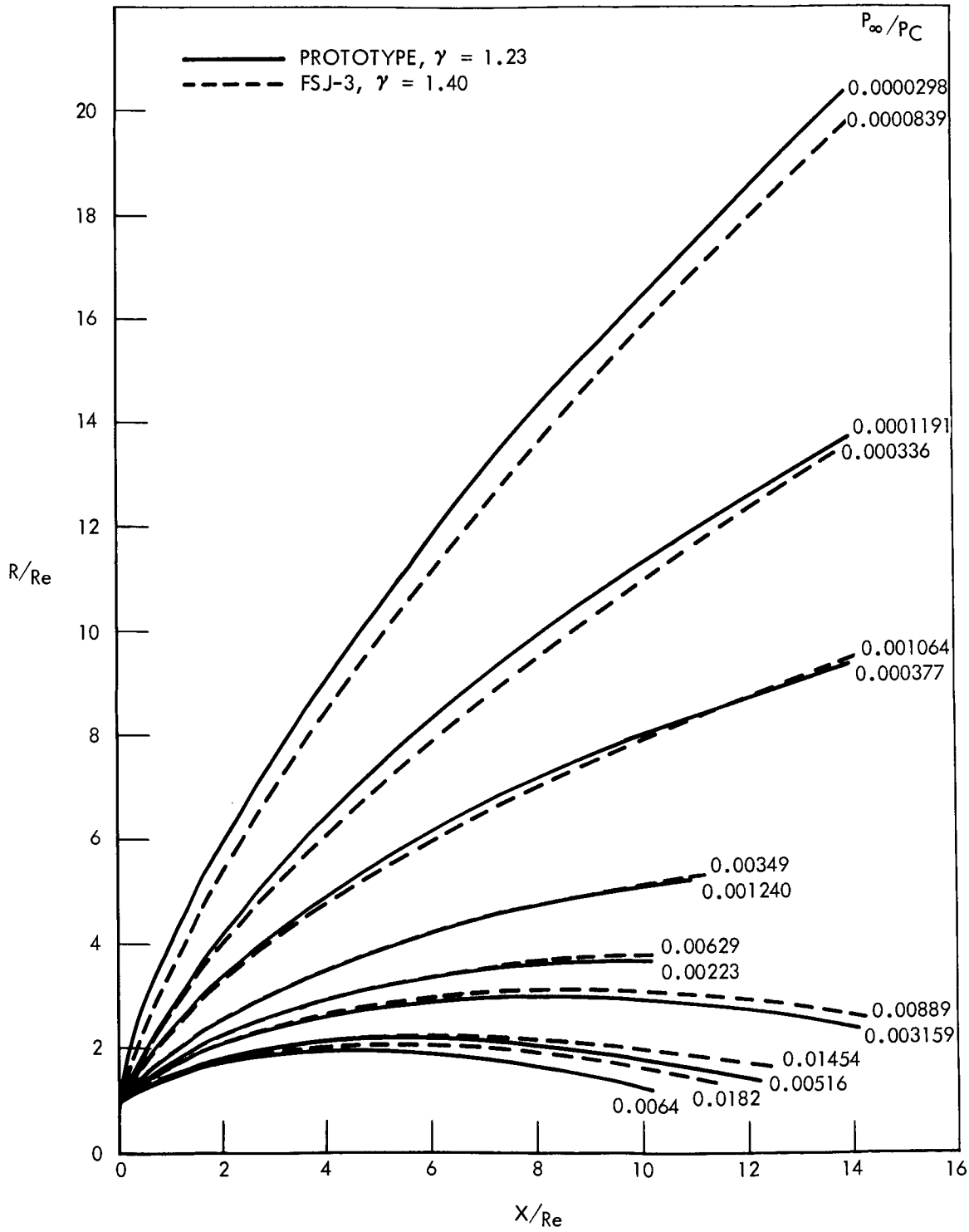

Figure 13. Computed Plume Shape Comparisons

~~CONFIDENTIAL~~

CO[redacted]

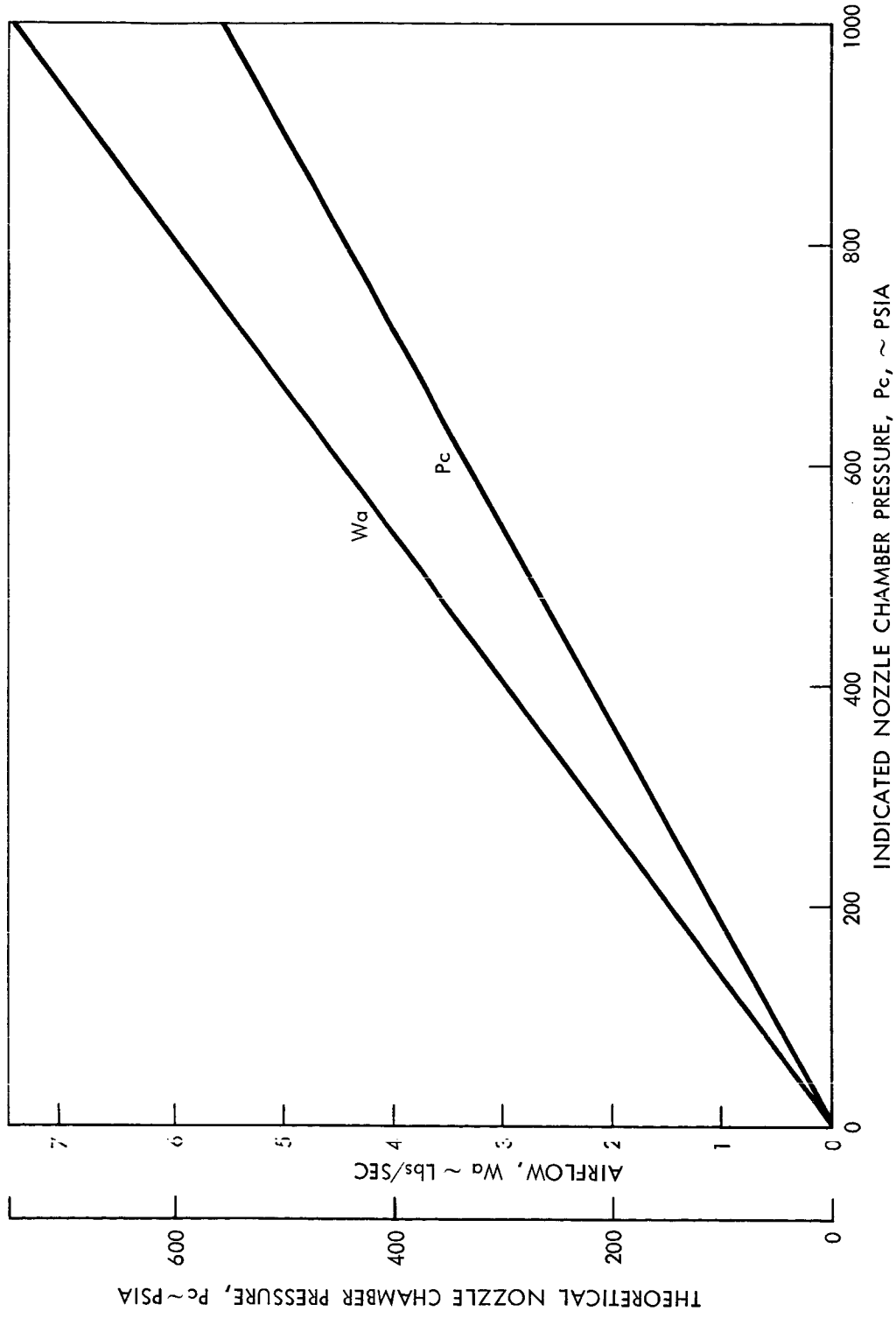

Figure 14. Airflow and Theoretical Chamber Pressure Versus Indicated Chamber Pressure, P_{c_1}

[redacted]

V. DISCUSSION

FORCE AND MOMENT DATA

Axial force, normal force, and apex pitching moment coefficient curves from tests of the 0.105 scale FS-2 model have been superimposed on Figures 21, 22, 23, and 24 in Appendix A. The differences shown are probably due to one or more of the following reasons.

1. Small model configuration differences. FS-2 was configuration $E_{48}T_9C_2$ and FSJ-3 was configuration $E_{65}T_{28}C_{40}N_8$.

2. Flow field interference of the air pipe inside the FSJ-3 model tower

3. Deletion of the CM nose on the FSJ-3 model

4. Force transmission through the rubber seal between the CM (metric) and the air pipe (nonmetric) of the FSJ-3 model.

5. At M = 0.7, the tunnel flow conditions in tunnel A (FSJ-3 test) are unknown because the tunnel was not designed for subsonic operation and therefore has not been calibrated.

The axial force coefficient data from the FSJ-3 tests at Mach numbers of 1.48, 1.98, and 2.99 were obviously in error because of sting effects; apparently caused by the undesirable size and shape of the yaw actuator. The plotted data presented in Appendix A were corrected for these effects by increasing the axial force coefficient by an amount equal the average base pressure discrepancy; that is

$$\Delta C_A = \Delta \overline{C_{p_B}} \tag{11}$$

The small changes in $C_{m_{cg}}$ due to these increases in C_A are well within the the tolerance band and have not been plotted. The C_A corrections are tabulated below. The tabulated data sheets presented in Appendix B are direct reproductions of data received from AEDC and have not been corrected for sting effects.

~~CONFIDENTIAL~~

ΔC_A at $M_\infty = 1.48$

	$C_T \longrightarrow 0$	1.08	1.50	1.96
α				
0	0.23	0.23	0.23	0.23
5	0.20	0.21	0.22	0.22
10	0.16	0.19	0.20	0.21
15	0.18	0.20	0.22	0.23
20	0.20	0.22	0.24	0.26
25	0.20	0.22	0.24	0.26
30	0.26	0.28	0.29	0.30
35	0.22	0.23	0.24	0.24
40	0.20	0.18	0.18	0.18

ΔC_A at $M_\infty = 1.98$

	$C_T \longrightarrow 0$	1.13	1.56	2.00
α				
0	0.12	0.11	0.11	0.10
5	0.10	0.09	0.09	0.09
10	0.08	0.08	0.08	0.08
15	0.07	0.07	0.07	0.07
20	0.06	0.06	0.06	0.06
25	0.06	0.06	0.06	0.06
30	0.07	0.07	0.07	0.07
35	0.07	0.07	0.07	0.07
40	0.06	0.07	0.07	0.07
45	0.05	0.06	0.06	0.06
50	0.04	0.06	0.06	0.06

ΔC_A at $M_\infty = 2.99$

	$C_T \longrightarrow 0$	1.65	2.30	2.94
α				
0	0.05	0.05	0.05	0.05
5	0.04	0.04	0.04	0.04
10	0.02	0.02	0.02	0.02
15	0.01	0.01	0.01	0.01
20	0	0	0	0
25	0	0	0	0
30	0.07	0.02	0.02	0.02
35	0.04	0.01	0.01	0.01
40	0.02	0	0	0
45	0.01	0	0	0
50	0	0	0	0

PRESSURE DATA

A small percentage of the pressure data taken during the tests is presented in plotted form in Appendix A. These plots show the conditions at which the jet impinges on the command module. It is obvious that sufficient data were not obtained to precisely define maximum impingement pressures along the windward ray at all applicable Mach numbers, angles of attack, and thrust levels. This is because the test program was designed primarily to obtain force and stability data. The remainder of the pressure data is presented in the tabulated form, only, in Appendix B.

SCHLIEREN PHOTOGRAPHS

Figures 15 through 20 are selected Schlieren photographs taken during the test. Because of the window brace which always obliterates an important part of the flow field, the photographs are not as useful as desirable. The photographs at 1.48 Mach number indicate an undesirable flow condition aft of the model which probably contributed to the sting effects.

DATA REDUCTION

The AEDC data reduction program was set up to provide aerodynamic force and moment coefficient data about the command module apex and about a stability axis (reference CG location) for the total LEV. Component force and moment coefficients were computed about the command module apex only. Center of pressure distance from the CM apex were reduced to the dimensionless form X_{cp}/D. Lift-to-drag ratio was calculated for the LEV.

Command module surface pressures were reduced to ratio form, P/P_o. and to coefficient form, $P-P_\infty/q_\infty$. Nozzle plenum chamber pressures were reduced to the ratio form P_c/P_∞.

DATA ACCURACY

Five factors were considered in the determination of the accuracy of the data from this test. These were:

- Model reference area and length tolerances
- Dynamic pressure (q_∞) measurement accuracy
- Force and moment measurement accuracies
- Data system accuracies
- Zero shifts

[redacted]

The probable errors listed below were obtained by taking the root-sum-square of the individual estimated errors.

Maximum Probable Errors

M	C_A	C_N	C_{m_A}	$C_{m_{cg}}$	C_P (percent)
0.7	±0.102	±0.0482	±0.0181	±0.0184	±10.8
1.48	±0.0078	±0.0077	±0.0082	±0.0082	±1.57
1.98	±0.0109	±0.0127	±0.0084	±0.0084	±1.85
2.99	±0.0129	±0.0161	±0.0091	±0.0091	±2.04
3.99	±0.0141	±0.0164	±0.0125	±0.0125	±2.08
4.99	±0.0225	±0.0225	±0.0268	±0.0268	±2.05
5.97	±0.0280	±0.0270	±0.0374	±0.0374	±1.84

CONFIDENTIAL

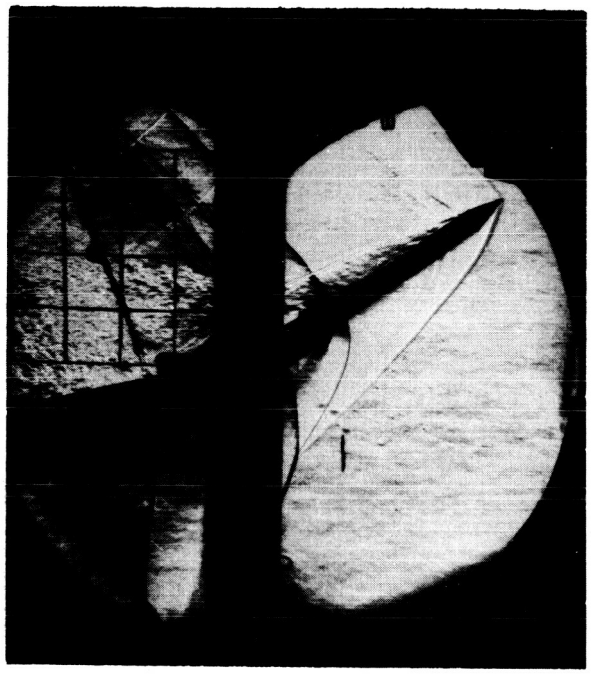

$M_\infty = 1.48$, $\alpha = 35^\circ$,

$C_T = 0$

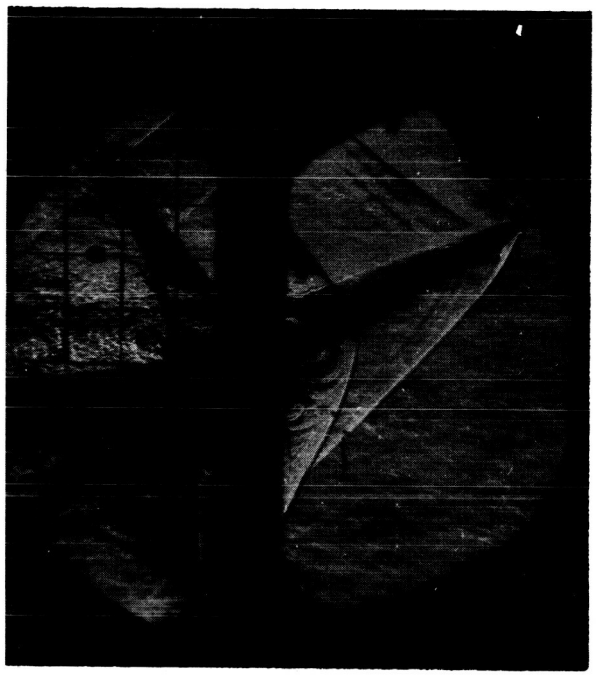

$M_\infty = 1.48$, $\alpha = 30^\circ$,

$C_T = 1.08$

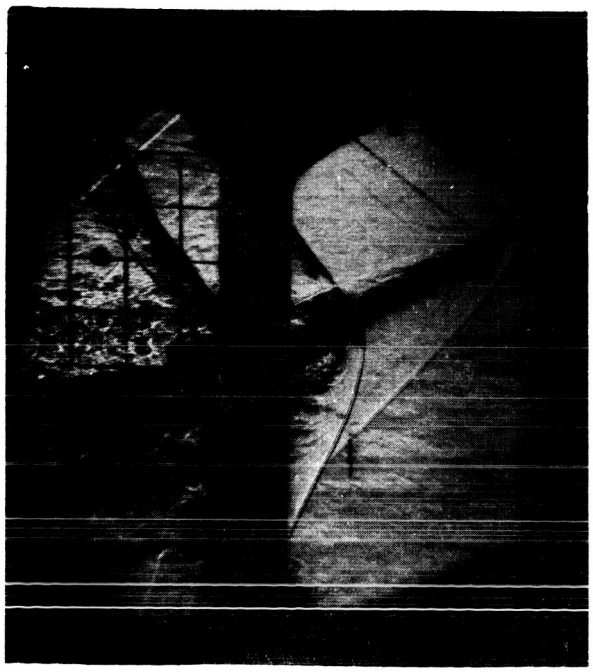

$M_\infty = 1.48$, $\alpha = 30^\circ$,

$C_T = 1.50$

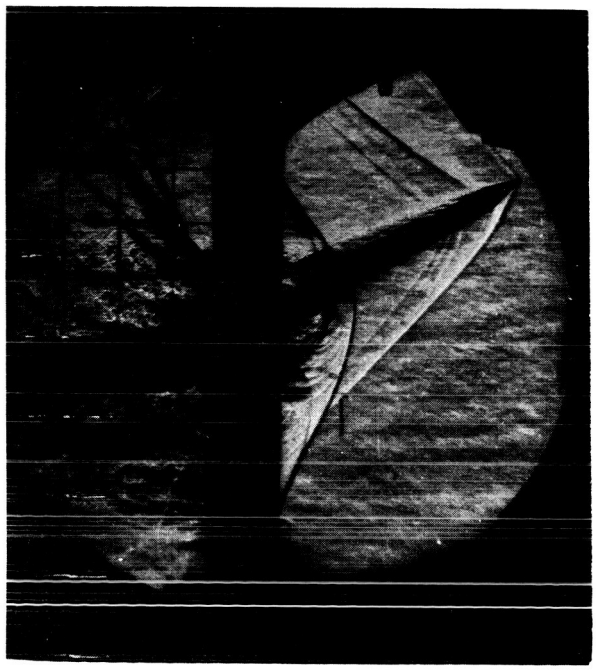

$M_\infty = 1.48$, $\alpha = 30^\circ$,

$C_T = 1.88$

Figure 15. Schlieren Photographs at $M_\infty = 1.48$

CONFIDENTIAL

CONFIDENTIAL

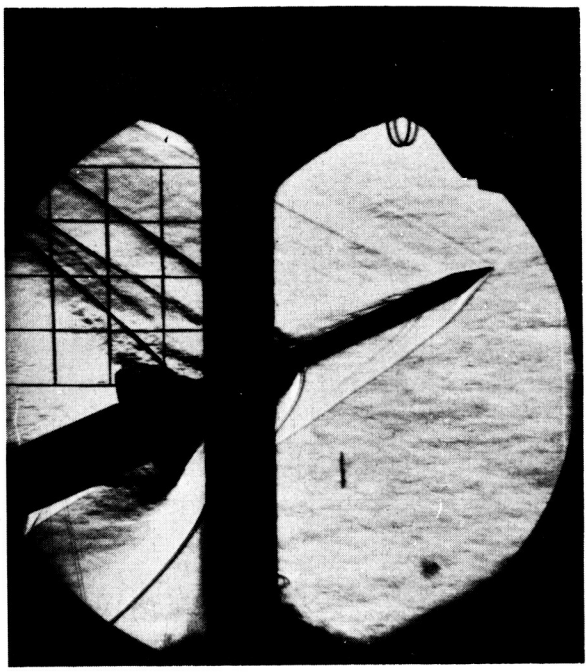

$M_\infty = 1.98$, $\alpha = 25^\circ$,

$C_T = 0$

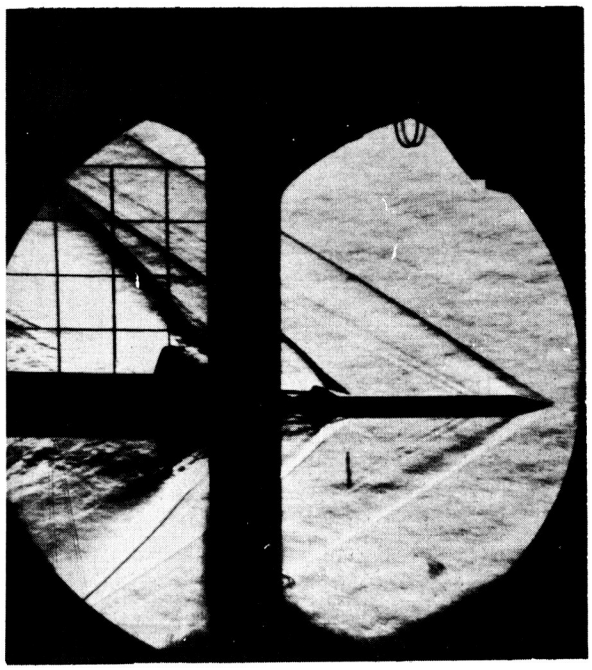

$M_\infty = 1.98$, $\alpha = 0^\circ$,

$C_T = 0$

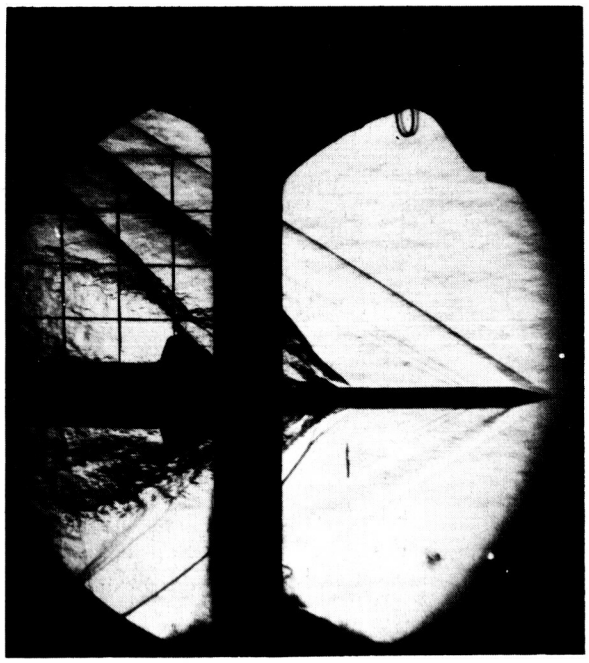

$M_\infty = 1.98$, $\alpha = 0^\circ$,

$C_T = 2.00$

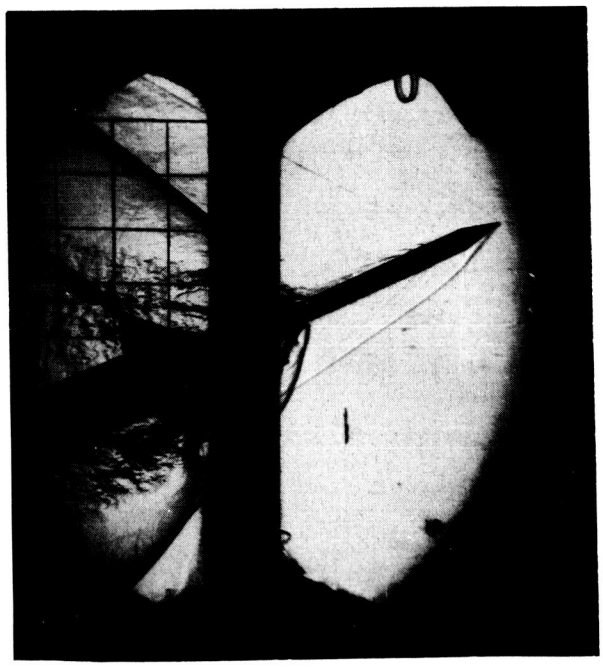

$M_\infty = 1.98$, $\alpha = 25^\circ$,

$C_T = 2.00$

Figure 16. Schlieren Photographs at $M_\infty = 1.98$

CONFIDENTIAL

CON~~FIDENTIAL~~

$M_\infty = 1.98$, $\alpha = 50^o$,

$C_T = 0$

$M_\infty = 1.98$, $\alpha = 50^o$,

$C_T = 1.14$

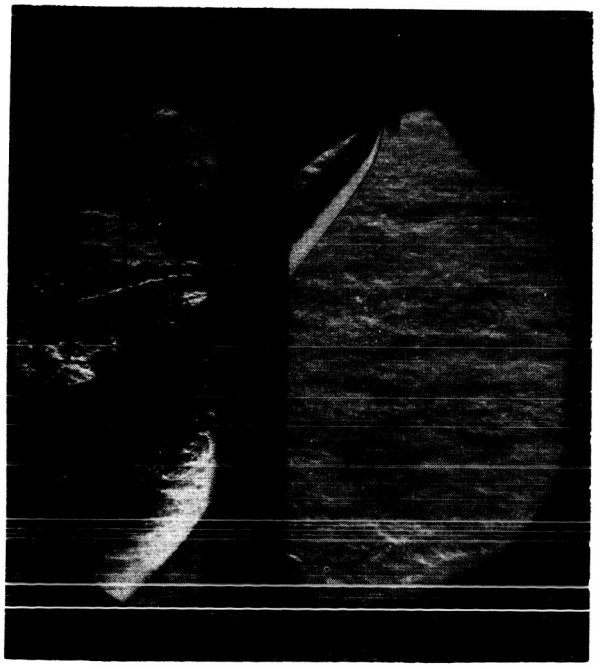

$M_\infty = 1.98$, $\alpha = 50^o$,

$C_T = 1.54$

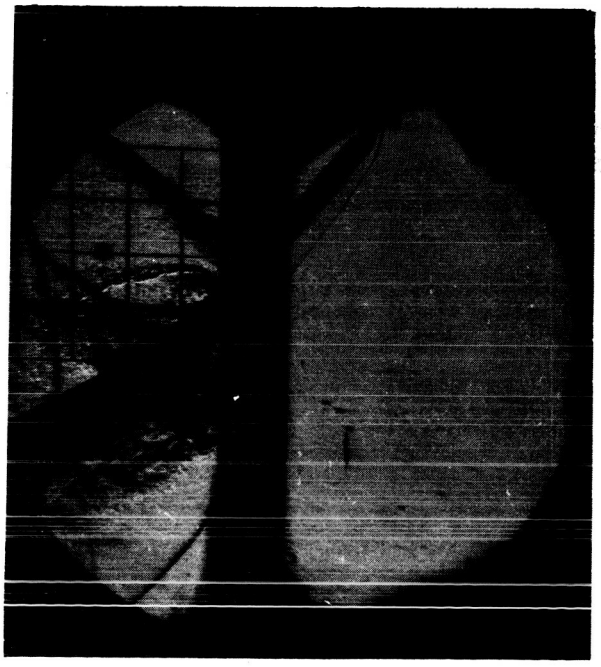

$M_\infty = 1.98$, $\alpha = 50^o$,

$C_T = 2.00$

Figure 16. Schlieren Photographs at $M_\infty = 1.98$ (Cont)

~~CONFIDENTIAL~~

CONFIDENTIAL

$M_\infty = 2.99$, $\alpha = 15^\circ$,

$C_T = 0$

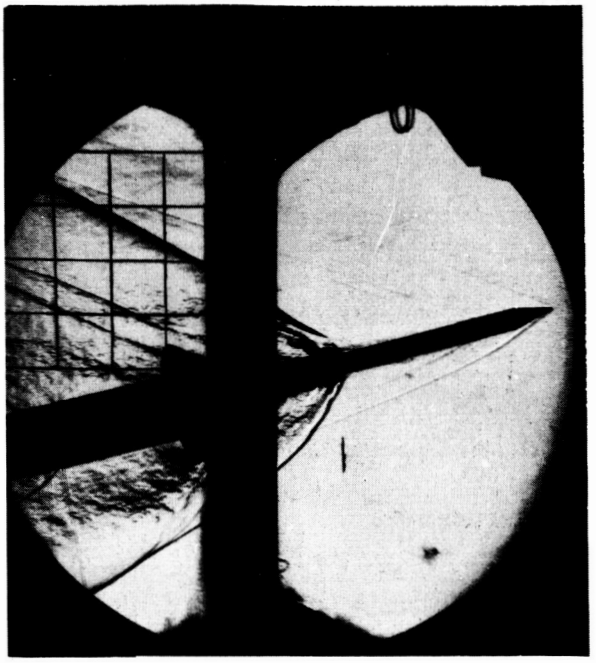

$M_\infty = 2.99$, $\alpha = 15^\circ$,

$C_T = 1.65$

$M_\infty = 2.99$, $\alpha = 10^\circ$,

$C_T = 2.30$

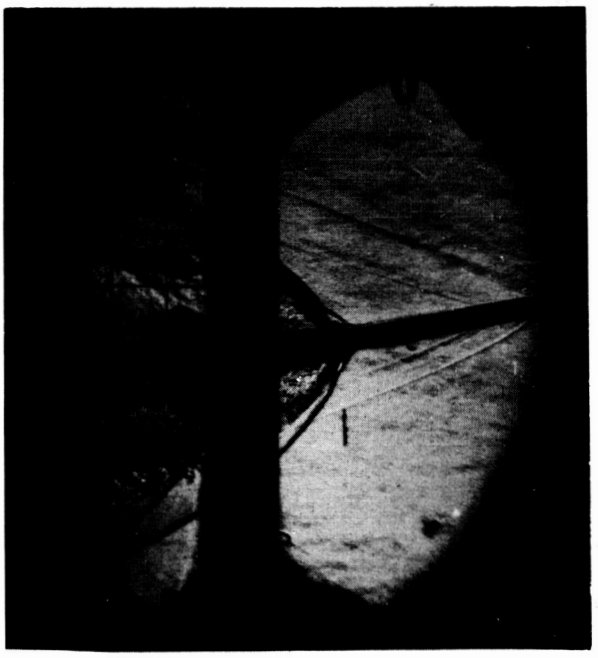

$M_\infty = 2.99$, $\alpha = 10^\circ$,

$C_T = 2.94$

Figure 17. Schlieren Photographs at $M_\infty = 2.99$

CONFIDENTIAL

CONFIDENTIAL

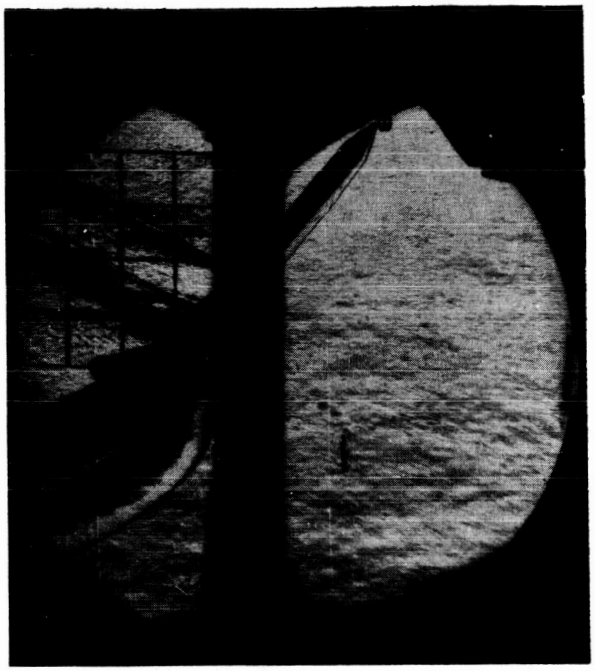

$M_\infty = 2.99$, $\alpha = 50^\circ$,

$C_T = 0$

$M_\infty = 2.99$, $\alpha = 50^\circ$,

$C_T = 1.60$

$M_\infty = 2.99$, $\alpha = 50^\circ$,

$C_T = 2.27$

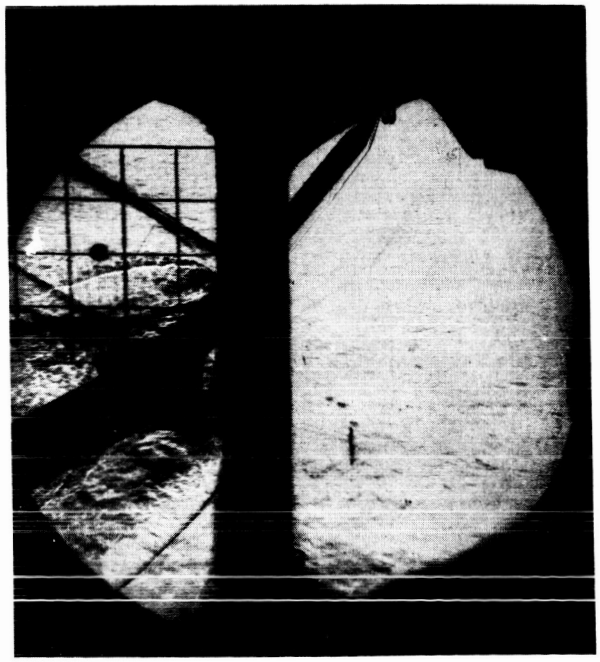

$M_\infty = 2.99$, $\alpha = 50^\circ$

$C_T = 2.91$

Figure 17. Schlieren Photographs at $M_\infty = 2.99$ (Cont)

CONFIDENTIAL

CONFIDENTIAL

$M_\infty = 3.99$, $\alpha = 25^\circ$,

$C_T = 5.14$

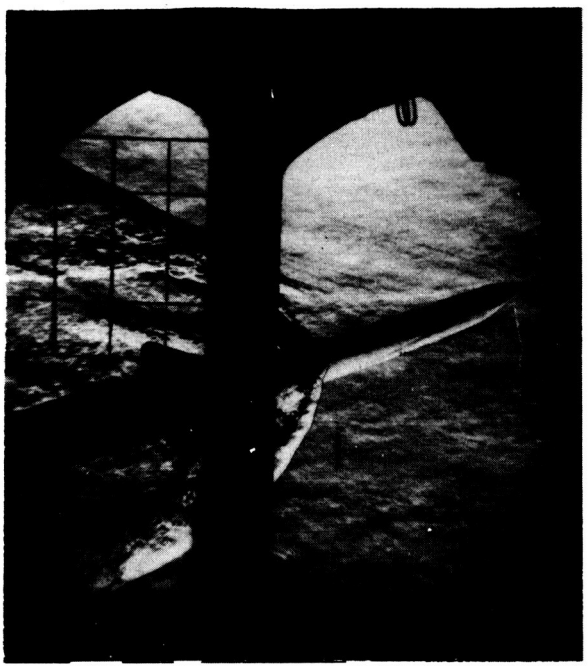

$M_\infty = 3.99$, $\alpha = 20^\circ$,

$C_T = 5.14$

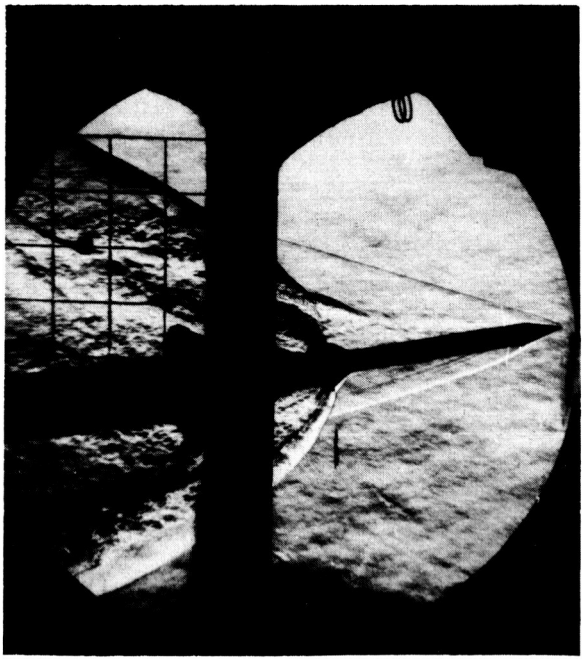

$M_\infty = 3.99$, $\alpha = 10^\circ$,

$C_T = 5.14$

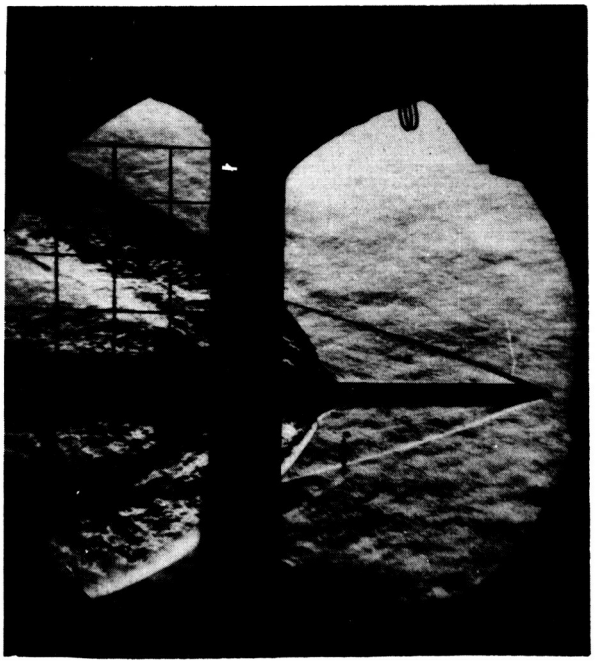

$M_\infty = 3.99$, $\alpha = 0^\circ$,

$C_T = 5.14$

Figure 18. Schlieren Photographs at $M_\infty = 3.99$

CONFIDENTIAL

CON~~FIDENTIAL~~

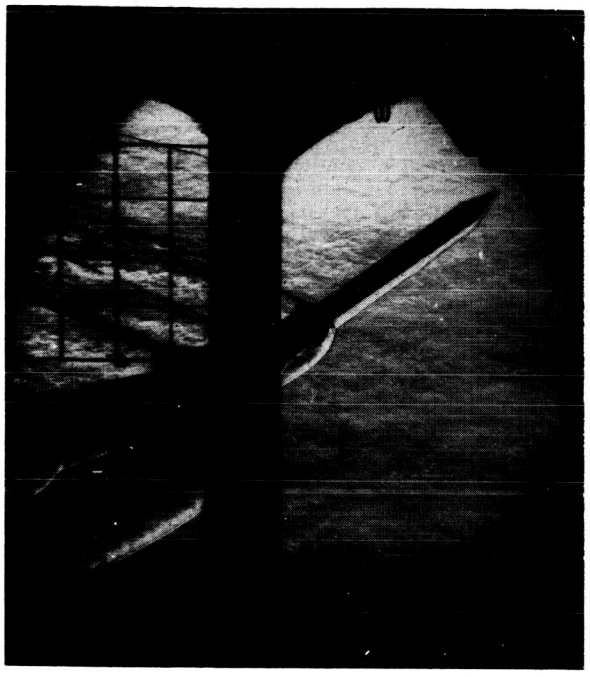

$M_\infty = 3.99$, $\alpha = 35^o$,

$C_T = 0$

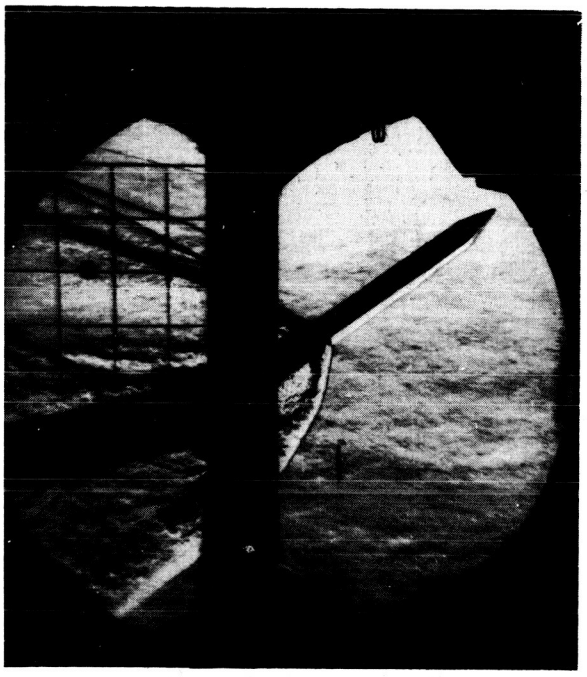

$M_\infty = 3.99$, $\alpha = 35^o$,

$C_T = 2.94$

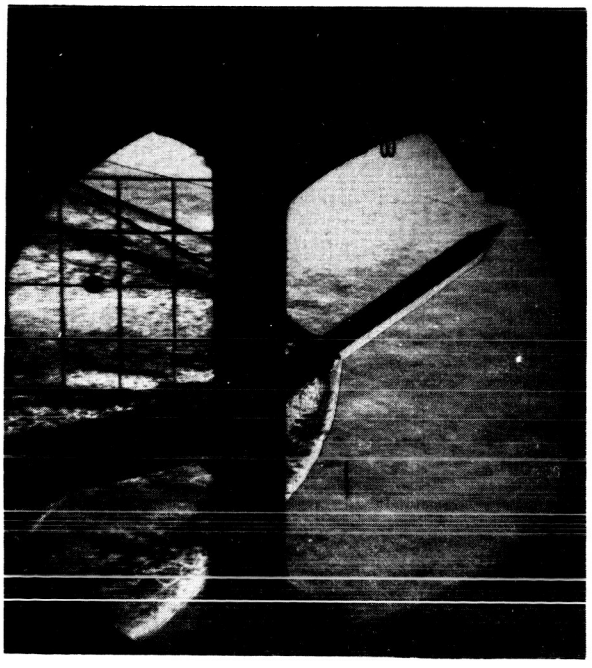

$M_\infty = 3.99$, $\alpha = 35^o$,

$C_T = 3.99$

$M_\infty = 3.99$, $\alpha = 35^o$

$C_T = 5.14$

Figure 18. Schlieren Photographs at $M_\infty = 3.99$ (Cont)

~~CONFIDENTIAL~~

~~CONFIDENTIAL~~

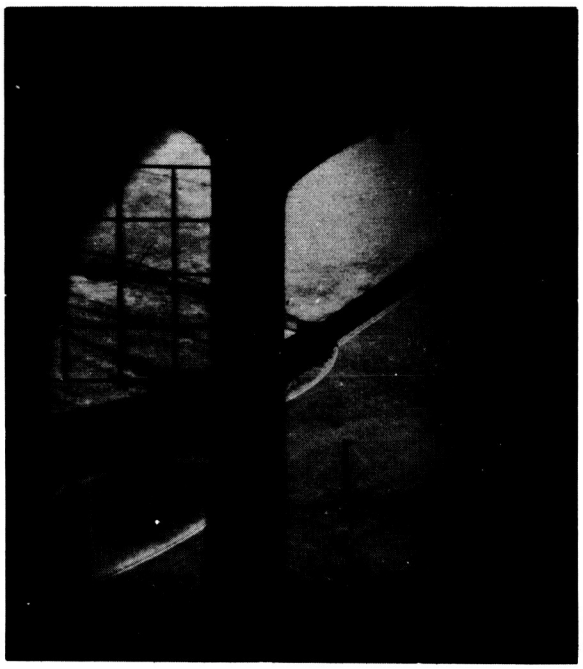

$M_\infty = 4.99$, $\alpha = 35^\circ$,

$C_T = 0$

$M_\infty = 4.99$, $\alpha = 35^\circ$,

$C_T = 7.66$

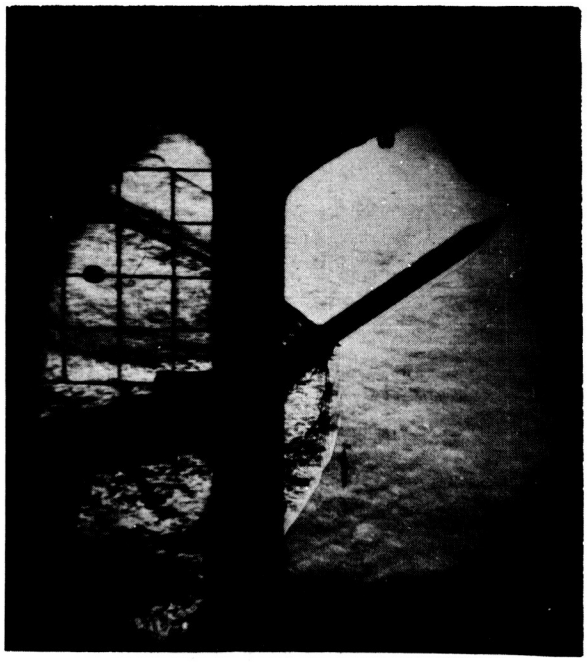

$M_\infty = 4.99$, $\alpha = 35^\circ$,

$C_T = 10.71$

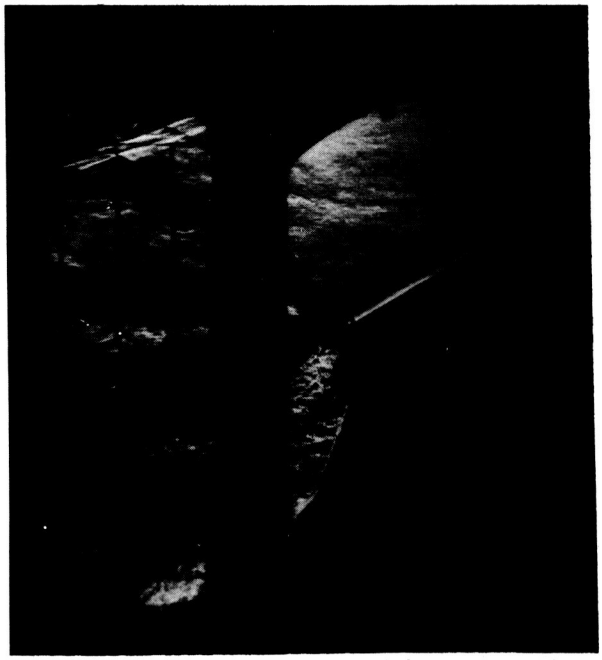

$M_\infty = 4.99$, $\alpha = 30^\circ$,

$C_T = 13.64$

Figure 19. Schlieren Photographs at $M_\infty = 4.99$

~~CONFIDENTIAL~~

CONFIDENTIAL

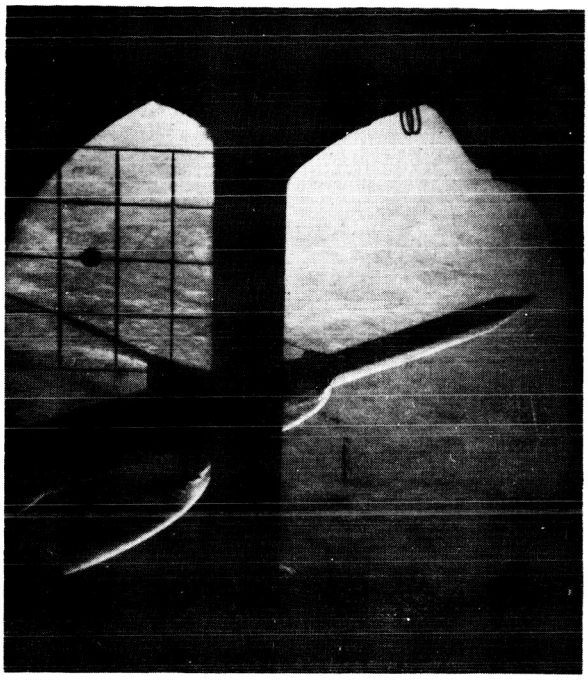

$M_\infty = 5.97$, $\alpha = 20^\circ$,

$C_T = 0$

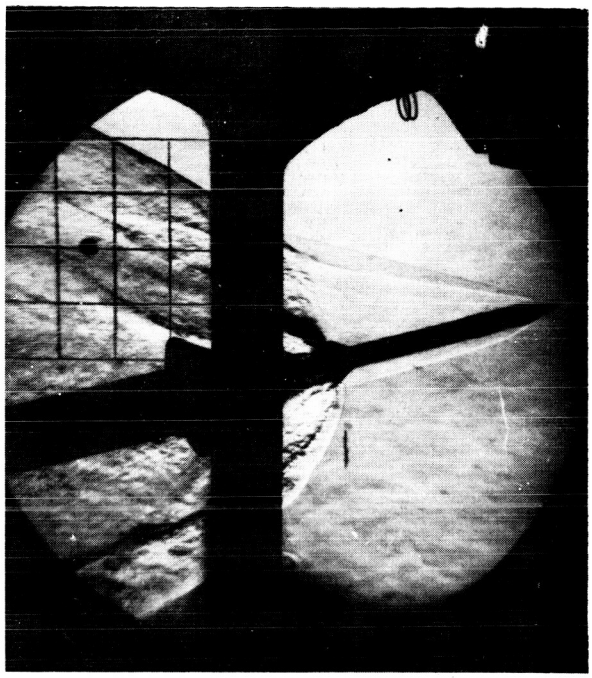

$M_\infty = 5.97$, $\alpha = 15^\circ$,

$C_T = 10.55$

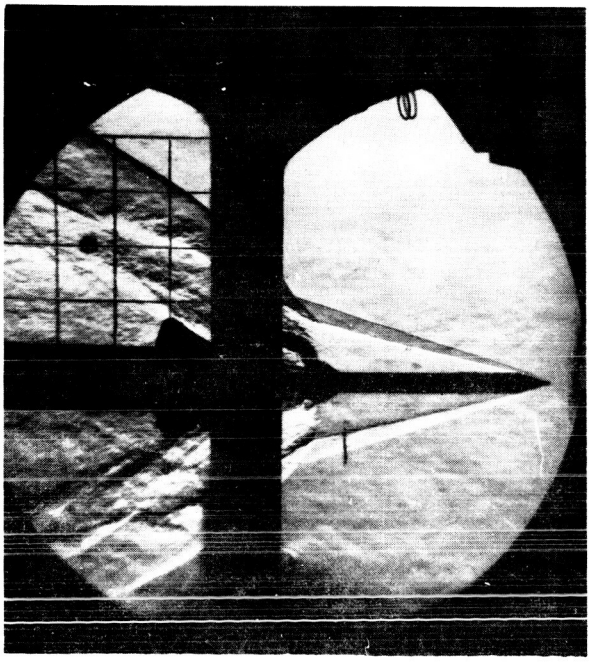

$M_\infty = 5.97$, $\alpha = 0^\circ$,

$C_T = 10.55$

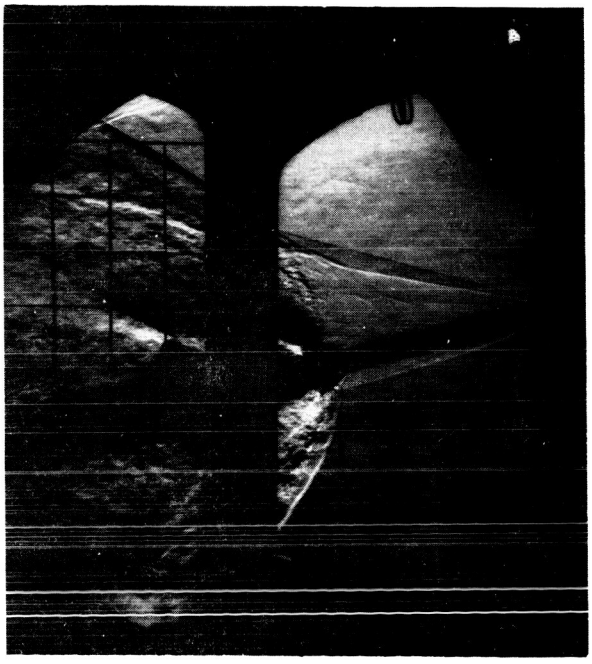

$M_\infty = 5.97$, $\alpha = 15^\circ$,

$C_T = 14.76$

Figure 20. Schlieren Photographs at $M_\infty = 5.97$

CONFIDENTIAL

CO[redacted]

APPENDIX A

PLOTTED DATA

[redacted]

~~CONFIDENTIAL~~

PLOTTED DATA INDEX

LAUNCH ESCAPE VEHICLE CHARACTERISTICS

Figure	Description	Page
21a	C_A vs α - $M_o = 0.7$	A-6
21b	C_N vs α	A-7
21c	C_{m_A} vs α	A-8
21d	$(X_{cp})_N/D$ vs α	A-9
21e	$C_{m_{cg}}$ vs α	A-10
21f	C_{A_1} vs α	A-11
21g	C_{A_2} vs α	A-12
21h	C_{N_1} vs α	A-13
21i	C_{N_2} vs α	A-14
21j	$C_{m_{A_1}}$ vs α	A-15
21k	$C_{m_{A_2}}$ vs α	A-16
22a	C_A vs α - $M_o = 1.48$	A-17
22b	C_N vs α	A-18
22c	C_{m_A} vs α	A-19
22d	$(X_{cp})_N/D$ vs α	A-20
22e	$C_{m_{cg}}$ vs α	A-21
22f	C_{A_1} vs α	A-22
22g	C_{A_2} vs α	A-23
22h	C_{N_1} vs α	A-24
22i	C_{N_2} vs α	A-25
22j	$C_{m_{A_1}}$ vs α	A-26
22k	$C_{m_{A_2}}$ vs α	A-27
23a	C_A vs α - $M_o = 1.98$	A-28
23b	C_N vs α	A-29
23c	C_{m_A} vs α	A-30

Figure	Description	Page
23d	$(X_{cp})_N/D$ vs α	A-31
23e	$C_{m_{cg}}$ vs α	A-32
23f	C_{A_1} vs α	A-33
23g	C_{A_2} vs α	A-34
23h	C_{N_1} vs α	A-35
23i	C_{N_2} vs α	A-36
23j	$C_{m_{A_1}}$ vs α	A-37
23k	$C_{m_{A_2}}$ vs α	A-38
24a	C_A vs α - $M_o = 2.99$	A-39
24b	C_N vs α	A-40
24c	C_{m_A} vs α	A-41
24d	$(X_{cp})_N/D$ vs α	A-42
24e	$C_{m_{cg}}$ vs α	A-43
24f	C_{A_1} vs α	A-44
24g	C_{A_2} vs α	A-45
24h	C_{N_1} vs α	A-46
24i	C_{N_2} vs α	A-47
24j	$C_{m_{A_1}}$ vs α	A-48
24k	$C_{m_{A_2}}$ vs α	A-49
25a	C_A vs α - $M_o = 3.99$	A-50
25b	C_N vs α	A-51
25c	C_{m_A} vs α	A-52
25d	$(X_{cp})_N/D$ vs α	A-53
25e	$C_{m_{cg}}$ vs α	A-54
25f	C_{A_1} vs α	A-55
25g	C_{A_2} vs α	A-56
25h	C_{N_1} vs α	A-57
25i	C_{N_2} vs α	A-58
25j	$C_{m_{A_1}}$ vs α	A-59
25k	$C_{m_{A_2}}$ vs α	A-60

Figure	Description	Page
26a	C_A vs α - M_o = 4.99	A-61
26b	C_N vs α	A-62
26c	C_{m_A} vs α	A-63
26d	$(X_{cp})_N/D$ vs α	A-64
26e	$C_{m_{cg}}$ vs α	A-65
26f	C_{A_1} vs α	A-66
26g	C_{A_2} vs α	A-67
26h	C_{N_1} vs α	A-68
26i	C_{N_2} vs α	A-69
26j	$C_{m_{A_1}}$ vs α	A-70
26k	$C_{m_{A_2}}$ vs α	A-71
27a	C_A vs α - M_o = 5.97	A-72
27b	C_N vs α	A-73
27c	C_{m_A} vs α	A-74
27d	$(X_{cp})_N/D$ vs α	A-75
27e	$C_{m_{cg}}$ vs α	A-76
27f	C_{A_1} vs α	A-77
27g	C_{A_2} vs α	A-78
27h	C_{N_1} vs α	A-79
27i	C_{N_2} vs α	A-80
27j	$C_{m_{A_1}}$ vs α	A-81
27k	$C_{m_{A_2}}$ vs α	A-82
28a	C_A vs M_o - α = 0 degrees	A-83
28b	C_A vs M_o - α = 10 degrees	A-84
28c	C_A vs M_o - α = 20 degrees	A-85
28d	C_A vs M_o - α = 30 degrees	A-86
28e	C_A vs M_o - α = 40 degrees	A-87
28f	C_A vs M_o - α = 50 degrees	A-88

CO[redacted]

Figure	Description	Page
29a	$C_{P_{33}}$ vs α - $M_o = 0.7$	A-89
29b	$C_{P_{33}}$ vs α - $M_o = 1.48$	A-90
29c	$C_{P_{33}}$ vs α - $M_o = 1.98$	A-91
29d	$C_{P_{33}}$ vs α - $M_o = 2.99$	A-92
29e	$C_{P_{33}}$ vs α - $M_o = 3.99$	A-93
30a	$C_{P_{23}}$ vs α - $M_o = 1.48$	A-94
30b	$C_{P_{23}}$ vs α - $M_o = 1.98$	A-95
30c	$C_{P_{23}}$ vs α - $M_o = 2.99$	A-96
30d	$C_{P_{23}}$ vs α - $M_o = 3.99$	A-97
31a	$C_{P_{15}}$ vs α - $M_o = 1.48$	A-98
31b	$C_{P_{15}}$ vs α - $M_o = 1.98$	A-99
31c	$C_{P_{15}}$ vs α - $M_o = 2.99$	A-100
31d	$C_{P_{15}}$ vs α - $M_o = 3.99$	A-101
32a	C_{P_7} vs α - $M_o = 1.48$	A-102
32b	C_{P_7} vs α - $M_o = 1.98$	A-103
32c	C_{P_7} vs α - $M_o = 2.99$	A-104
32d	C_{P_7} vs α - $M_o = 3.99$	A-105
33	C_P vs $S/_r$ at $M_o = 1.98$, α = 0 degrees	A-106
34	C_P vs $S/_r$ at $M_o = 1.98$, α = 5 degrees	A-112
35	C_P vs $S/_r$ at $M_o = 1.98$, α = 10 degrees	A-118
36	C_P vs $S/_r$ at $M_o = 1.98$, α = 15 degrees	A-124
37	C_P vs $S/_r$ at $M_o = 1.98$, α = 20 degrees	A-130
38	C_P vs $S/_r$ at $M_o = 1.98$, α = 30 degrees	A-136
39	C_P vs $S/_r$ at $M_o = 1.98$, α = 40 degrees	A-142
40	C_P vs $S/_r$ at $M_o = 1.98$, α = 50 degrees	A-148

[redacted]

~~CONFIDENTIAL~~

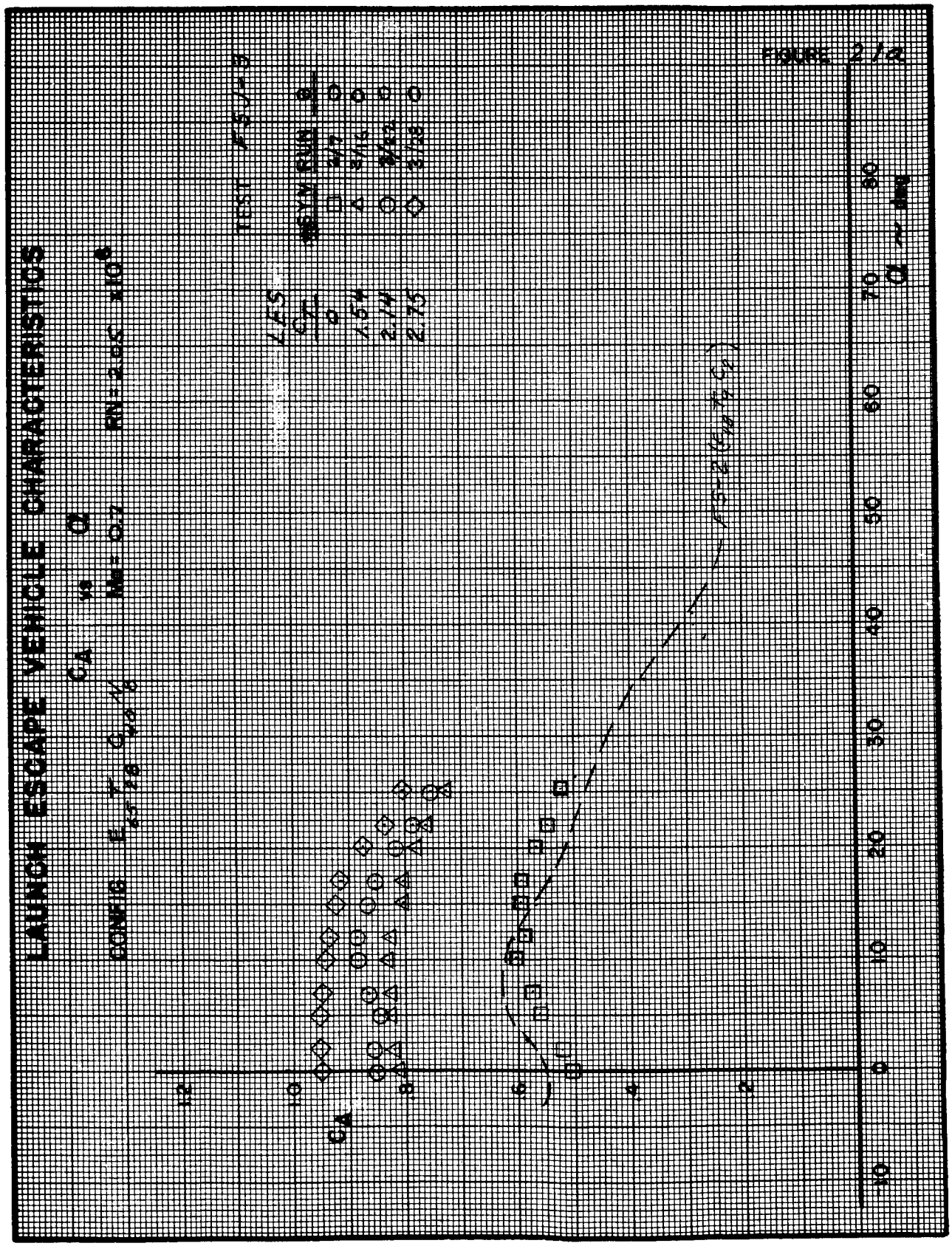

~~CONFIDENTIAL~~

CO[redacted]

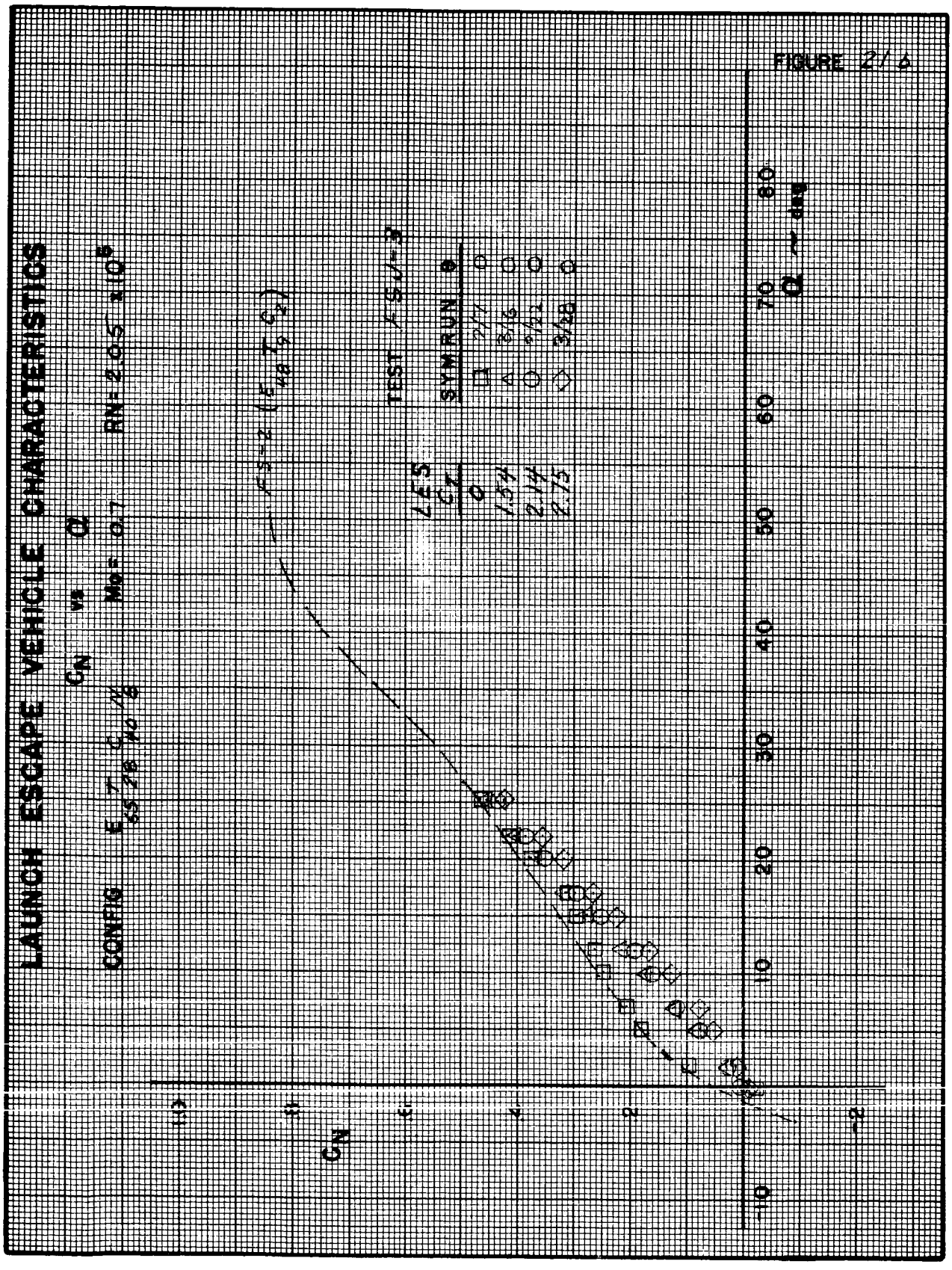

FIGURE 2/6

[redacted]

~~CONFIDENTIAL~~

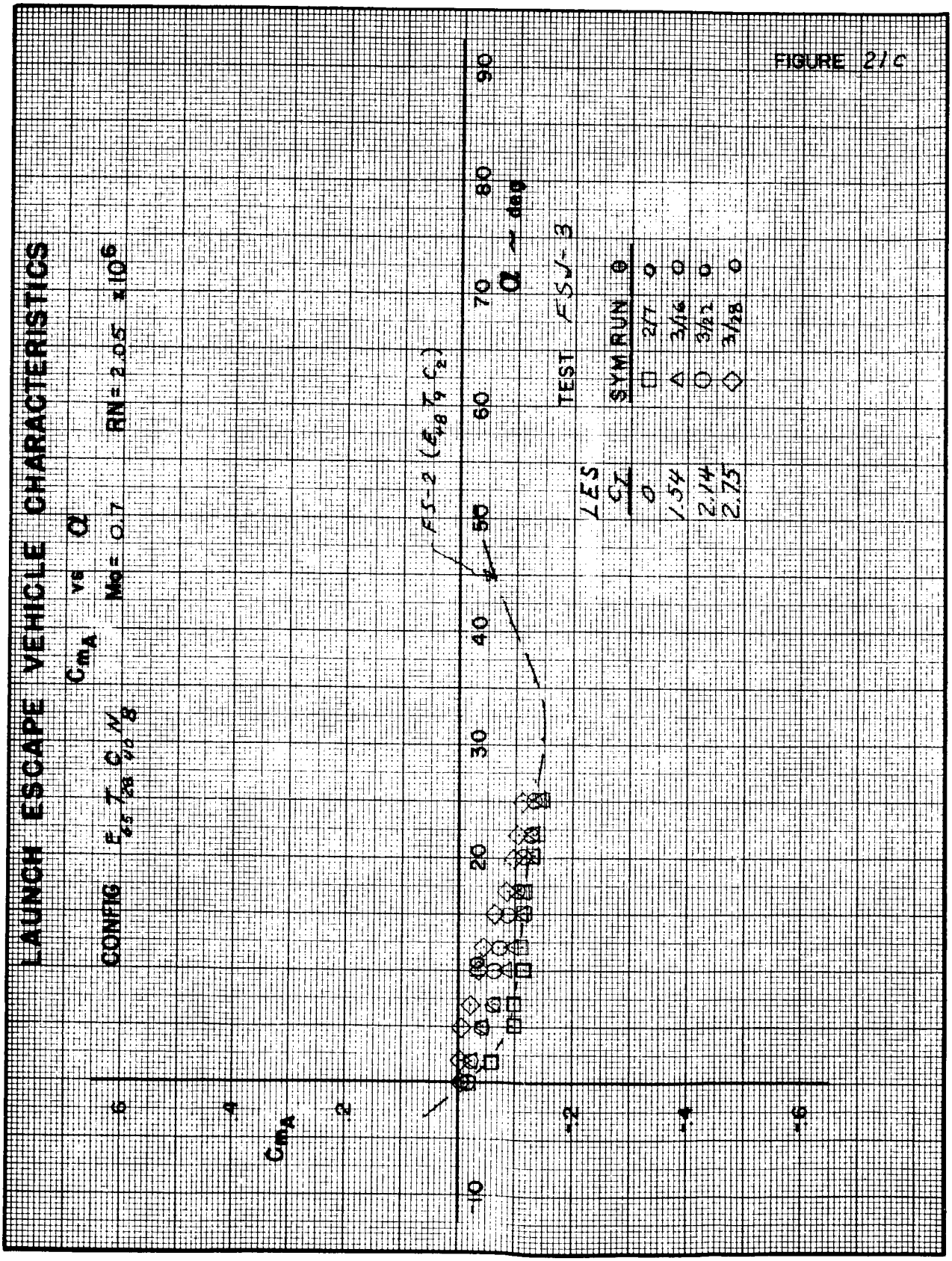

FIGURE 21c

~~CONFIDENTIAL~~

CON[redacted]

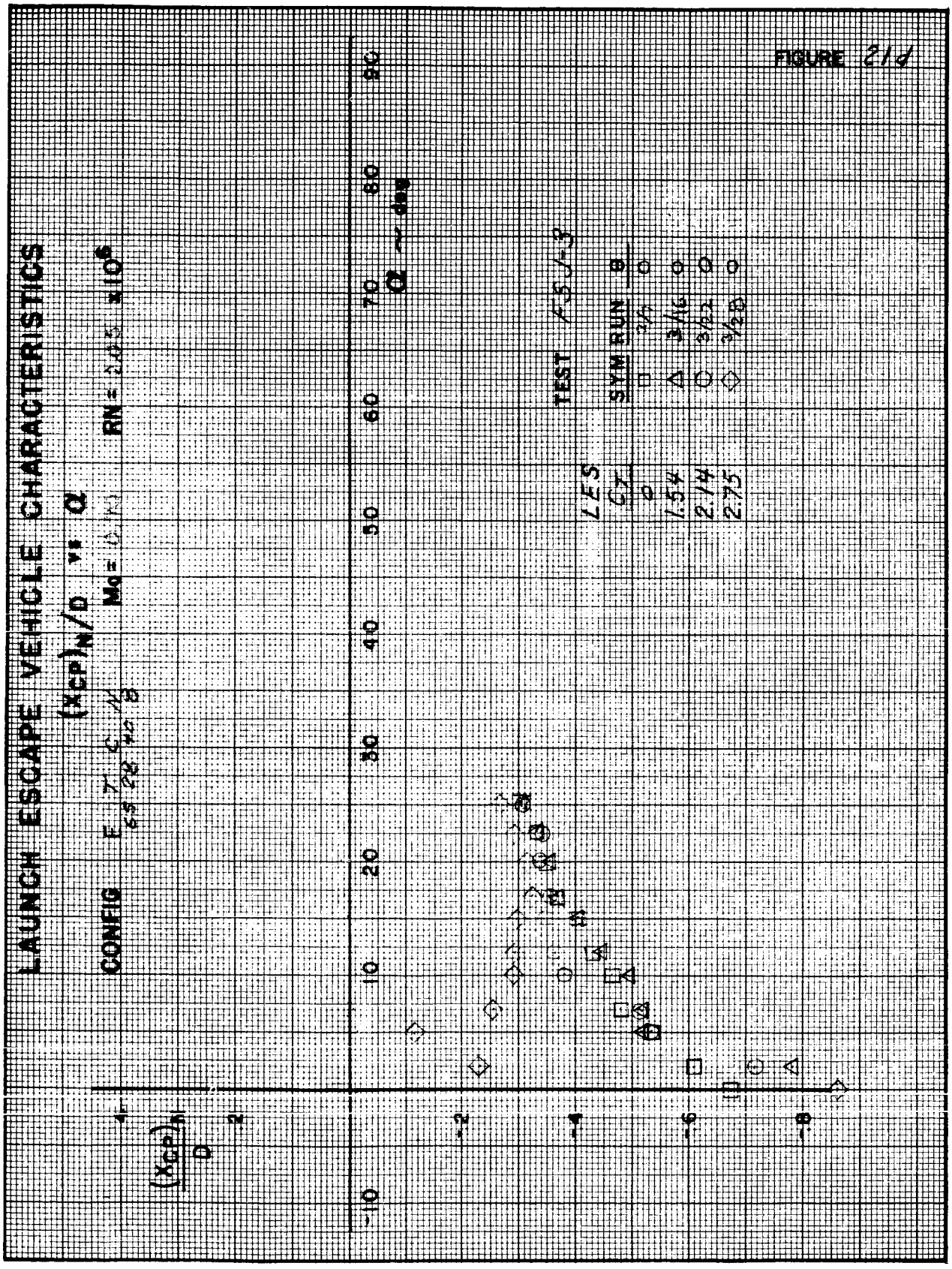

FIGURE 21d

[redacted]

~~CONFIDENTIAL~~

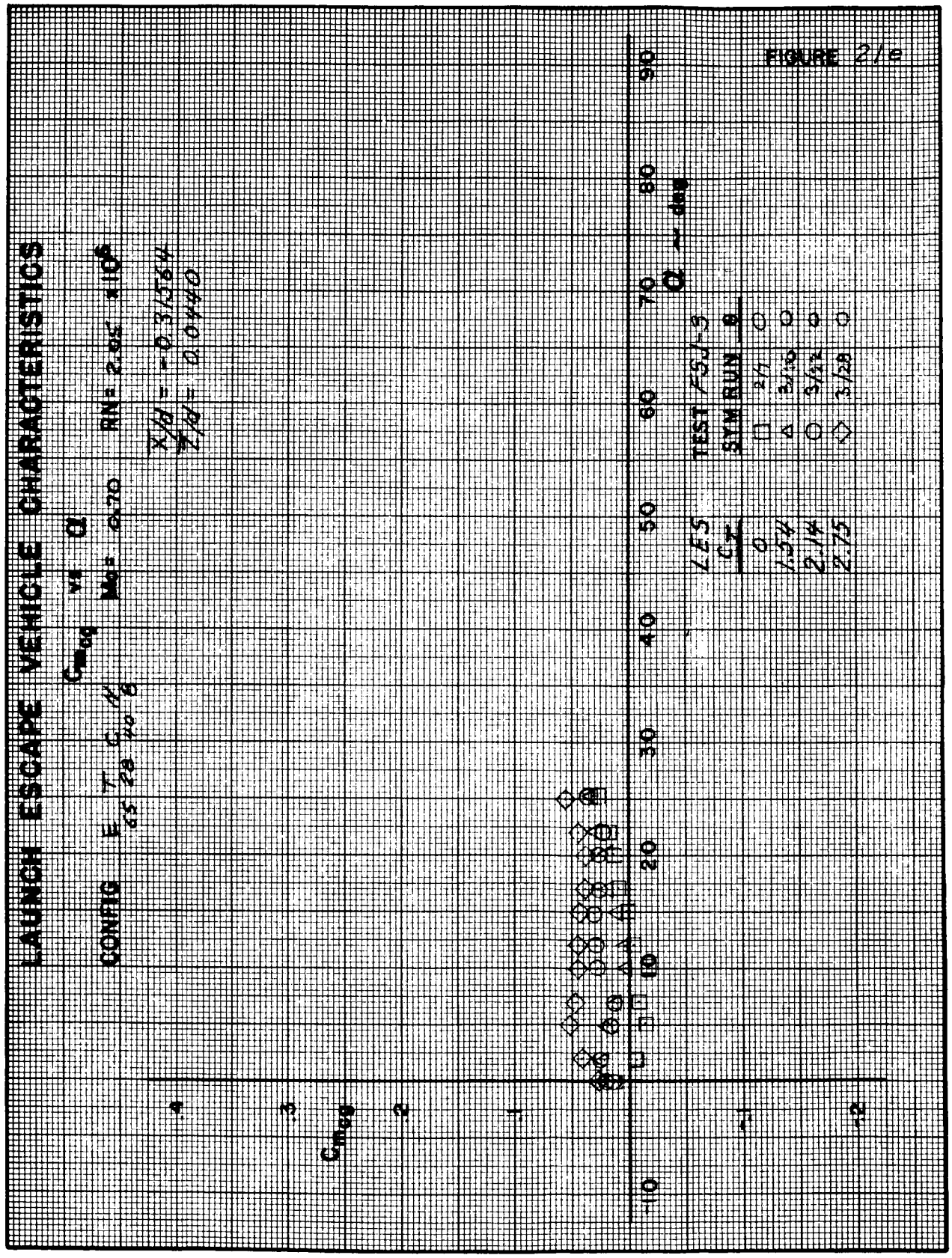

FIGURE 21e

~~CONFIDENTIAL~~

CONFIDENTIAL

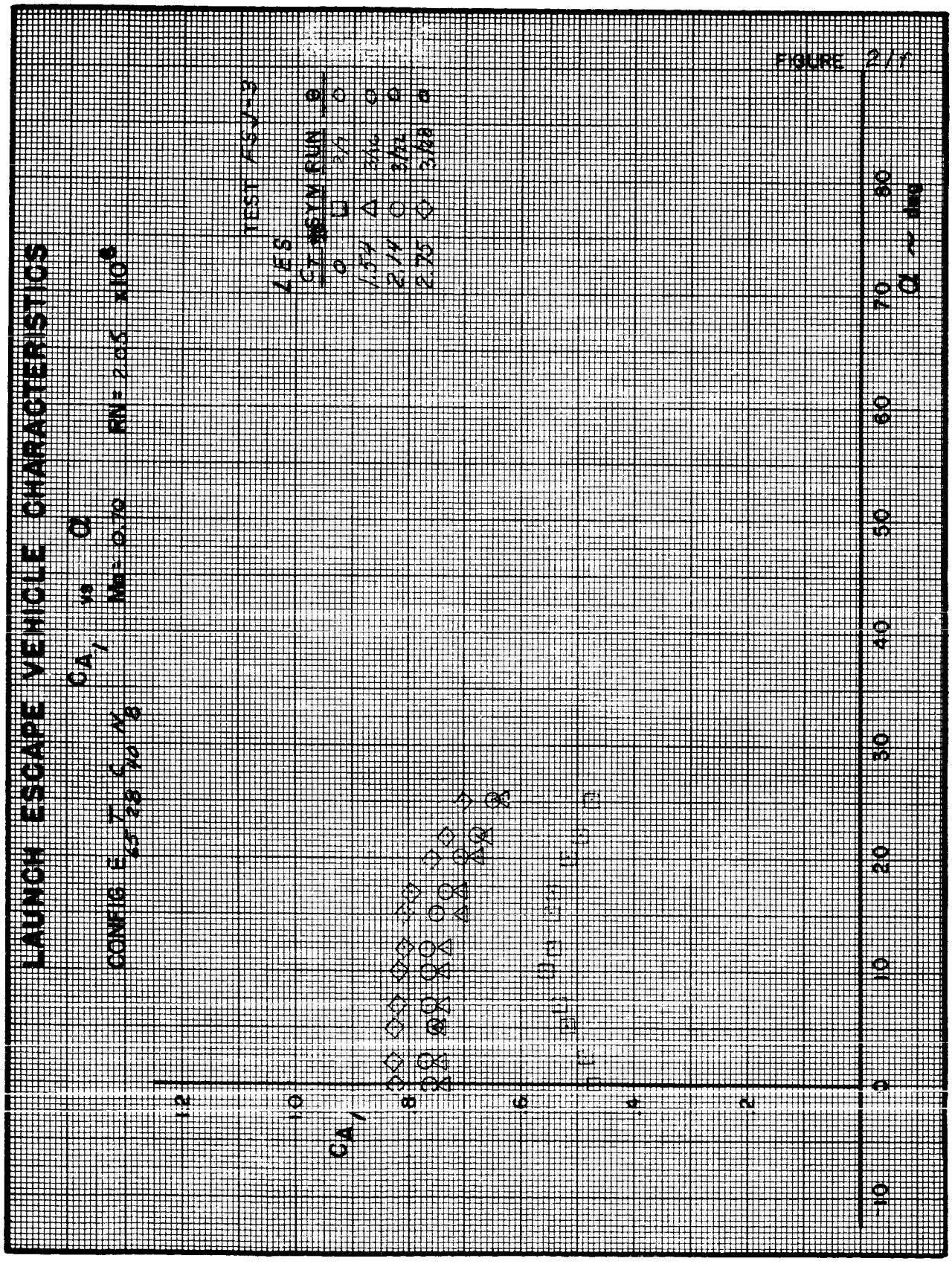

FIGURE 21

CONFIDENTIAL

~~CONFIDENTIAL~~

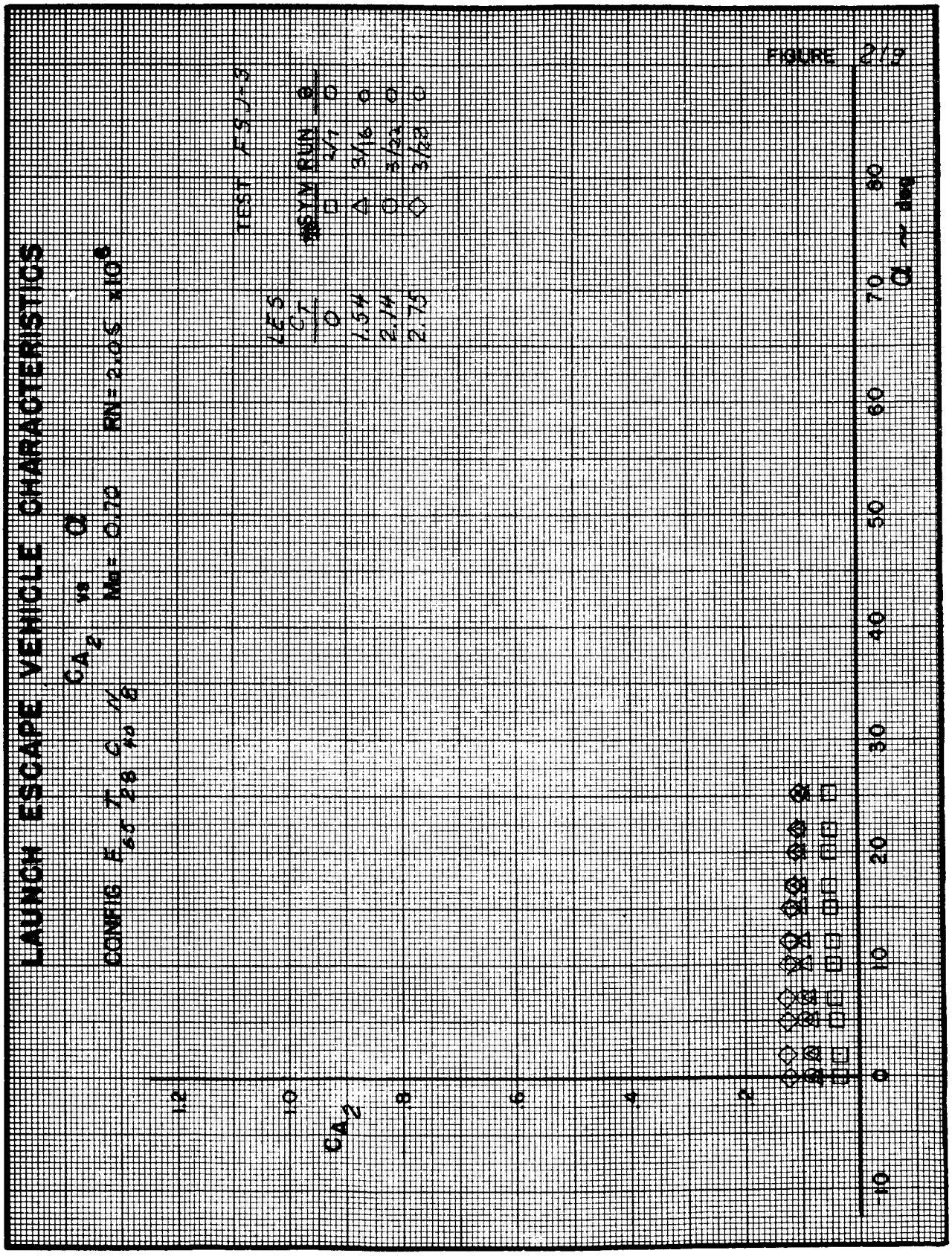

FIGURE 2/9

~~CONFIDENTIAL~~

CON[redacted]

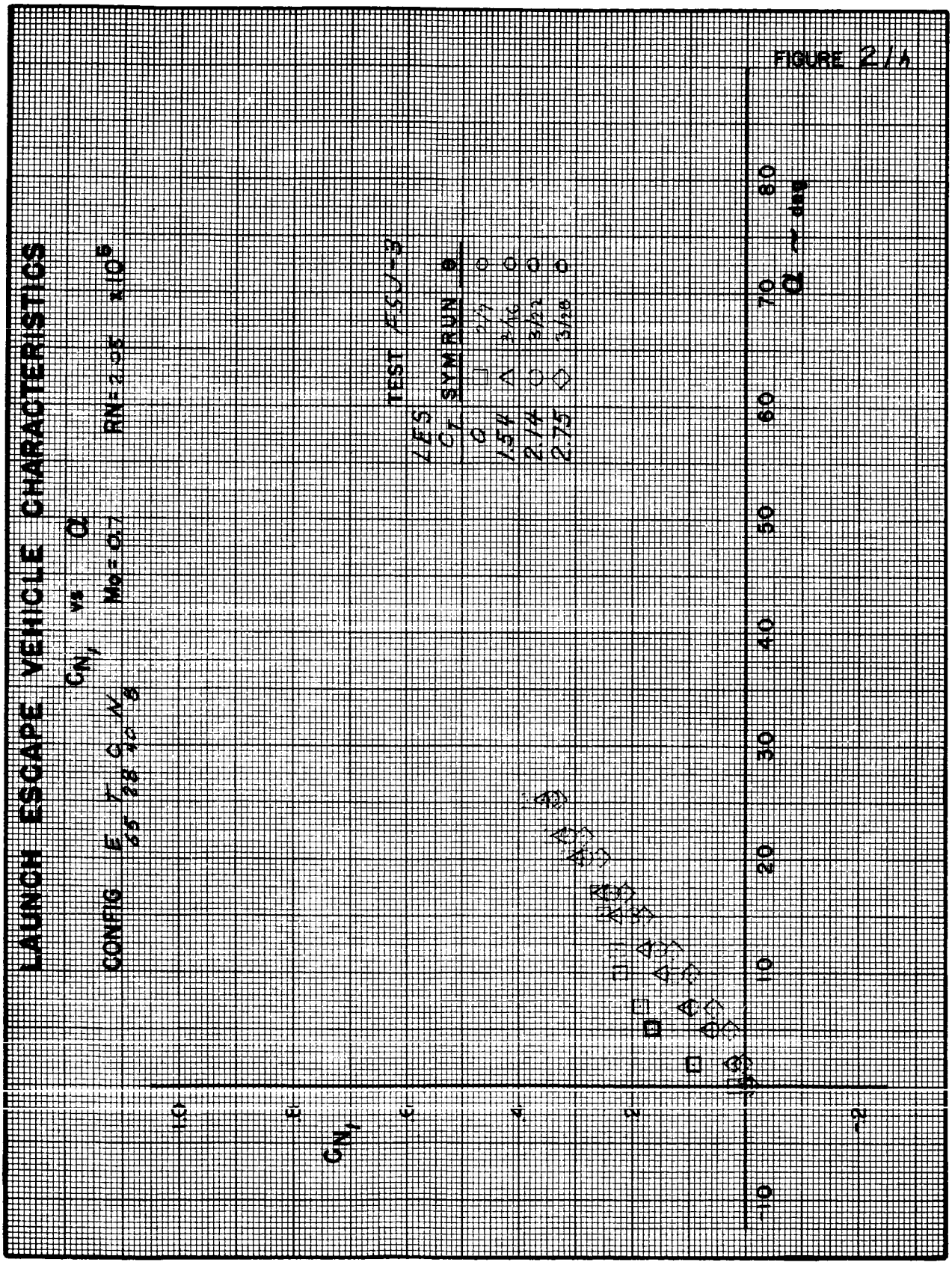

FIGURE 2/A

~~CONFIDENTIAL~~

~~CONFIDENTIAL~~

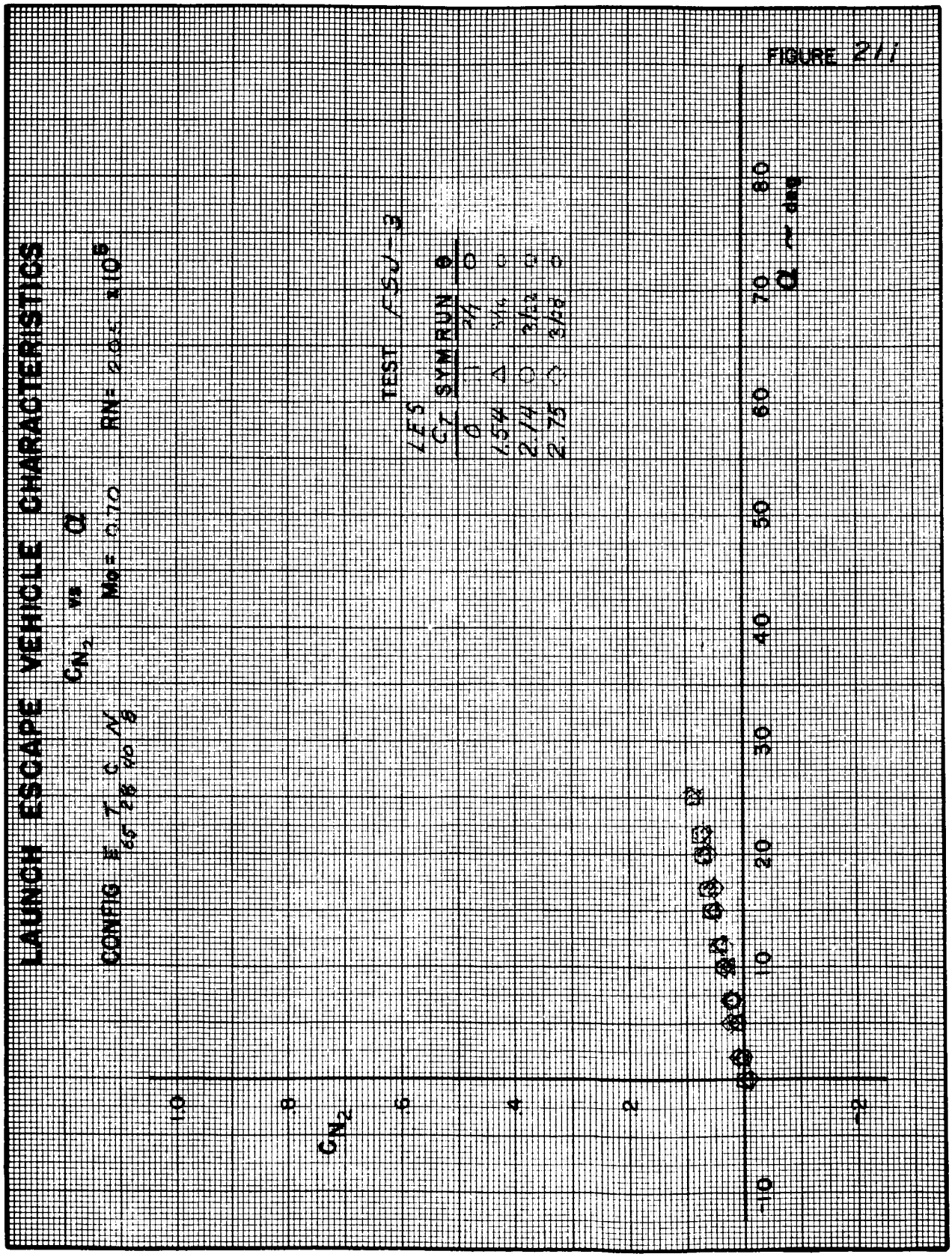

FIGURE 211

~~CONFIDENTIAL~~

CONFIDENTIAL

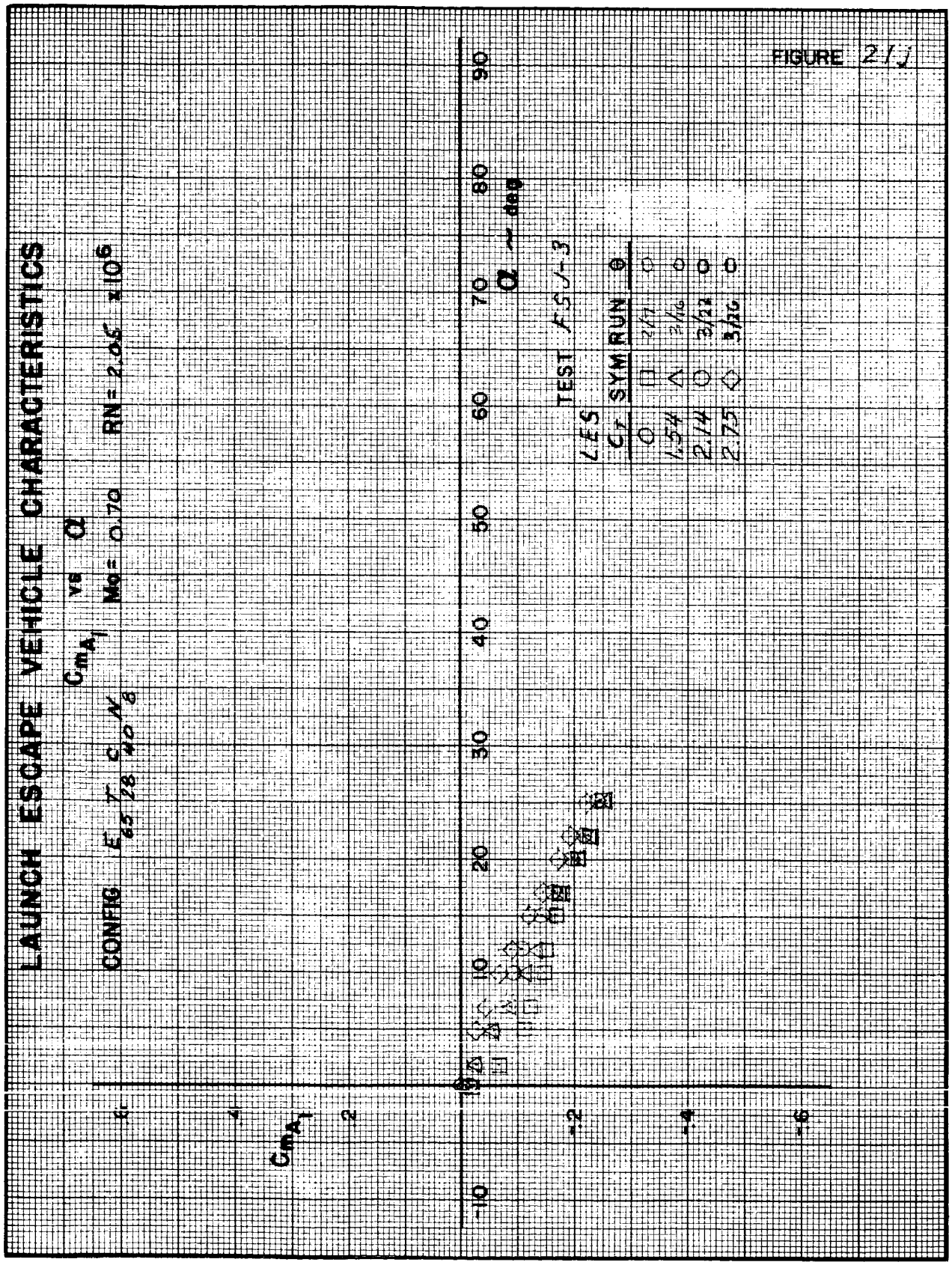

FIGURE 21

CONFIDENTIAL

~~CONFIDENTIAL~~

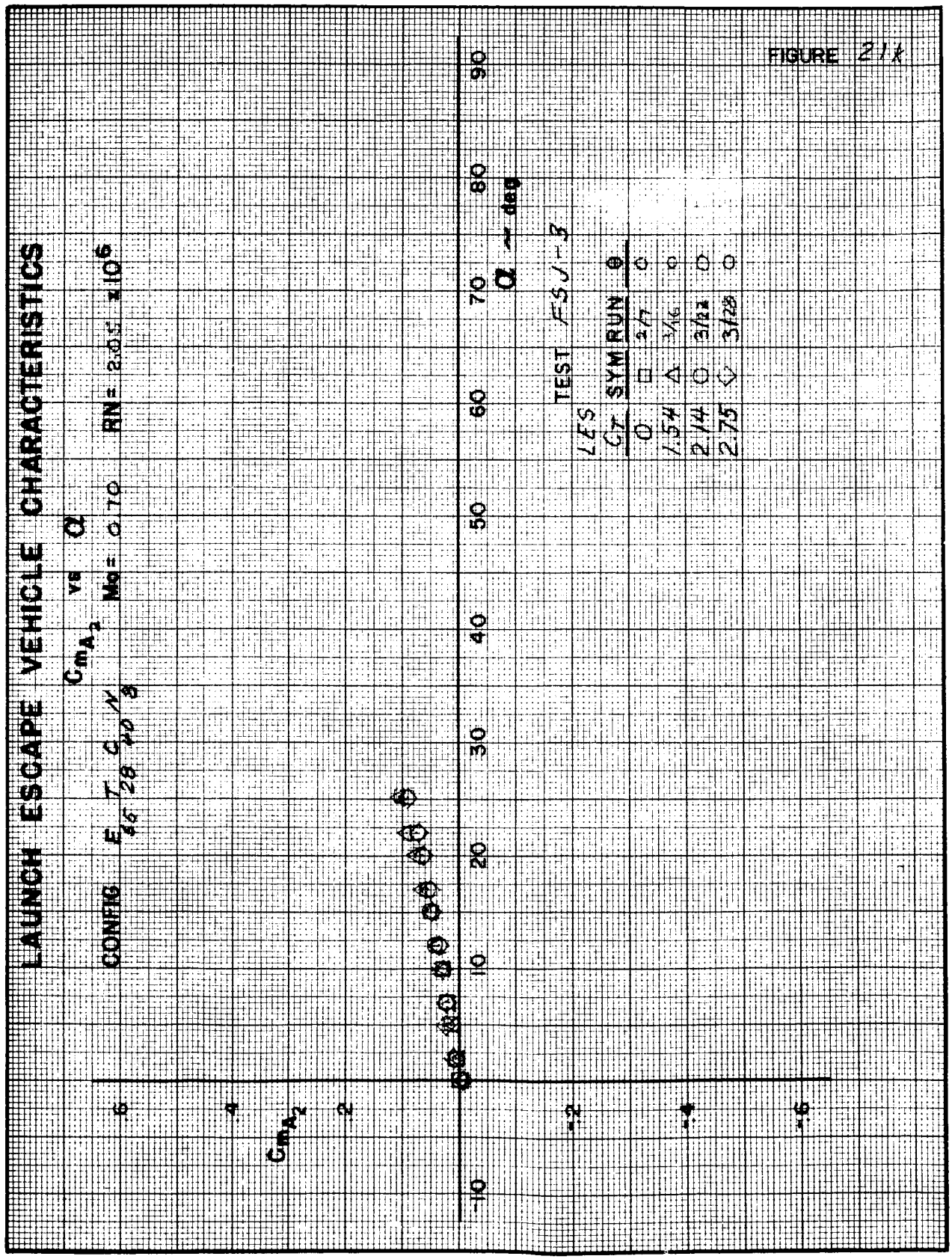

~~CONFIDENTIAL~~

CON[redacted]

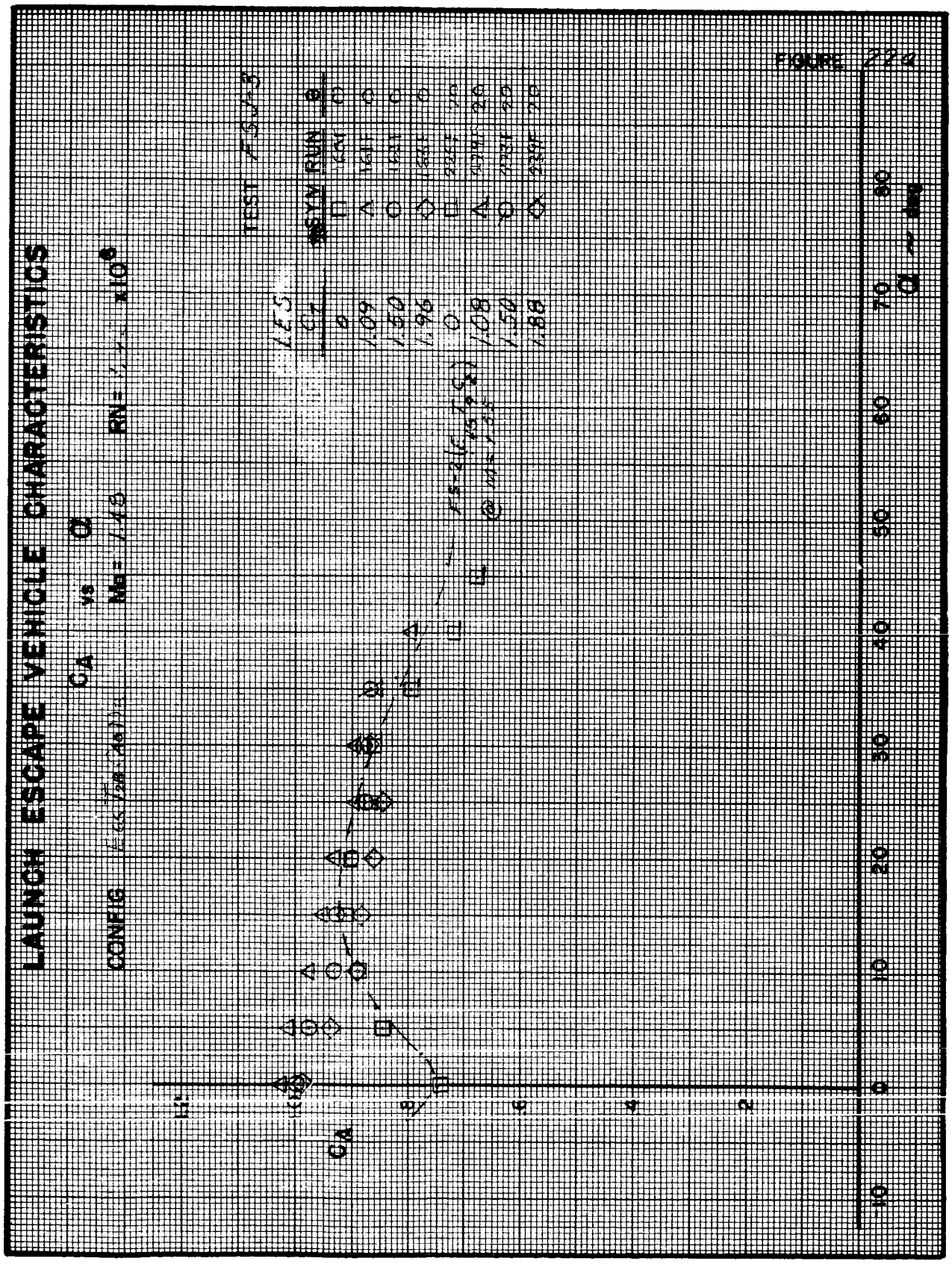

FIGURE 22a

[redacted]

~~CONFIDENTIAL~~

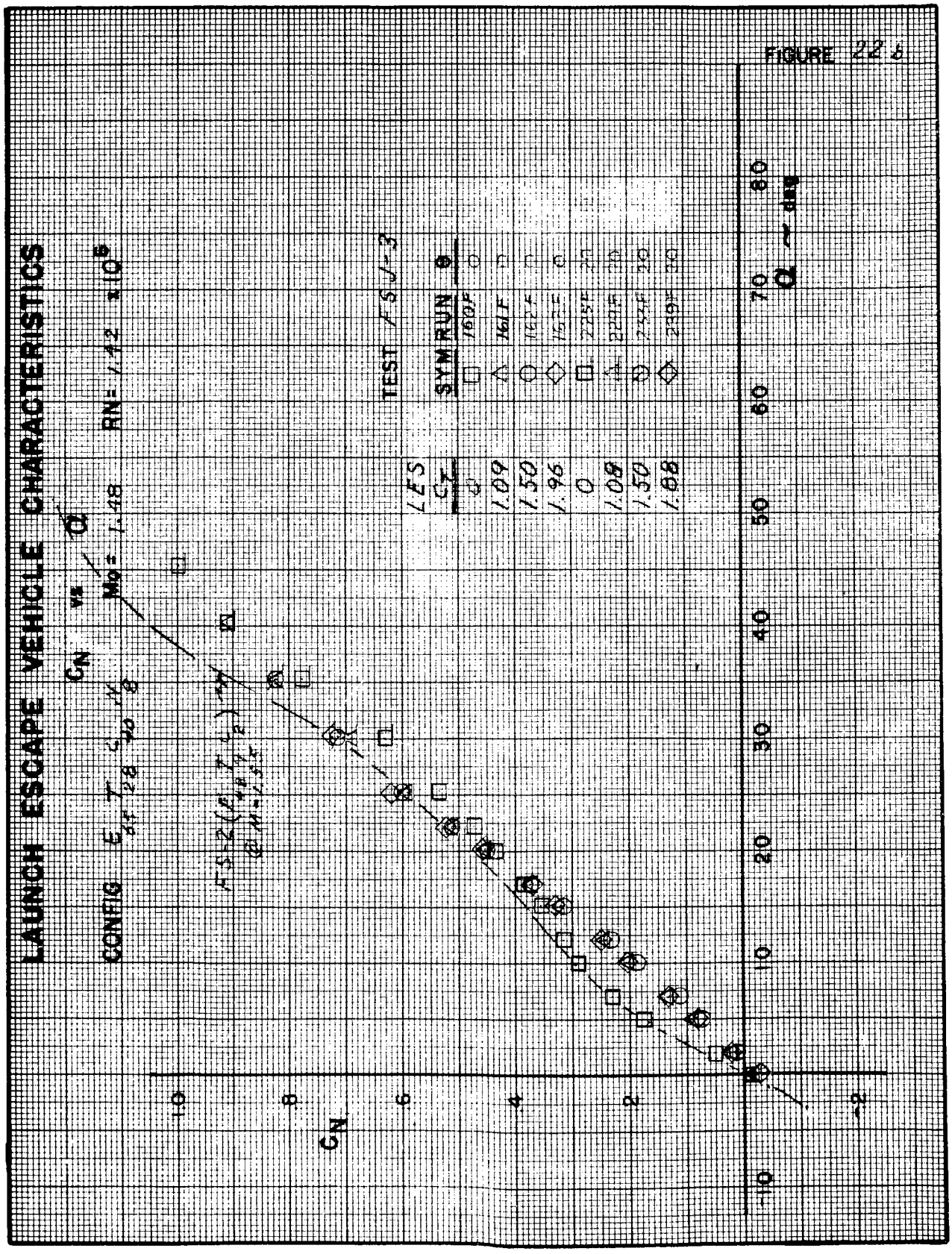

FIGURE 22.8

~~CONFIDENTIAL~~

CONFIDENTIAL

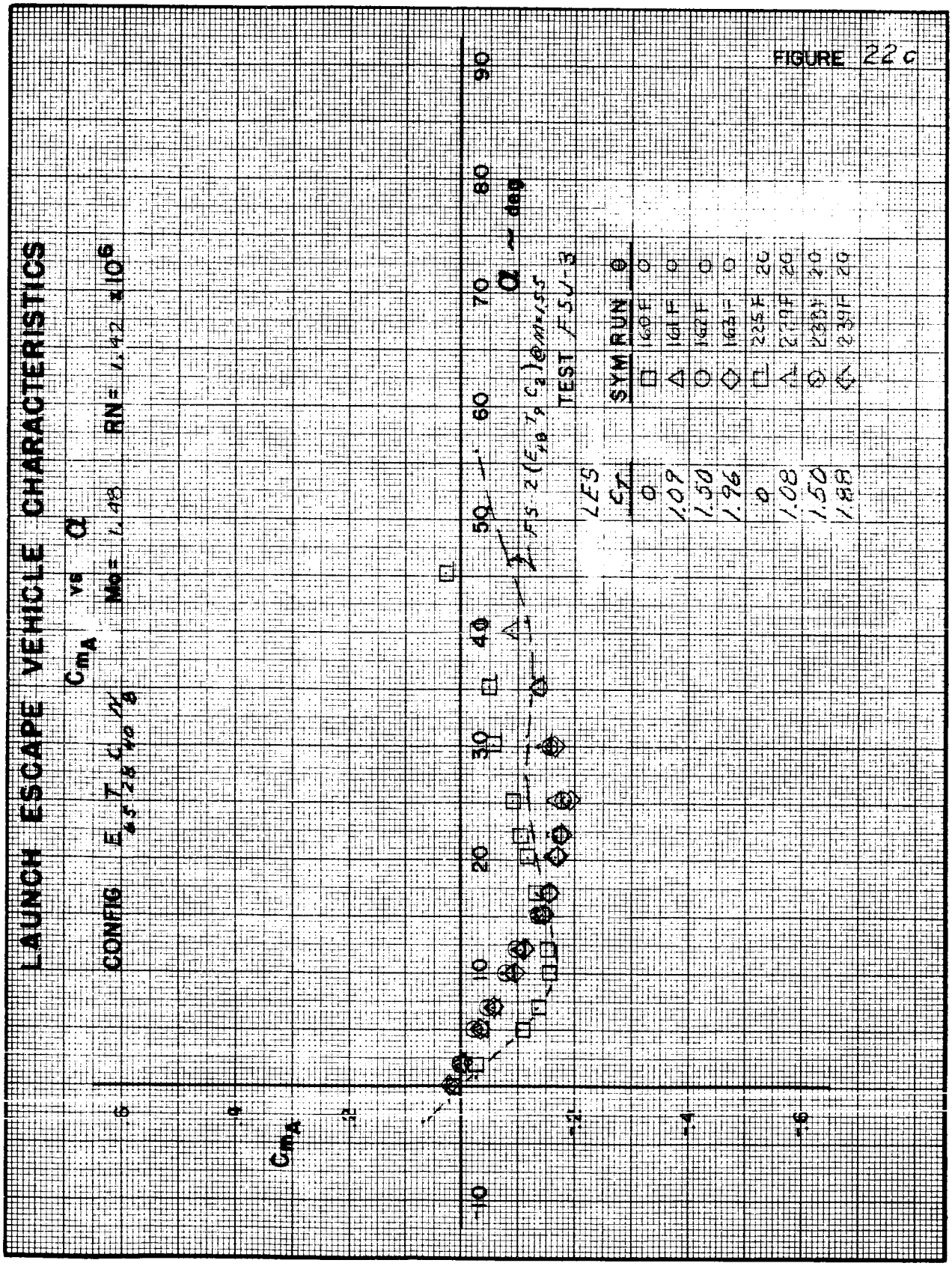

FIGURE 22c

CONFIDENTIAL

~~CONFIDENTIAL~~

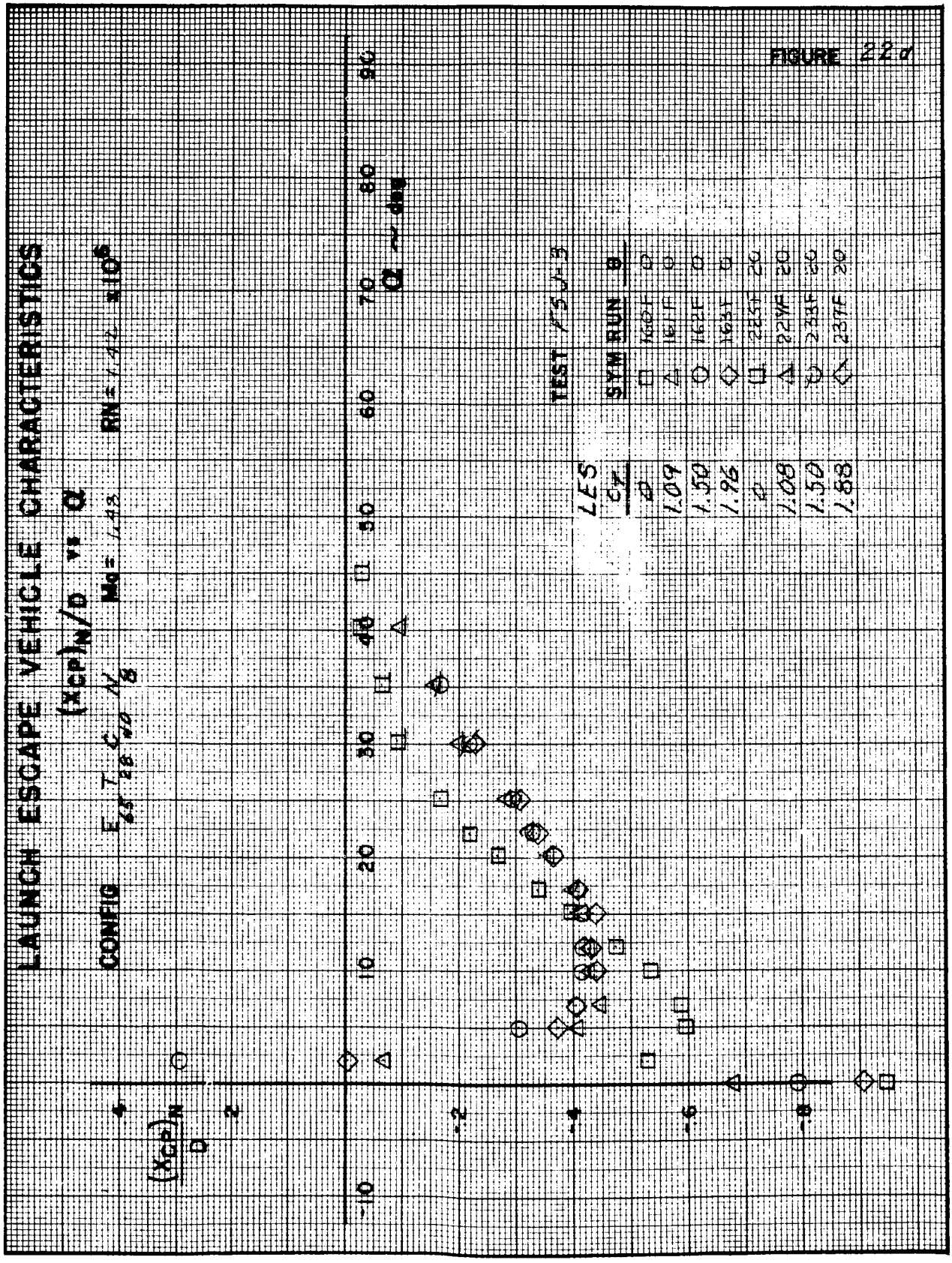

FIGURE 22d

~~CONFIDENTIAL~~

CO[redacted]

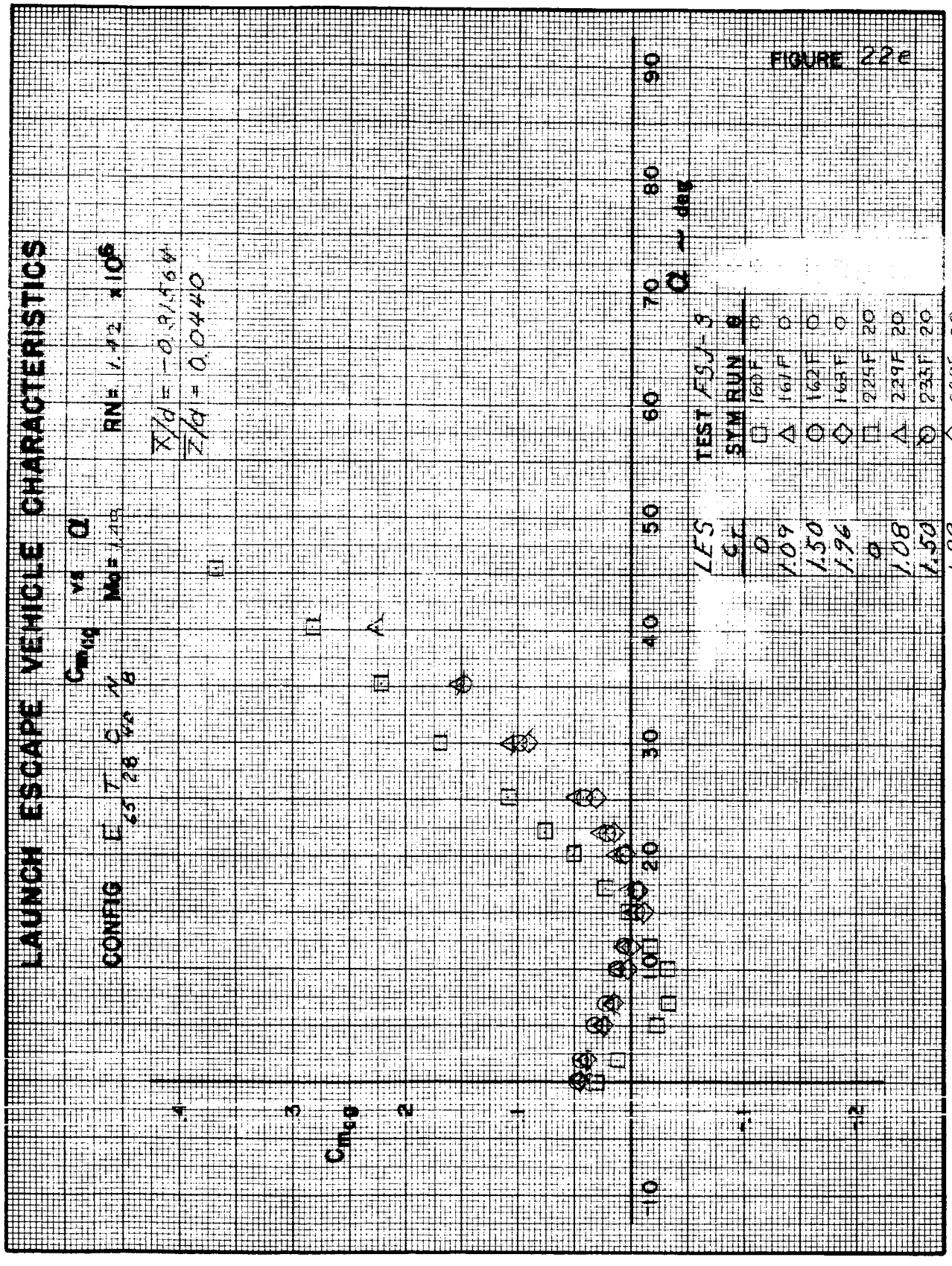

[redacted]

~~CONFIDENTIAL~~

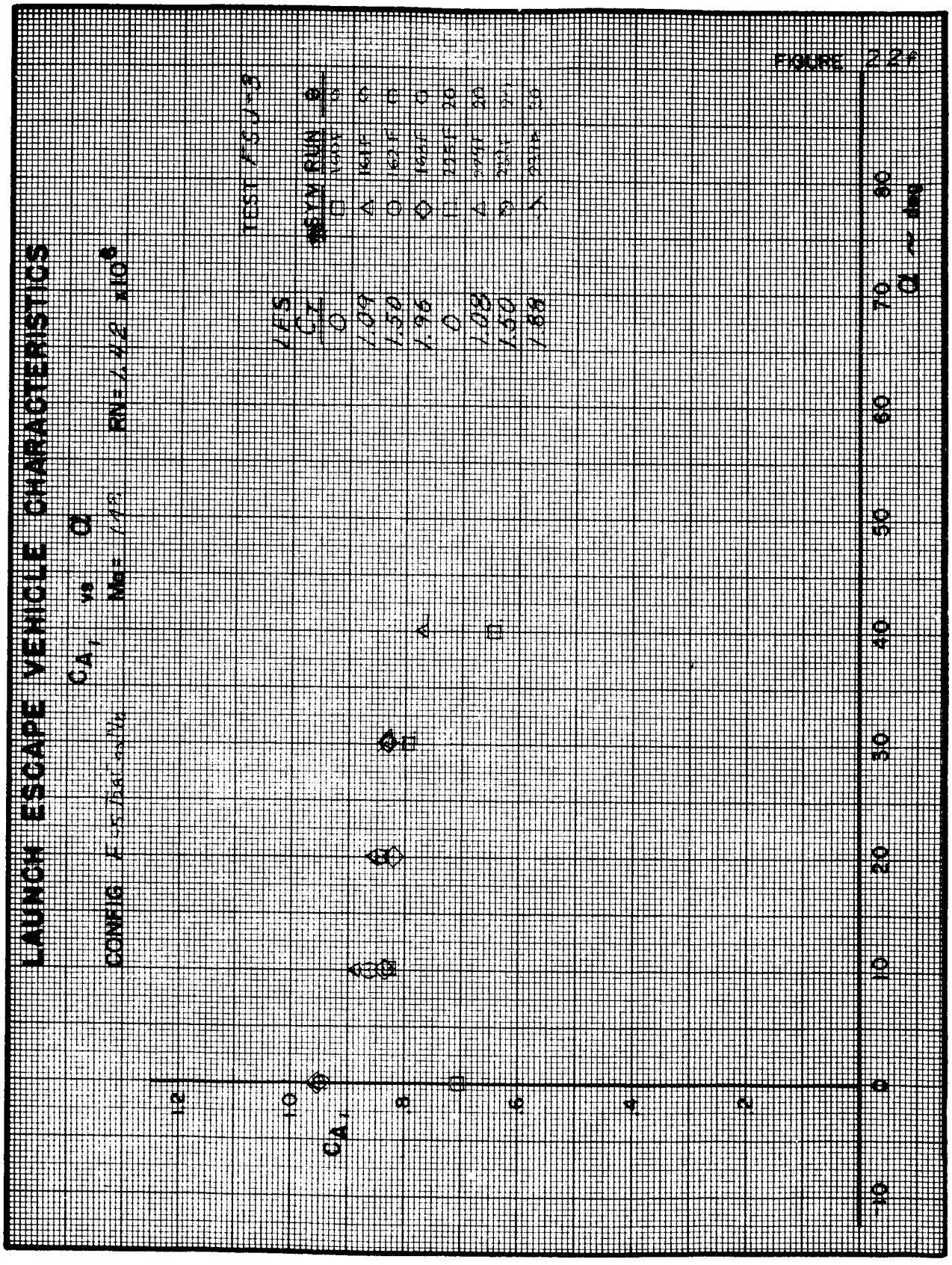

FIGURE 22

~~CONFIDENTIAL~~

CO[redacted]

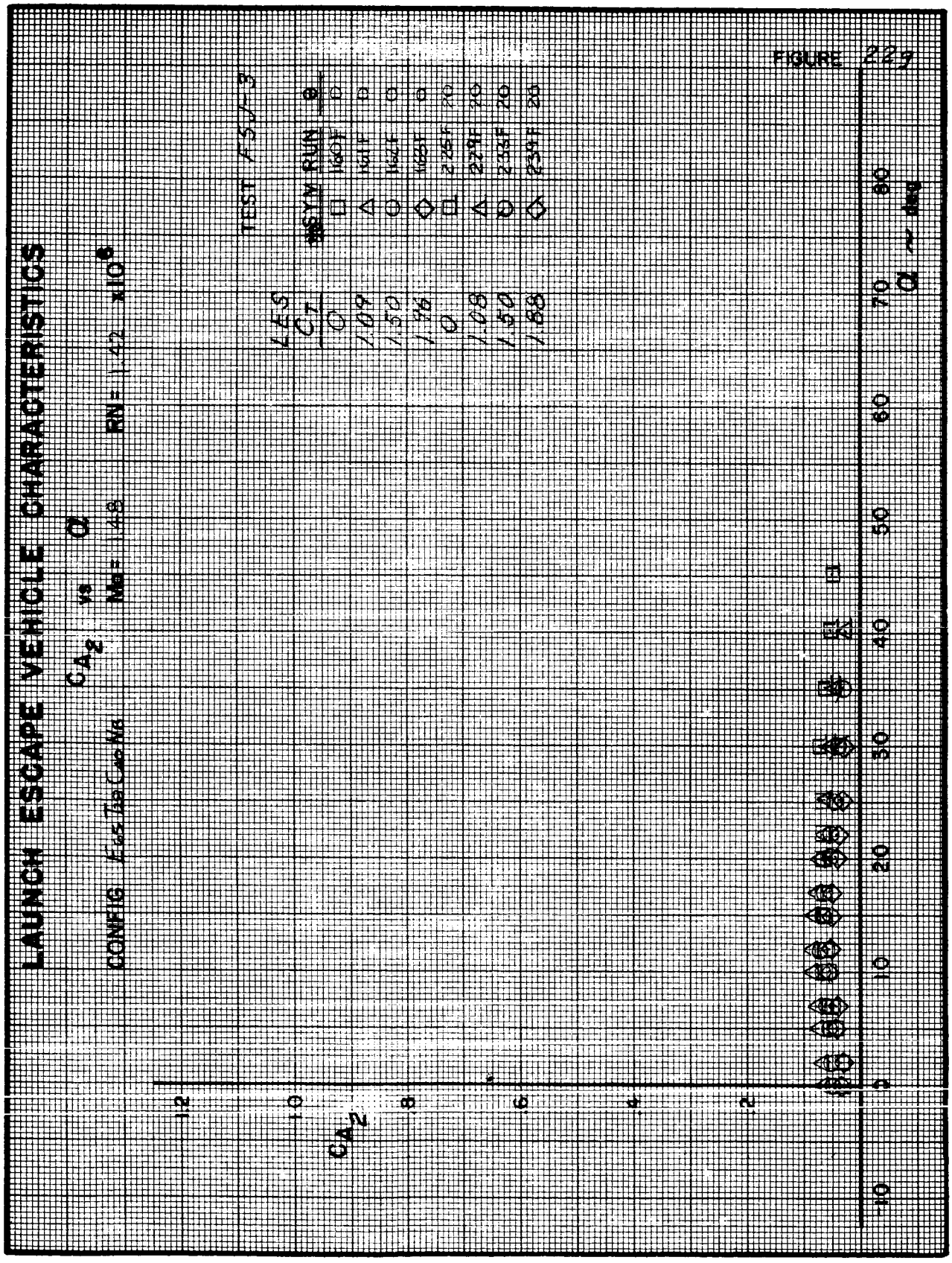

[redacted]

~~CONFIDENTIAL~~

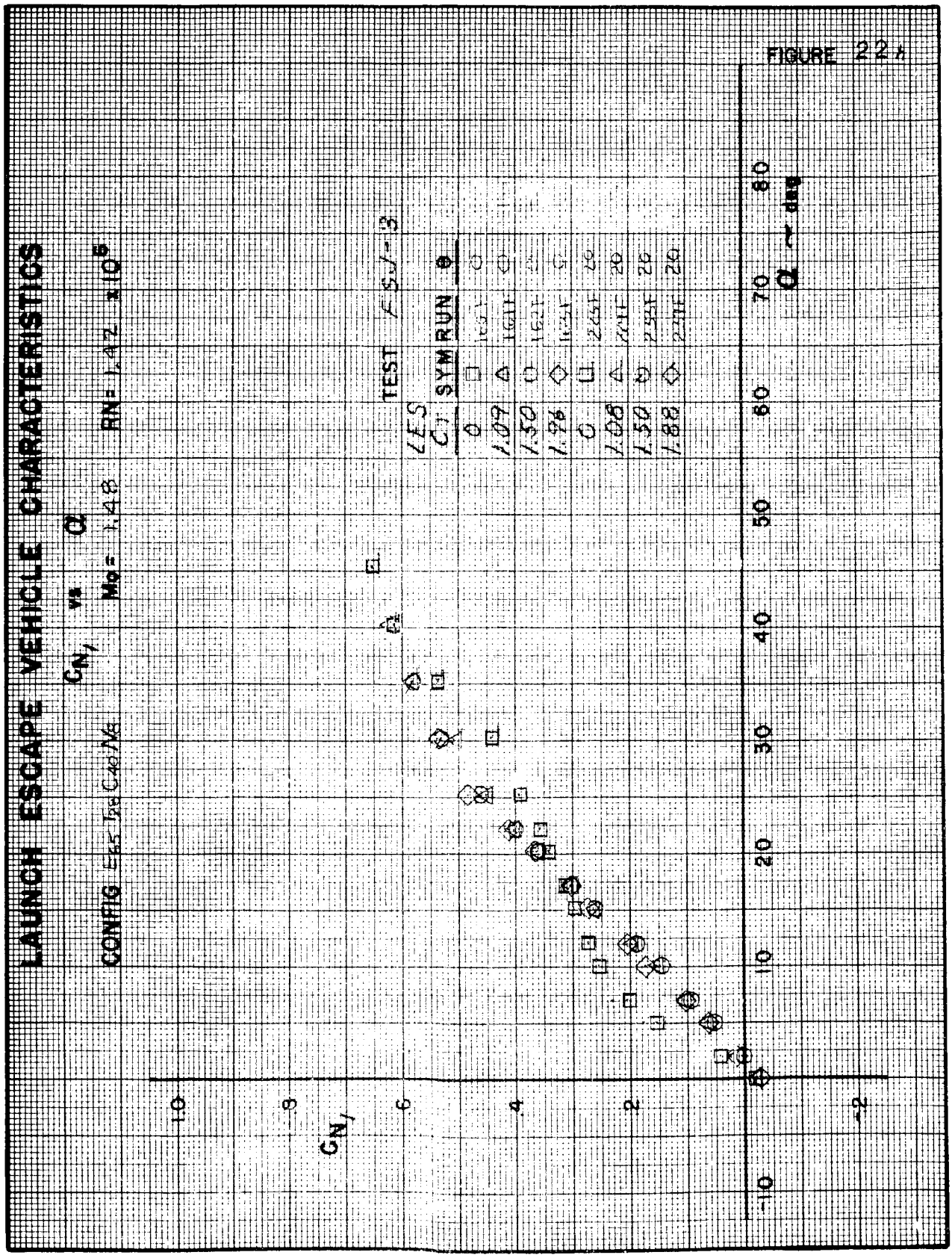

FIGURE 22 h

~~CONFIDENTIAL~~

CONFIDENTIAL

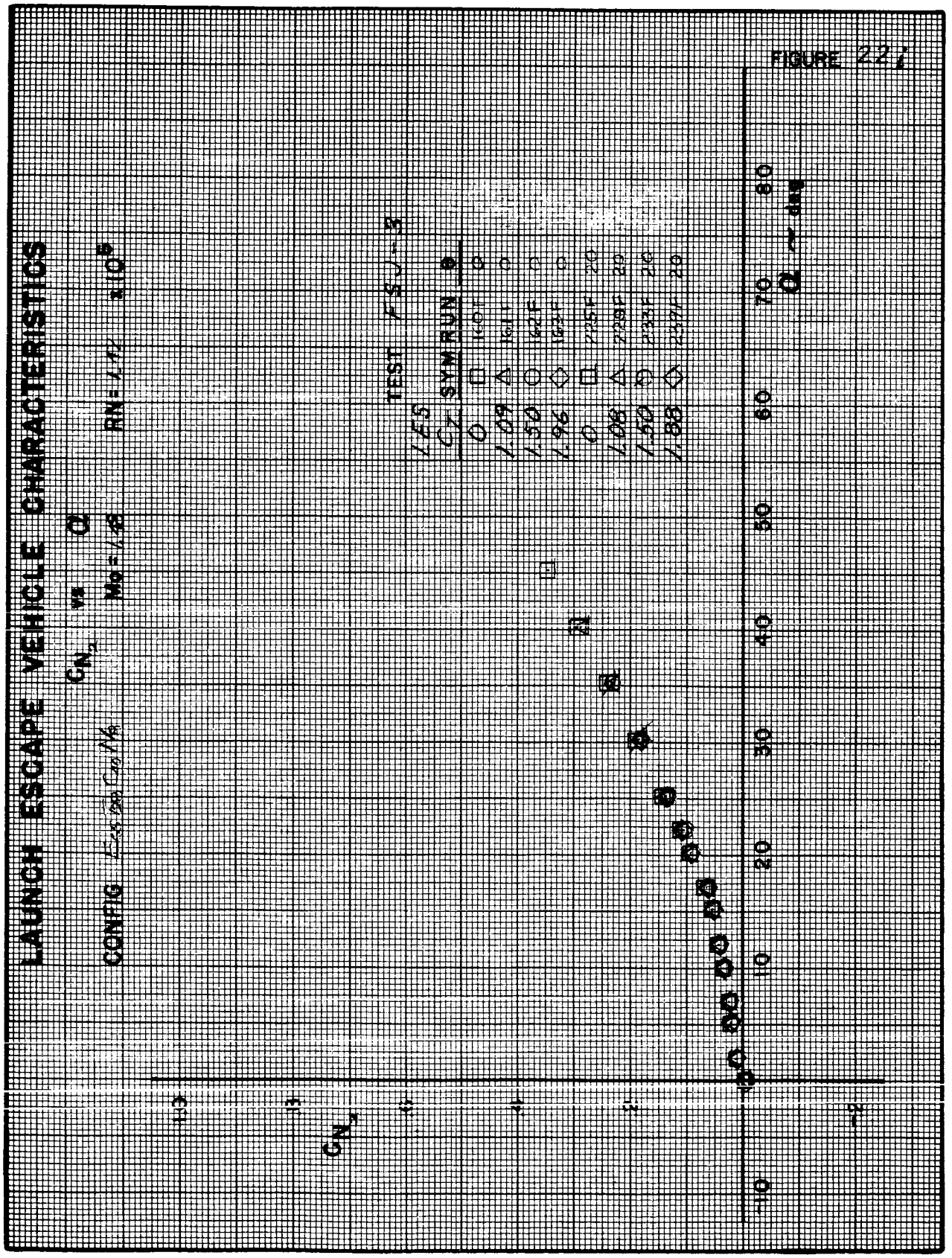

FIGURE 22

CONFIDENTIAL

~~CONFIDENTIAL~~

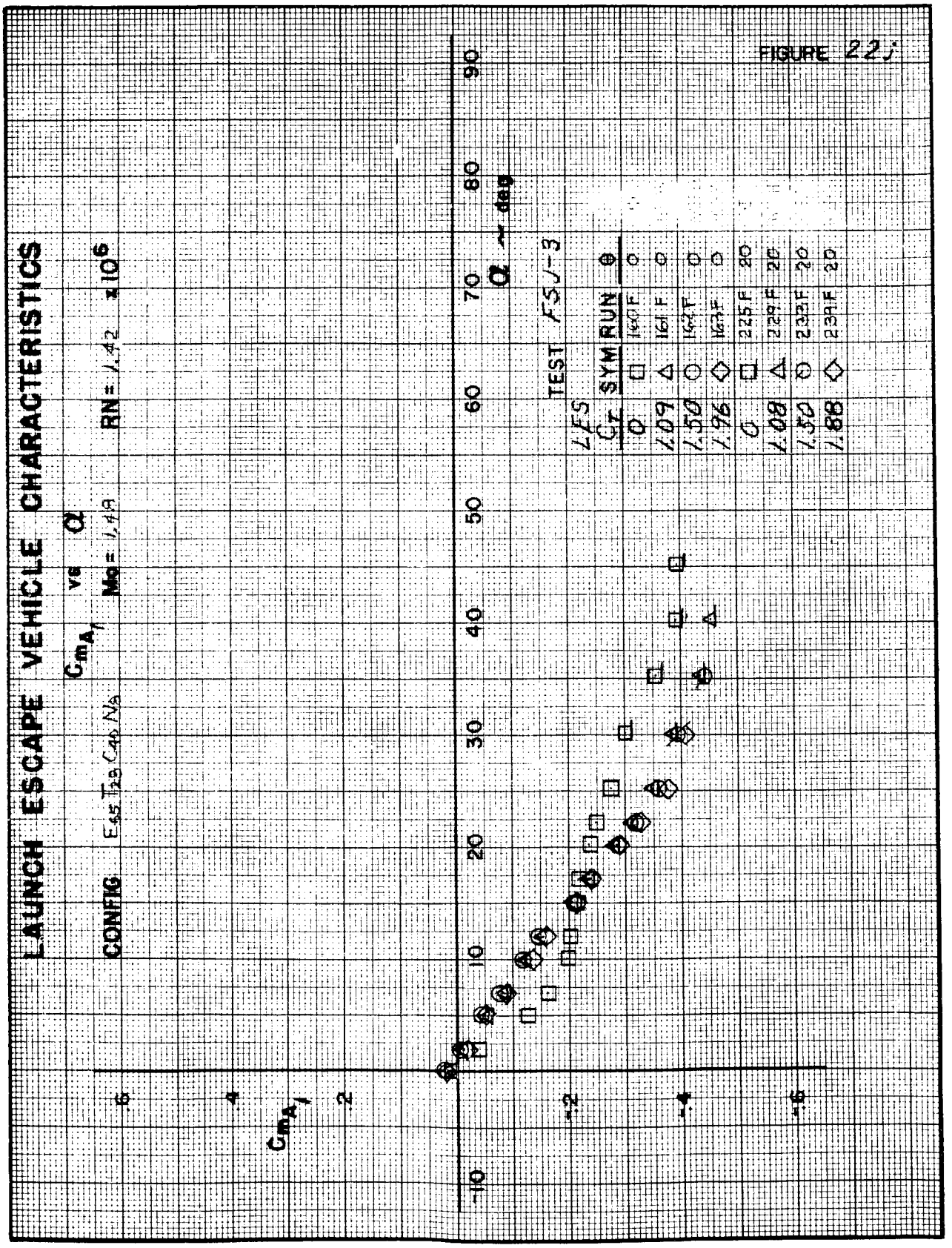

FIGURE 22.

~~CONFIDENTIAL~~

CO[redacted]

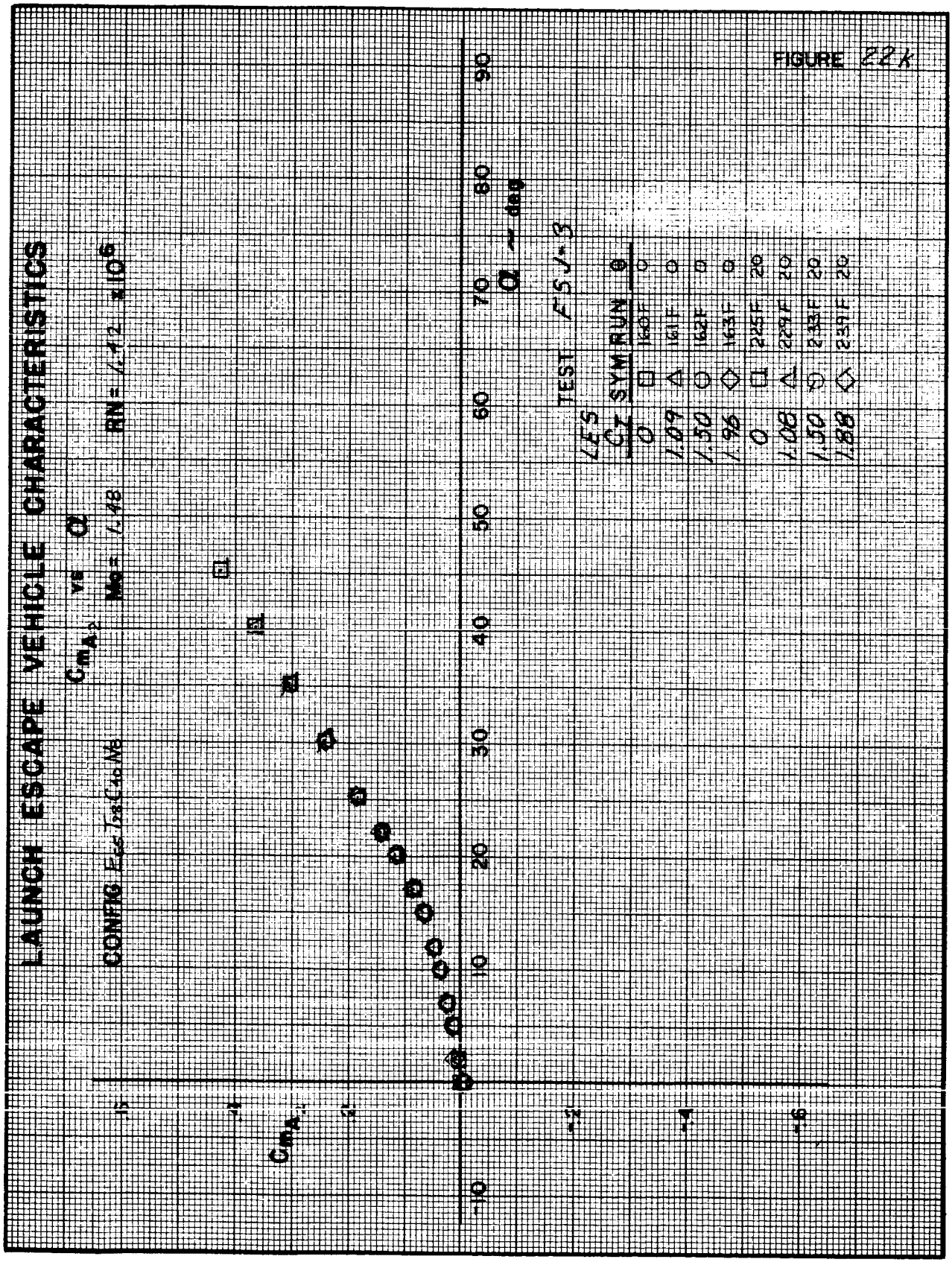

[redacted]

~~CONFIDENTIAL~~

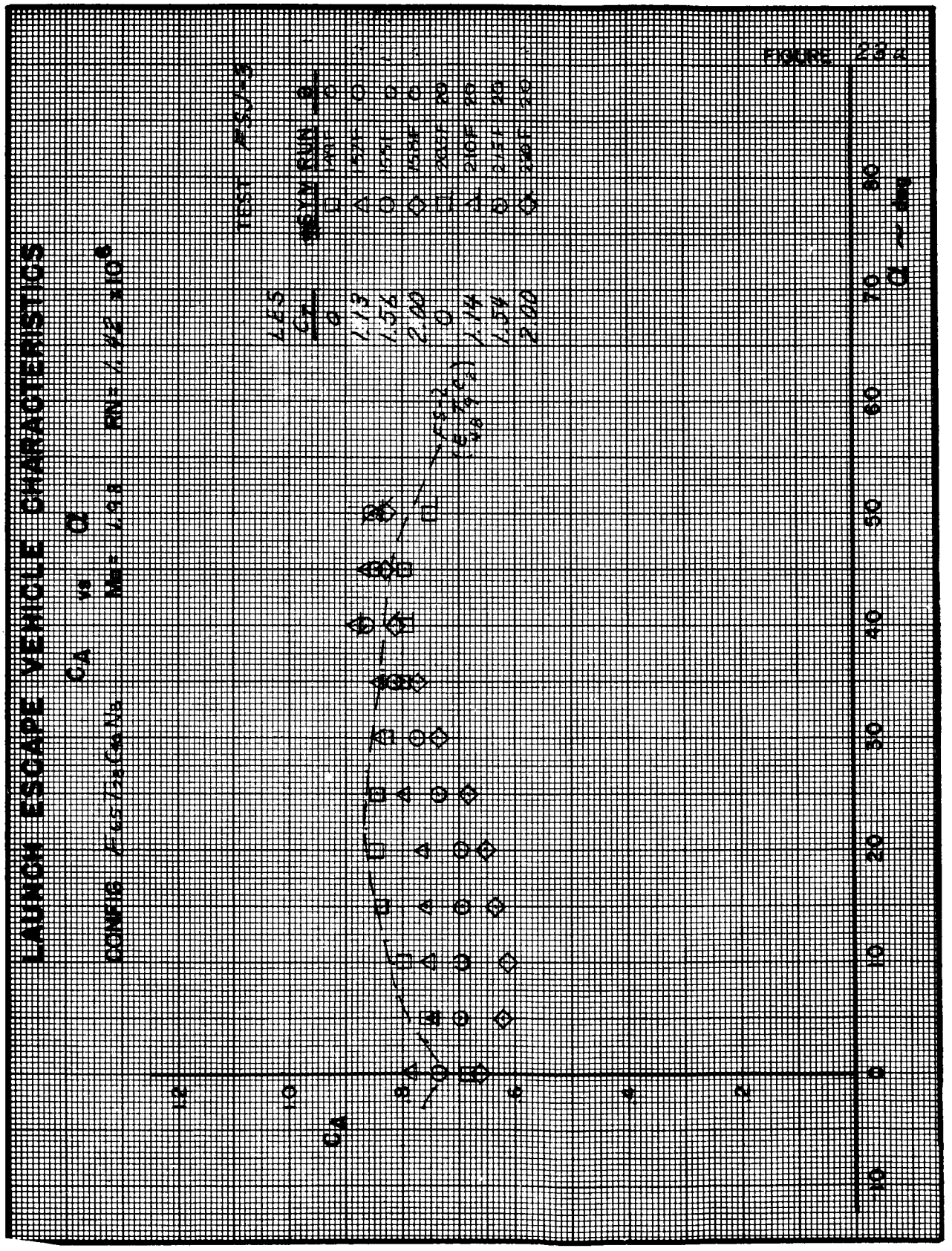

FIGURE 23a

~~CONFIDENTIAL~~

CON[redacted]

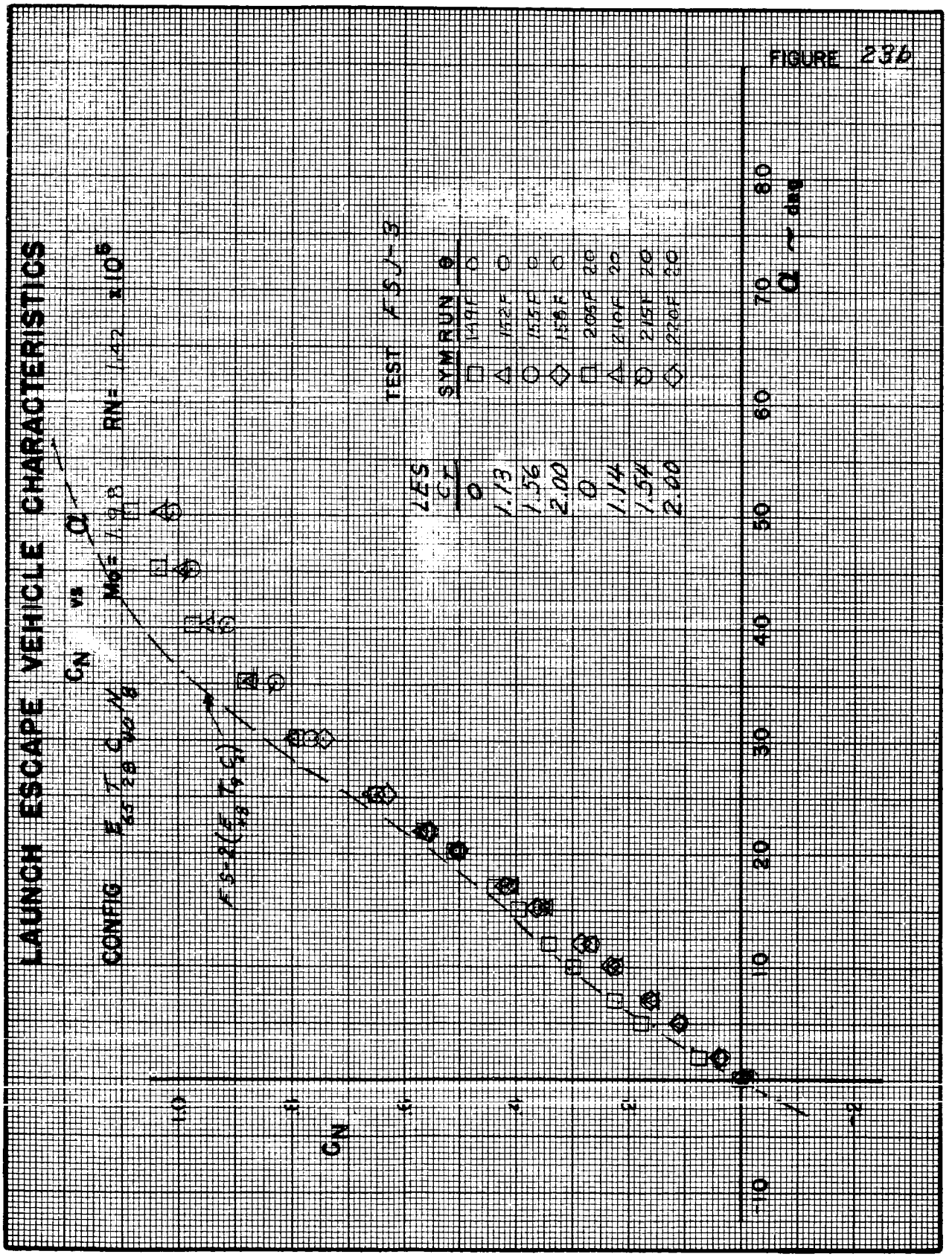

FIGURE 23b

~~CONFIDENTIAL~~

~~CONFIDENTIAL~~

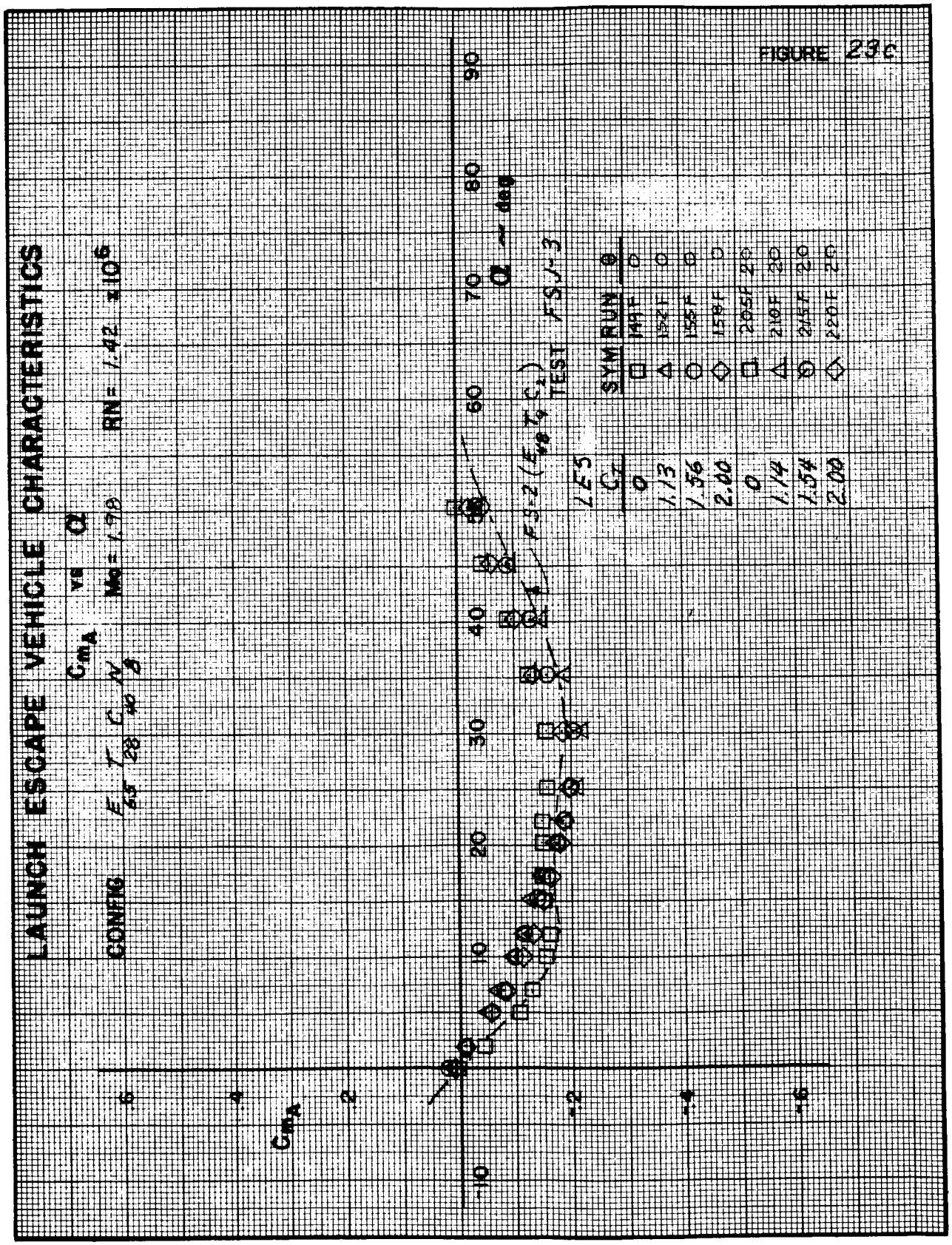

FIGURE 23c

~~CONFIDENTIAL~~

CO[redacted]

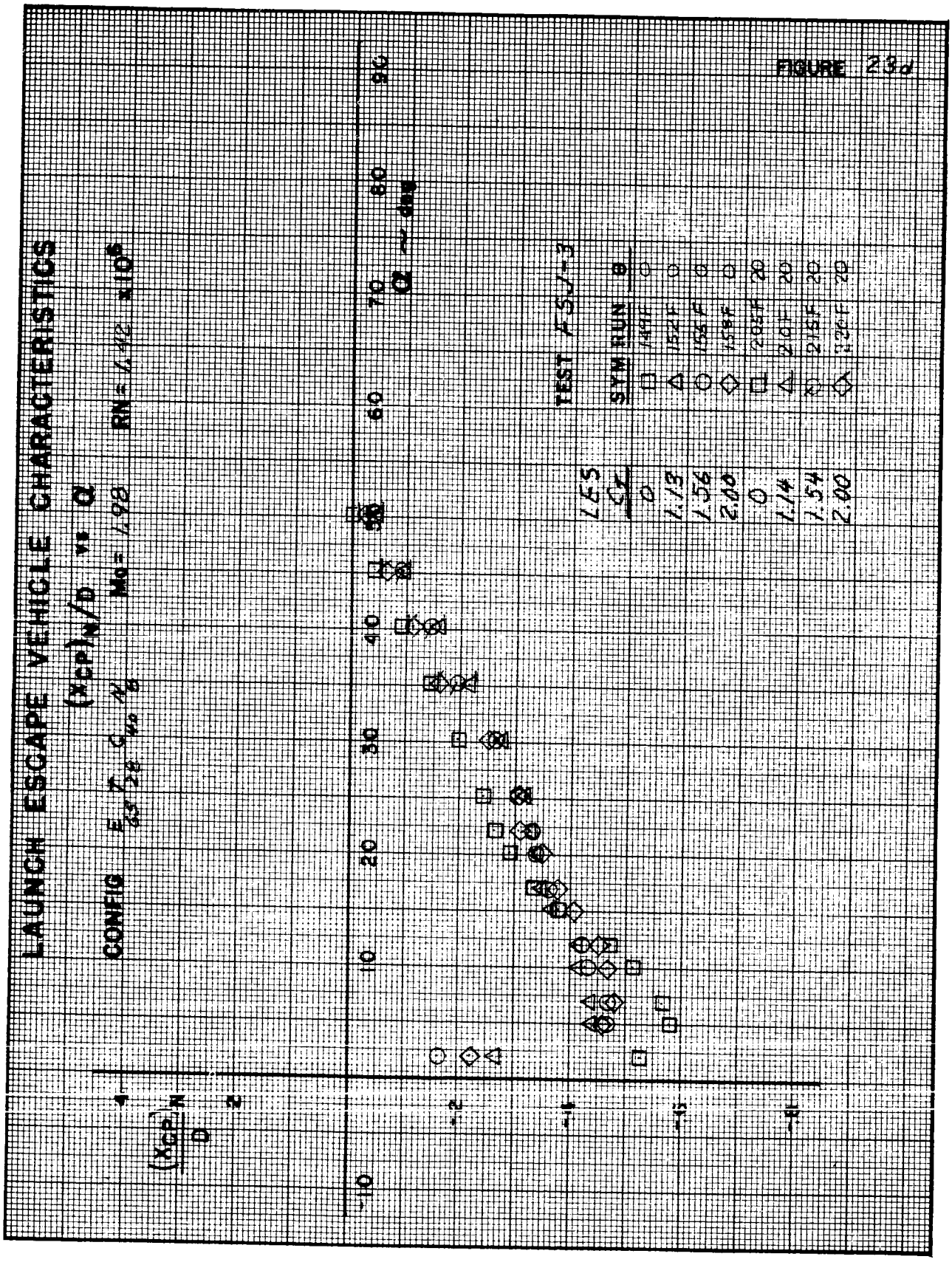

FIGURE 23d

[redacted]

~~CONFIDENTIAL~~

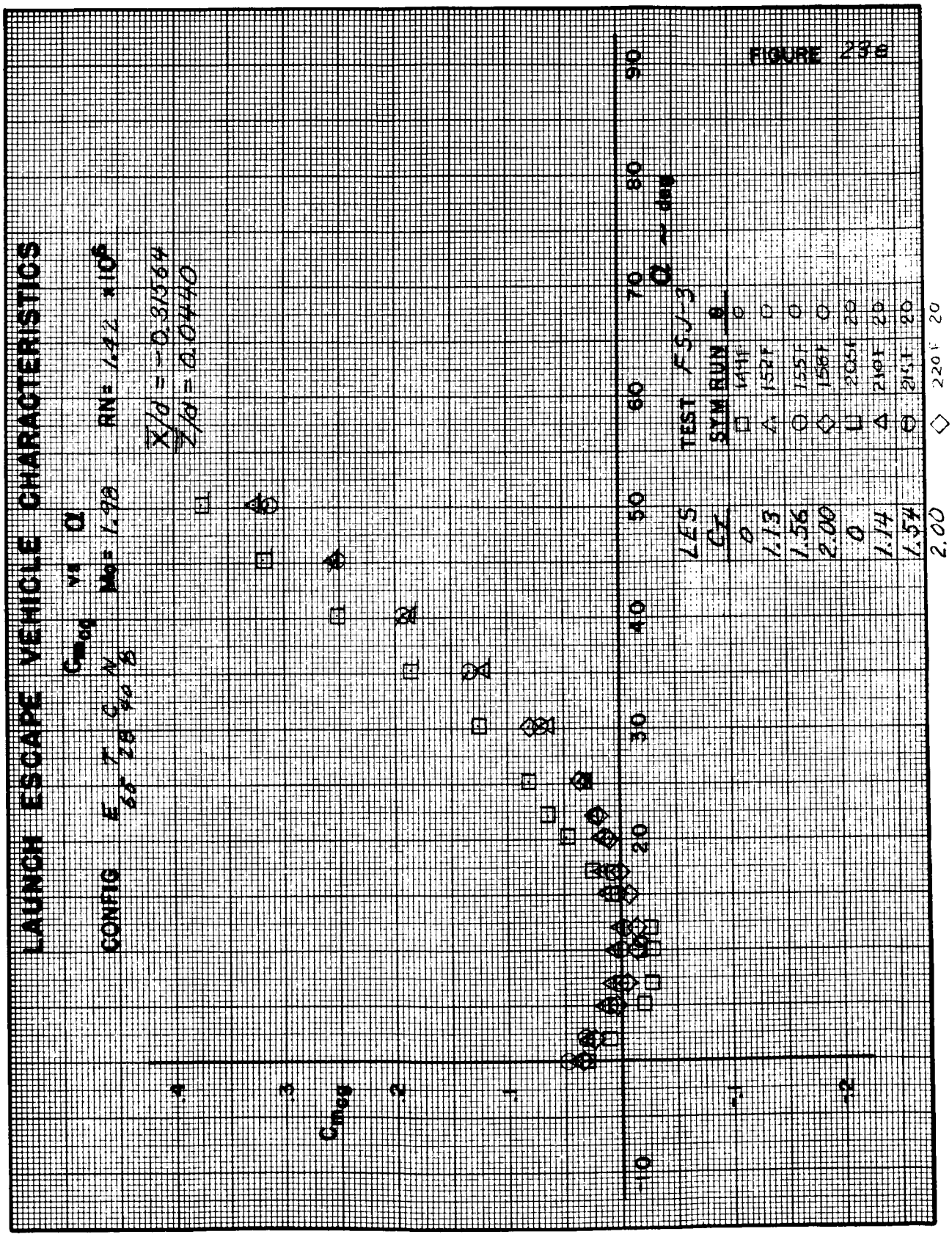

~~CONFIDENTIAL~~

CON[redacted]

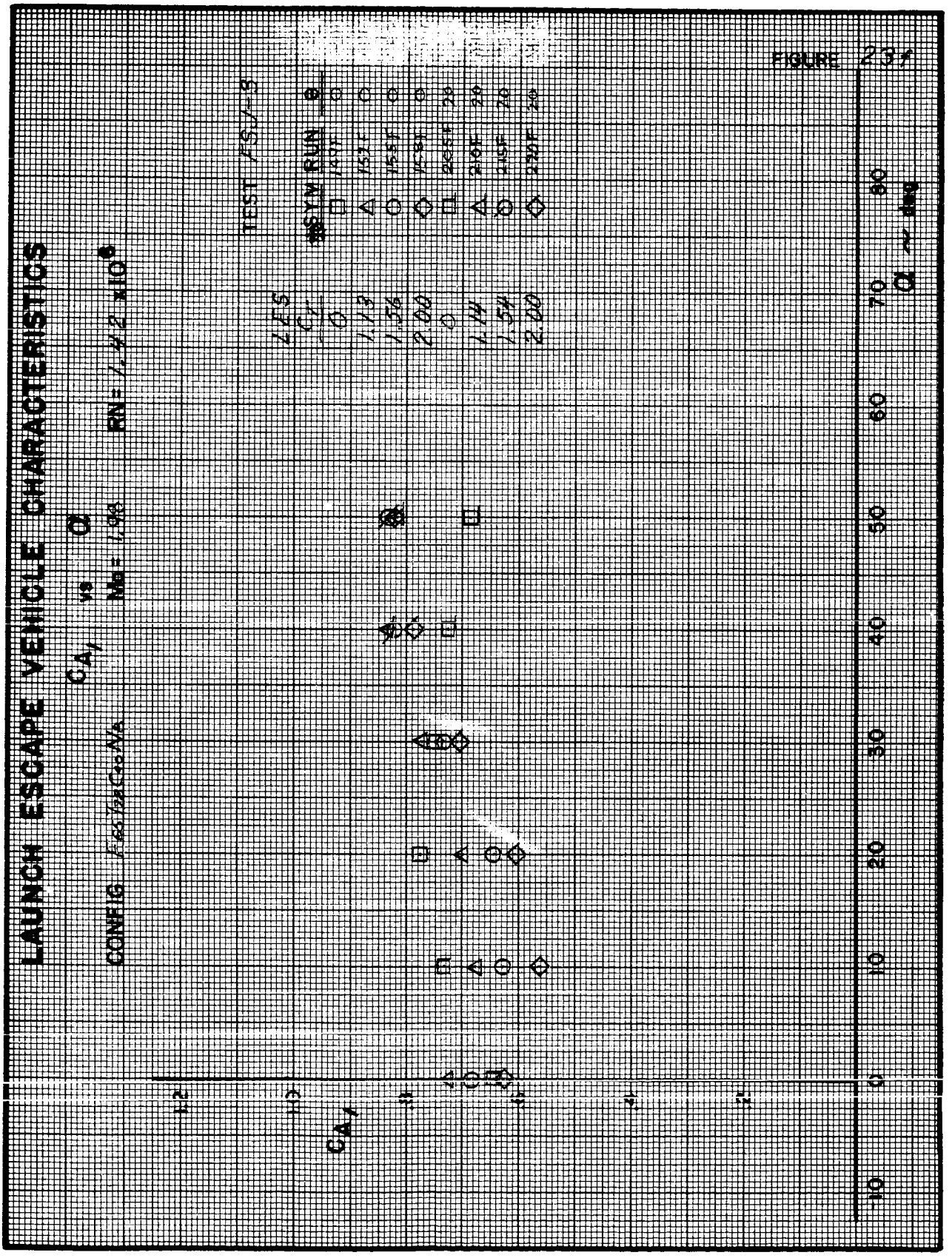

FIGURE 23f

CONFIDENTIAL

~~CONFIDENTIAL~~

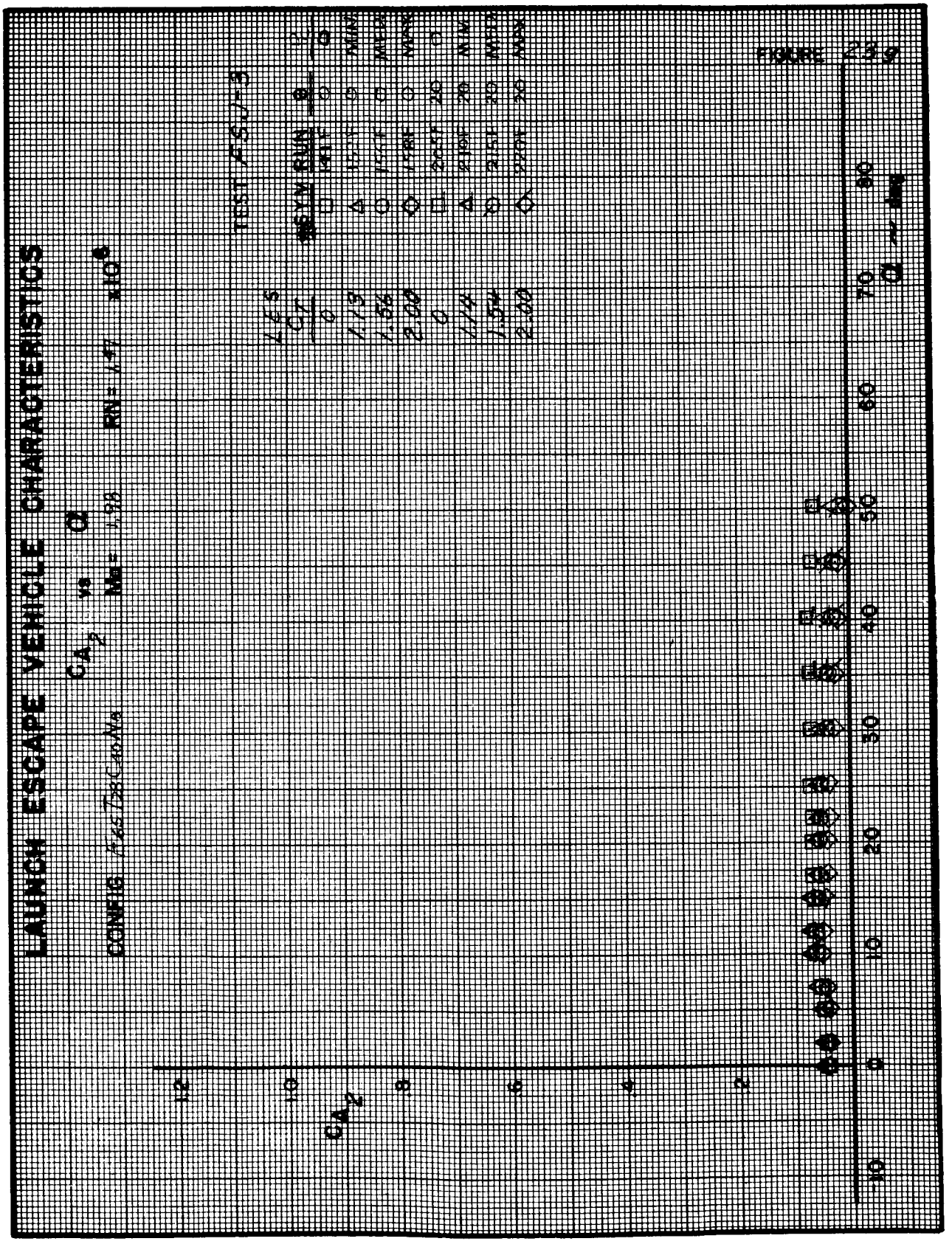

FIGURE 23.9

~~CONFIDENTIAL~~

CONFIDENTIAL

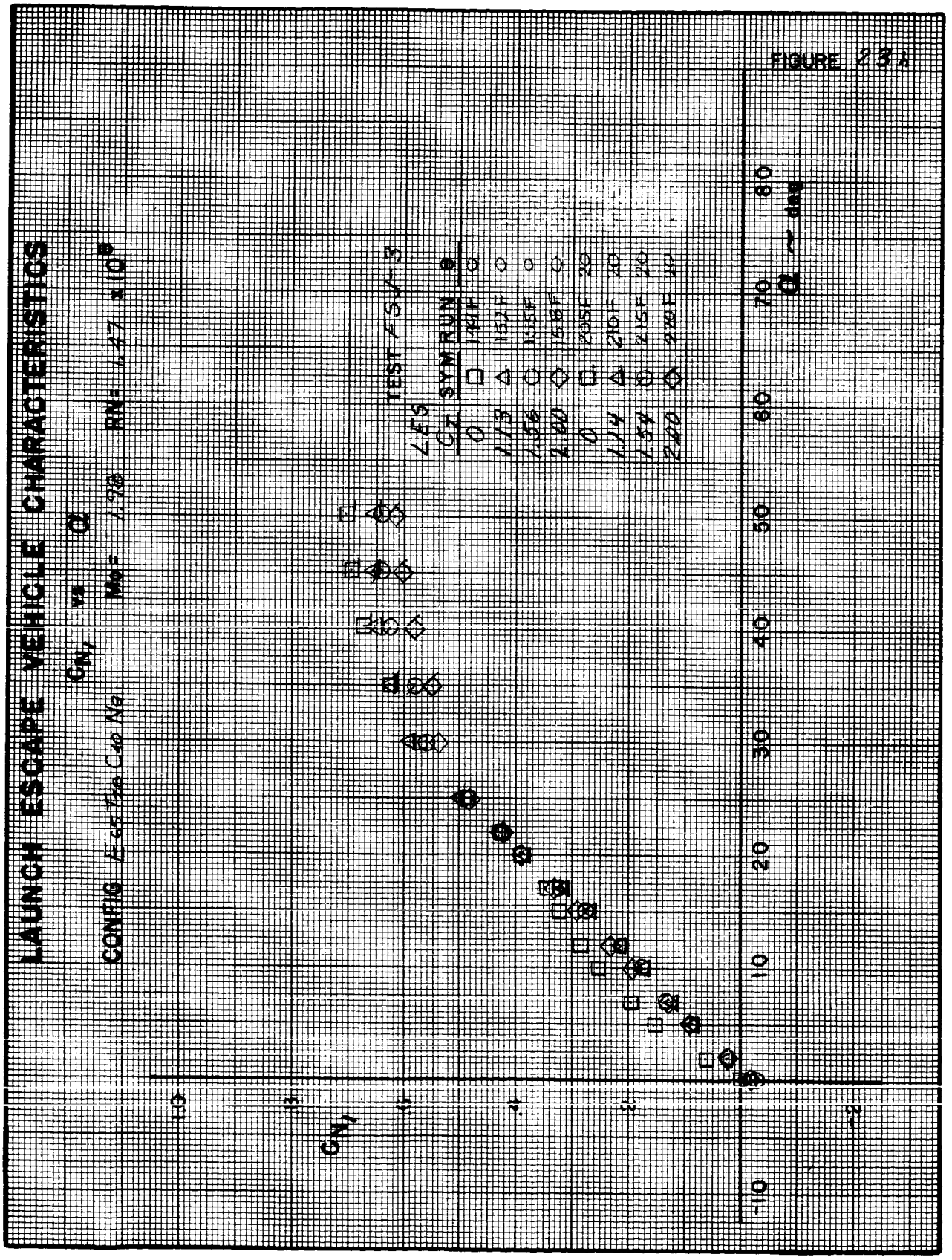

FIGURE 23A

CONFIDENTIAL

~~CONFIDENTIAL~~

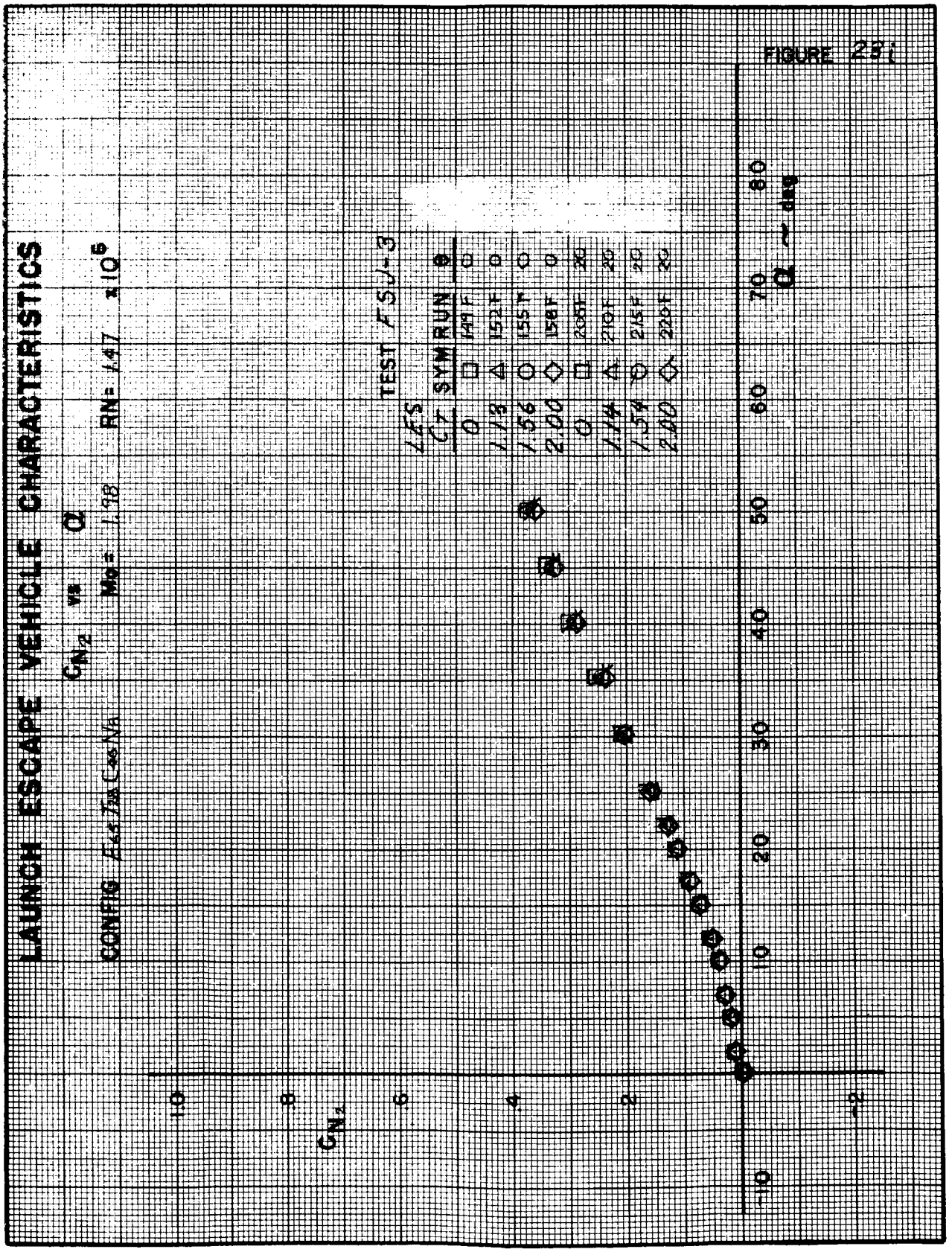

FIGURE 23i

~~CONFIDENTIAL~~

CONFIDENTIAL

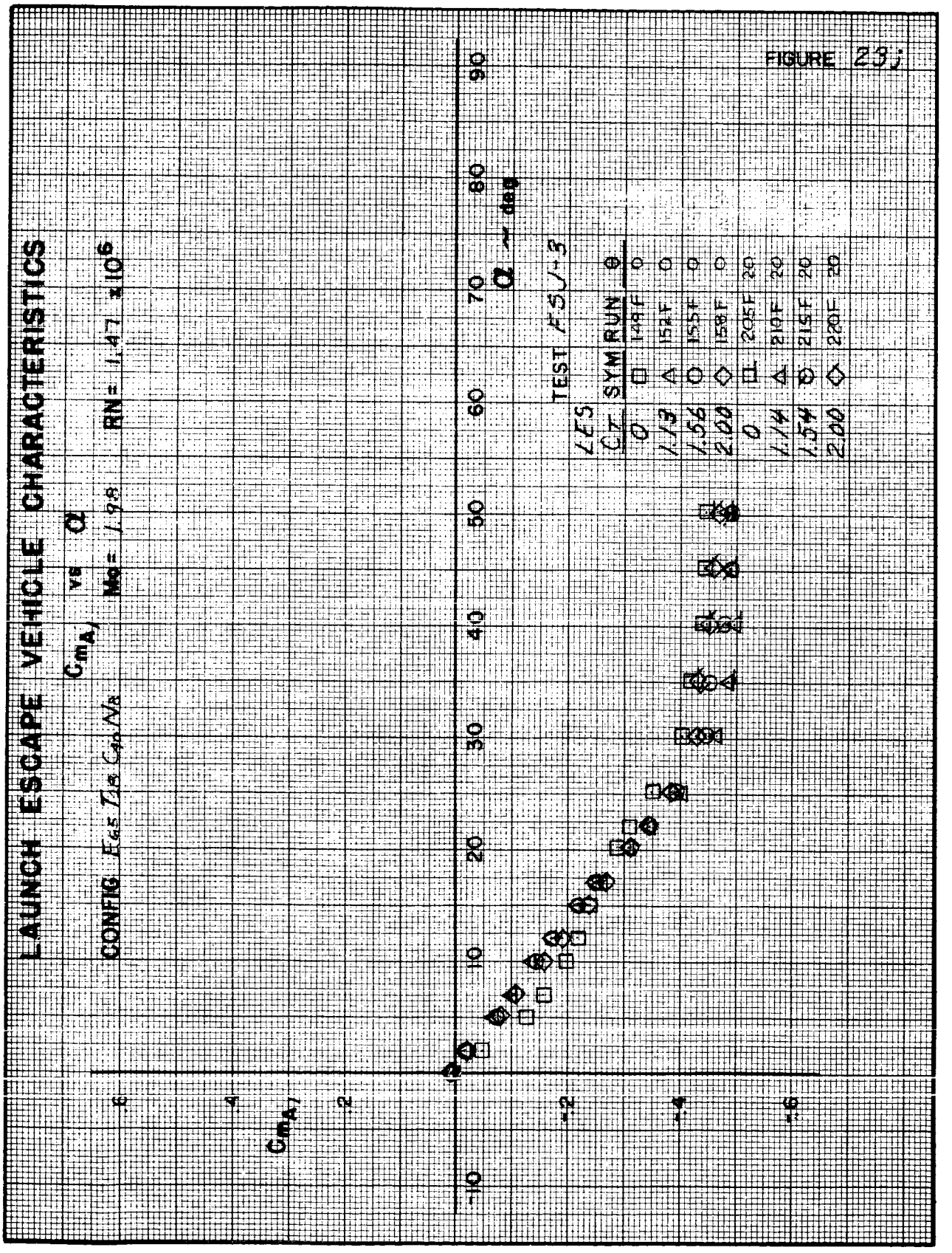

FIGURE 23j

CONFIDENTIAL

~~CONFIDENTIAL~~

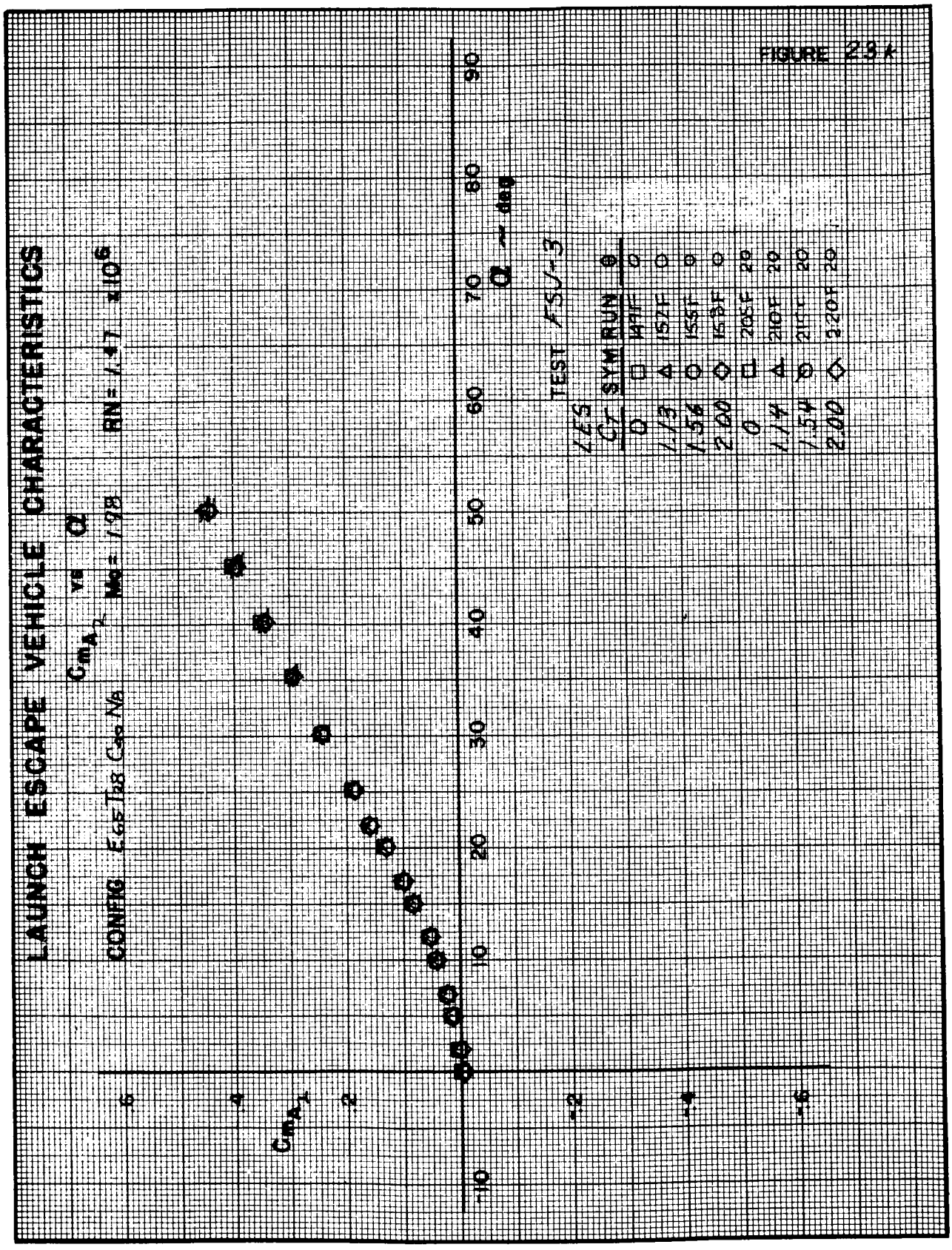

FIGURE 23A

~~CONFIDENTIAL~~

CON~~FIDENTIAL~~

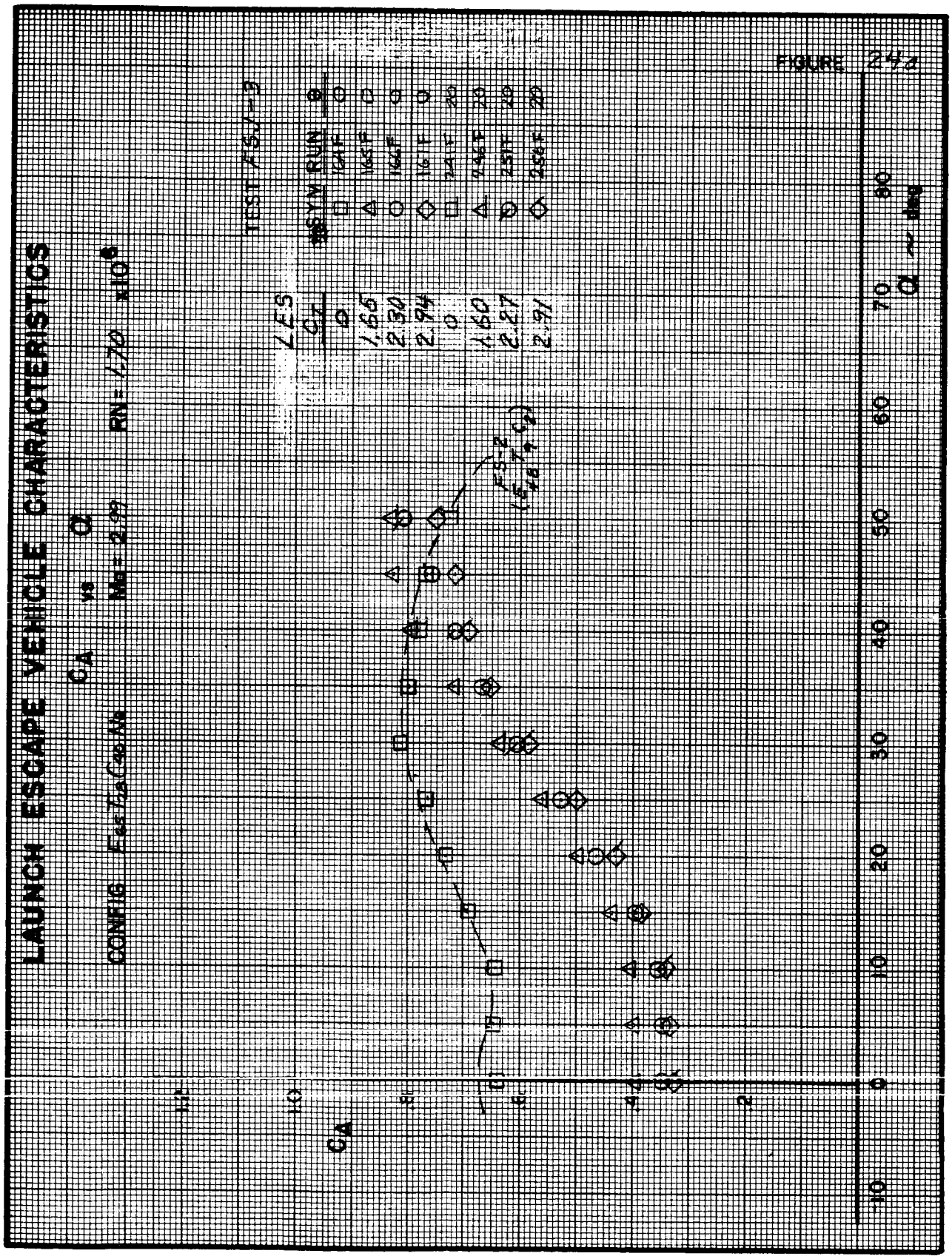

FIGURE 24a

~~CONFIDENTIAL~~

~~CONFIDENTIAL~~

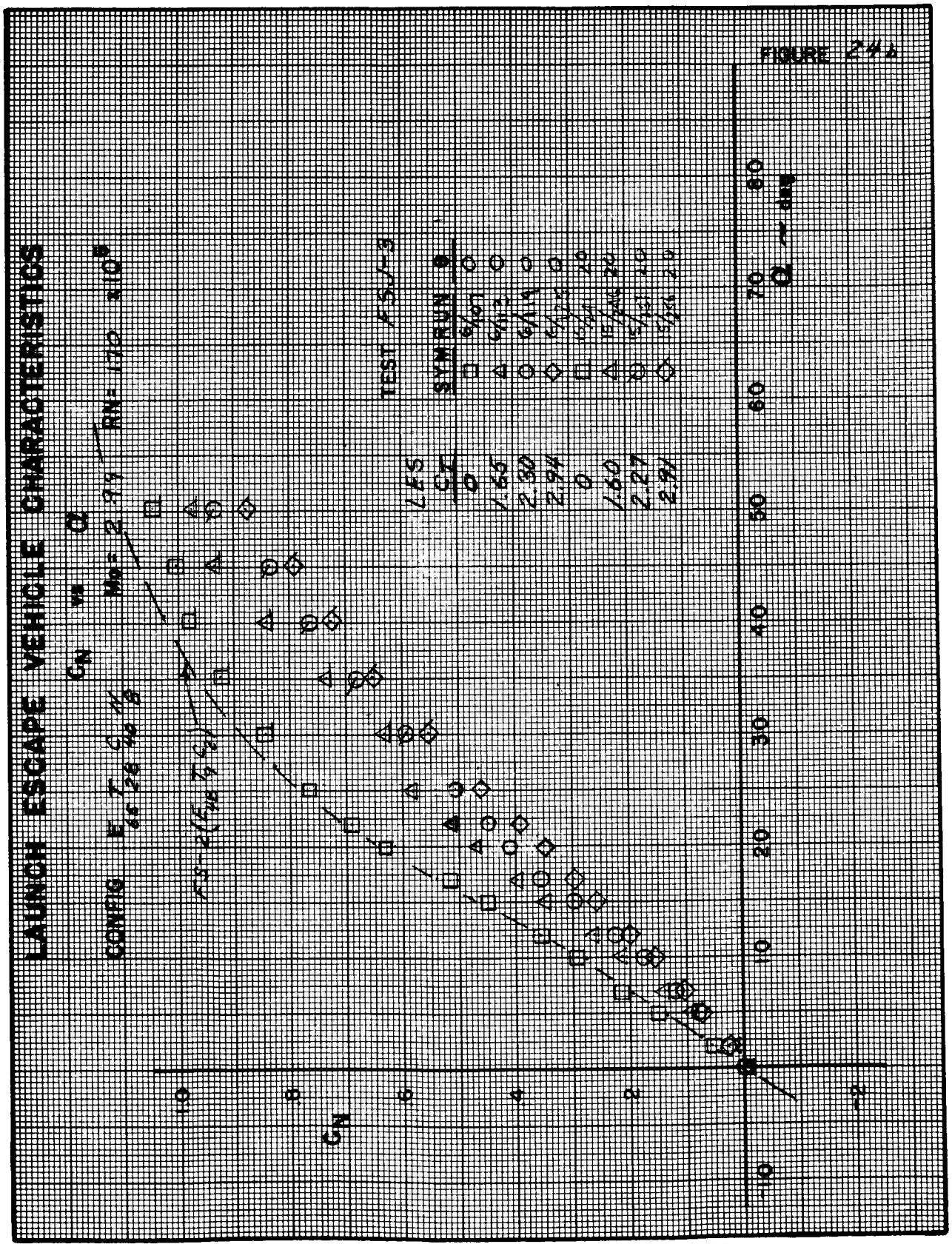

~~CONFIDENTIAL~~

CONFIDENTIAL

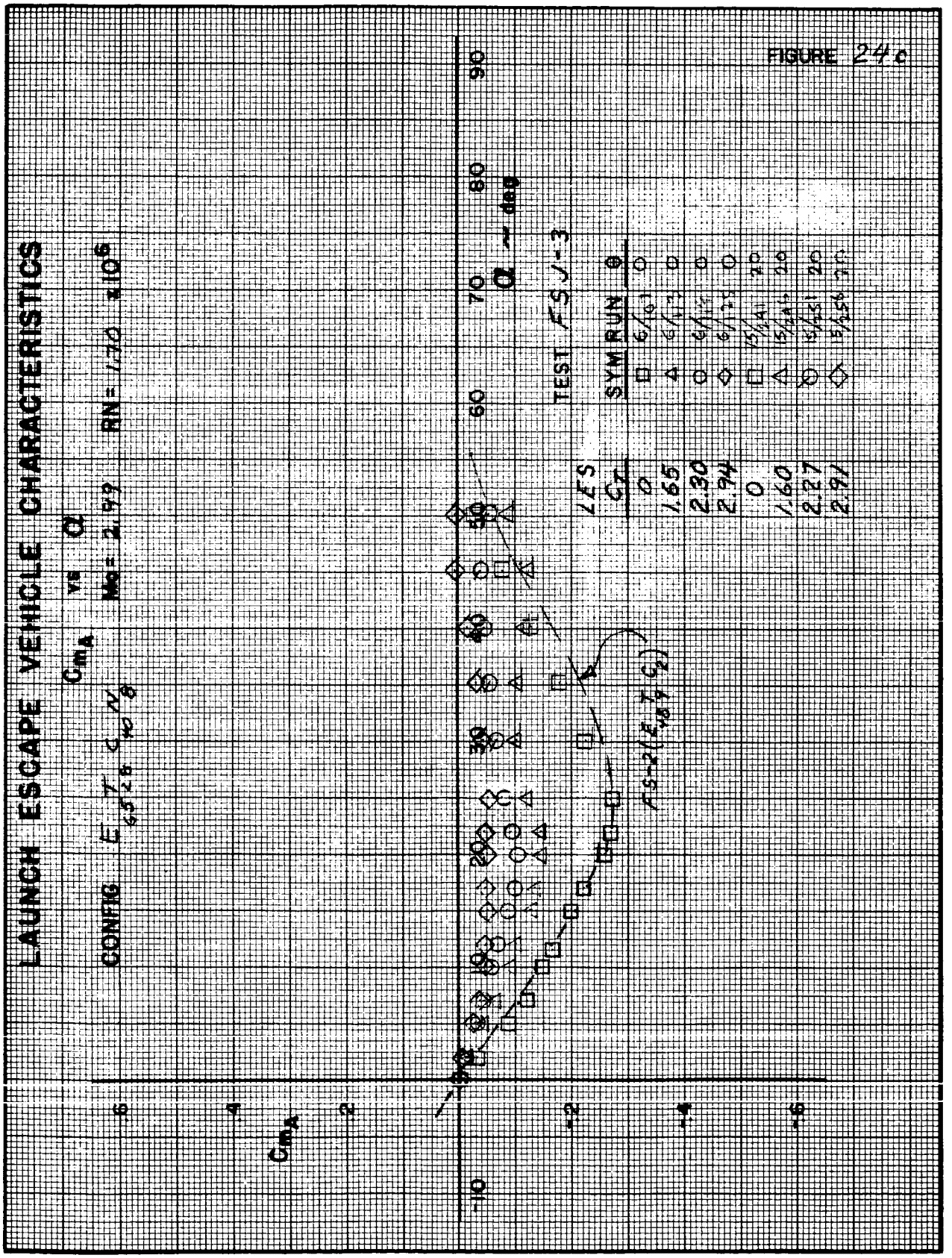

FIGURE 24c

CONFIDENTIAL

~~CONFIDENTIAL~~

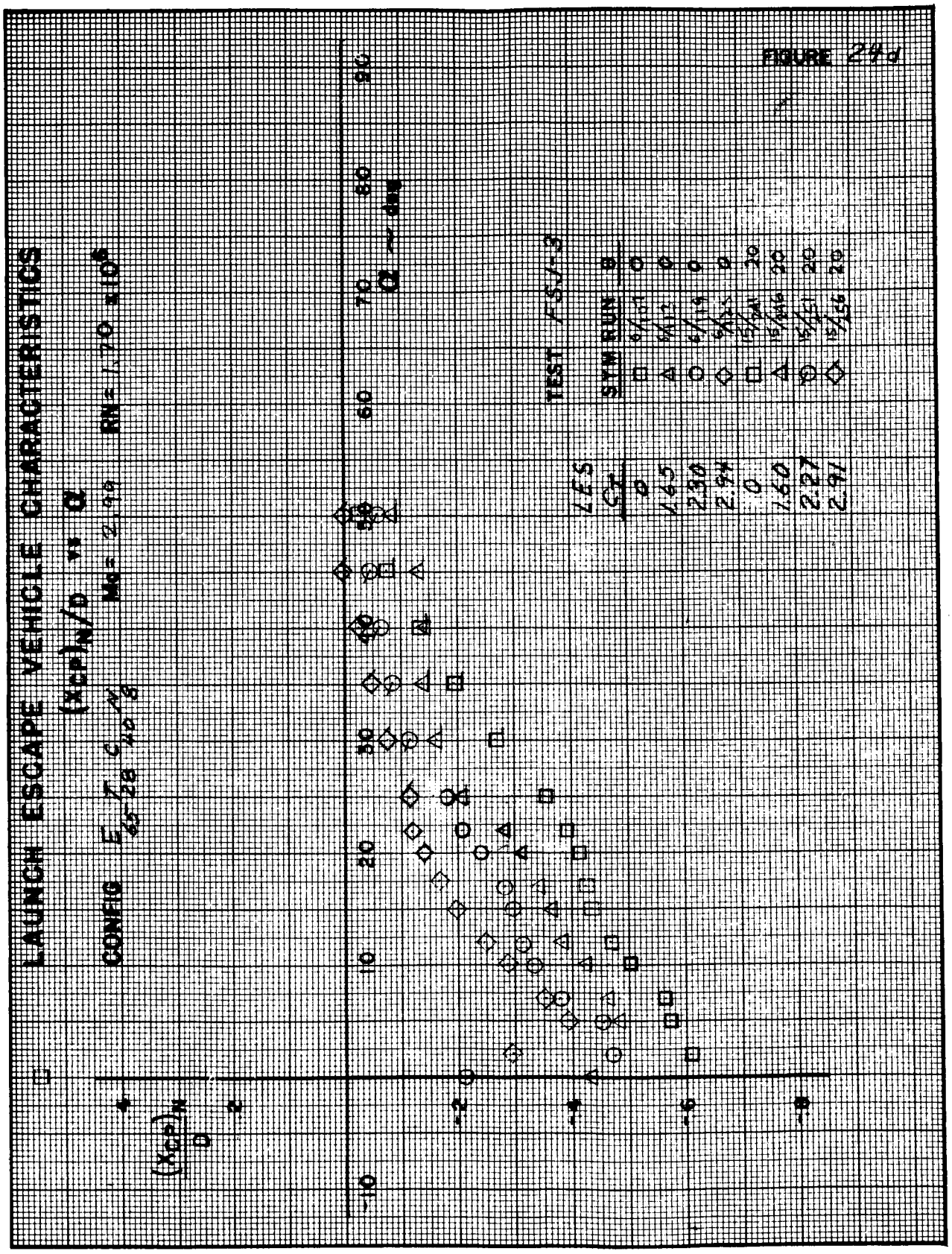

FIGURE 24d

~~CONFIDENTIAL~~

CONFIDENTIAL

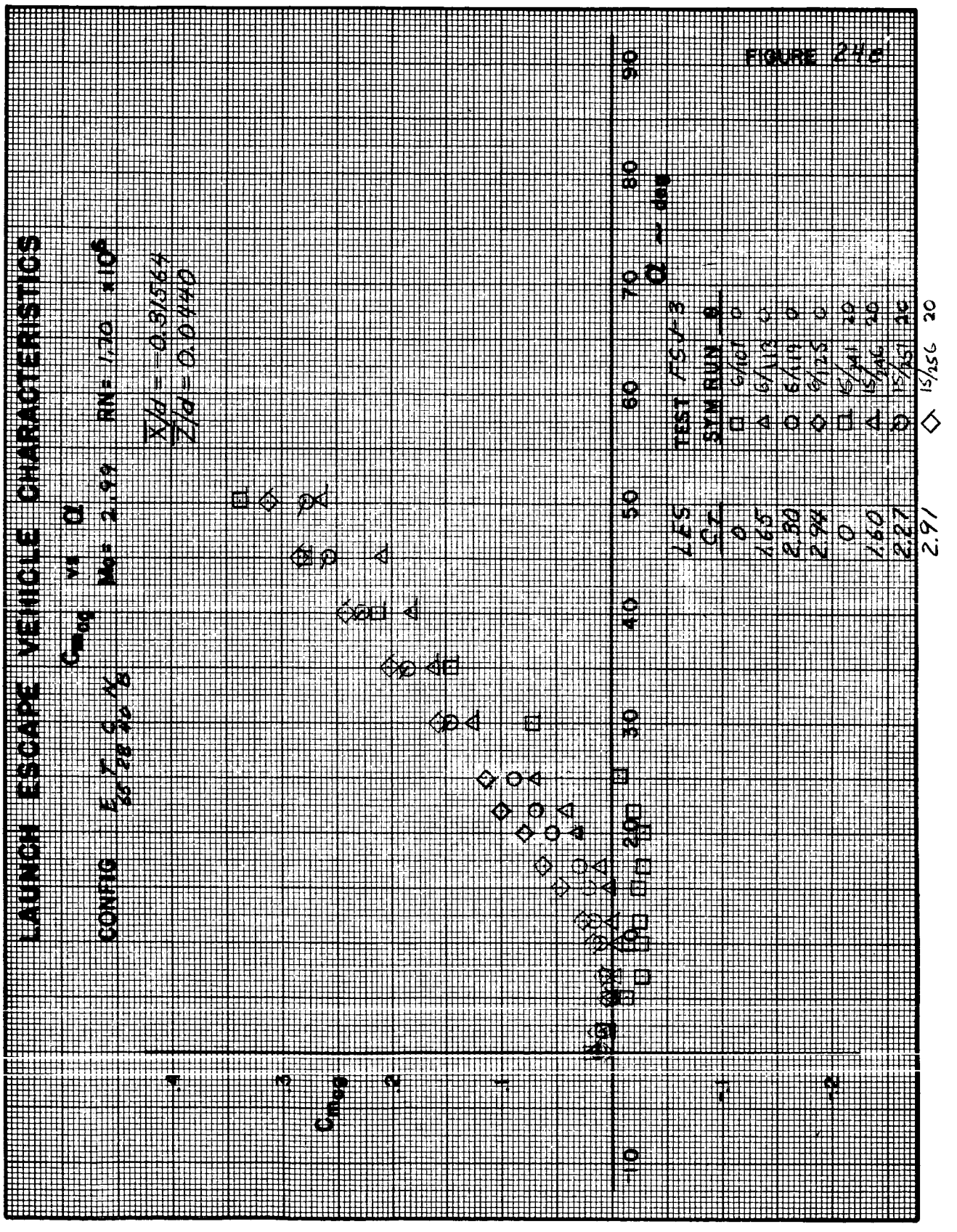

FIGURE 24

CONFIDENTIAL

~~CONFIDENTIAL~~

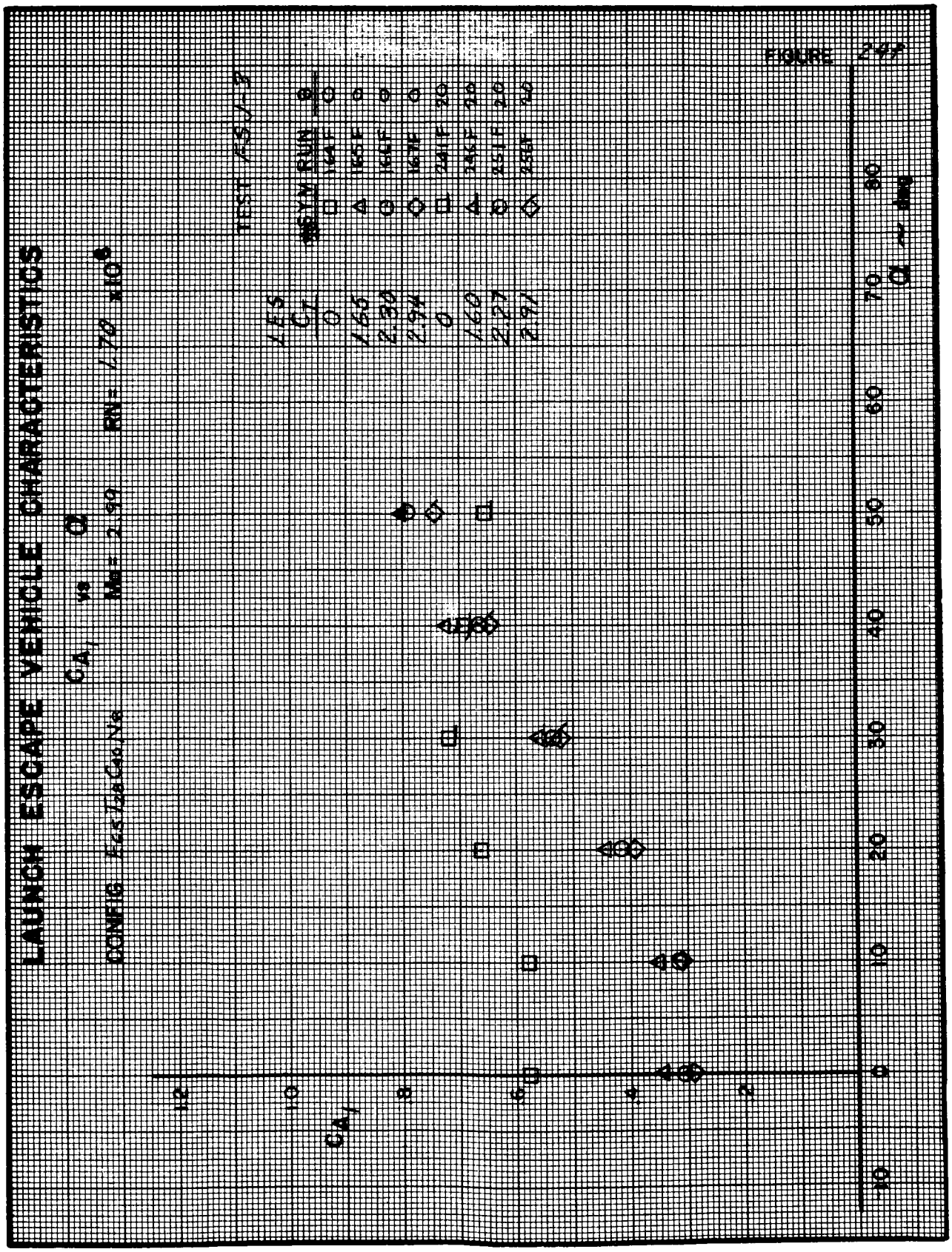

FIGURE 24

~~CONFIDENTIAL~~

CON[redacted]

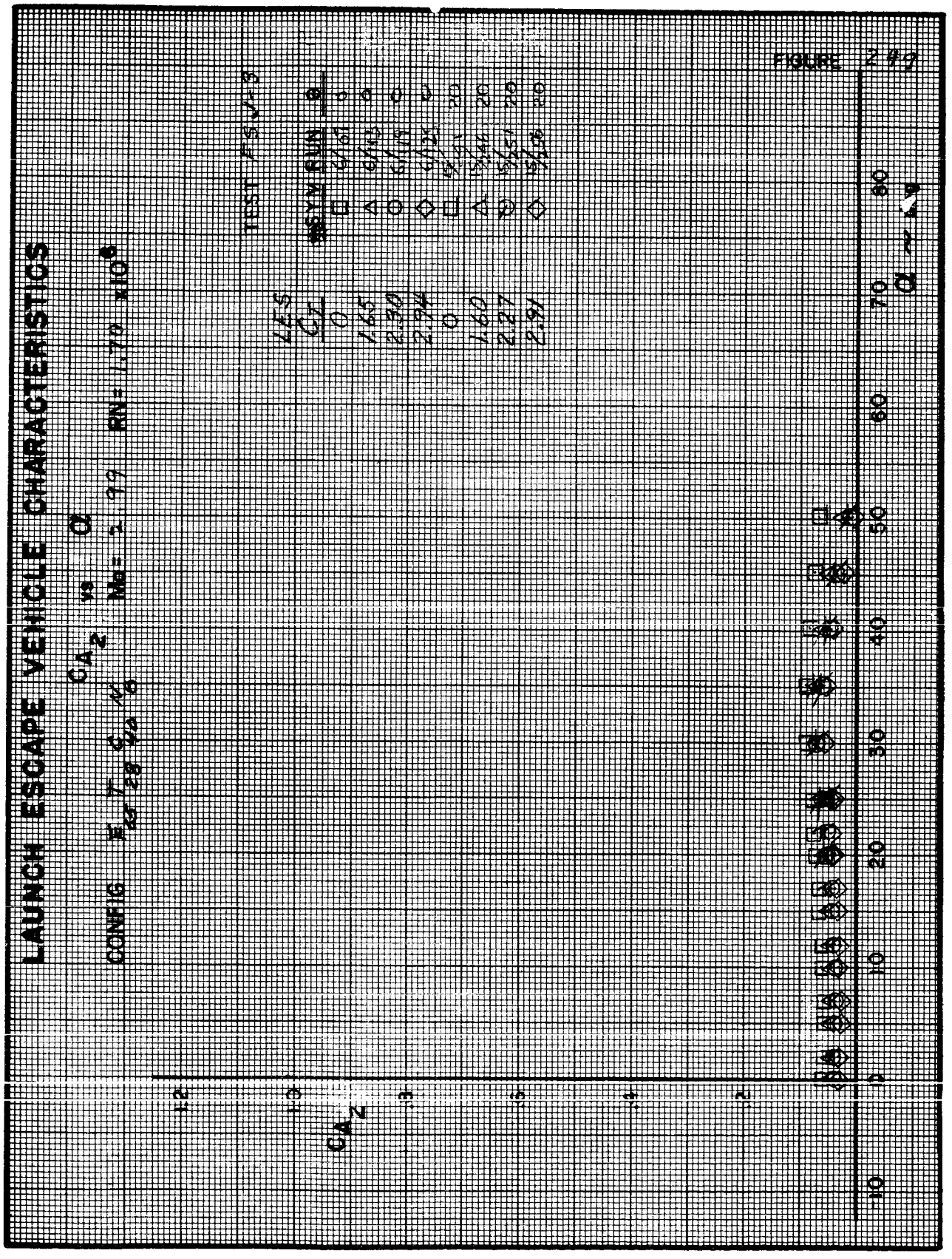

FIGURE 27

[redacted]

~~CONFIDENTIAL~~

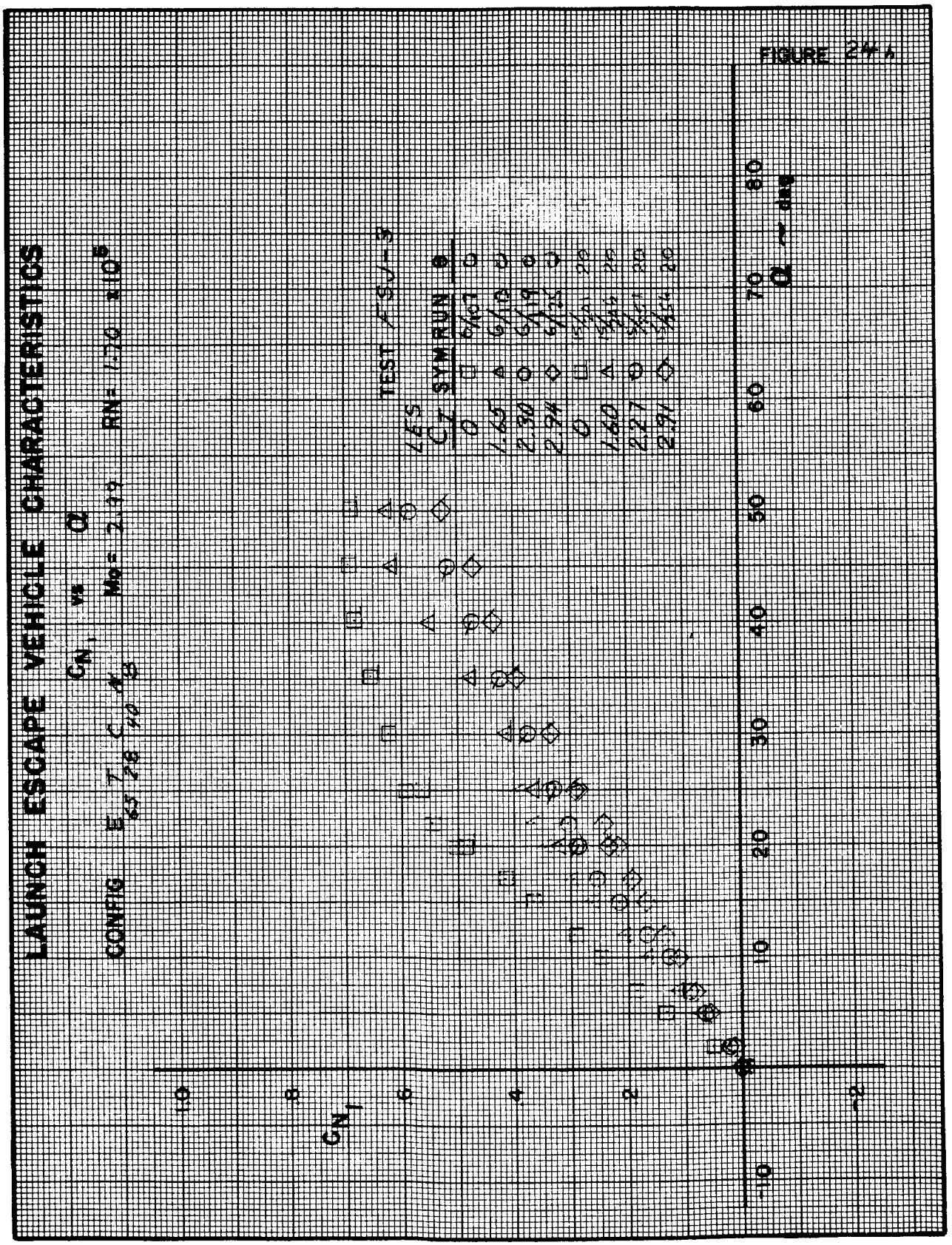

FIGURE 24 h

~~CONFIDENTIAL~~

CON[redacted]

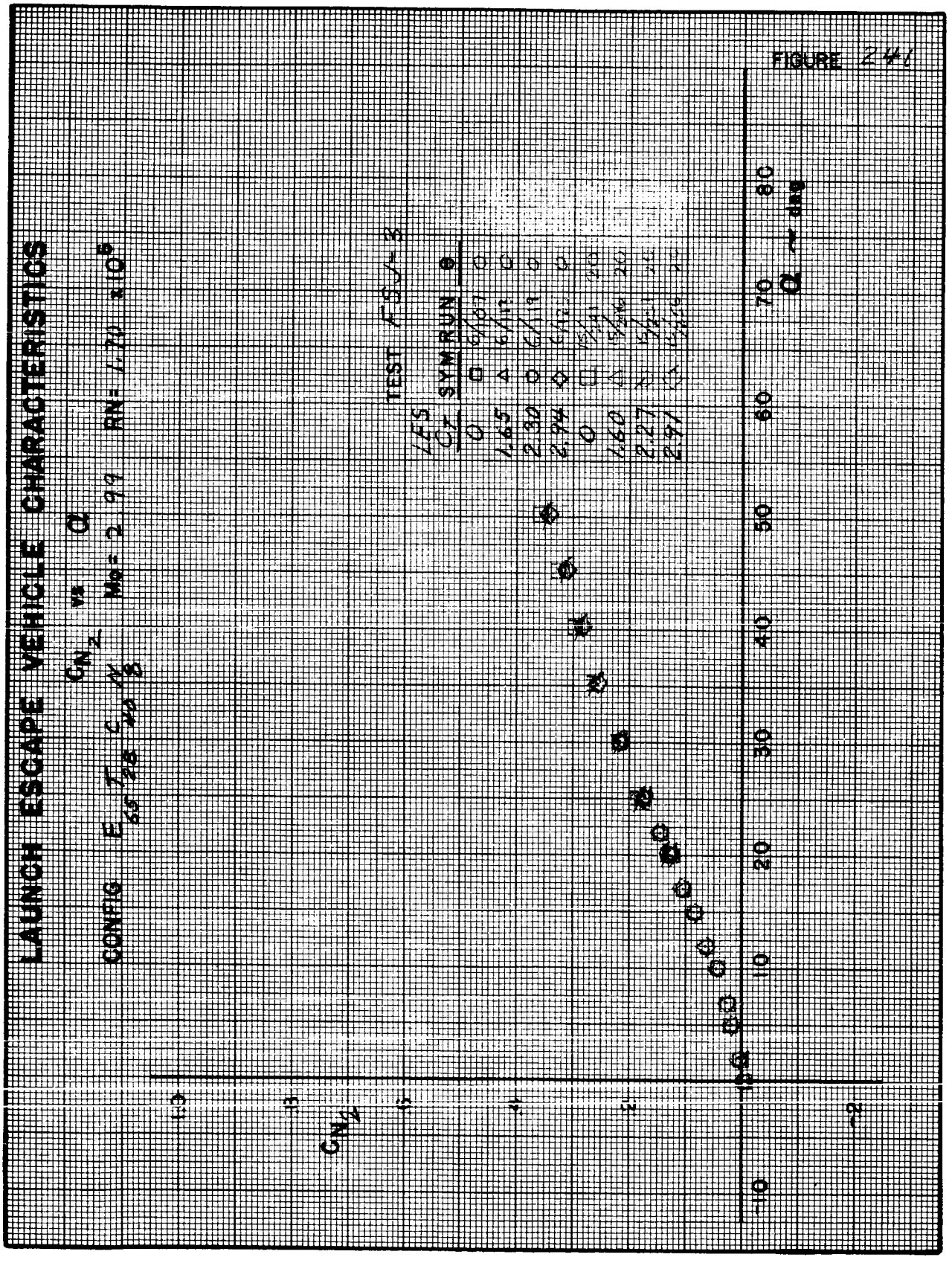

FIGURE 241

[redacted]

~~CONFIDENTIAL~~

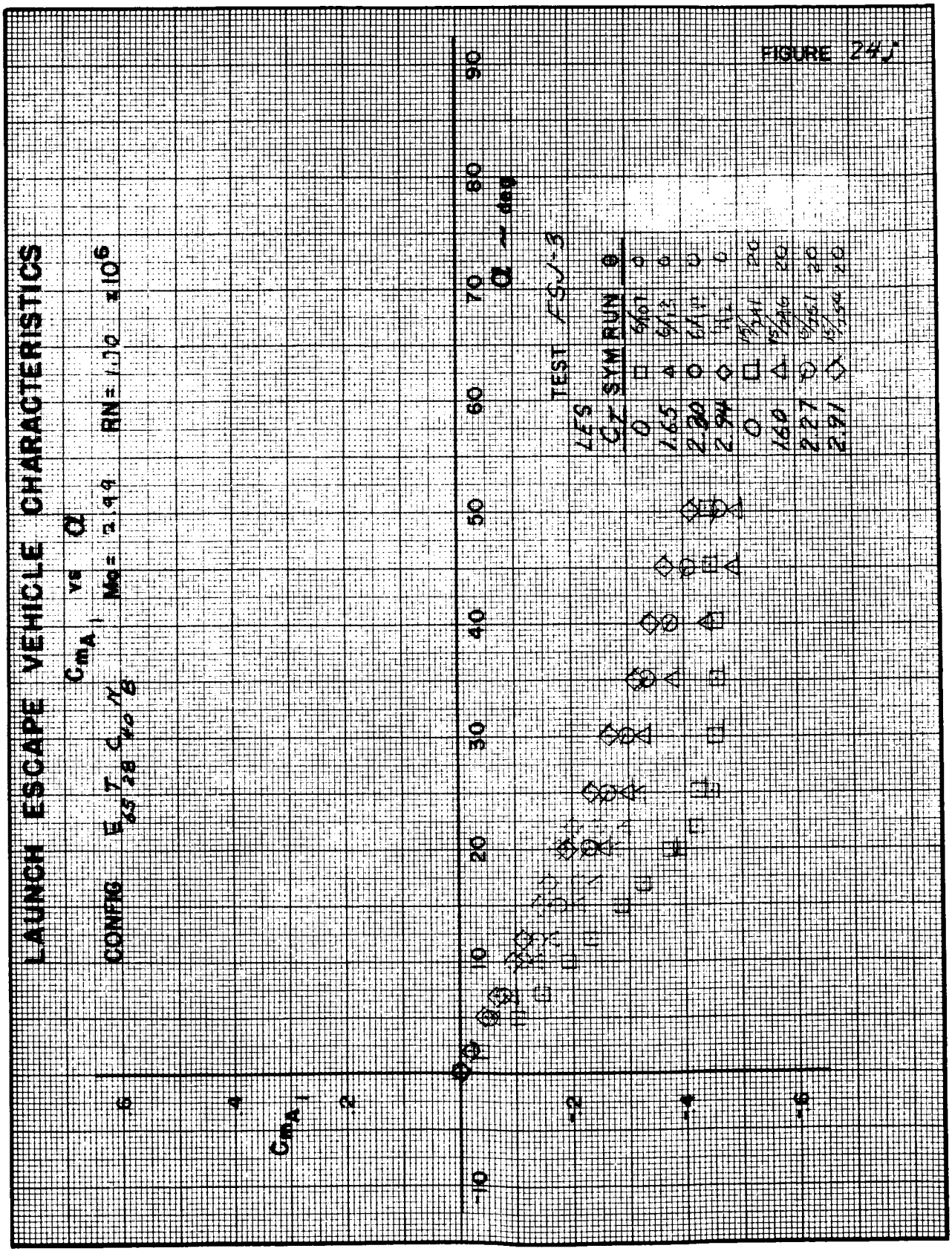

FIGURE 24

~~CONFIDENTIAL~~

CON~~FIDENTIAL~~

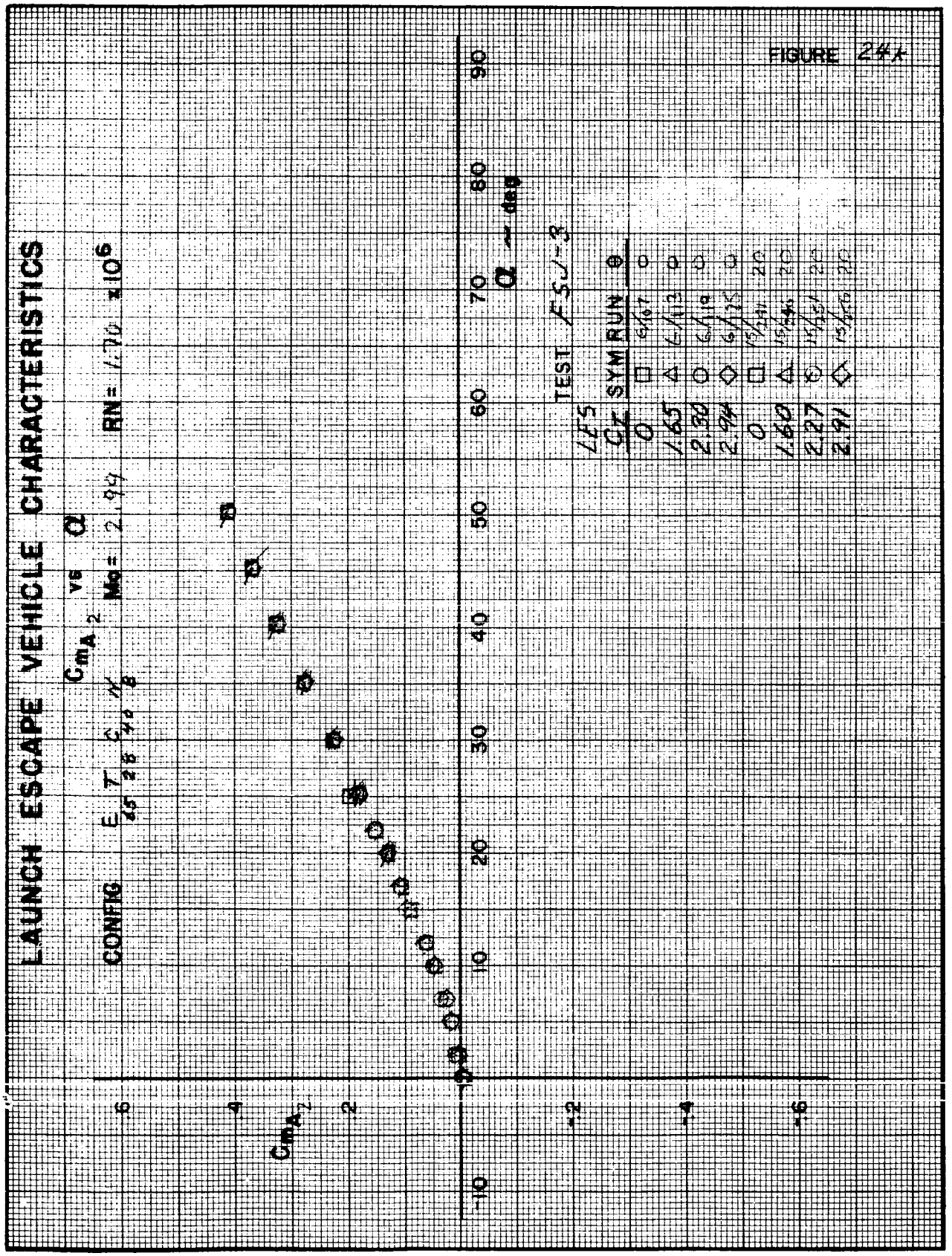

FIGURE 24A

~~CONFIDENTIAL~~

~~CONFIDENTIAL~~

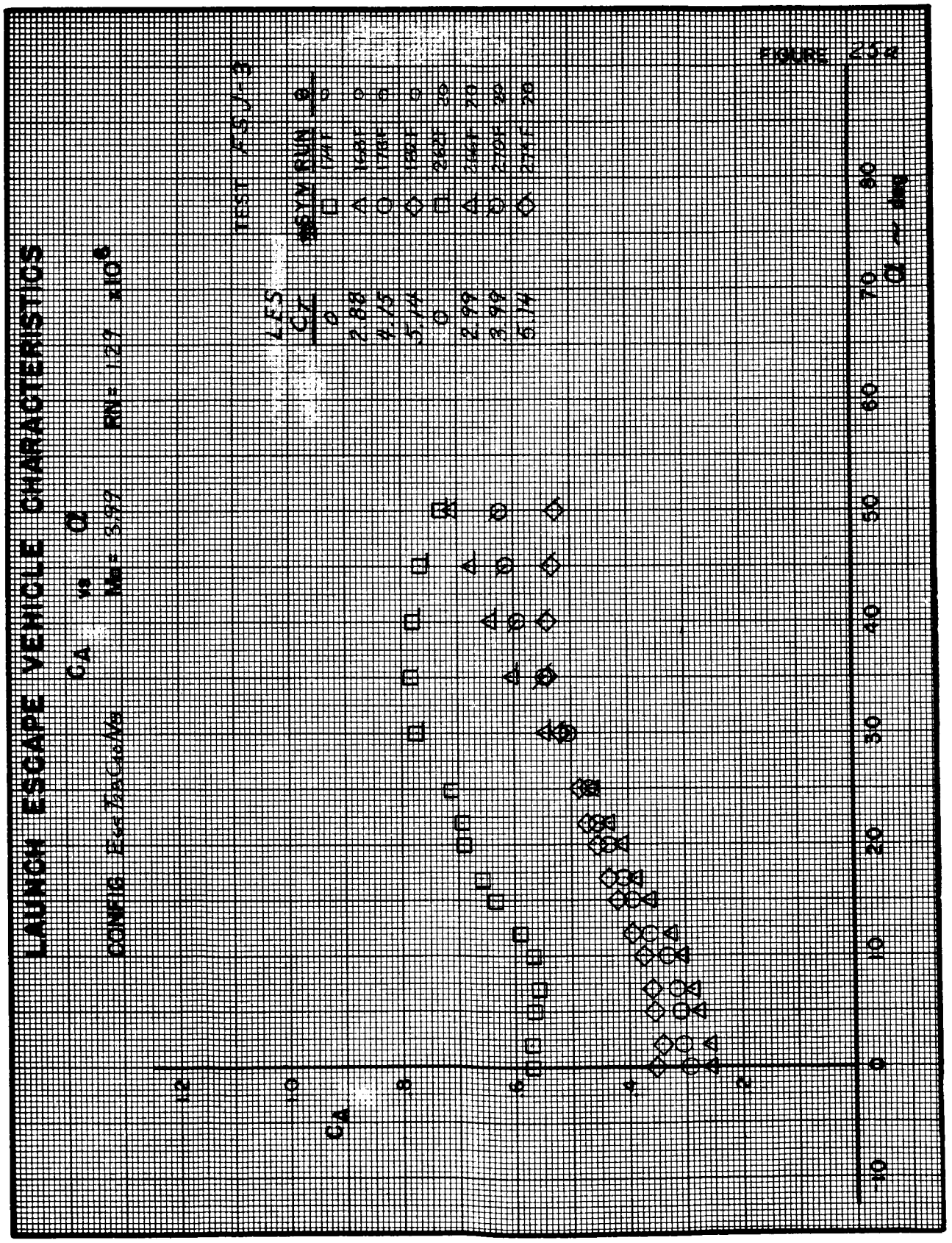

~~CONFIDENTIAL~~

CON[redacted]

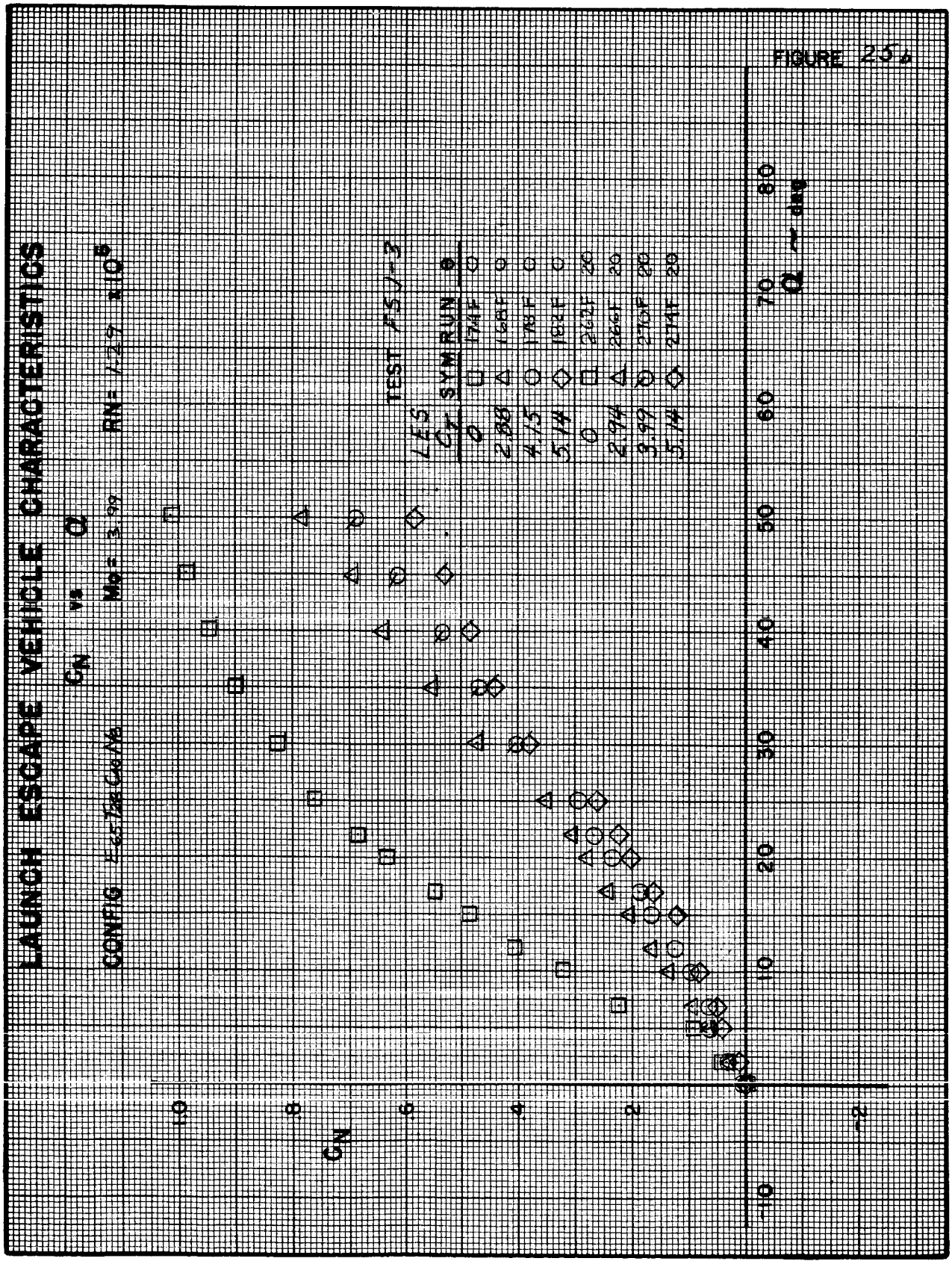

FIGURE 25.6

[redacted]

~~CONFIDENTIAL~~

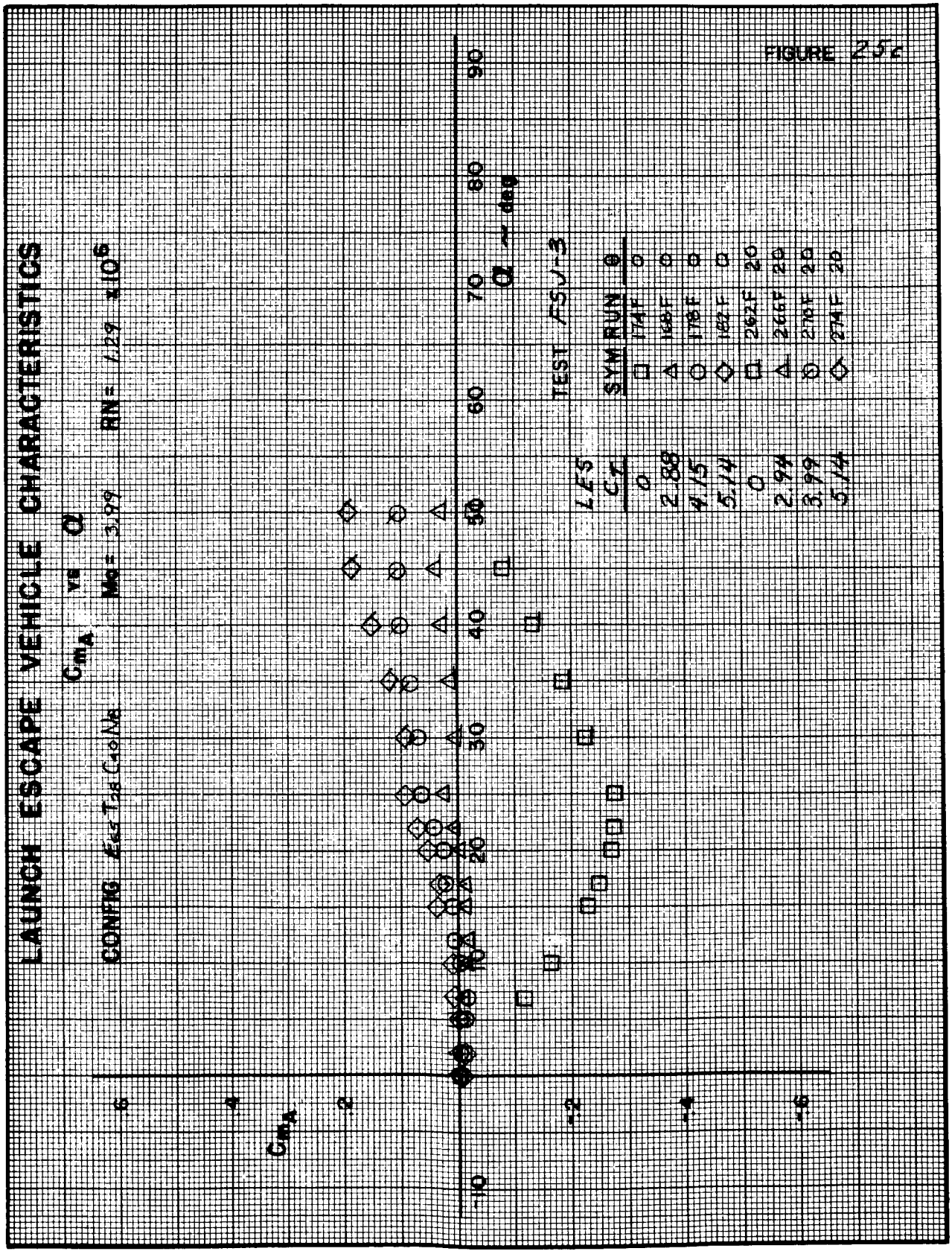

~~CONFIDENTIAL~~

CO[redacted]

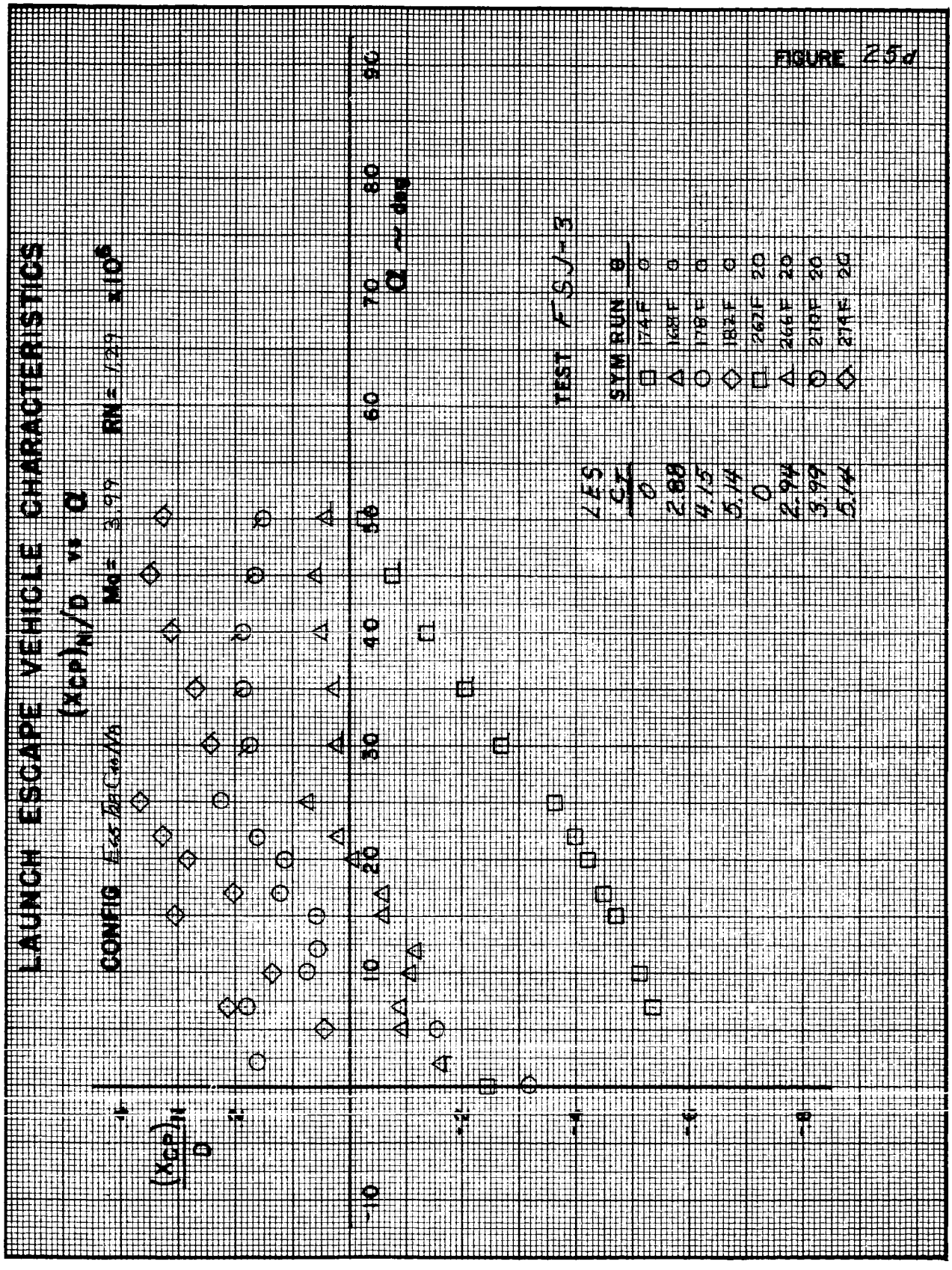

[redacted]

~~CONFIDENTIAL~~

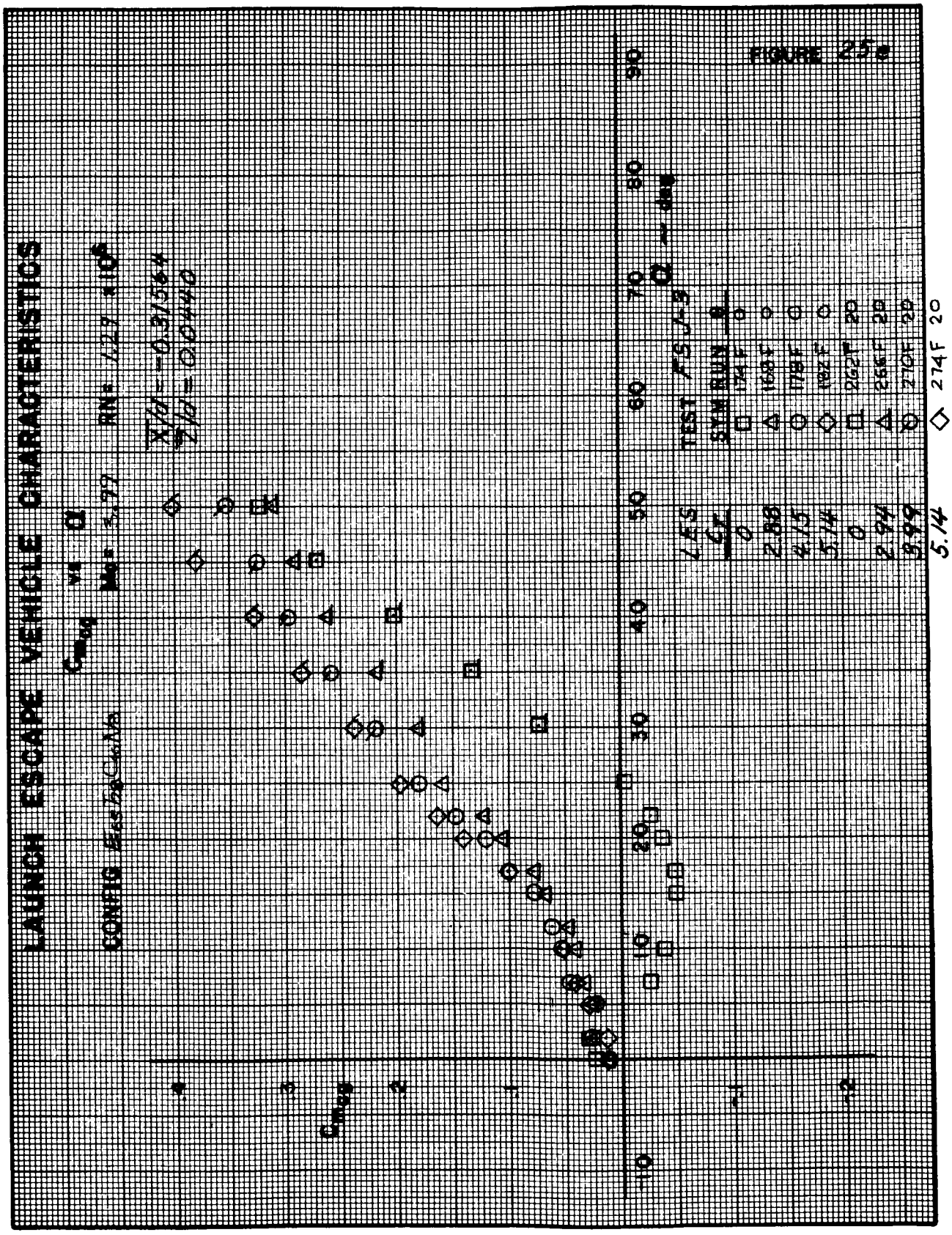

FIGURE 25e

~~CONFIDENTIAL~~

CON[redacted]

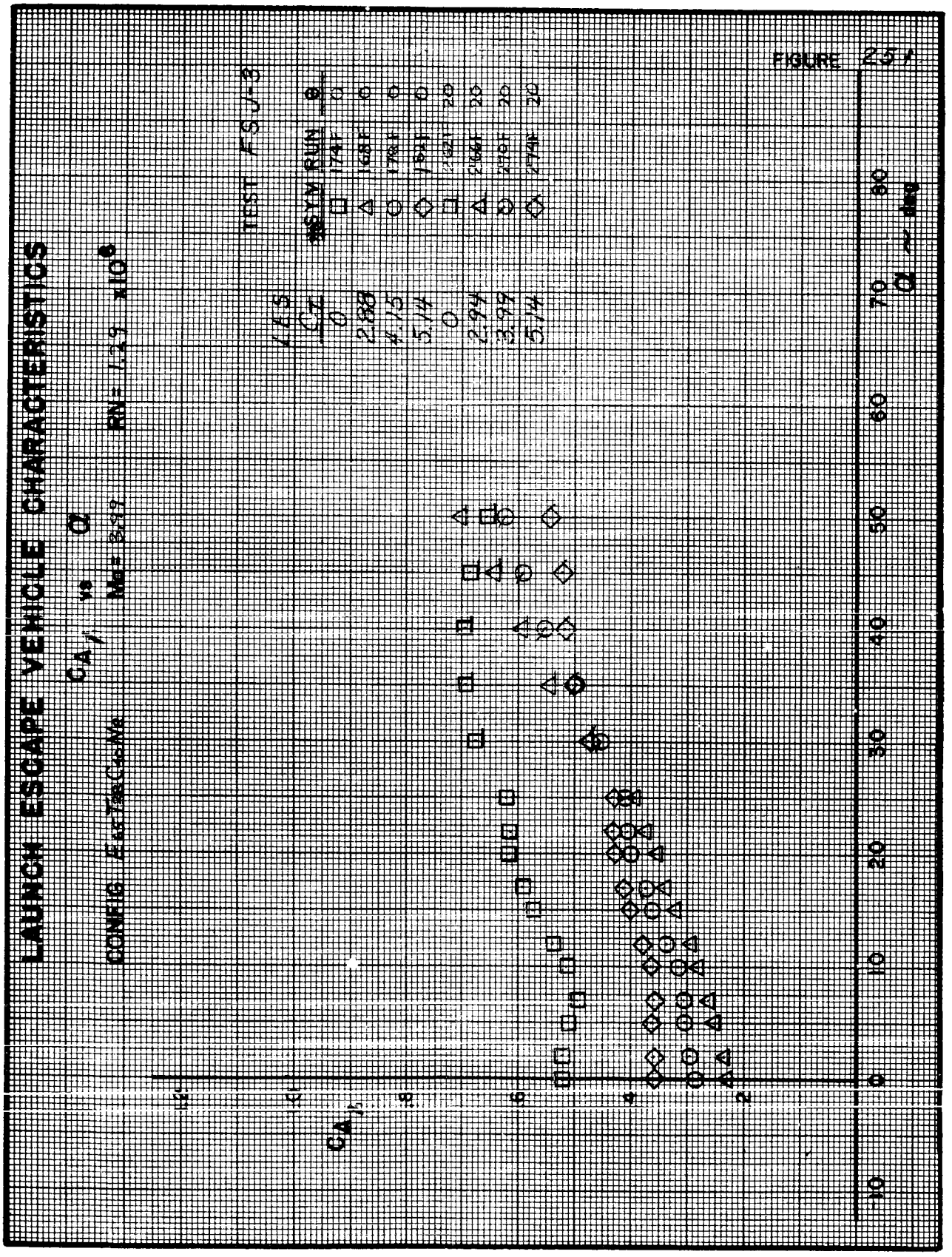

[redacted]

~~CONFIDENTIAL~~

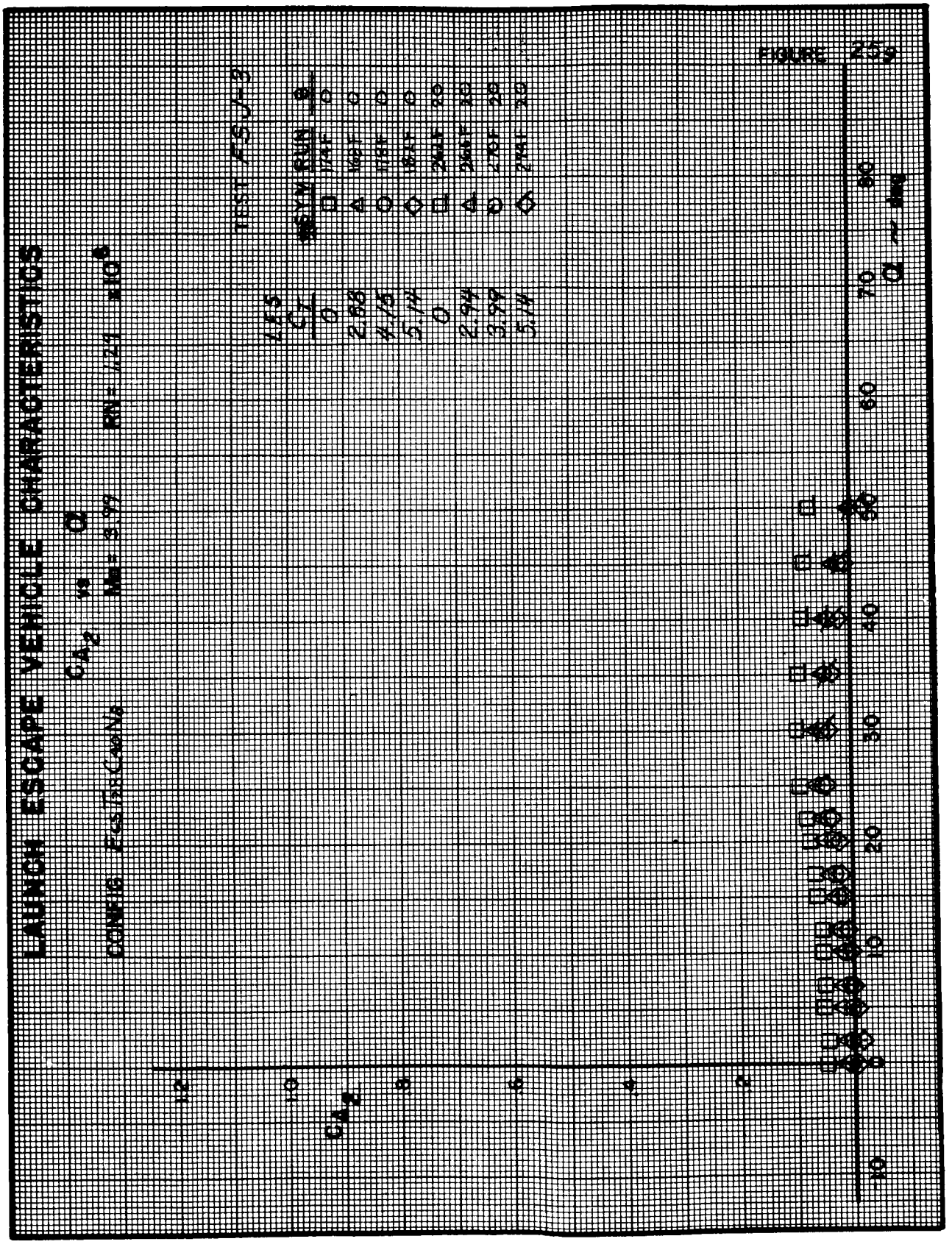

~~CONFIDENTIAL~~

CO[redacted]

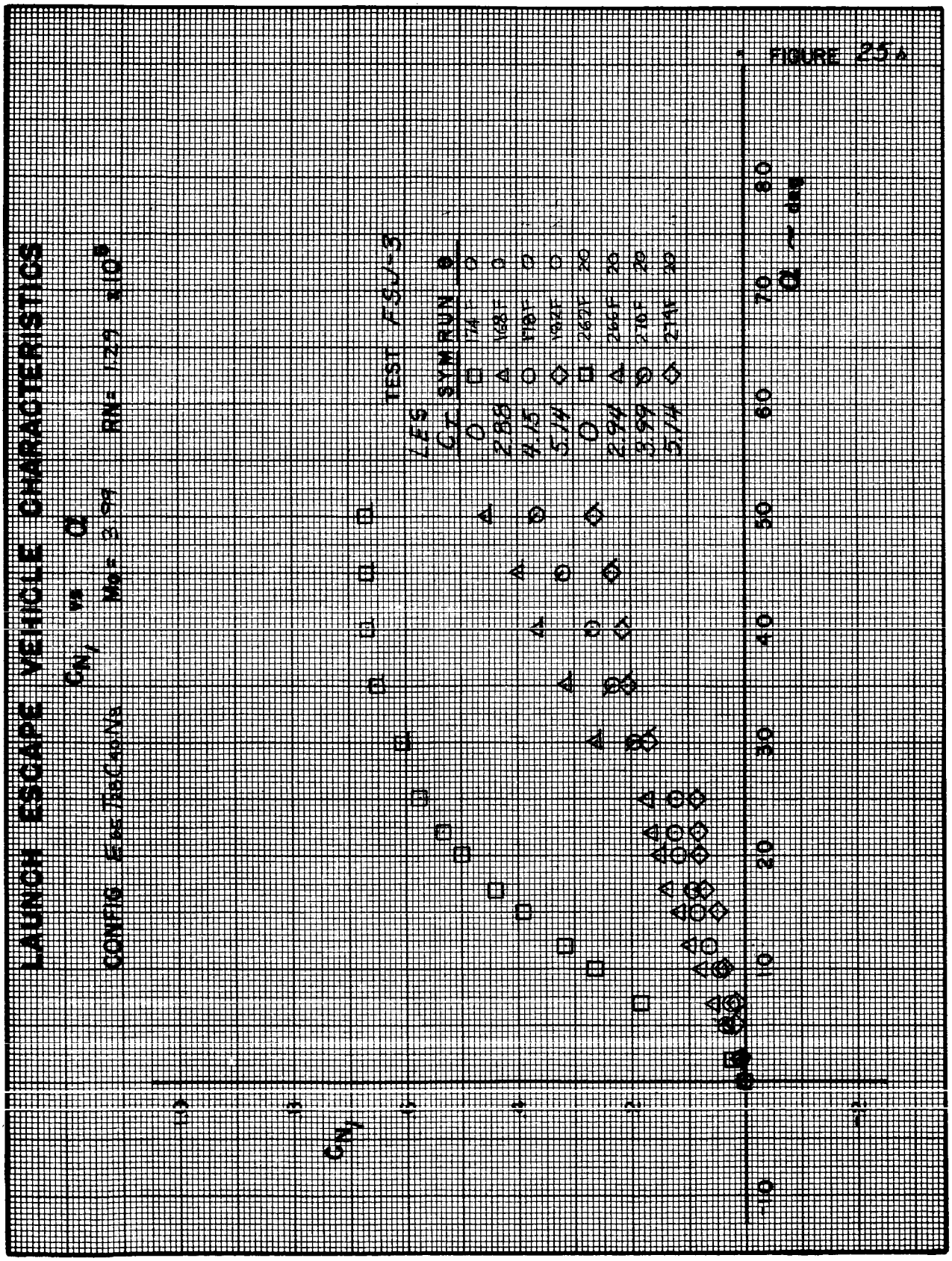

FIGURE 25A

[redacted]

~~CONFIDENTIAL~~

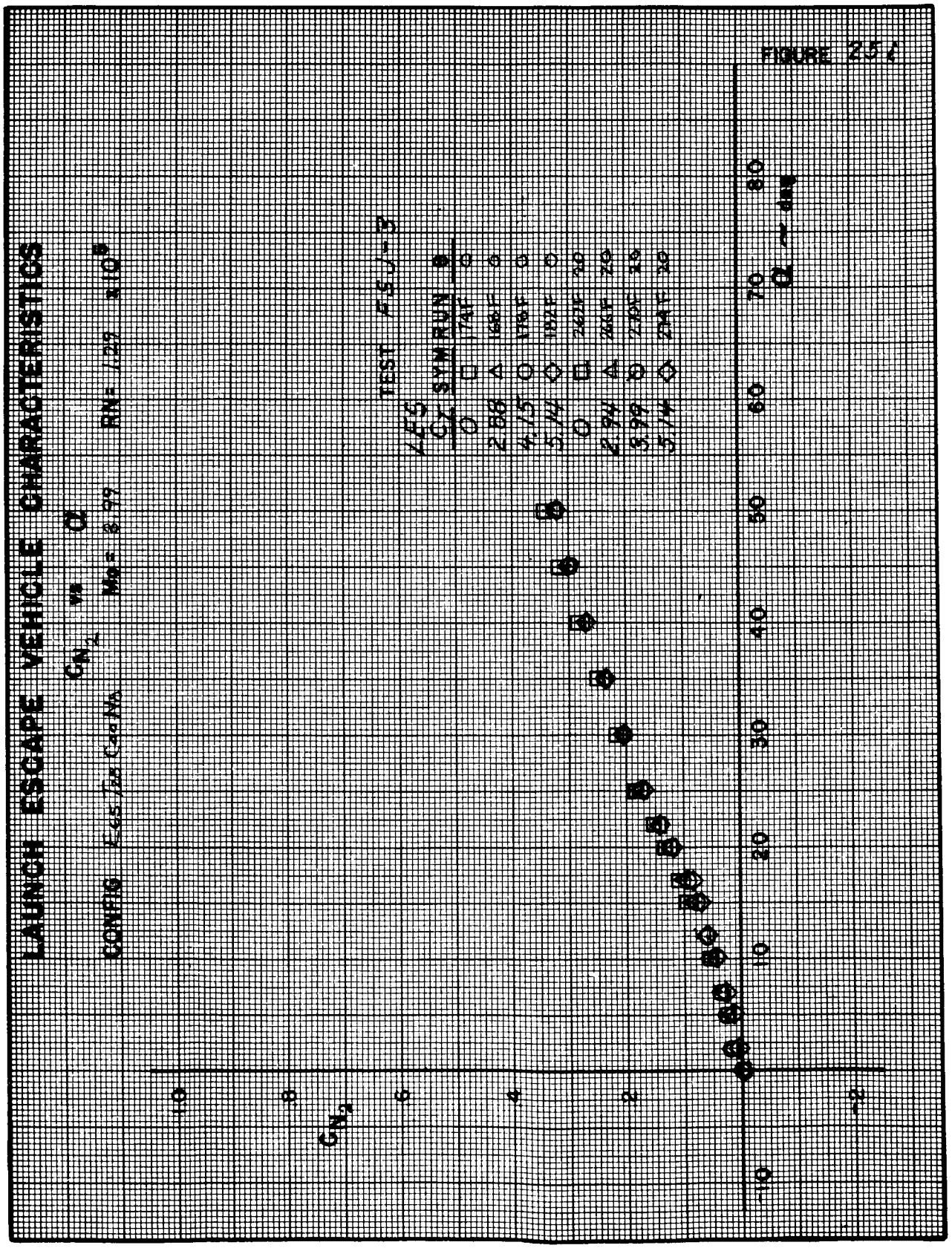

FIGURE 25.4

~~CONFIDENTIAL~~

CO[redacted]

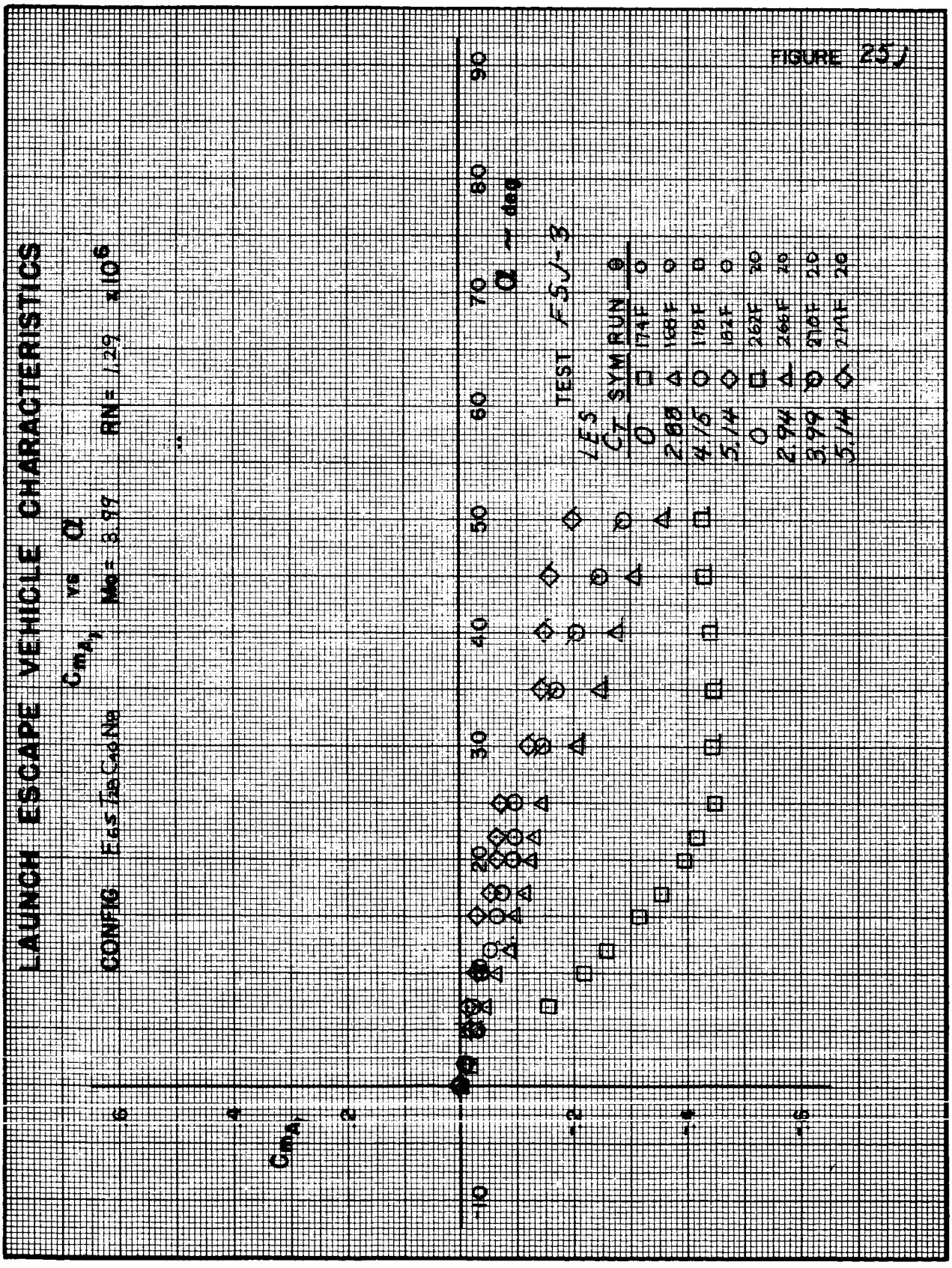

~~CONFIDENTIAL~~

~~CONFIDENTIAL~~

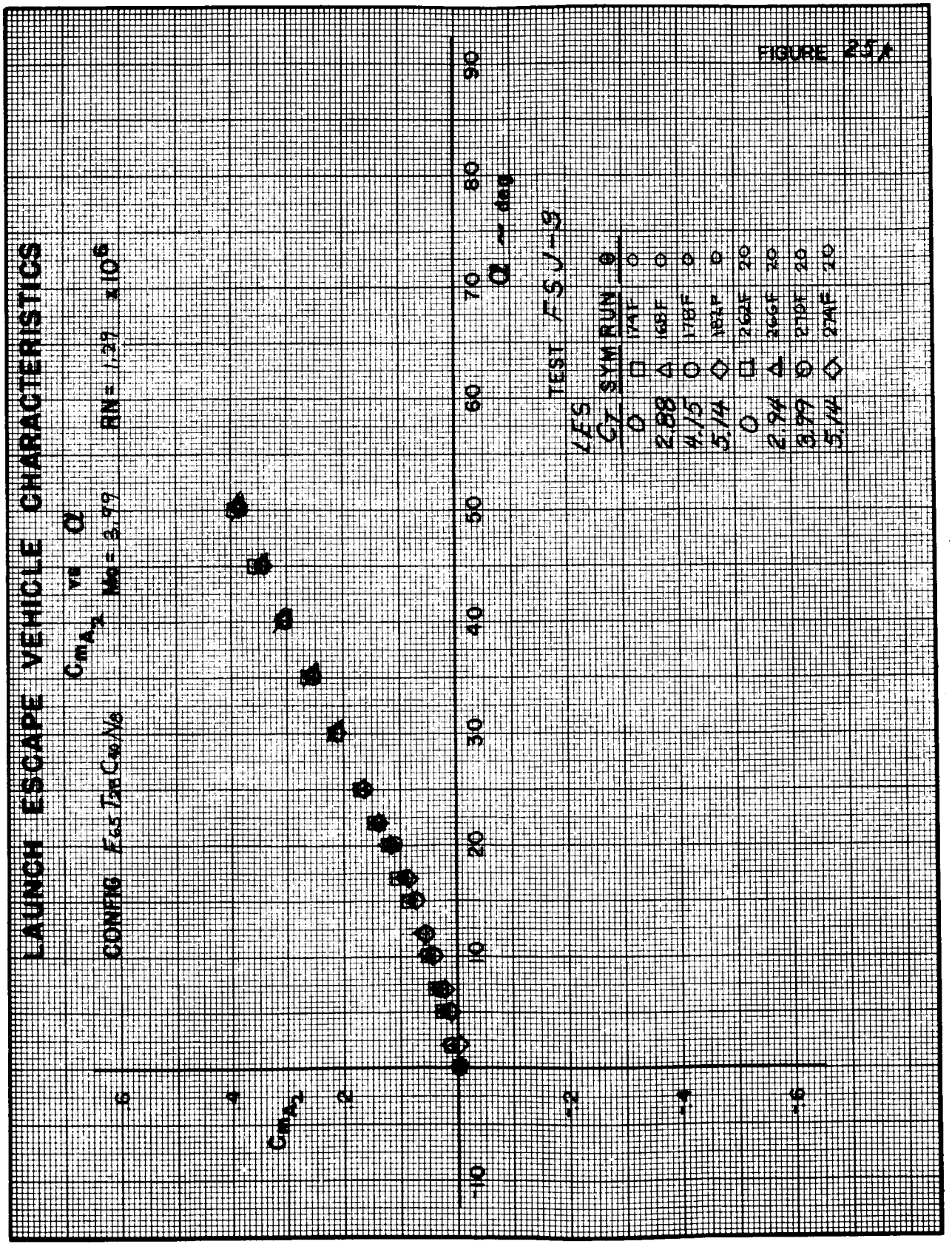

FIGURE 25

~~CONFIDENTIAL~~

CONFIDENTIAL

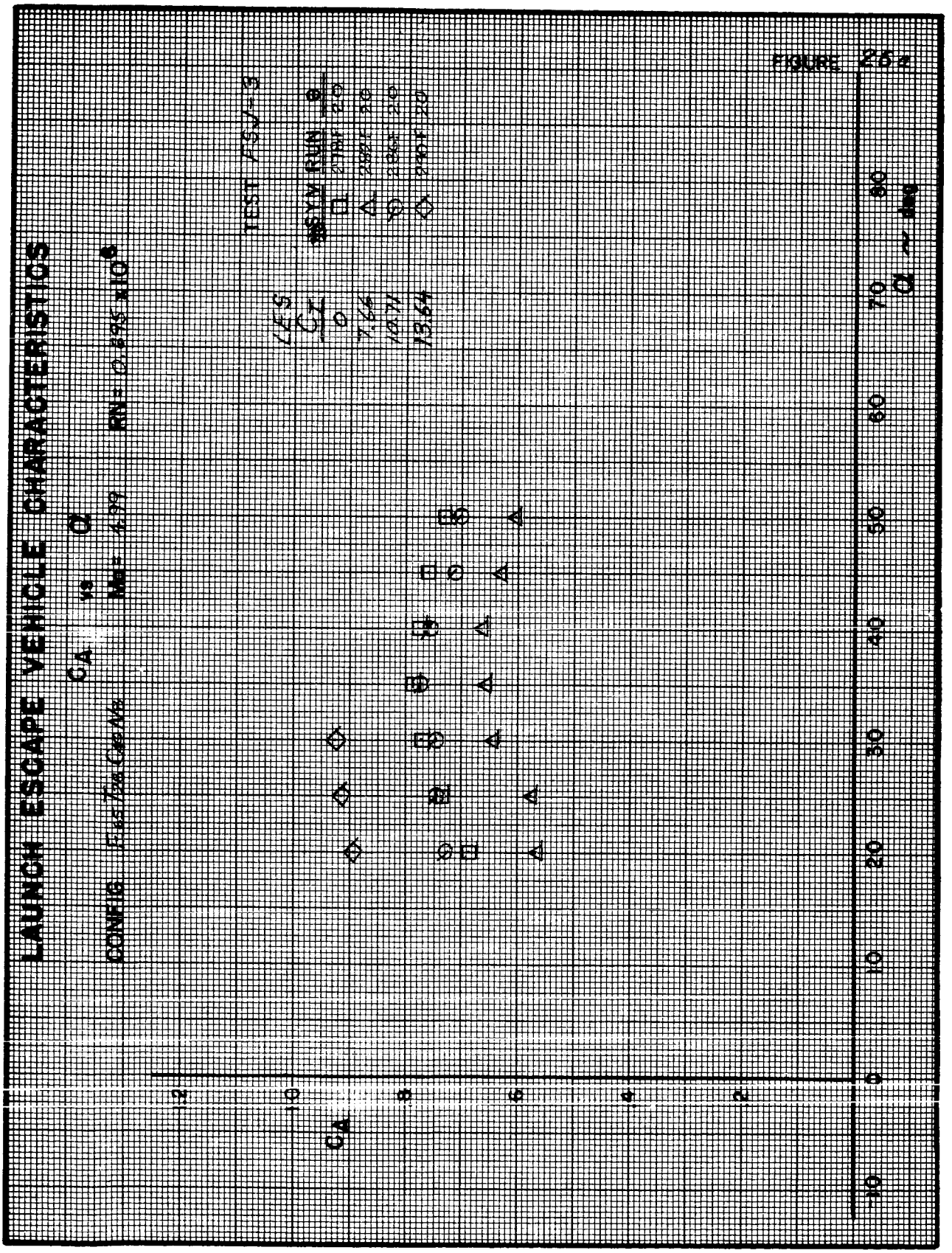

FIGURE 26a

CONFIDENTIAL

~~CONFIDENTIAL~~

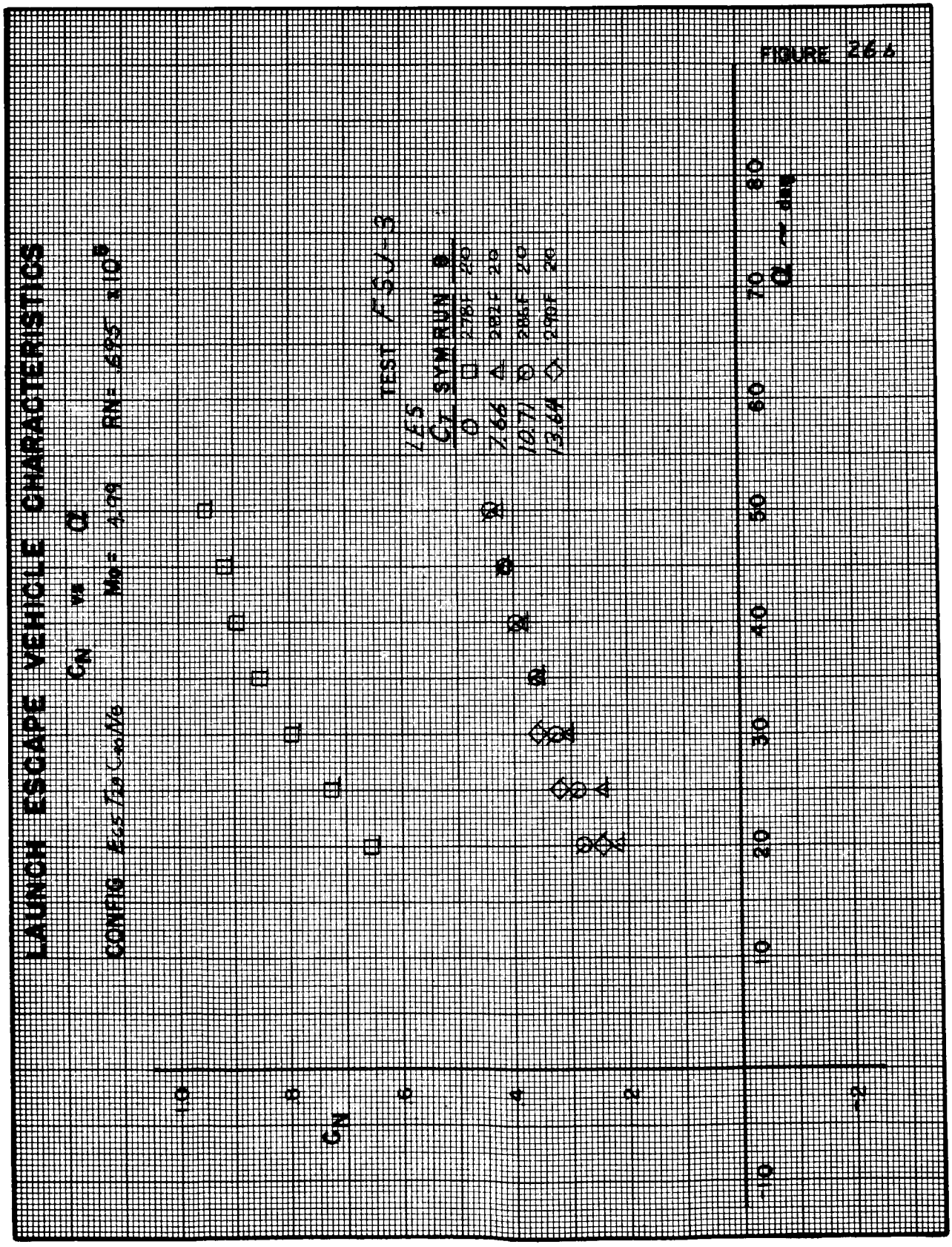

FIGURE 26.6

~~CONFIDENTIAL~~

CONFIDENTIAL

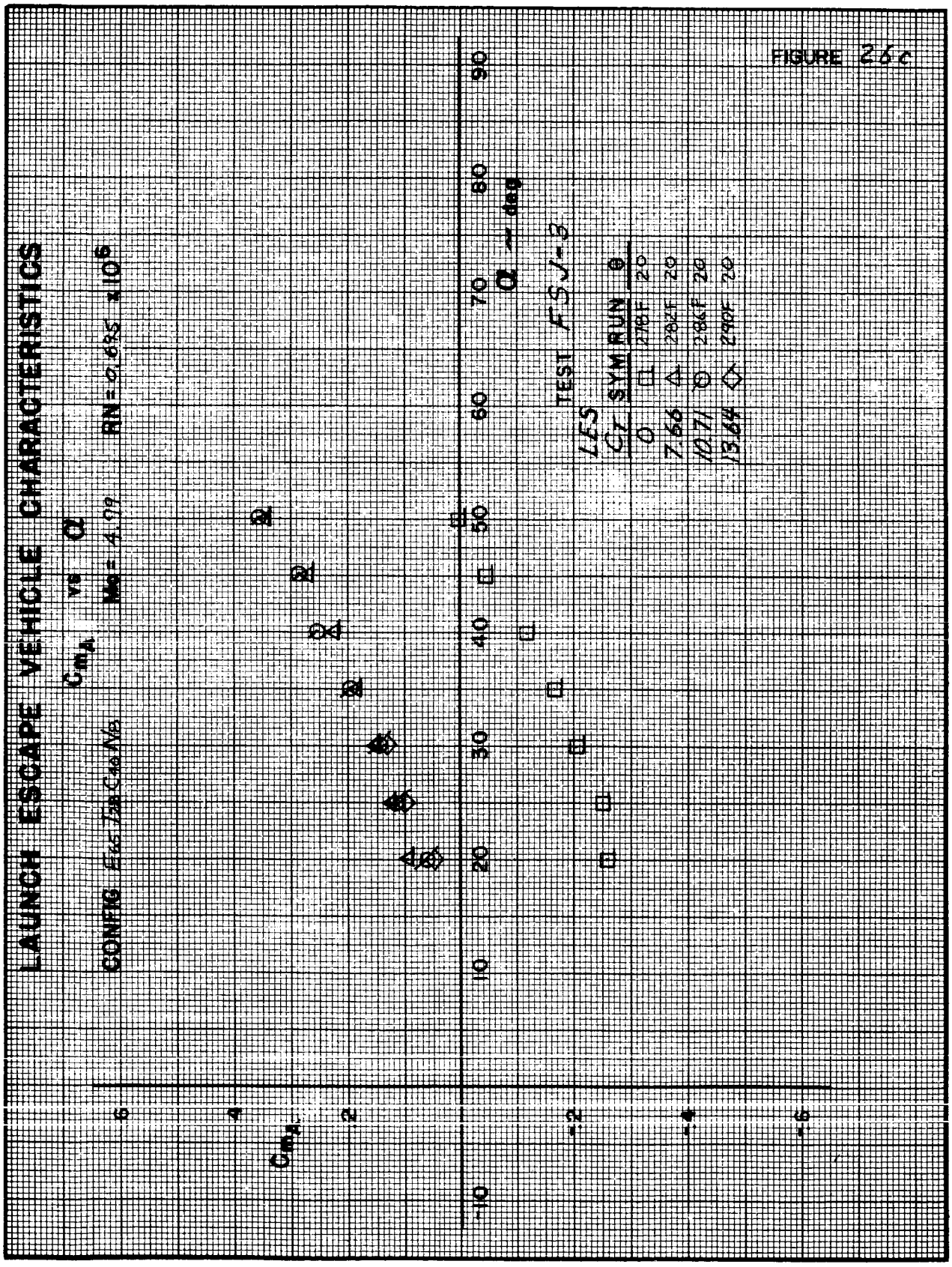

FIGURE 26c

CONFIDENTIAL

~~CONFIDENTIAL~~

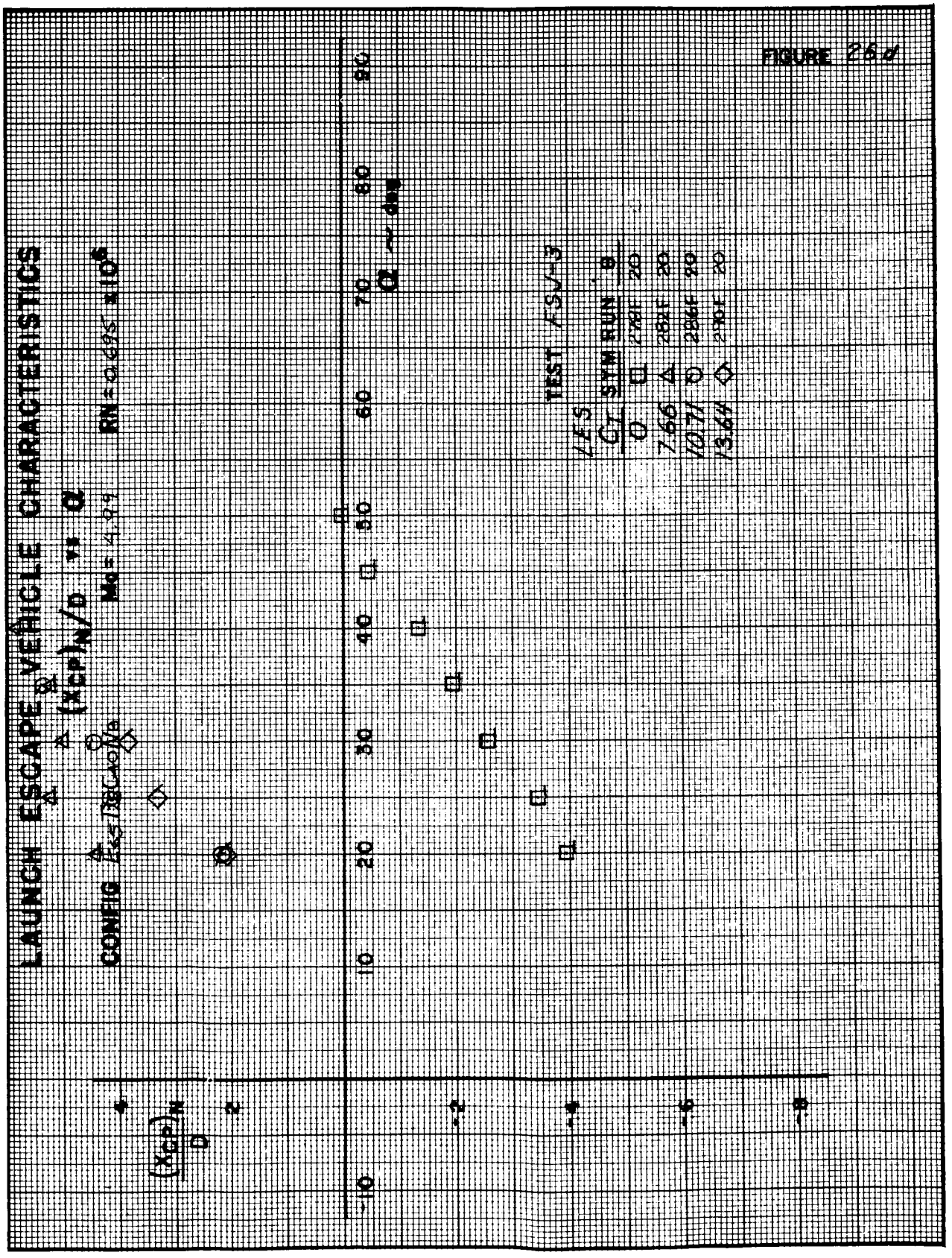

FIGURE 26d

~~CONFIDENTIAL~~

CONFIDENTIAL

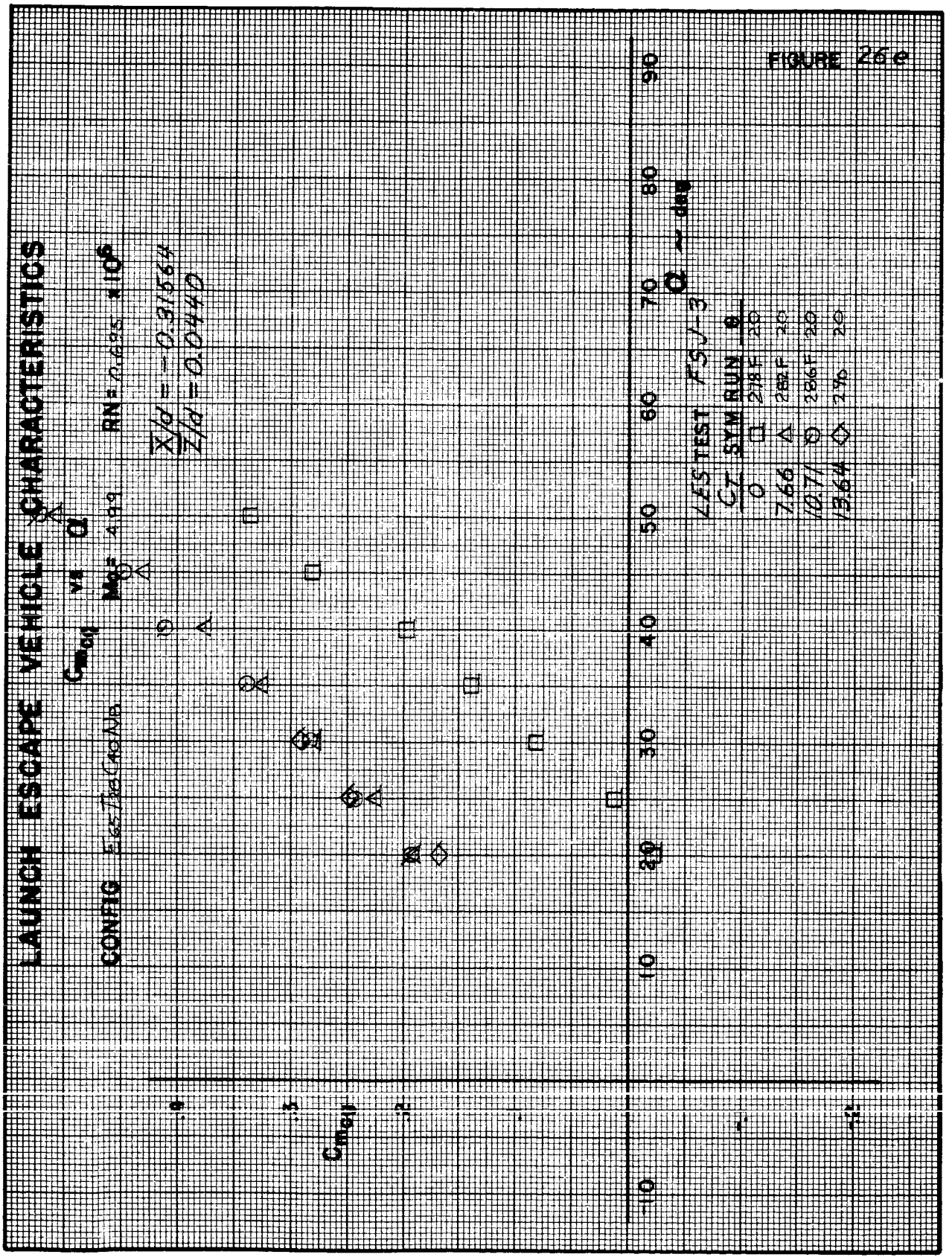

CONFIDENTIAL

~~CONFIDENTIAL~~

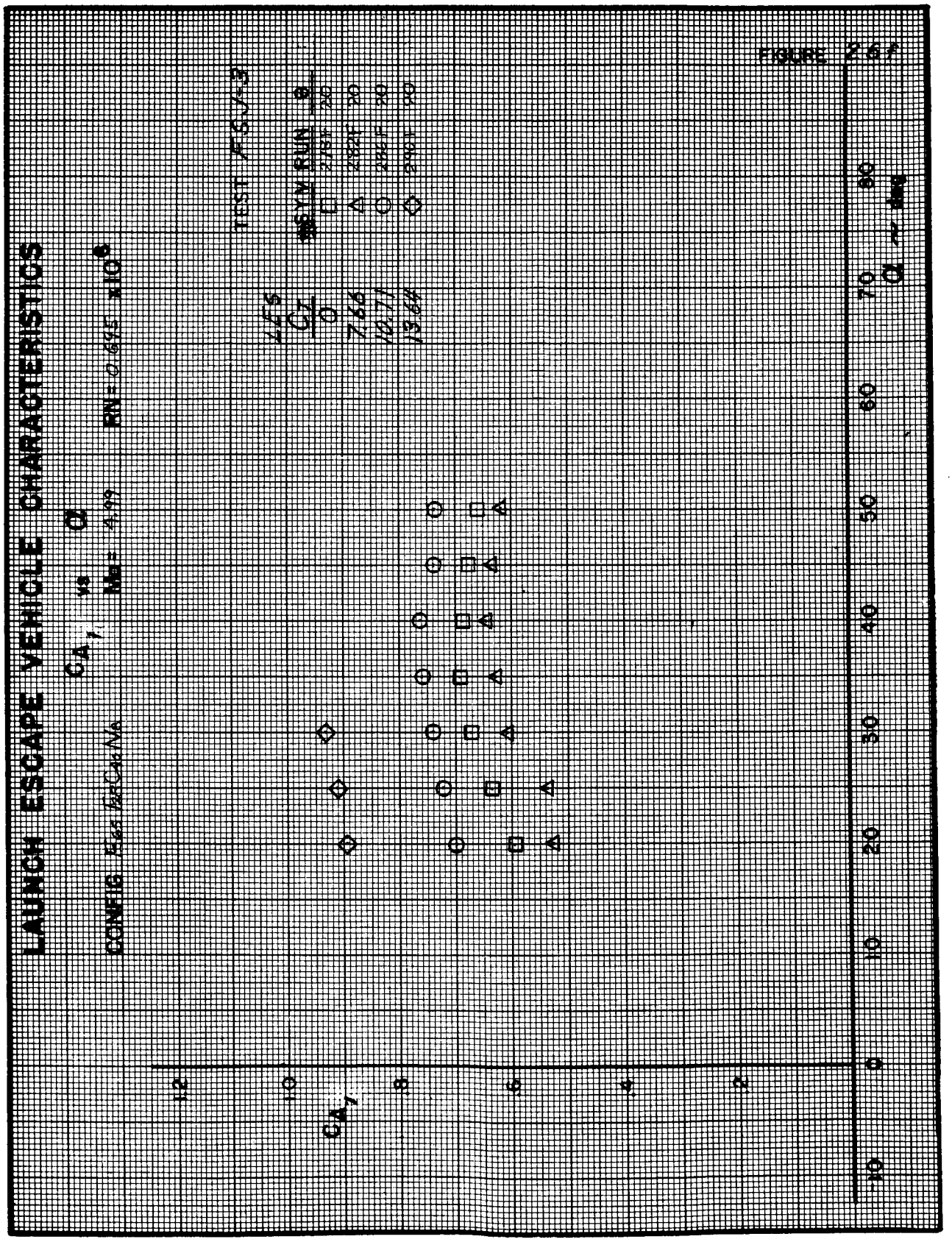

FIGURE 26

~~CONFIDENTIAL~~

CONFIDENTIAL

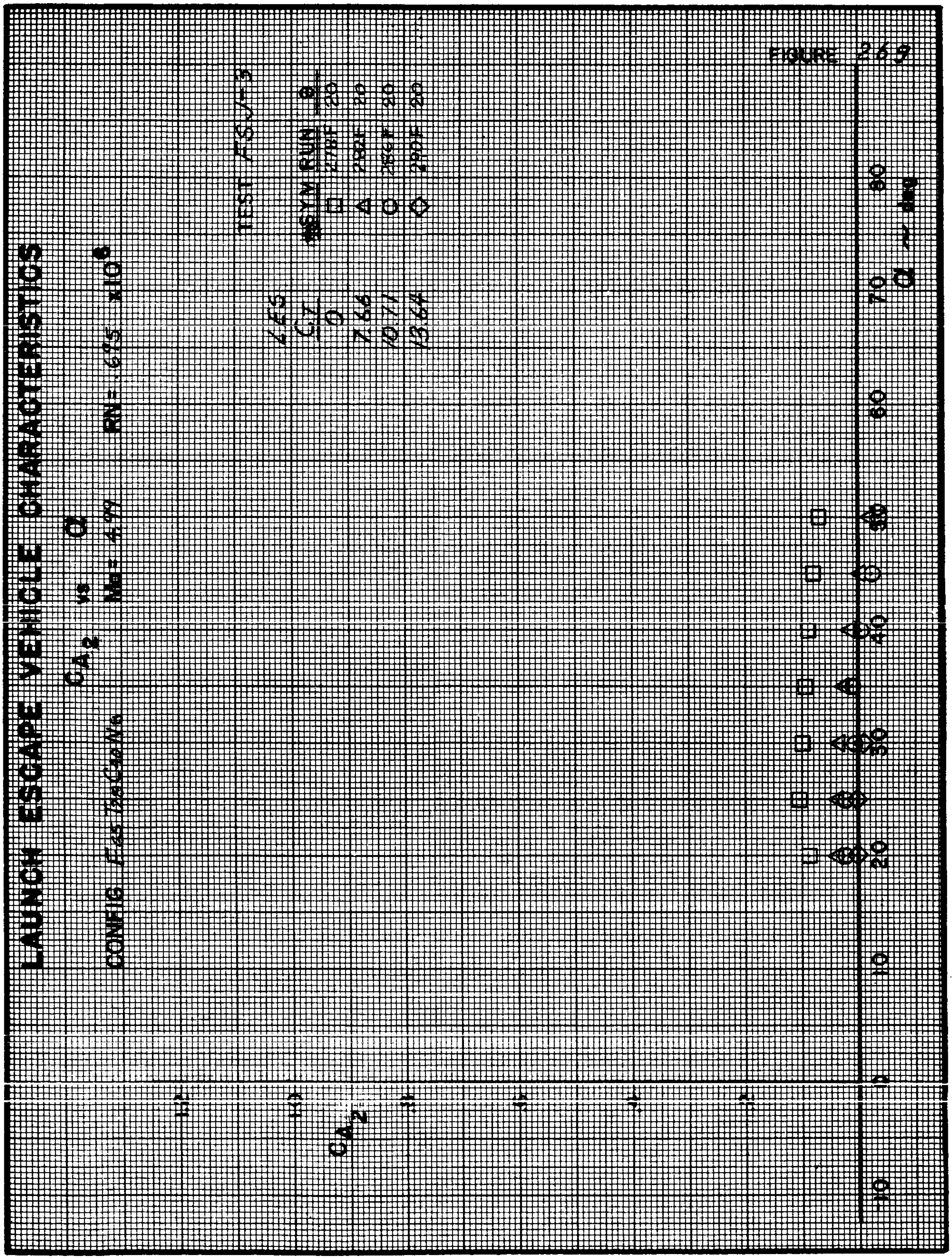

[redacted]

~~CONFIDENTIAL~~

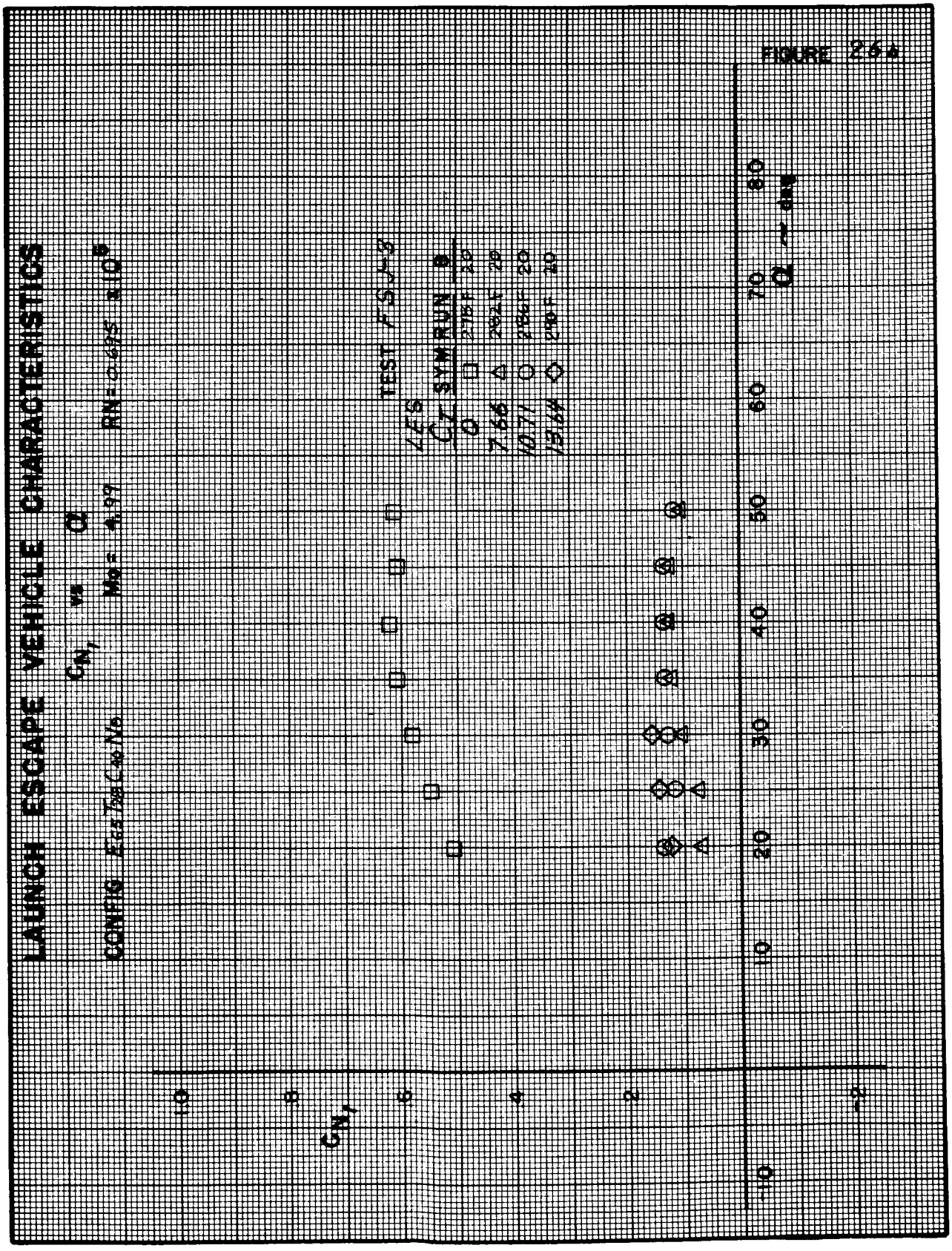

FIGURE 26a

~~CONFIDENTIAL~~

C[redacted]

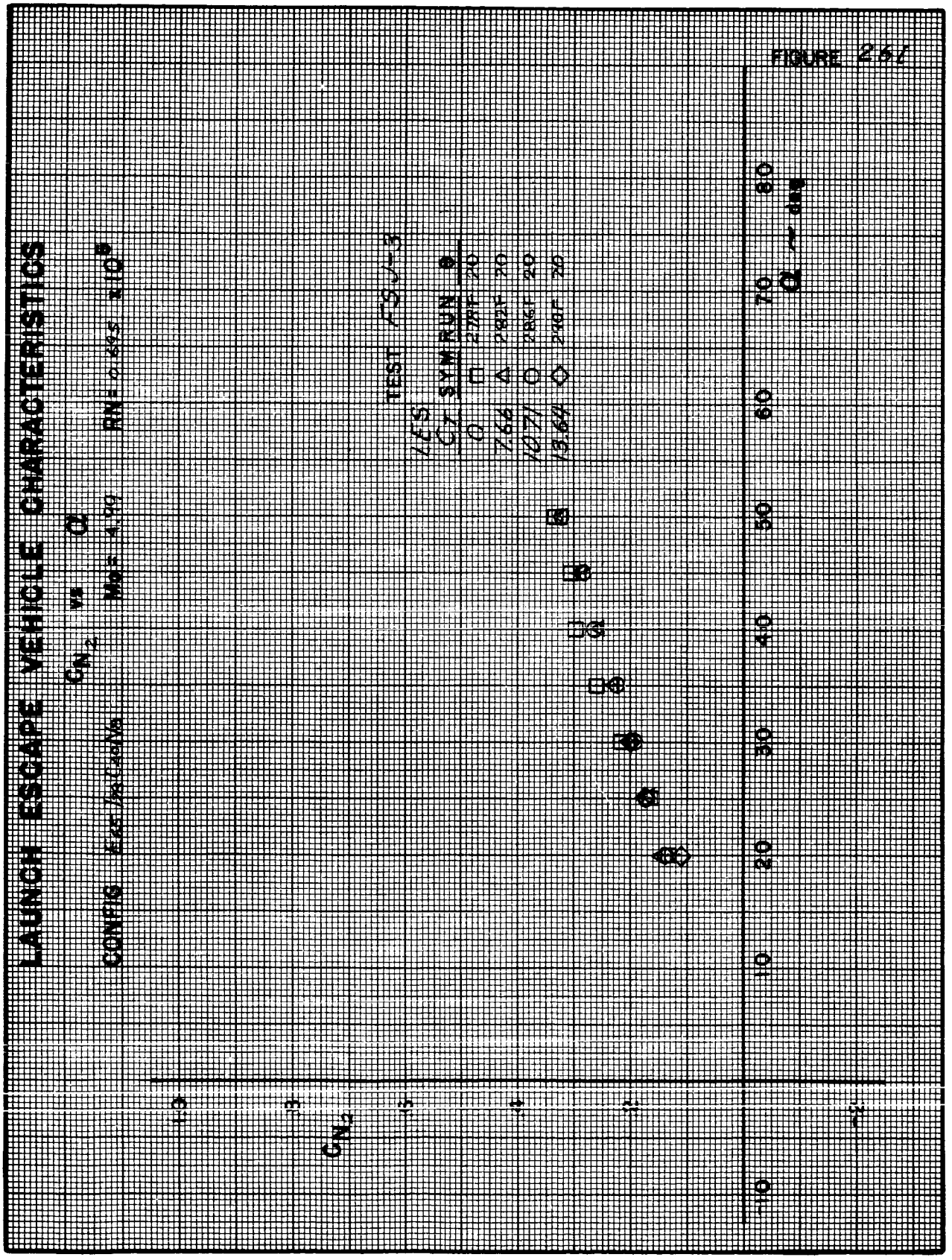

FIGURE 261

[redacted]

~~CONFIDENTIAL~~

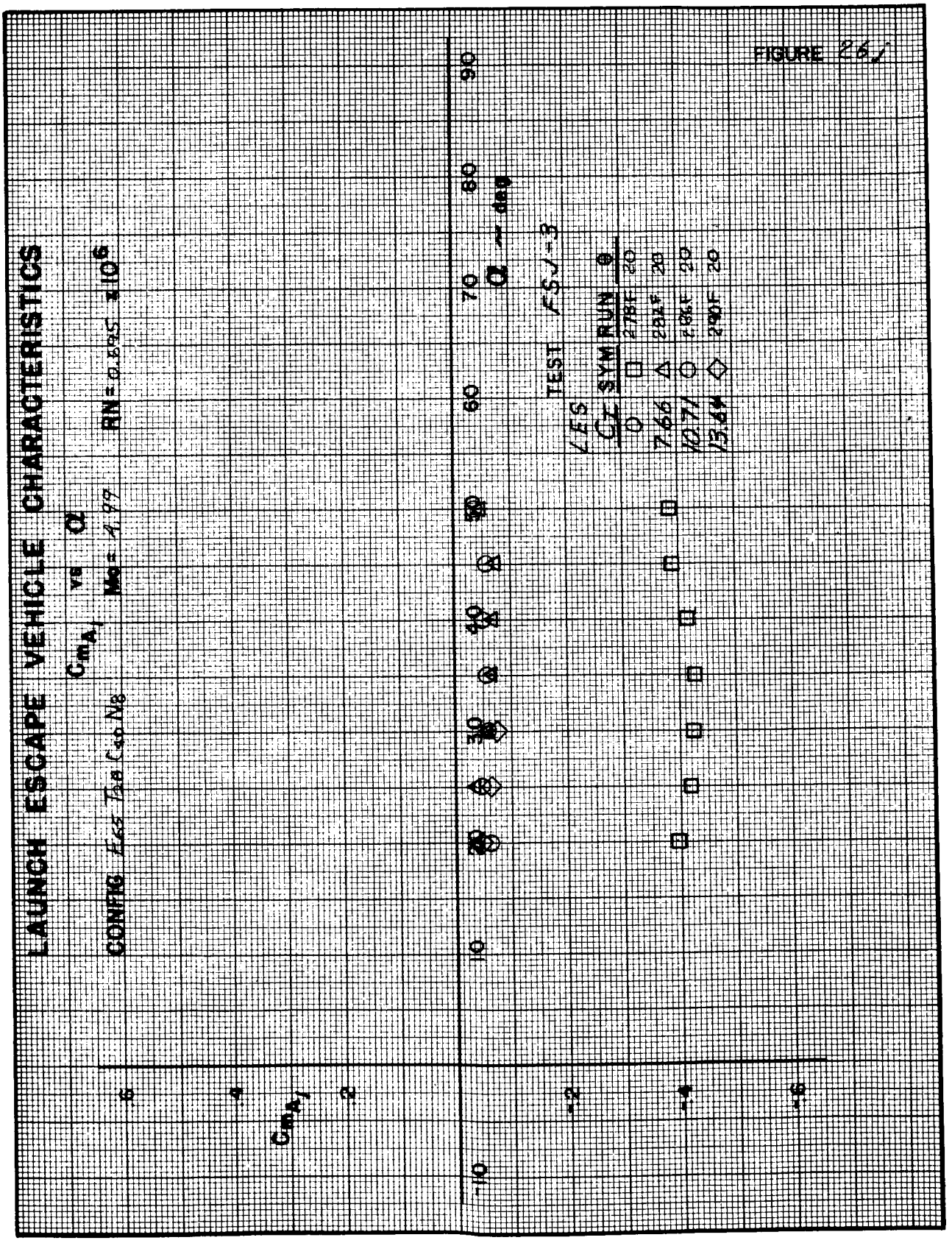

FIGURE 26

~~CONFIDENTIAL~~

~~CONFIDENTIAL~~

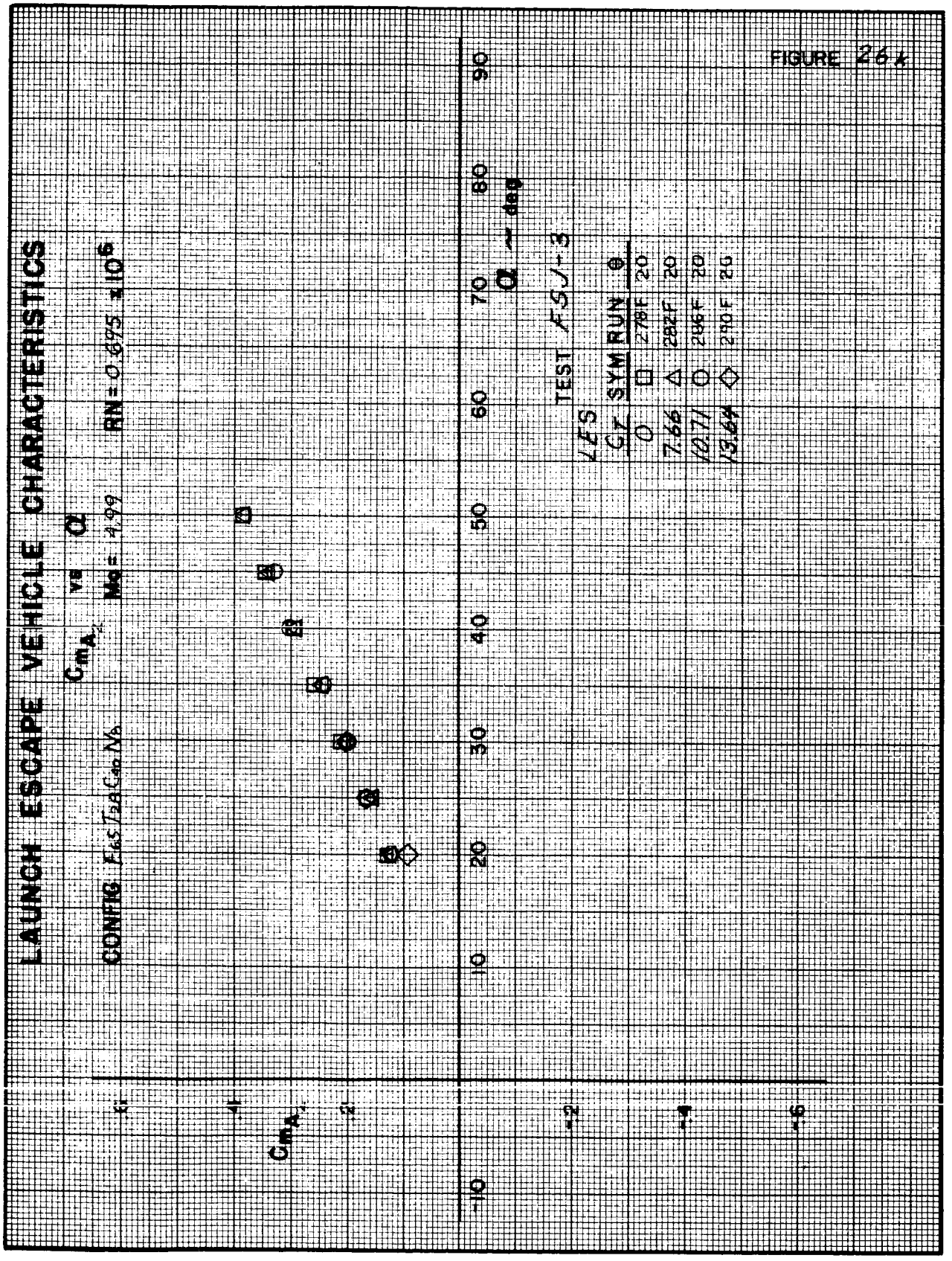

FIGURE 26 k

~~CONFIDENTIAL~~

~~CONFIDENTIAL~~

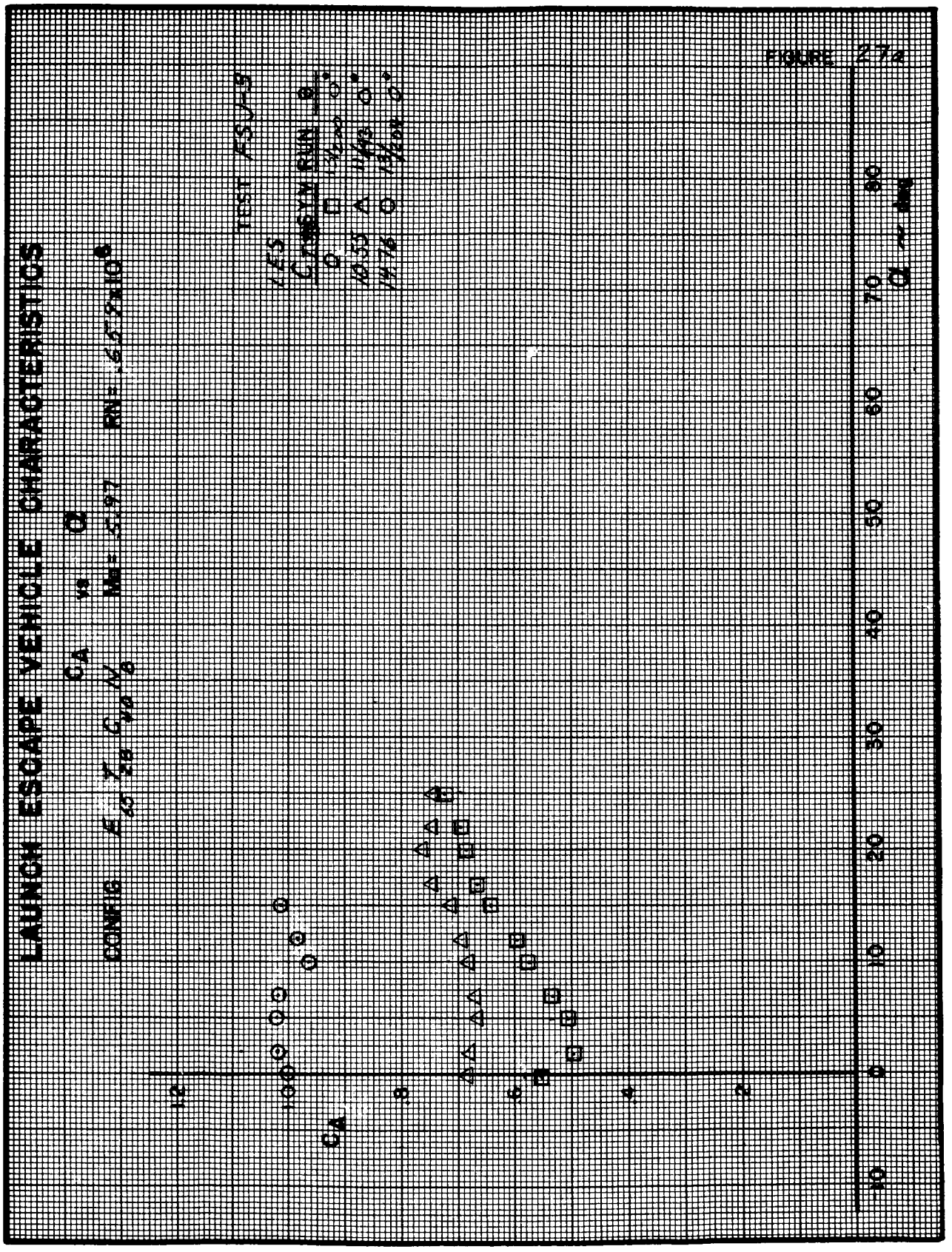

FIGURE 27a

~~CONFIDENTIAL~~

CONFIDENTIAL

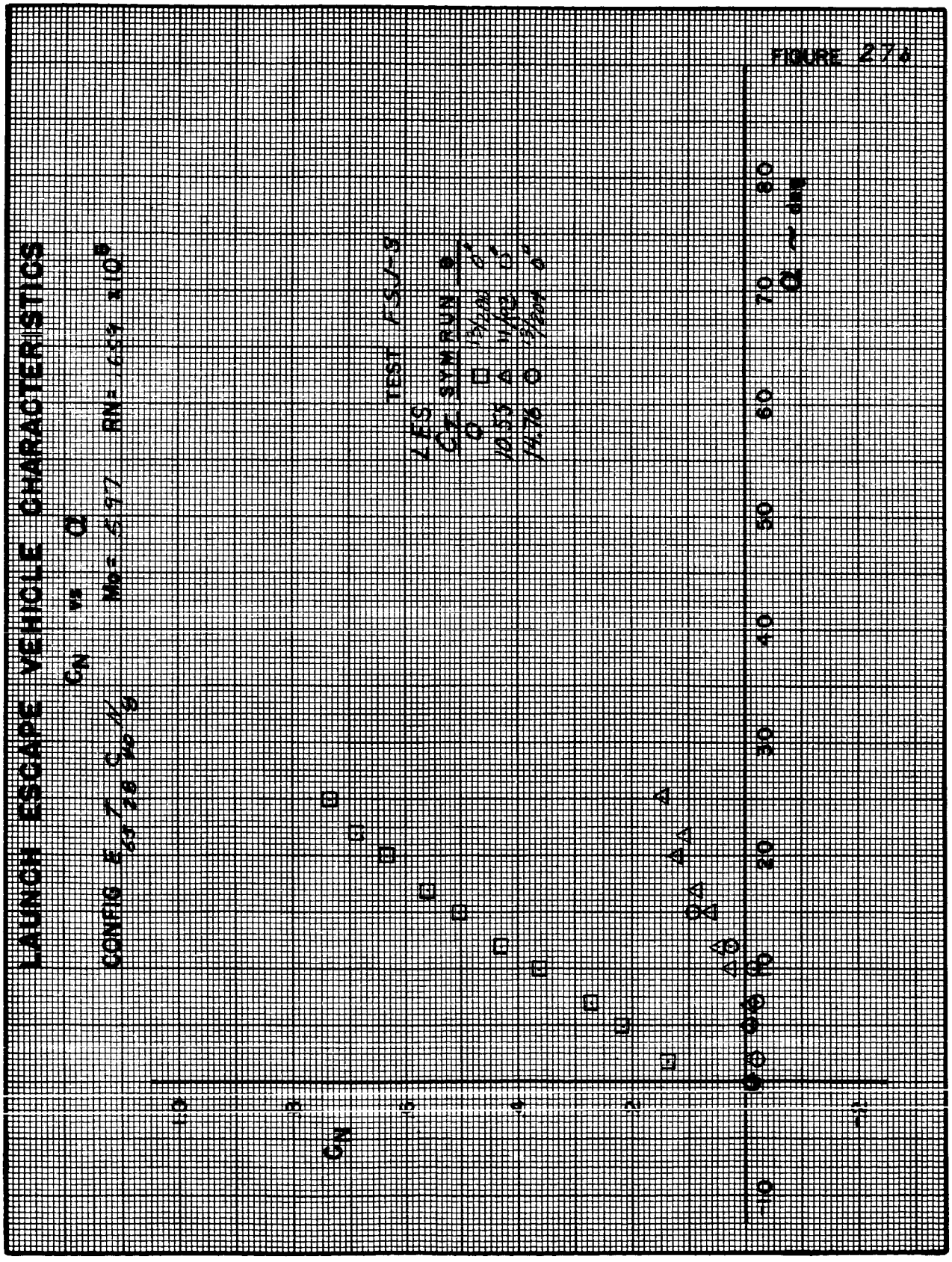

FIGURE 27a

CONFIDENTIAL

~~CONFIDENTIAL~~

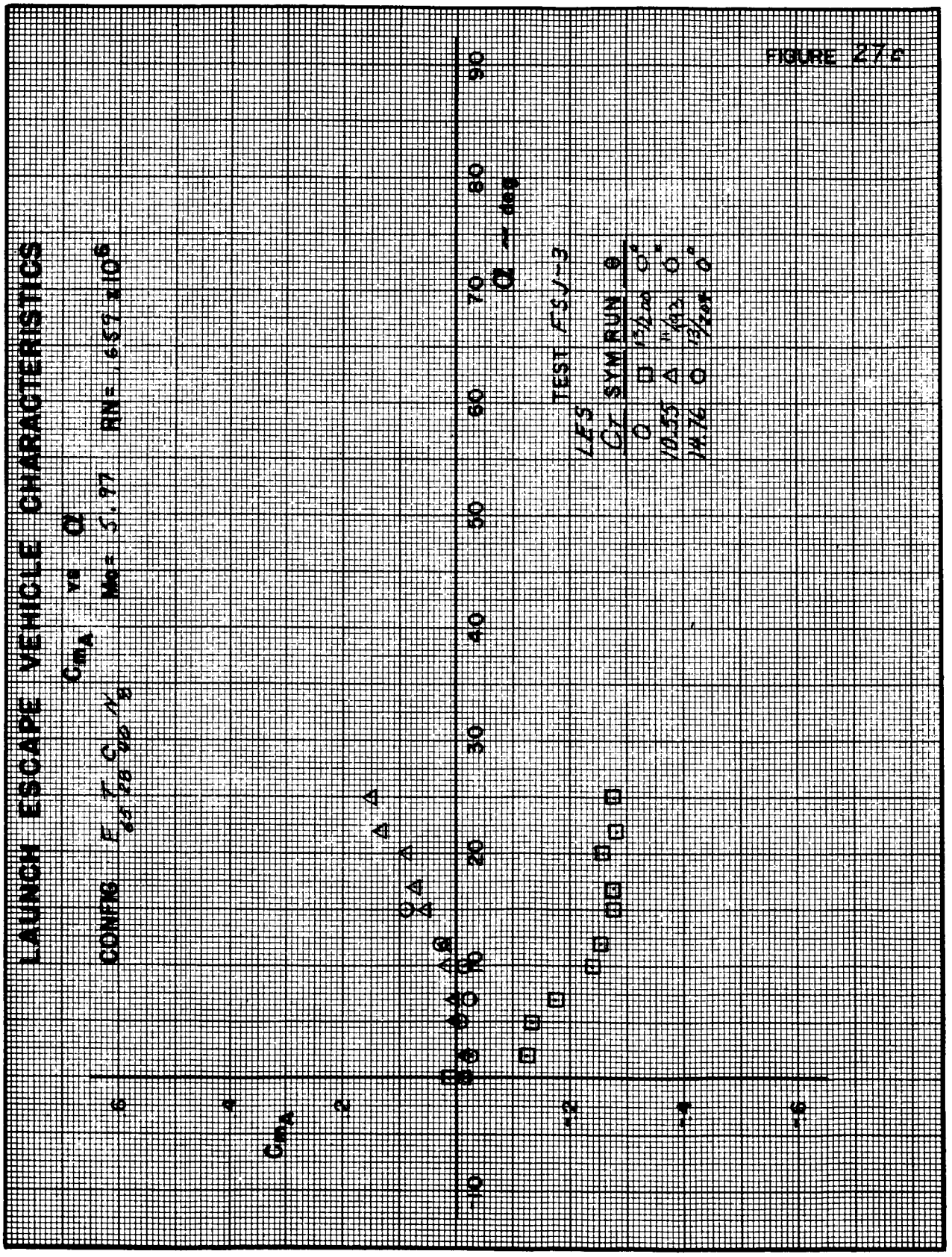

FIGURE 27c

~~CONFIDENTIAL~~

CONFIDENTIAL

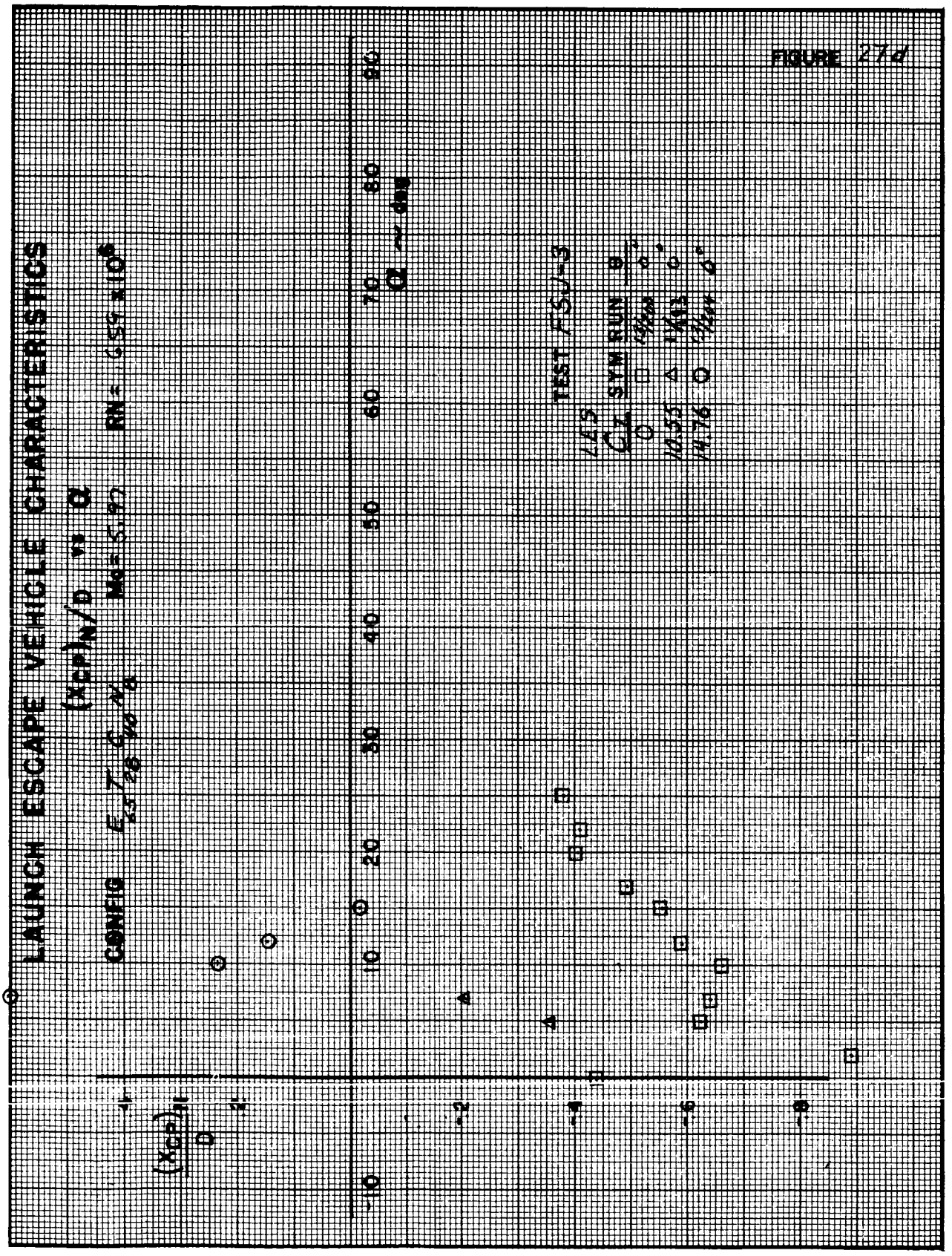

FIGURE 27d

CONFIDENTIAL

~~CONFIDENTIAL~~

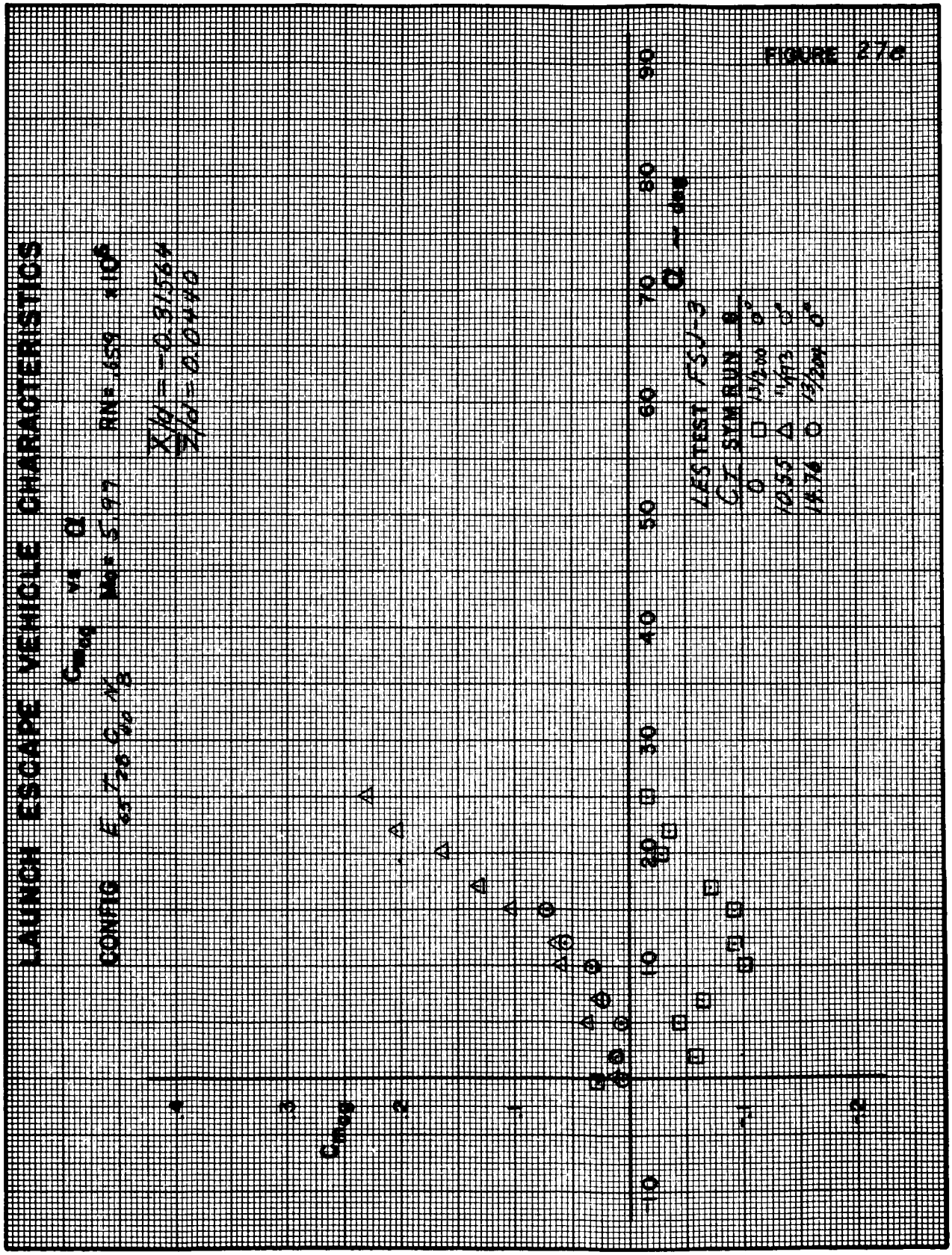

FIGURE 27e

~~CONFIDENTIAL~~

CONFIDENTIAL

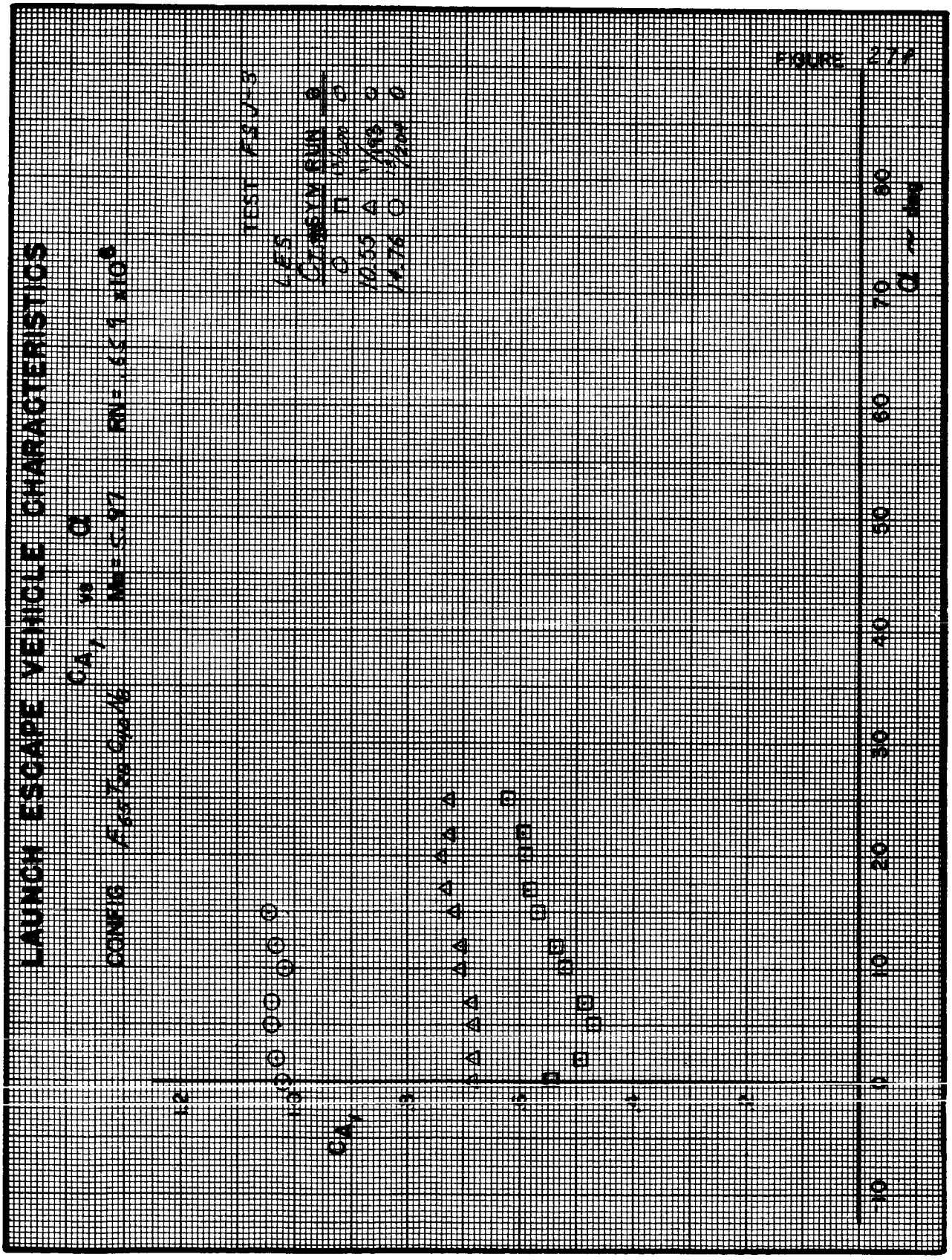

FIGURE 27

CONFIDENTIAL

~~CONFIDENTIAL~~

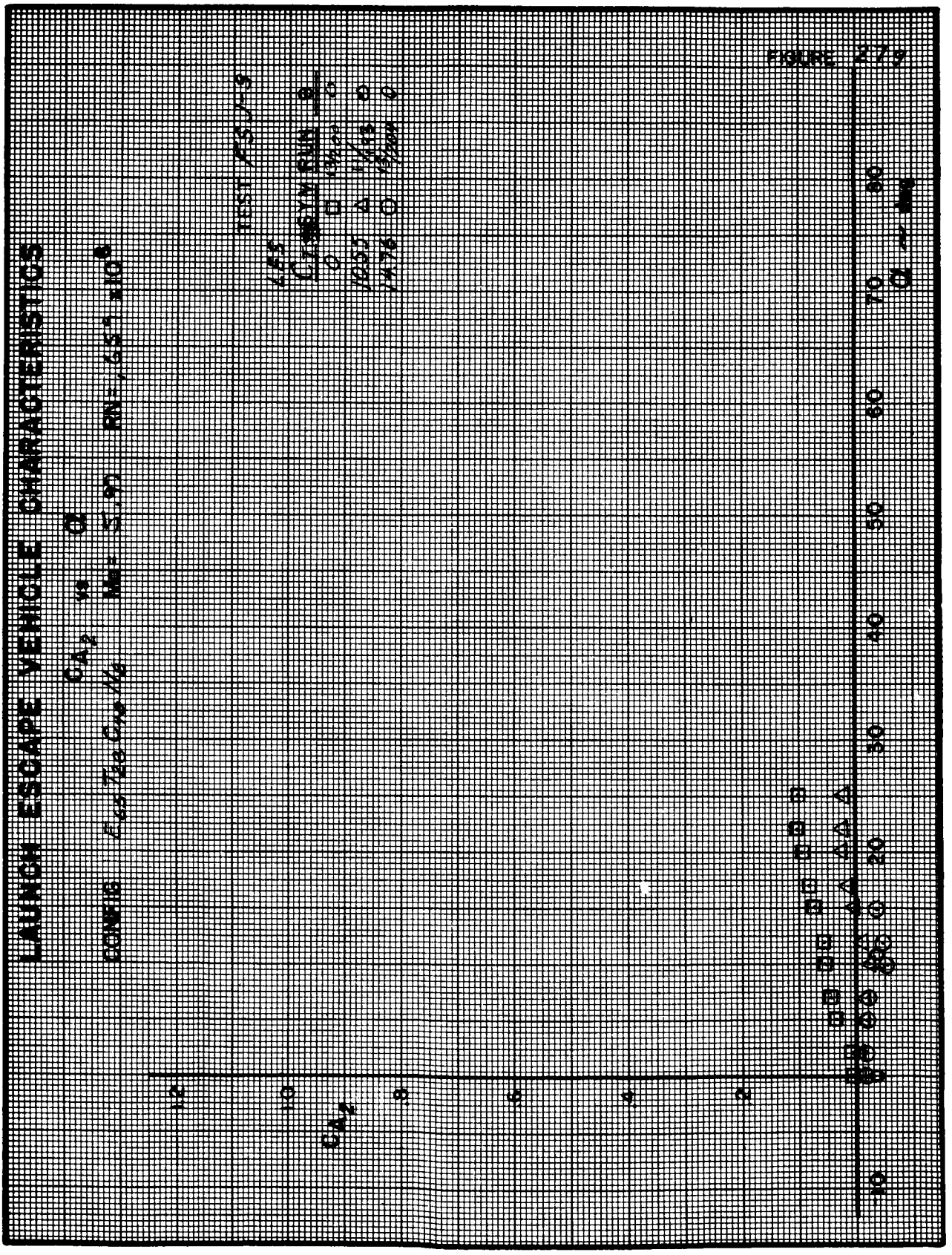

FIGURE 2.7.9

~~CONFIDENTIAL~~

CONFIDENTIAL

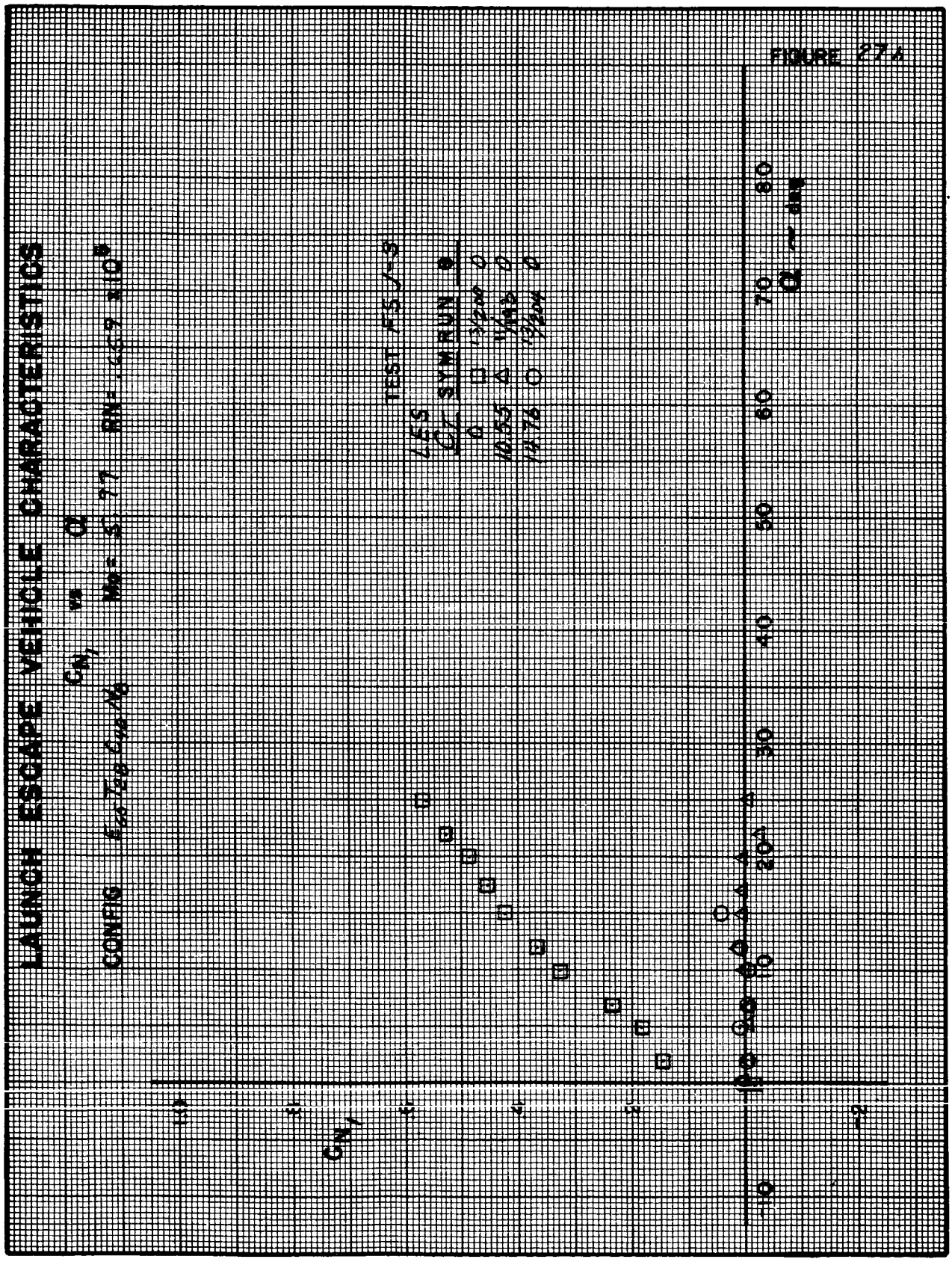

FIGURE 27A

CONFIDENTIAL

~~CONFIDENTIAL~~

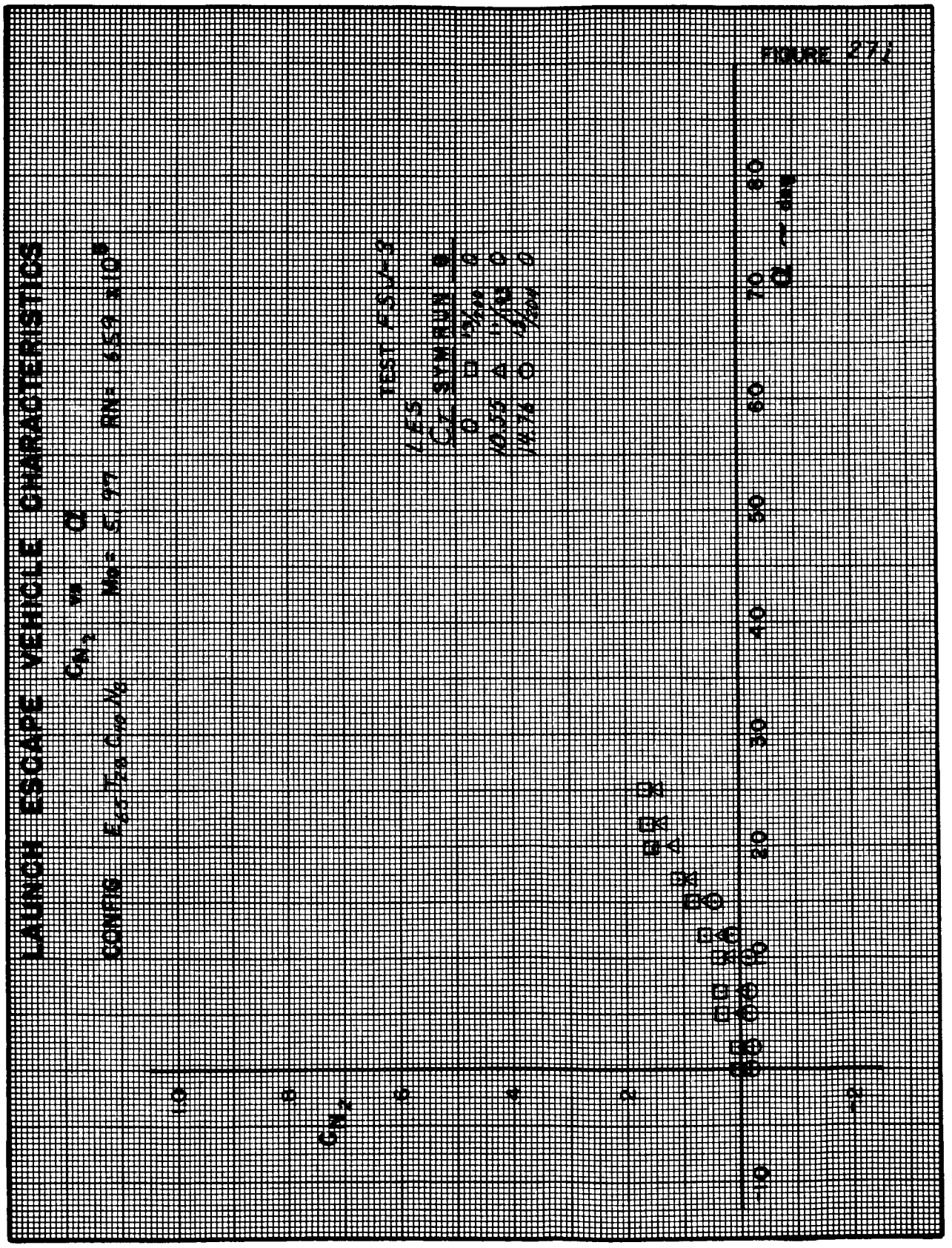

FIGURE 27.

~~CONFIDENTIAL~~

CONFIDENTIAL

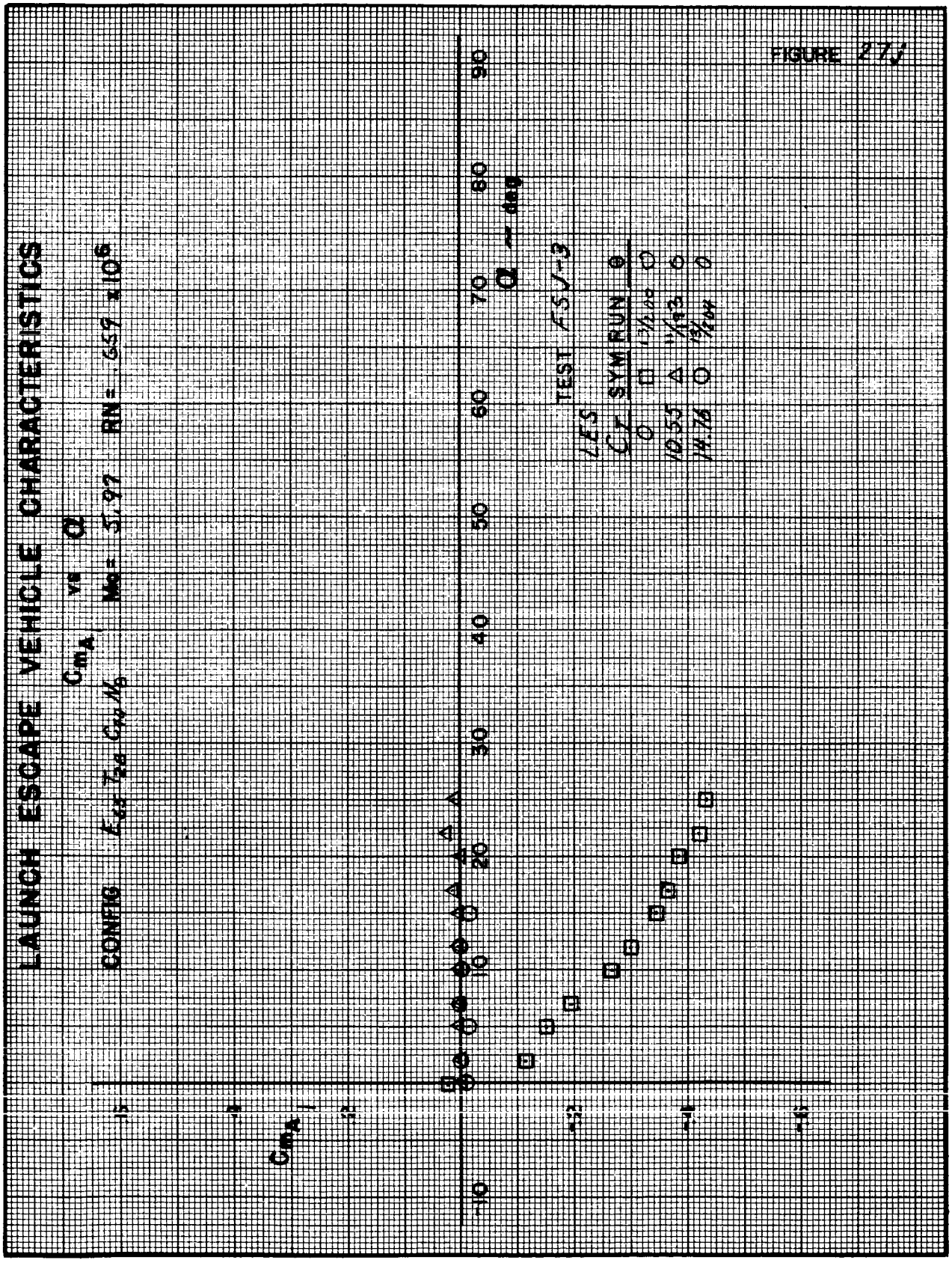

FIGURE 27

CONFIDENTIAL

~~CONFIDENTIAL~~

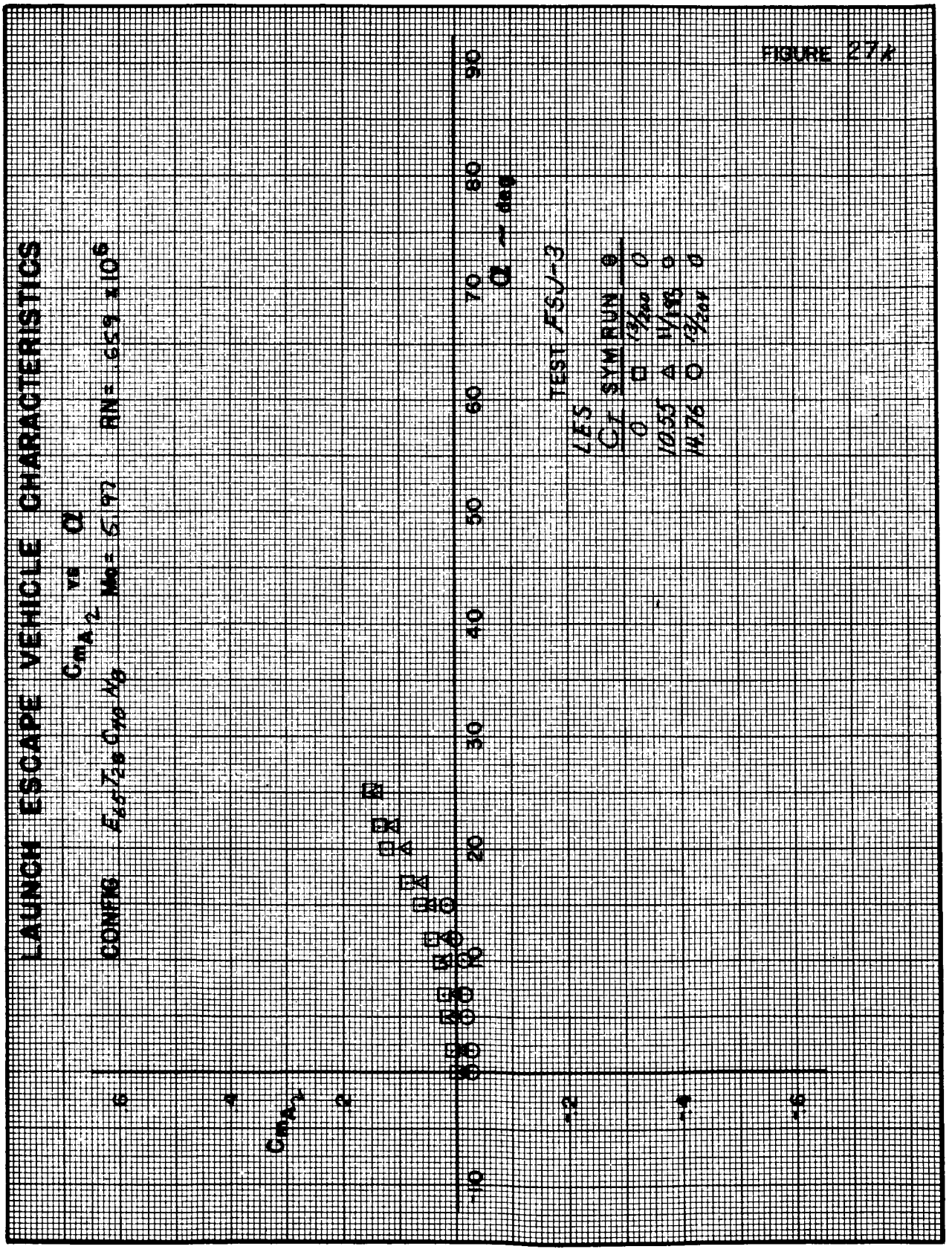

FIGURE 27k

~~CONFIDENTIAL~~

CONFIDENTIAL

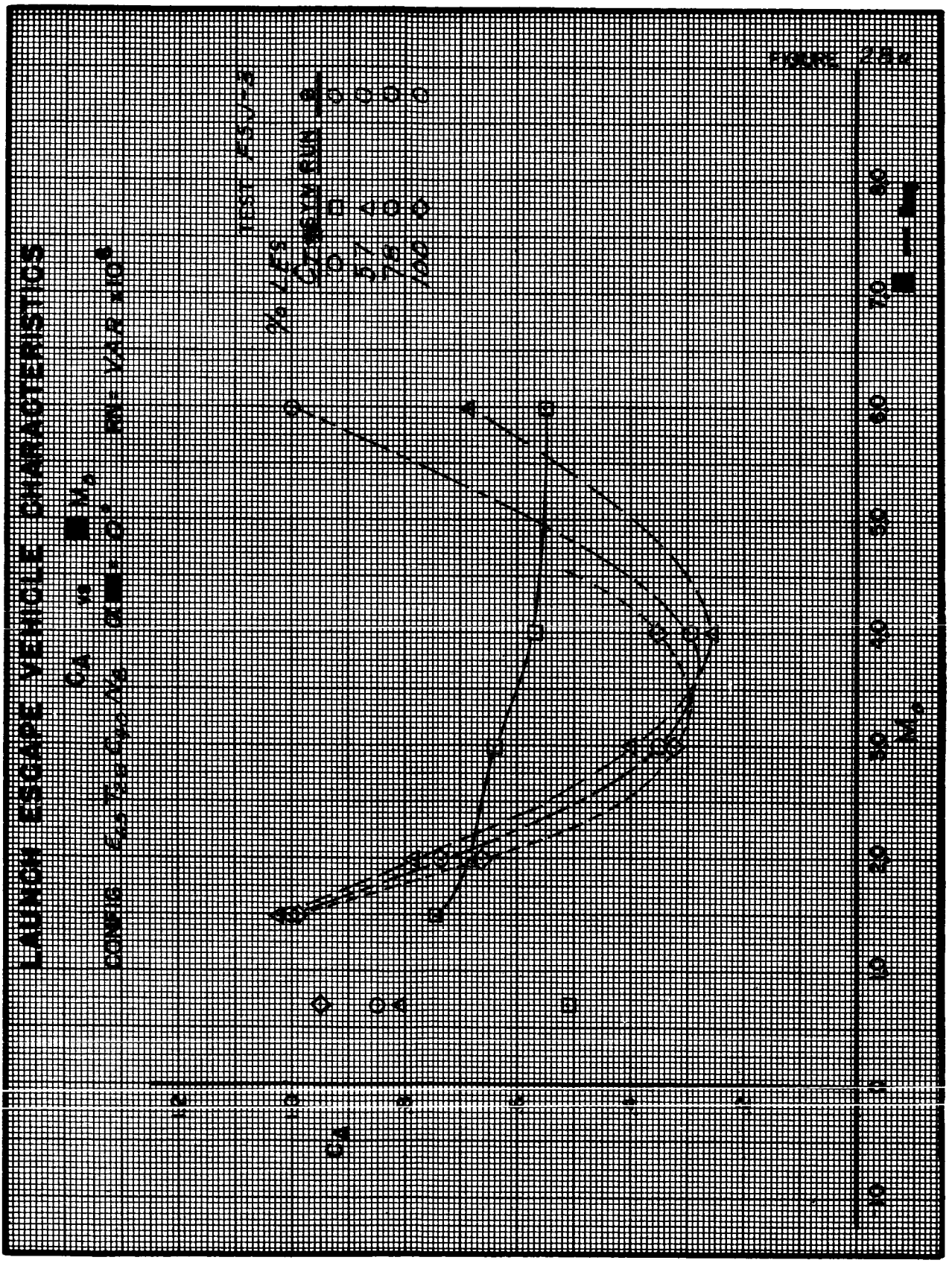

CONFIDENTIAL

CONFIDENTIAL

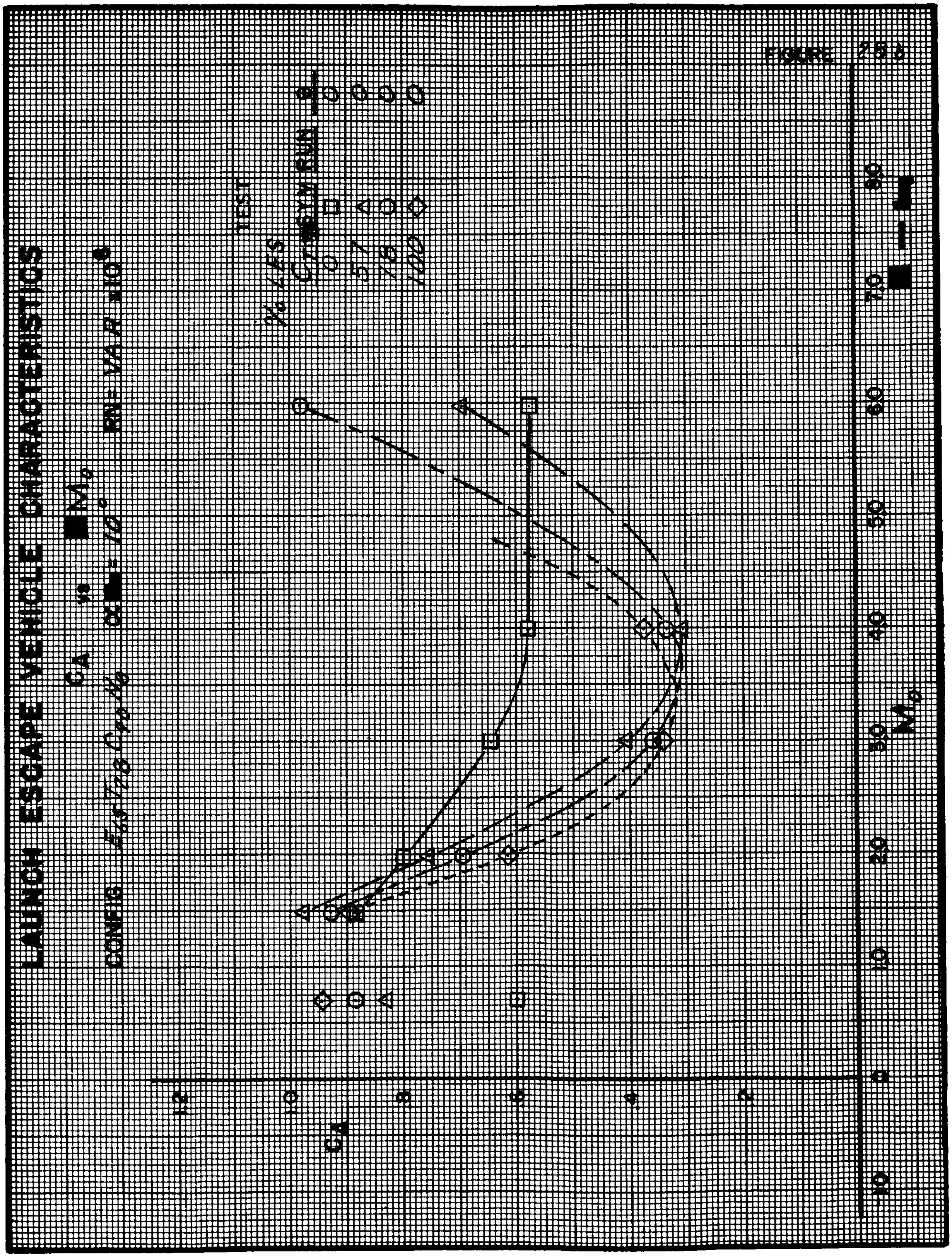

CONFIDENTIAL

CONFIDENTIAL

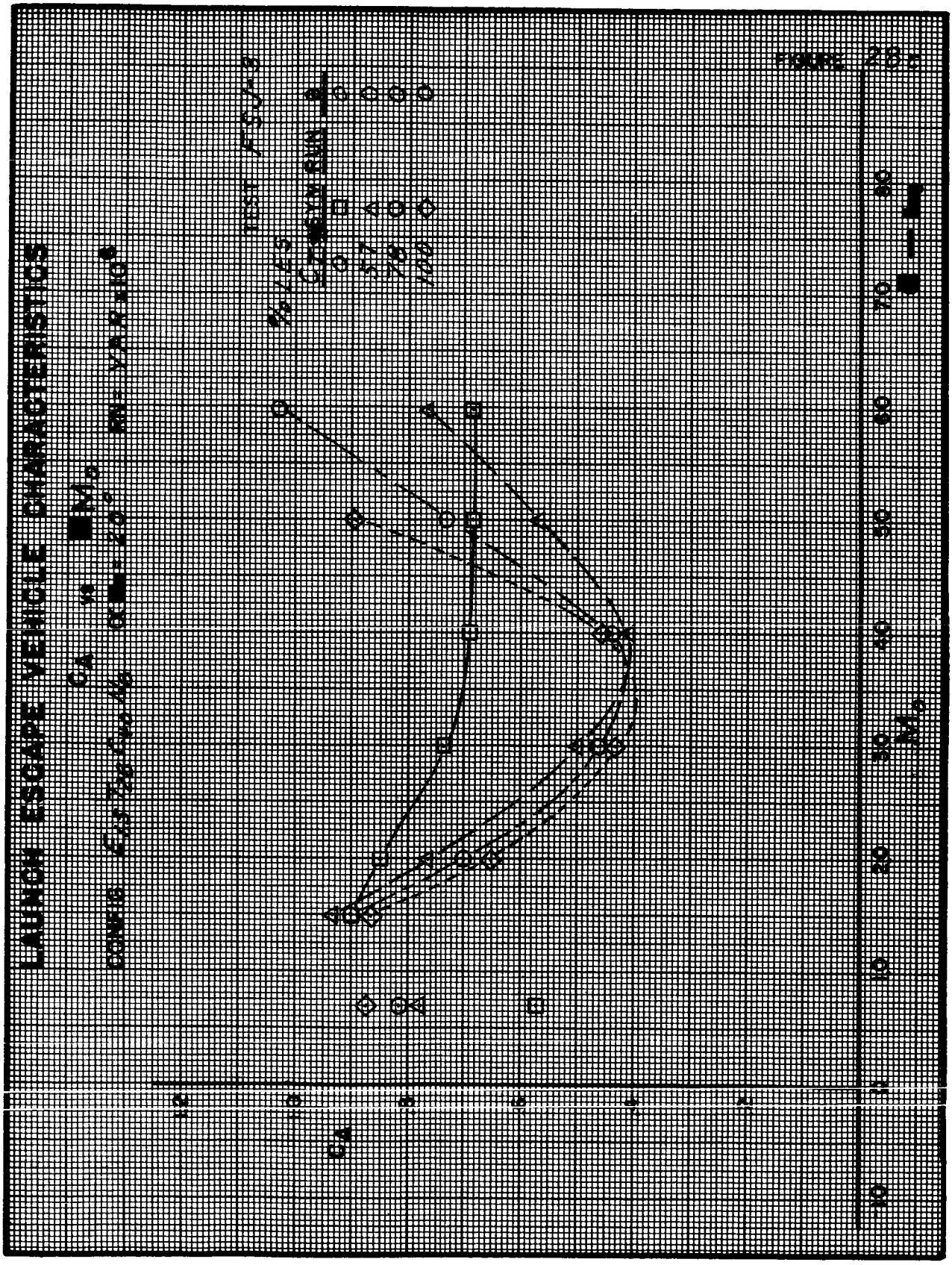

CONFIDENTIAL

~~CONFIDENTIAL~~

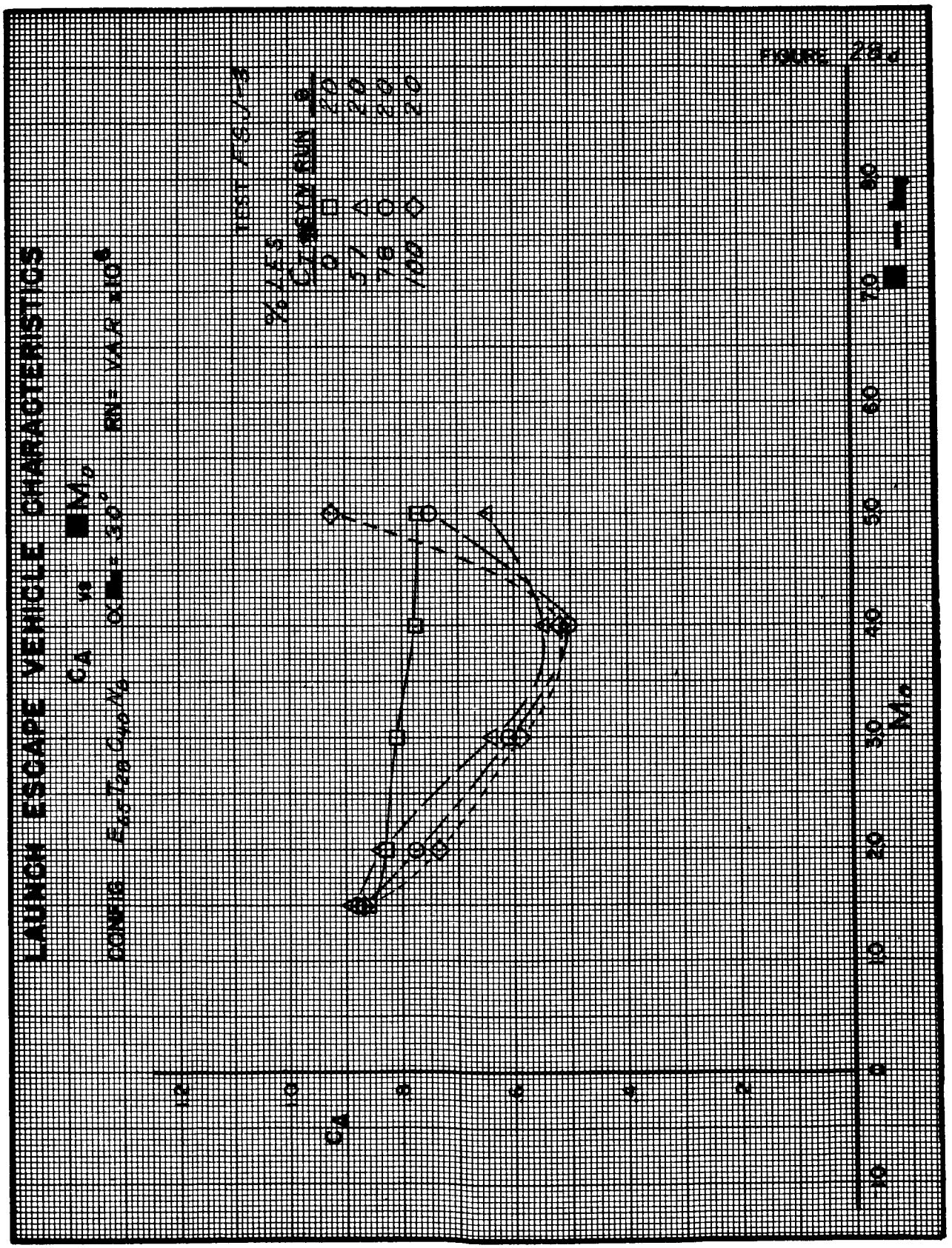

FIGURE 28d

~~CONFIDENTIAL~~

CONFIDENTIAL

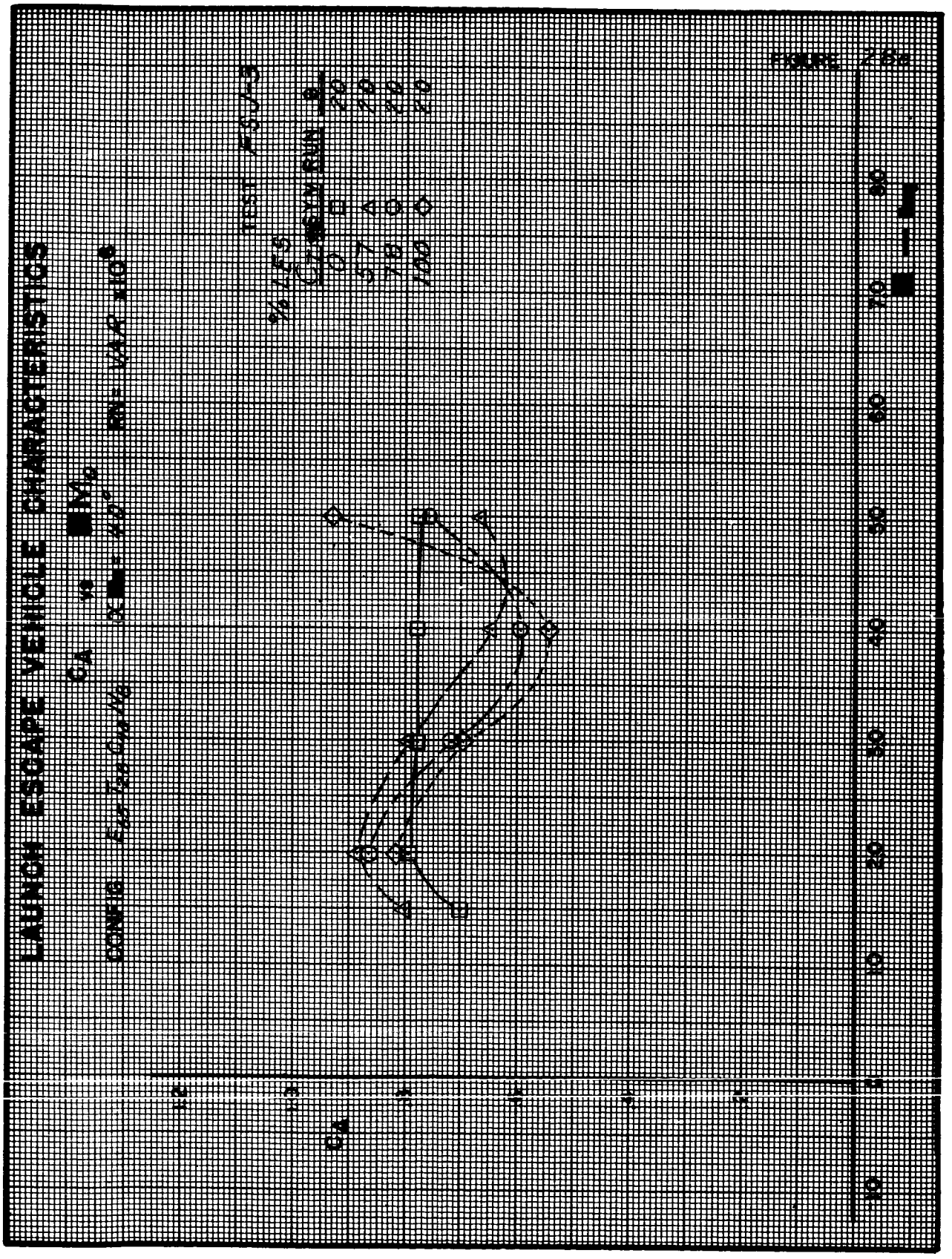

FIGURE 26a

CONFIDENTIAL

CONFIDENTIAL

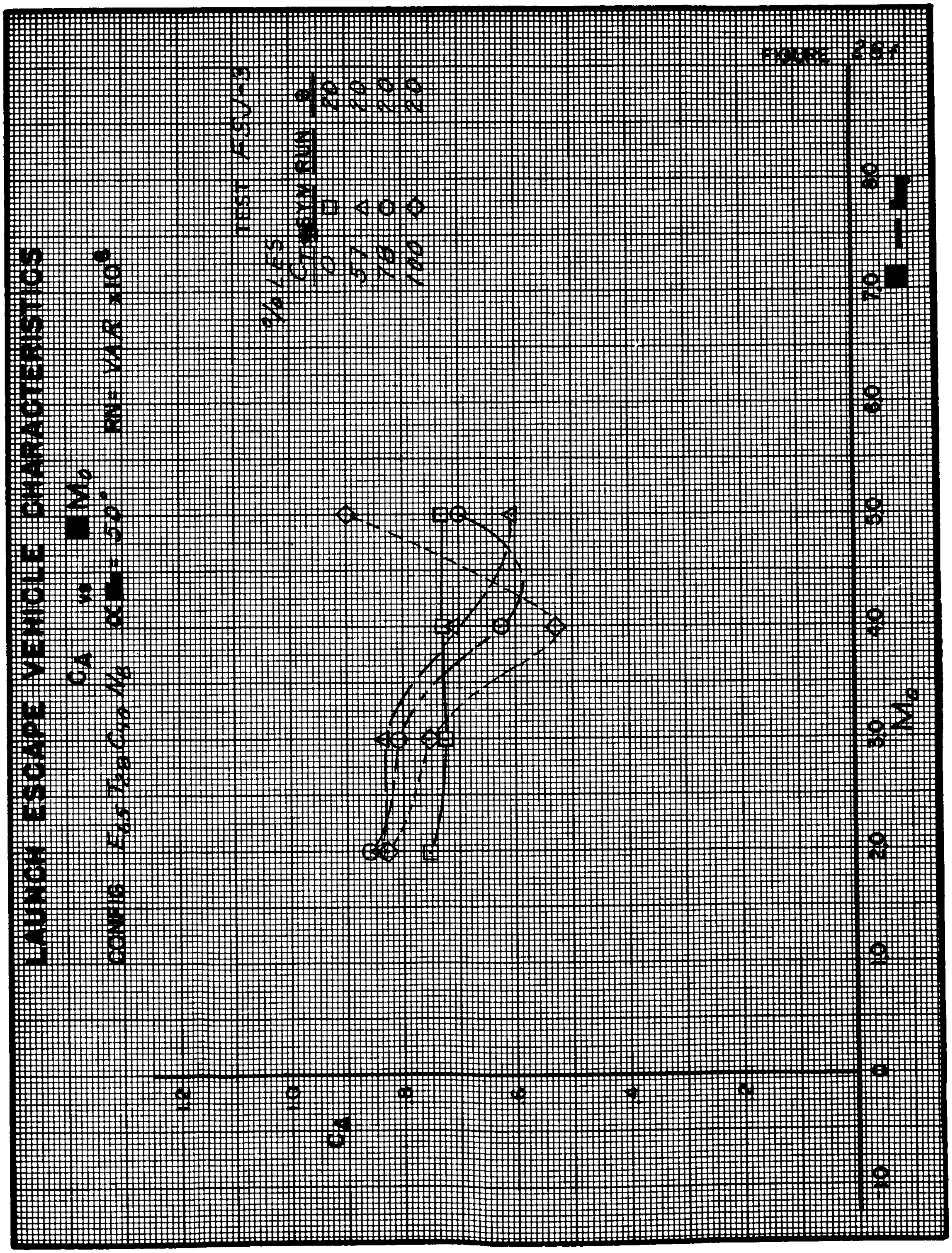

CONFIDENTIAL

FORM M-113-N2- (REV. 3-61)

PREPARED BY:	NORTH AMERICAN AVIATION, INC. SPACE and INFORMATION SYSTEMS DIVISION	PAGE NO. OF
CHECKED BY:		REPORT NO.
DATE:		MODEL NO.

[redacted]

FIGURE 29a

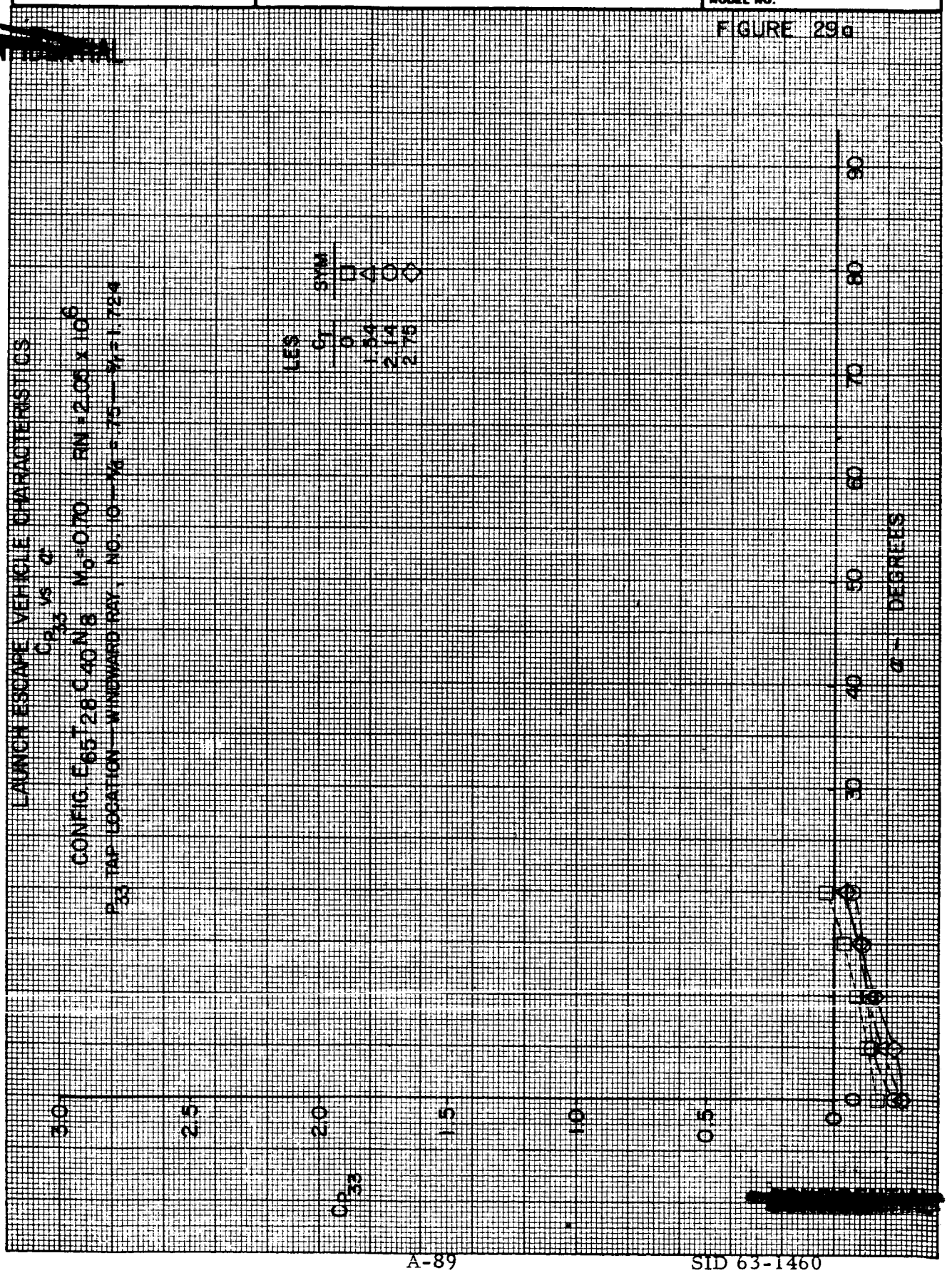

[redacted]

FORM M-113-N2- (REV. 3-61)

PREPARED BY:	NORTH AMERICAN AVIATION, INC. SPACE and INFORMATION SYSTEMS DIVISION	PAGE NO. OF
CHECKED BY:		REPORT NO.
DATE:		MODEL NO.

~~CONFIDENTIAL~~

FIGURE 29 b

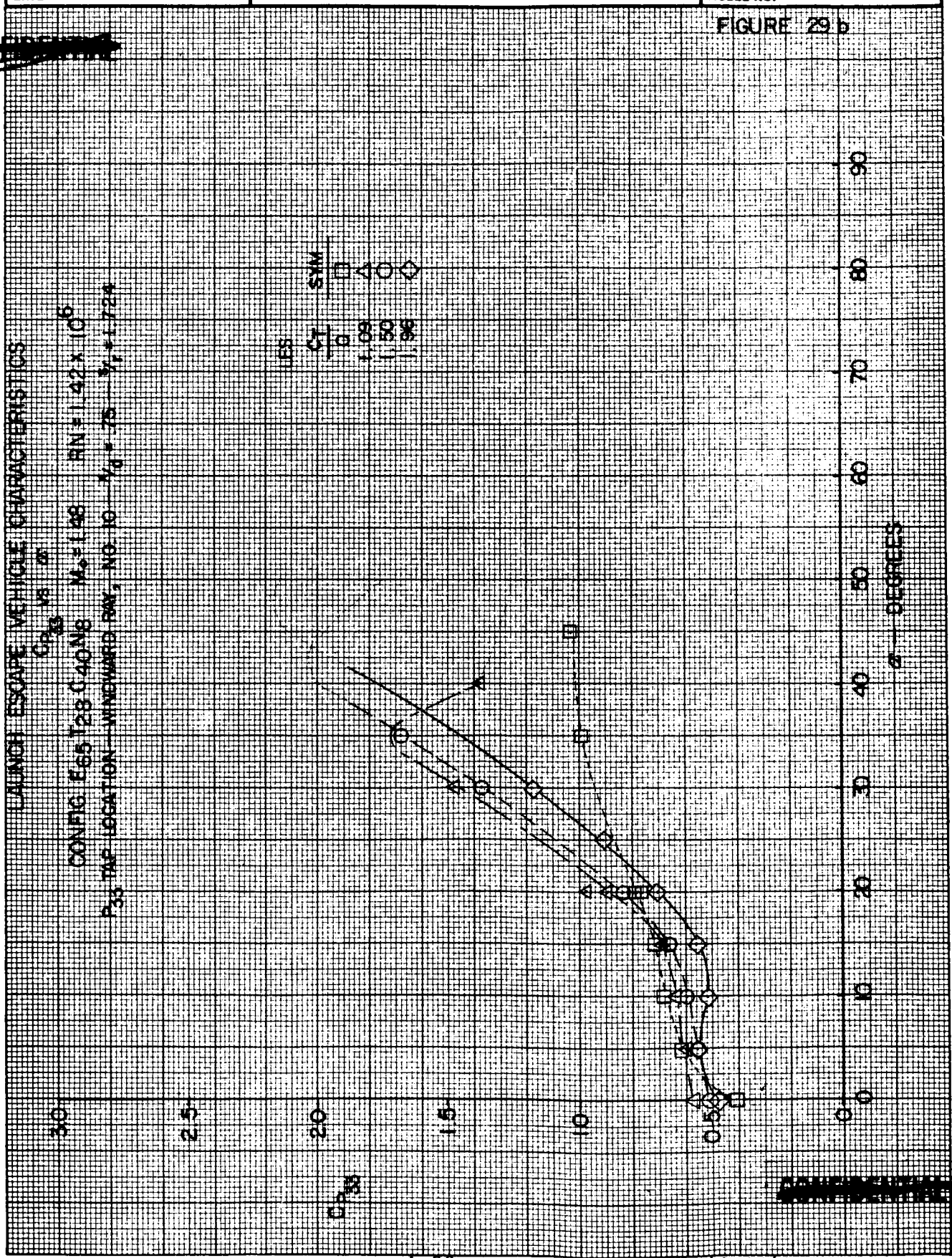

~~CONFIDENTIAL~~

FORM M-113-N2- (REV. 3-61)

PREPARED BY:	NORTH AMERICAN AVIATION, INC. SPACE and INFORMATION SYSTEMS DIVISION	PAGE NO. OF
CHECKED BY:		REPORT NO.
DATE:		MODEL NO.

[redacted]

FIGURE 29 c

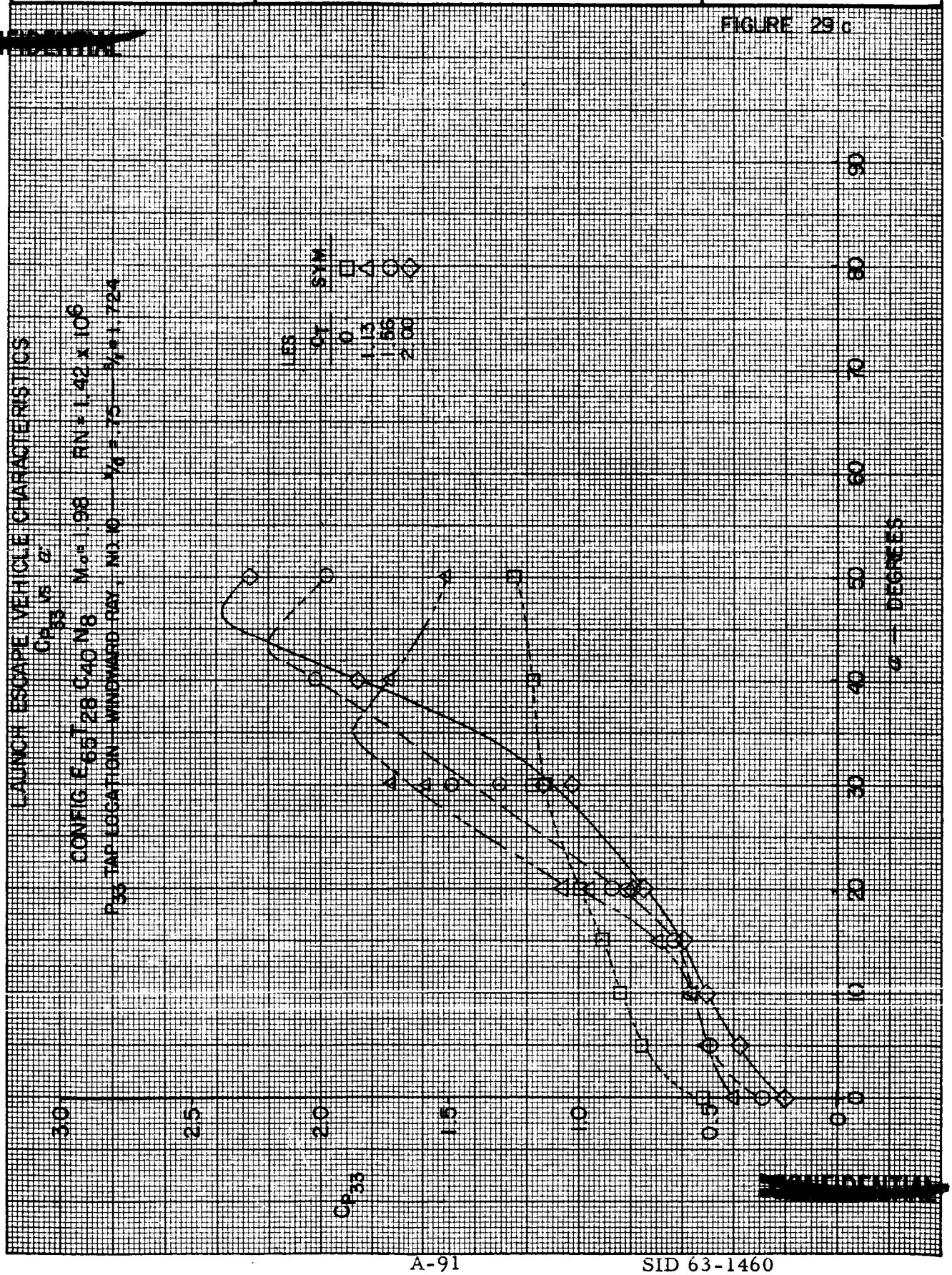

[redacted]

CONFIDENTIAL

FIGURE 29d

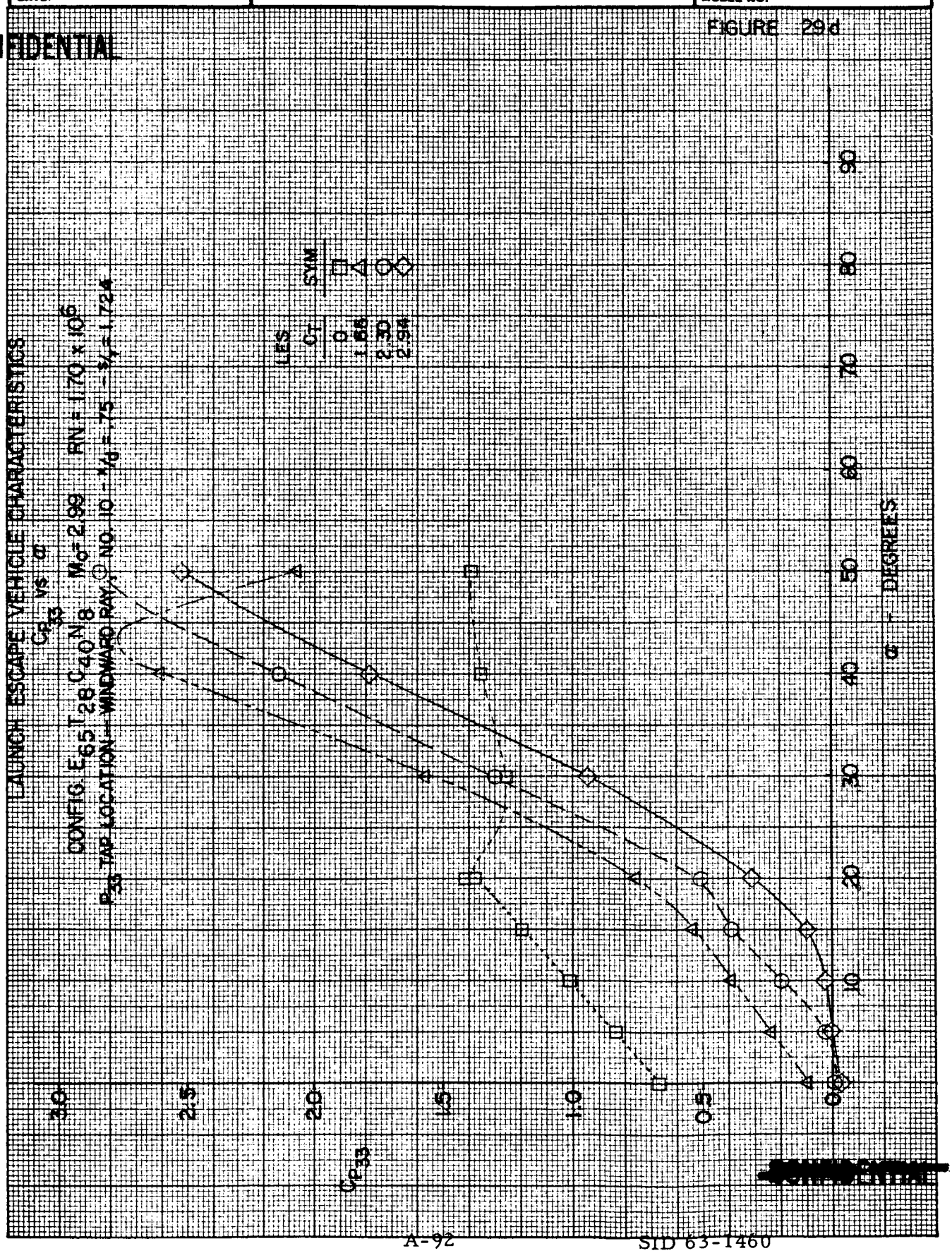

[redacted]

FORM M-113-N2- (REV. 3-61)

PREPARED BY:	NORTH AMERICAN AVIATION, INC. SPACE and INFORMATION SYSTEMS DIVISION	PAGE NO. OF
CHECKED BY:		REPORT NO.
DATE:		MODEL NO.

CON[redacted]

FIGURE 29e

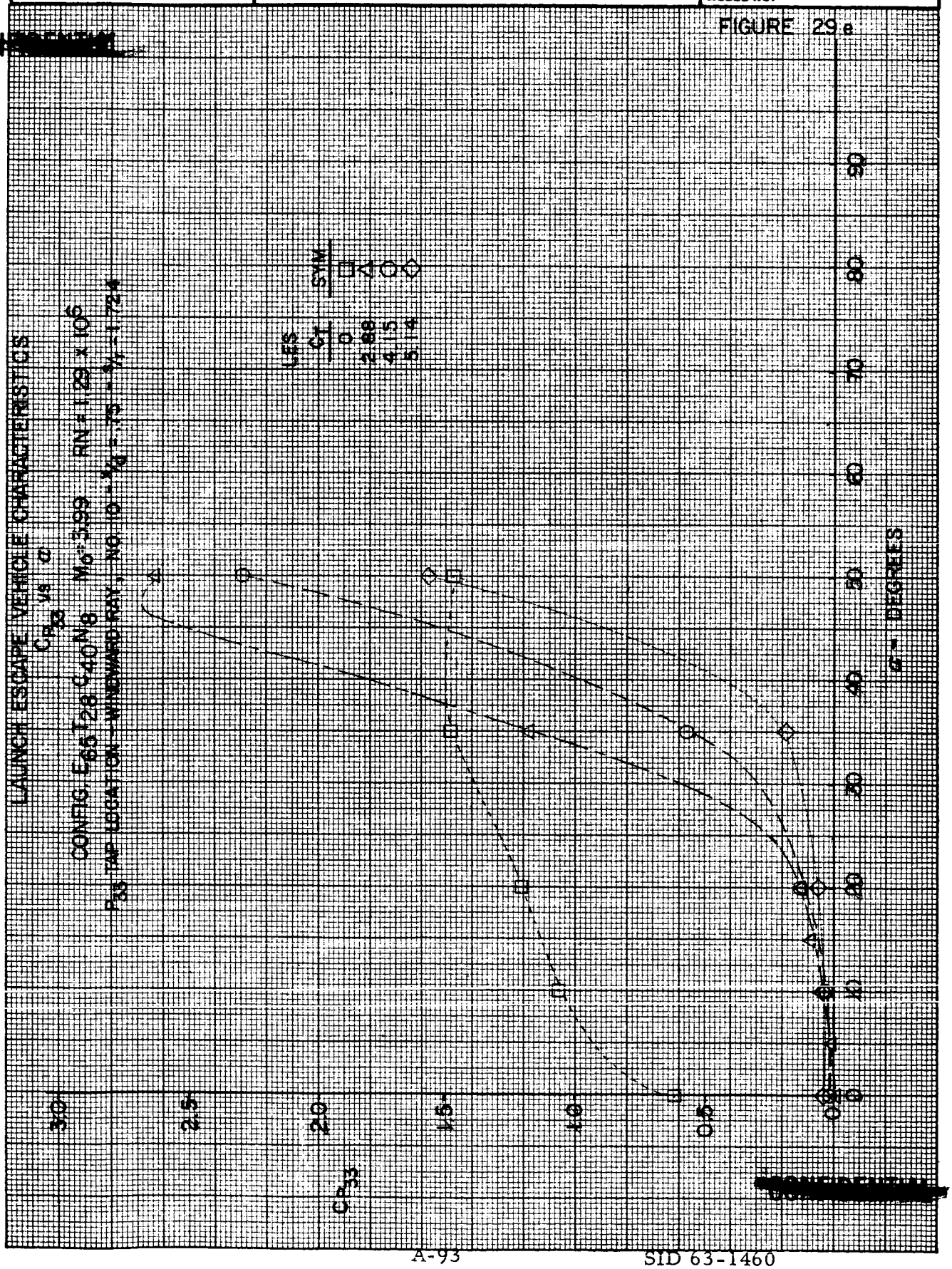

[redacted]

FIGURE 30 a

[redacted]

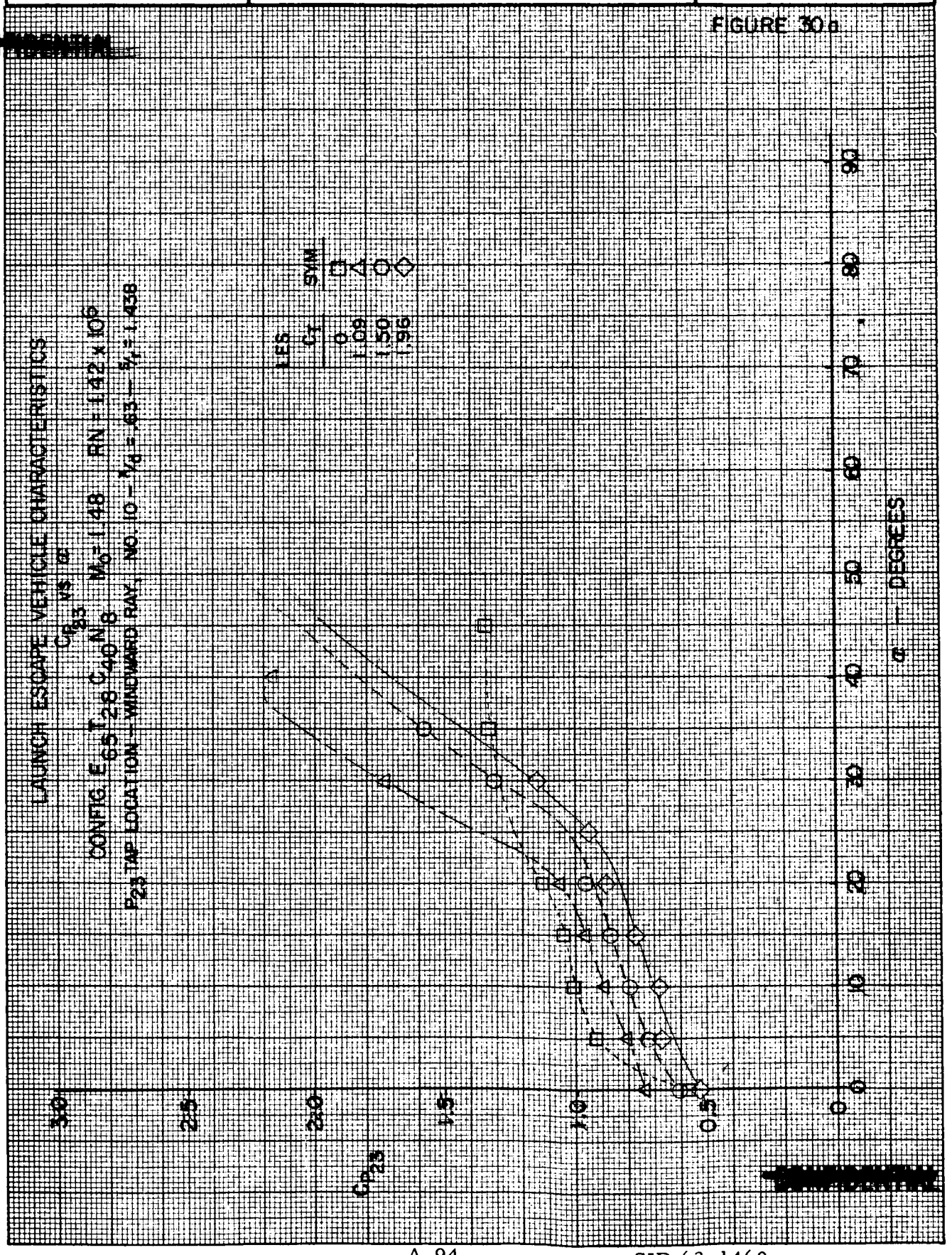

[redacted]

FORM M-113-N2- (REV. 3-61)

PREPARED BY:	NORTH AMERICAN AVIATION, INC. SPACE and INFORMATION SYSTEMS DIVISION	PAGE NO. OF
CHECKED BY:		REPORT NO.
DATE:		MODEL NO.

CON[redacted]TIAL

FIGURE 30 b

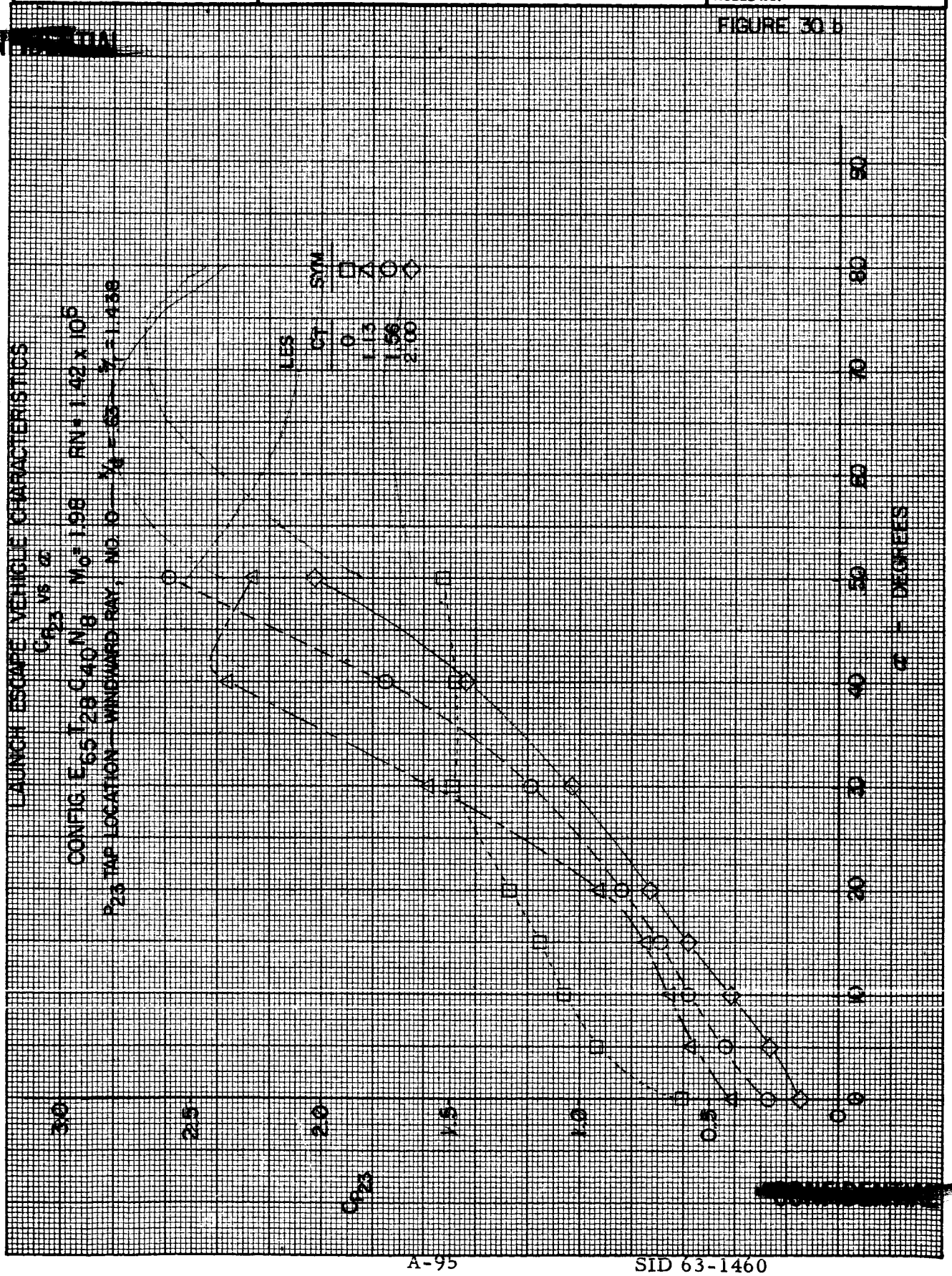

[redacted]

FIGURE 30c

[redacted]

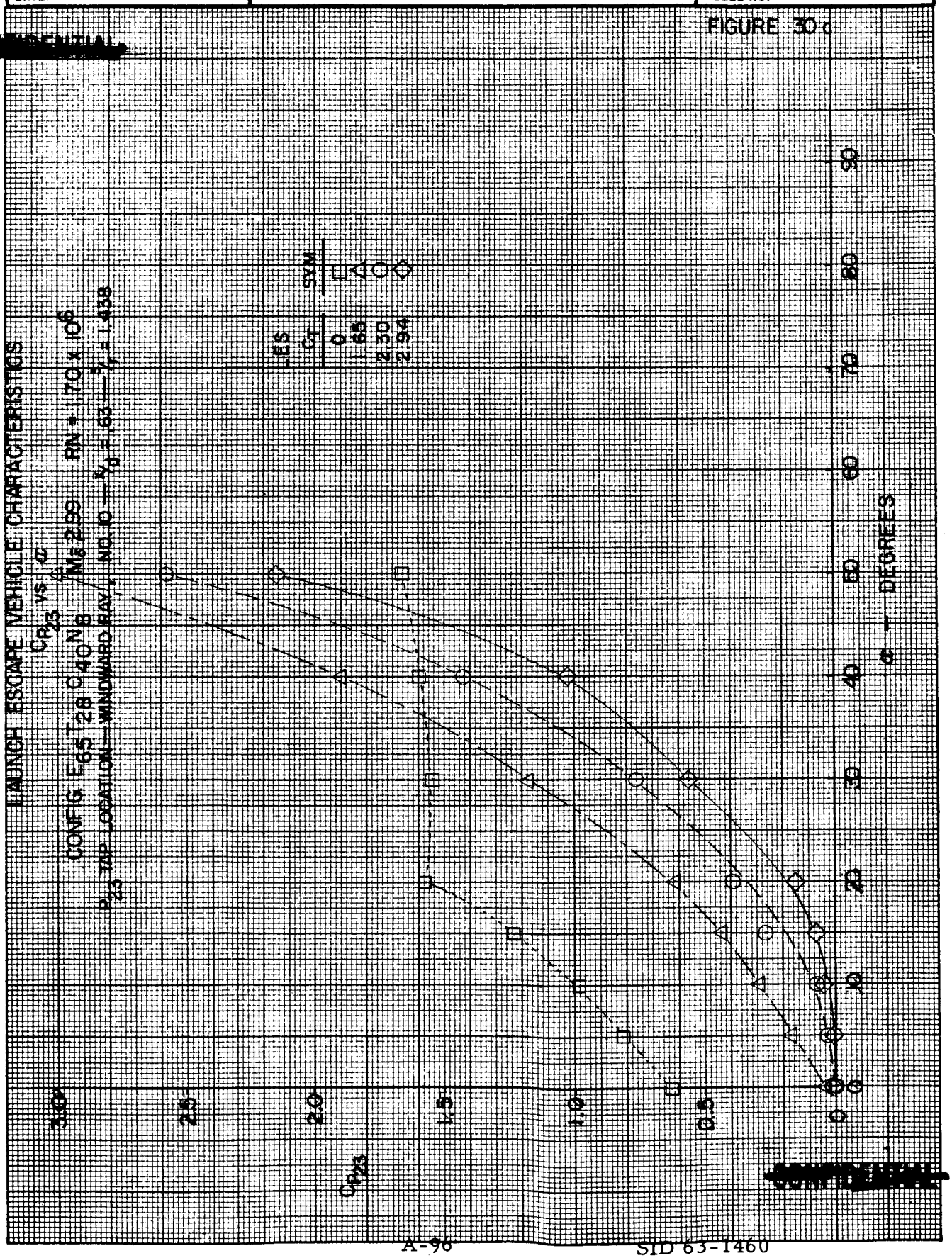

[redacted]

FORM M-113-N2- (REV. 3-61)

PREPARED BY:	NORTH AMERICAN AVIATION, INC. SPACE and INFORMATION SYSTEMS DIVISION	PAGE NO. OF
CHECKED BY:		REPORT NO.
DATE:		MODEL NO.

[redacted]

FIGURE 30 d

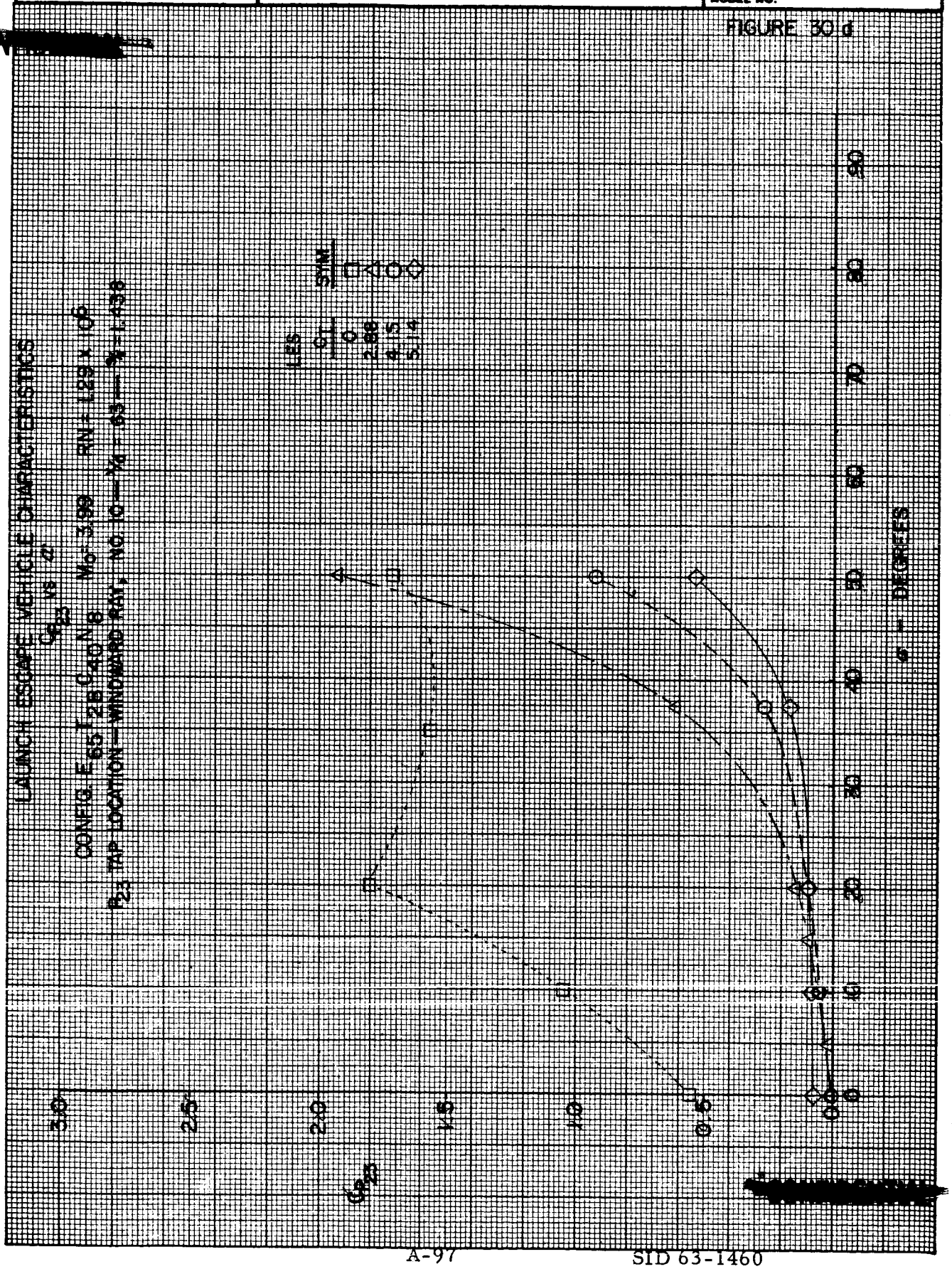

[redacted]

FIGURE 31a

[redacted]

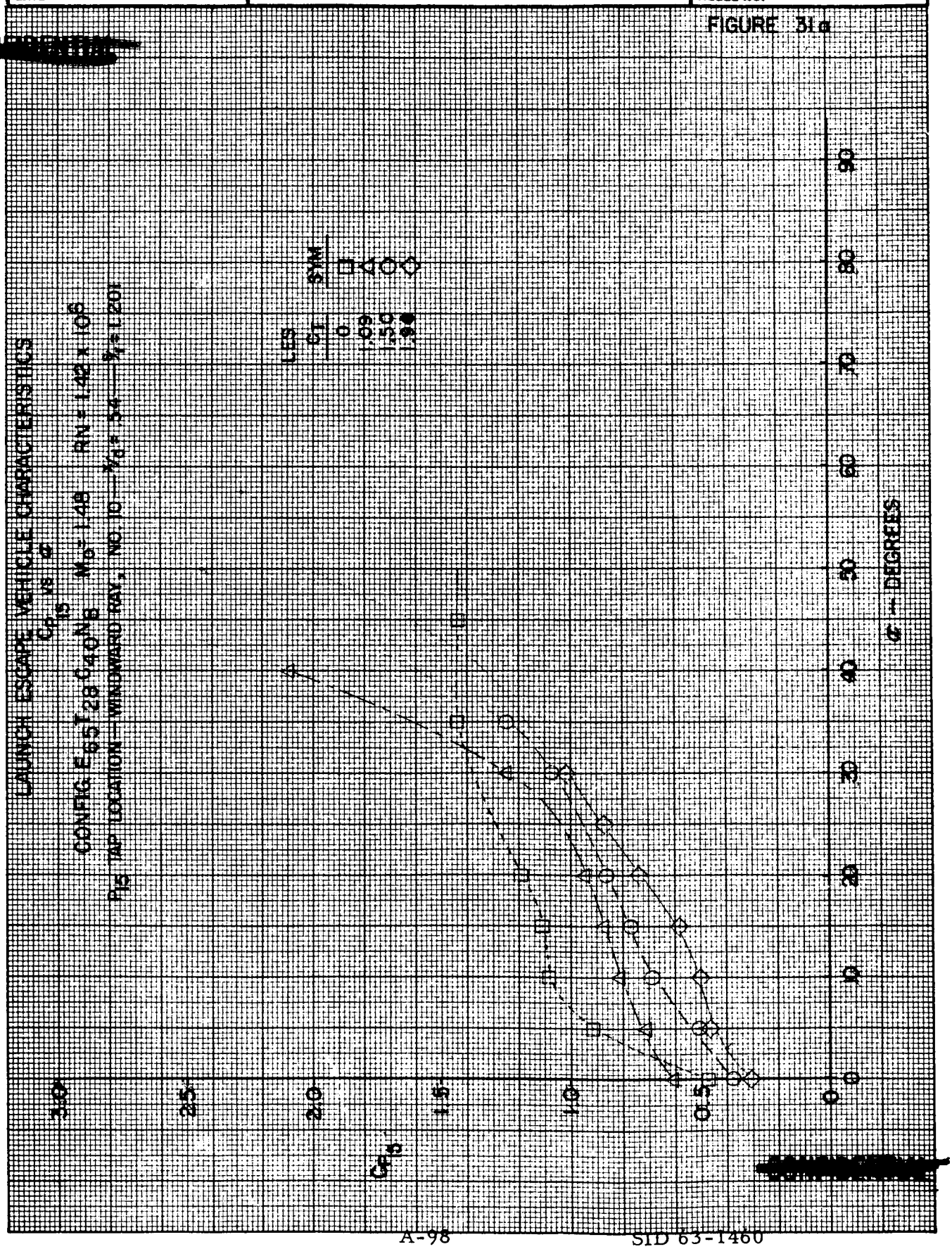

[redacted]

FORM N-113-N2- (REV. 3-61)

PREPARED BY:	NORTH AMERICAN AVIATION, INC. SPACE and INFORMATION SYSTEMS DIVISION	PAGE NO. OF
CHECKED BY:		REPORT NO.
DATE:		MODEL NO.

~~CONFIDENTIAL~~

FIGURE 31 b

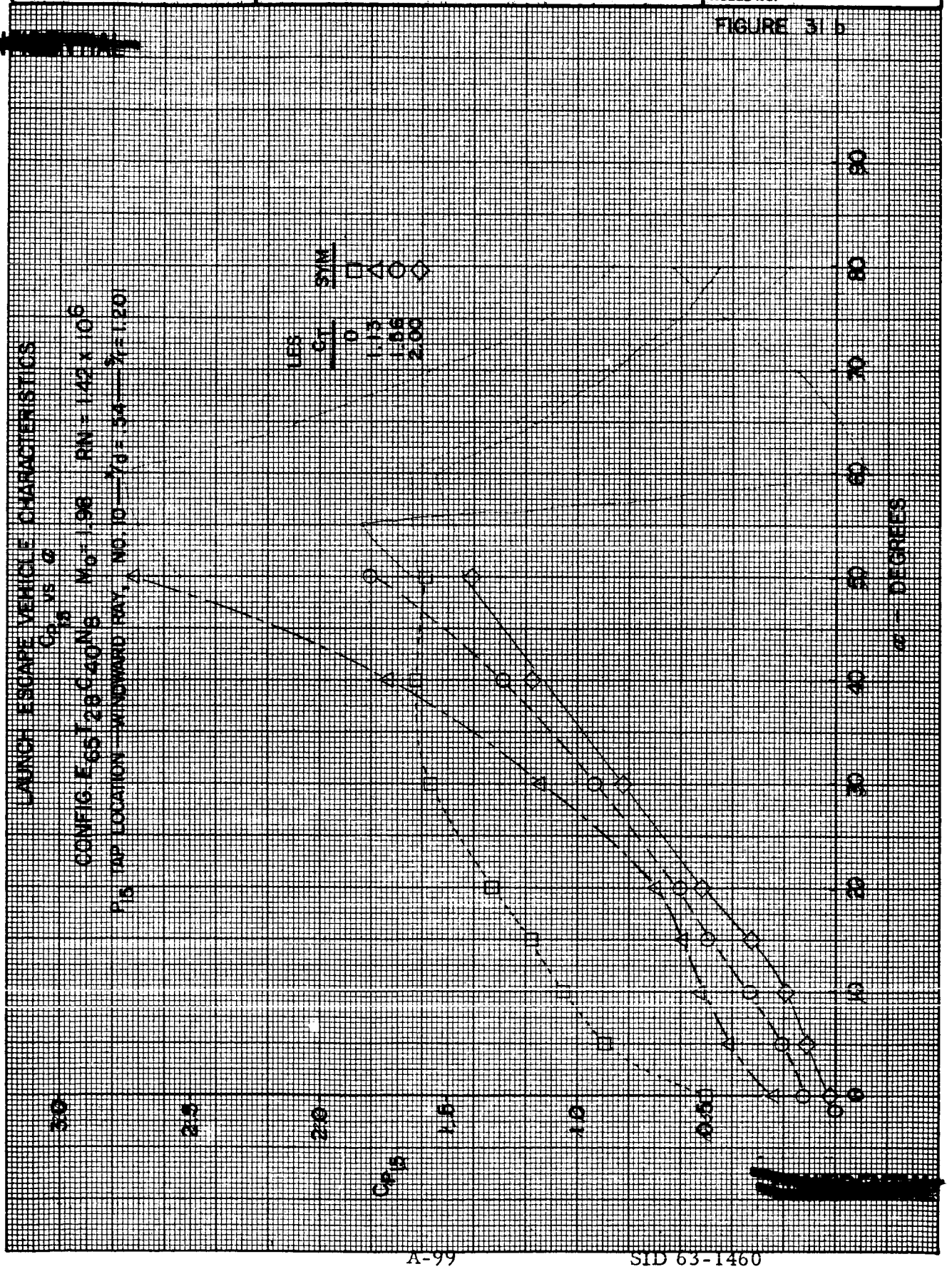

[redacted]

FORM M-113-N2- (REV. 3-61)

PREPARED BY:	NORTH AMERICAN AVIATION, INC. SPACE and INFORMATION SYSTEMS DIVISION	PAGE NO. OF
CHECKED BY:		REPORT NO.
DATE:		MODEL NO.

FIGURE 31 c

~~CONFIDENTIAL~~

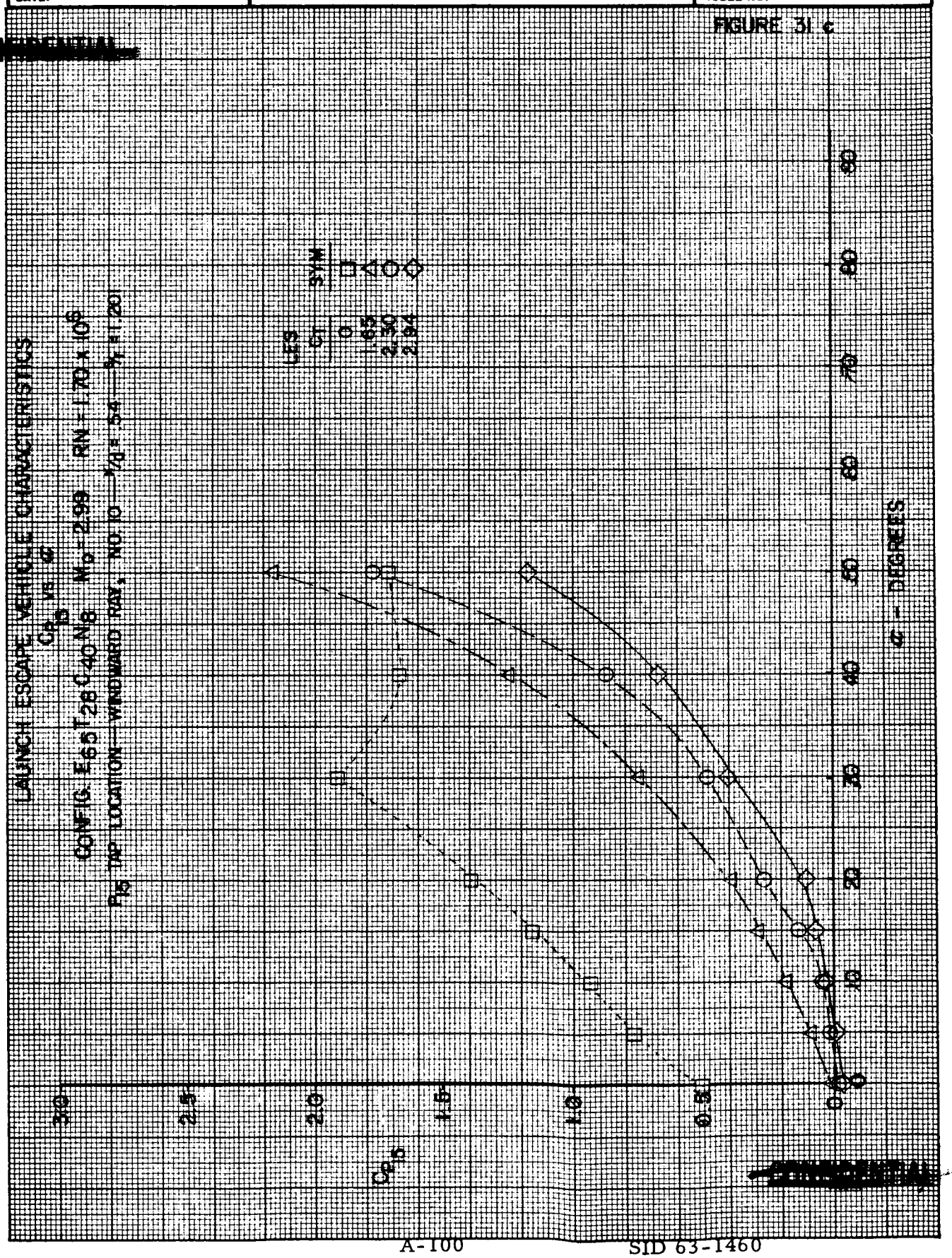

~~CONFIDENTIAL~~

FORM M-113-N2- (REV. 3-61)

PREPARED BY:	NORTH AMERICAN AVIATION, INC. SPACE and INFORMATION SYSTEMS DIVISION	PAGE NO. OF
CHECKED BY:		REPORT NO.
DATE:		MODEL NO.

[redacted]

FIGURE 31 d

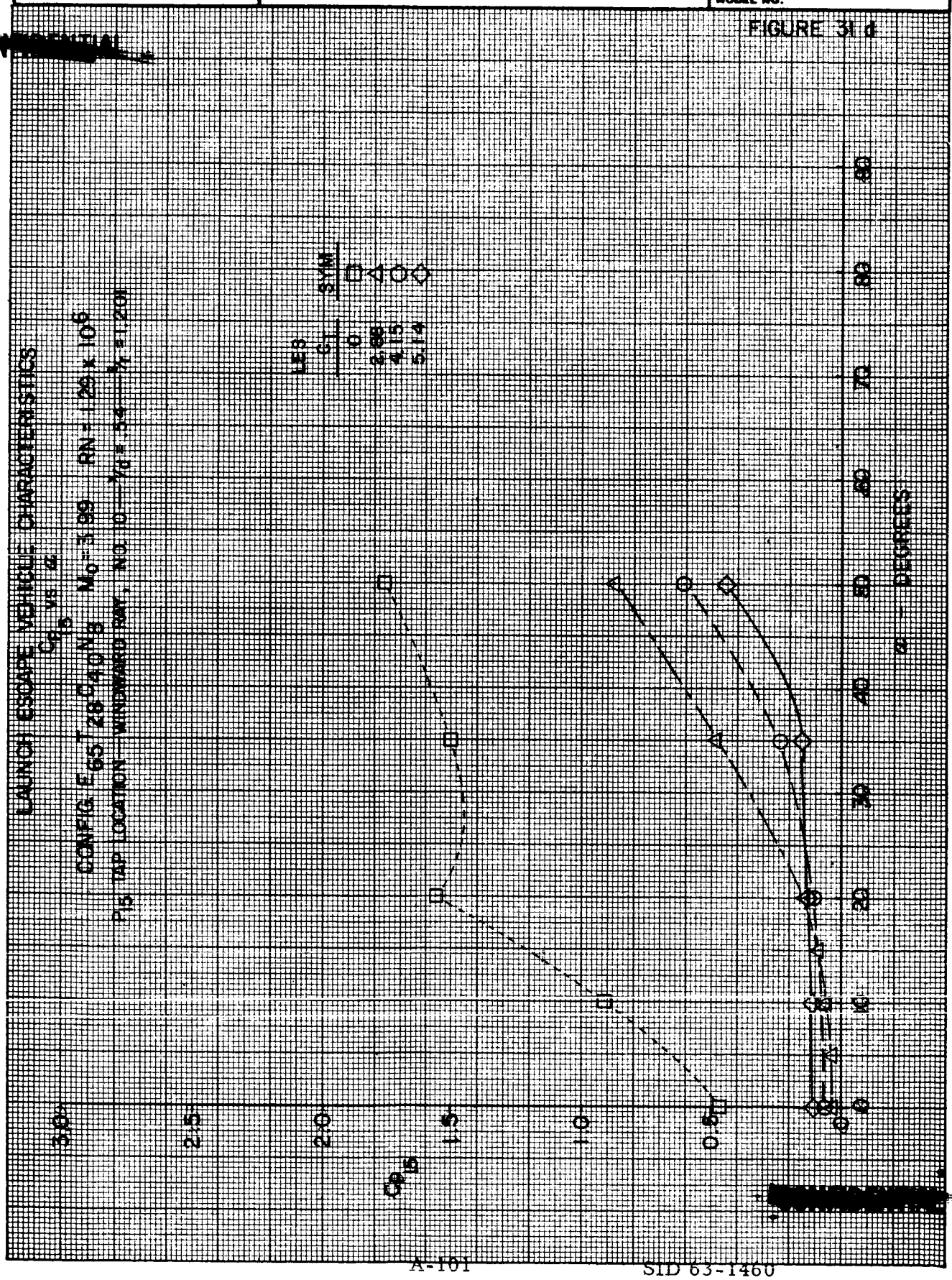

FORM M-113-N2- (REV. 3-61)

PREPARED BY:	NORTH AMERICAN AVIATION, INC. SPACE and INFORMATION SYSTEMS DIVISION	PAGE NO. OF
CHECKED BY:		REPORT NO.
DATE:		MODEL NO.

FIGURE 32a

~~CONFIDENTIAL~~

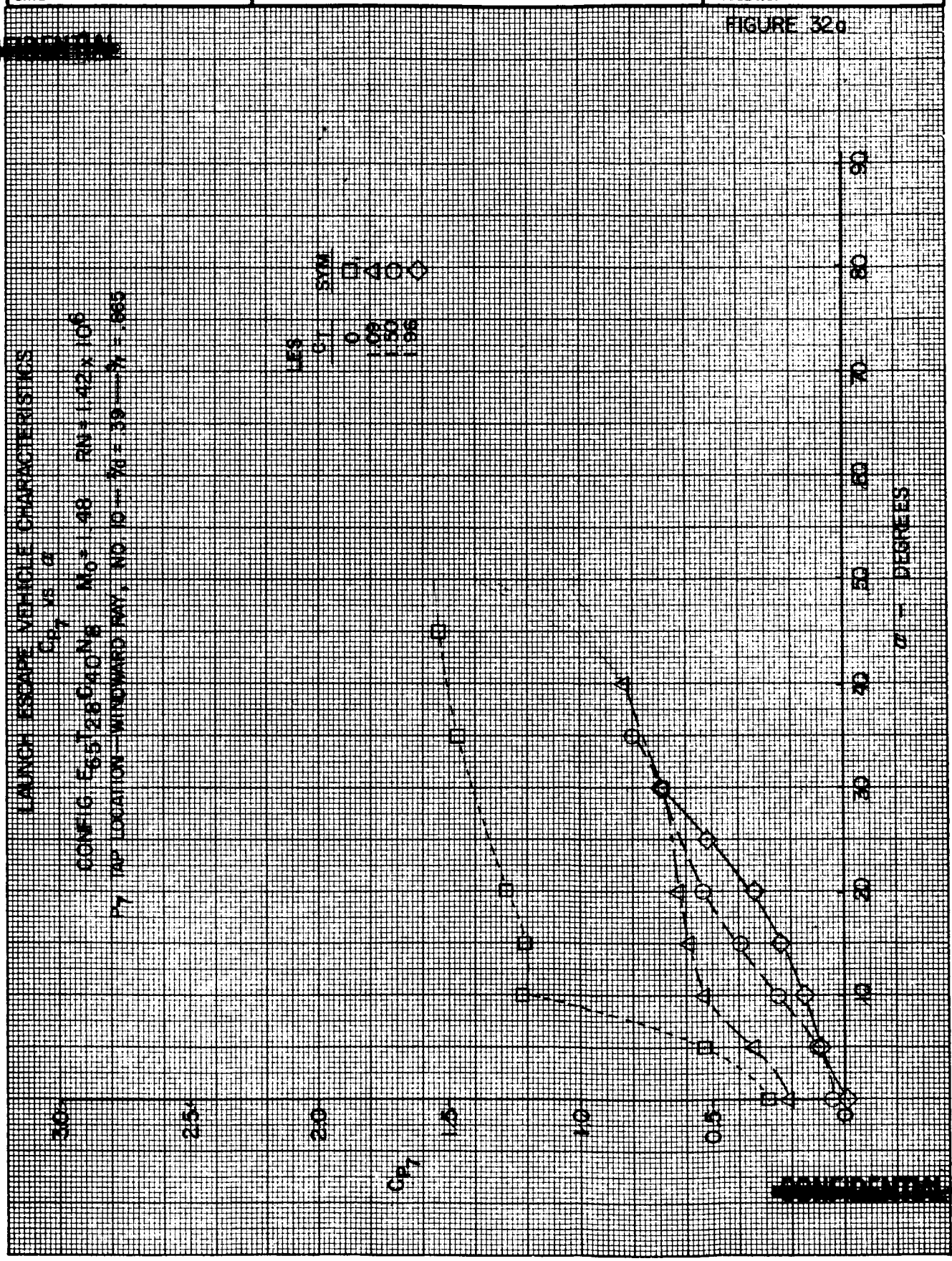

~~CONFIDENTIAL~~

FORM M-113-N2- (REV. 3-61)

PREPARED BY:	NORTH AMERICAN AVIATION, INC. SPACE and INFORMATION SYSTEMS DIVISION	PAGE NO. OF
CHECKED BY:		REPORT NO.
DATE:		MODEL NO.

[redacted]

FIGURE 32b

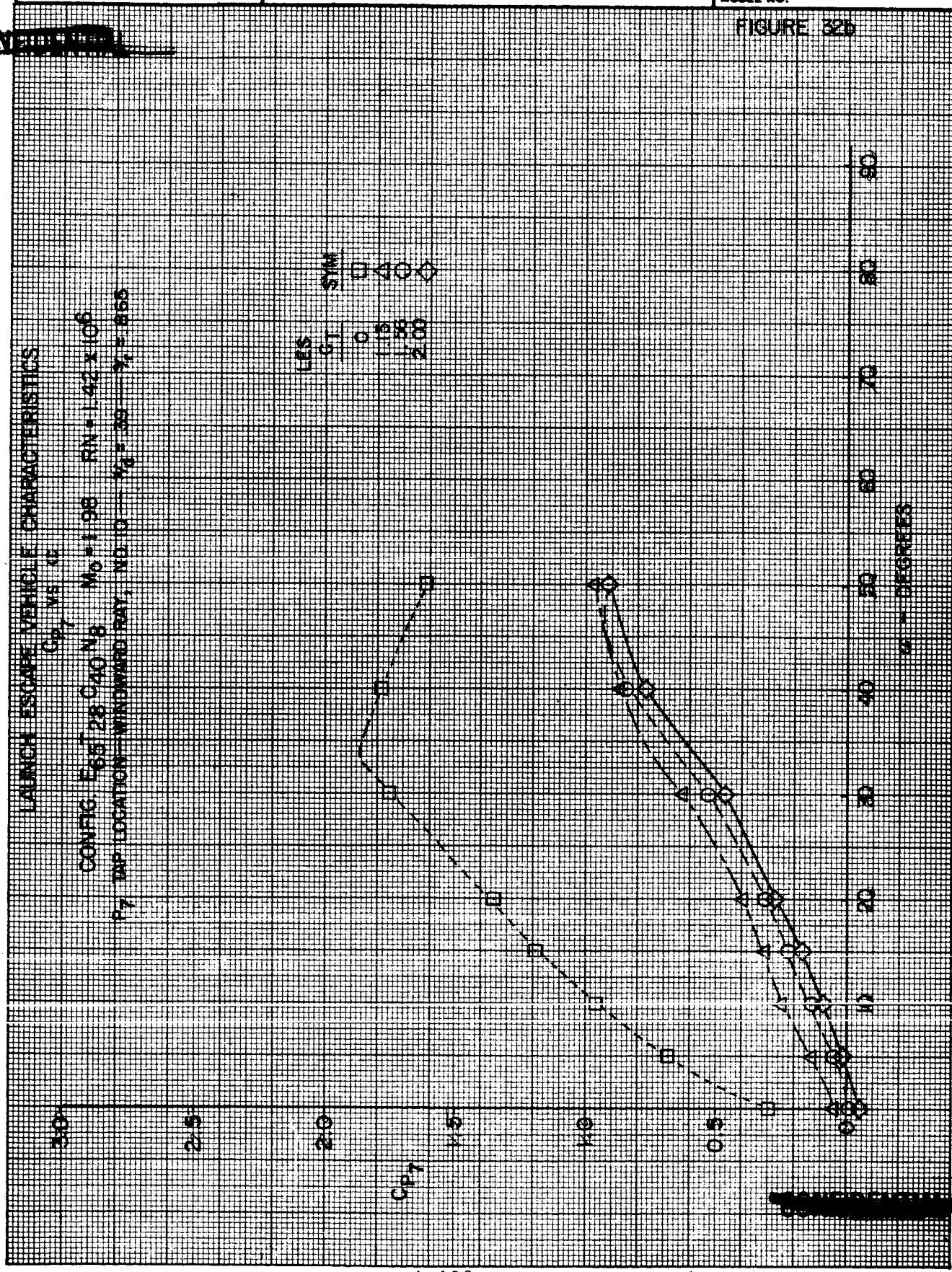

[redacted]

[redacted]

FIGURE 32 c

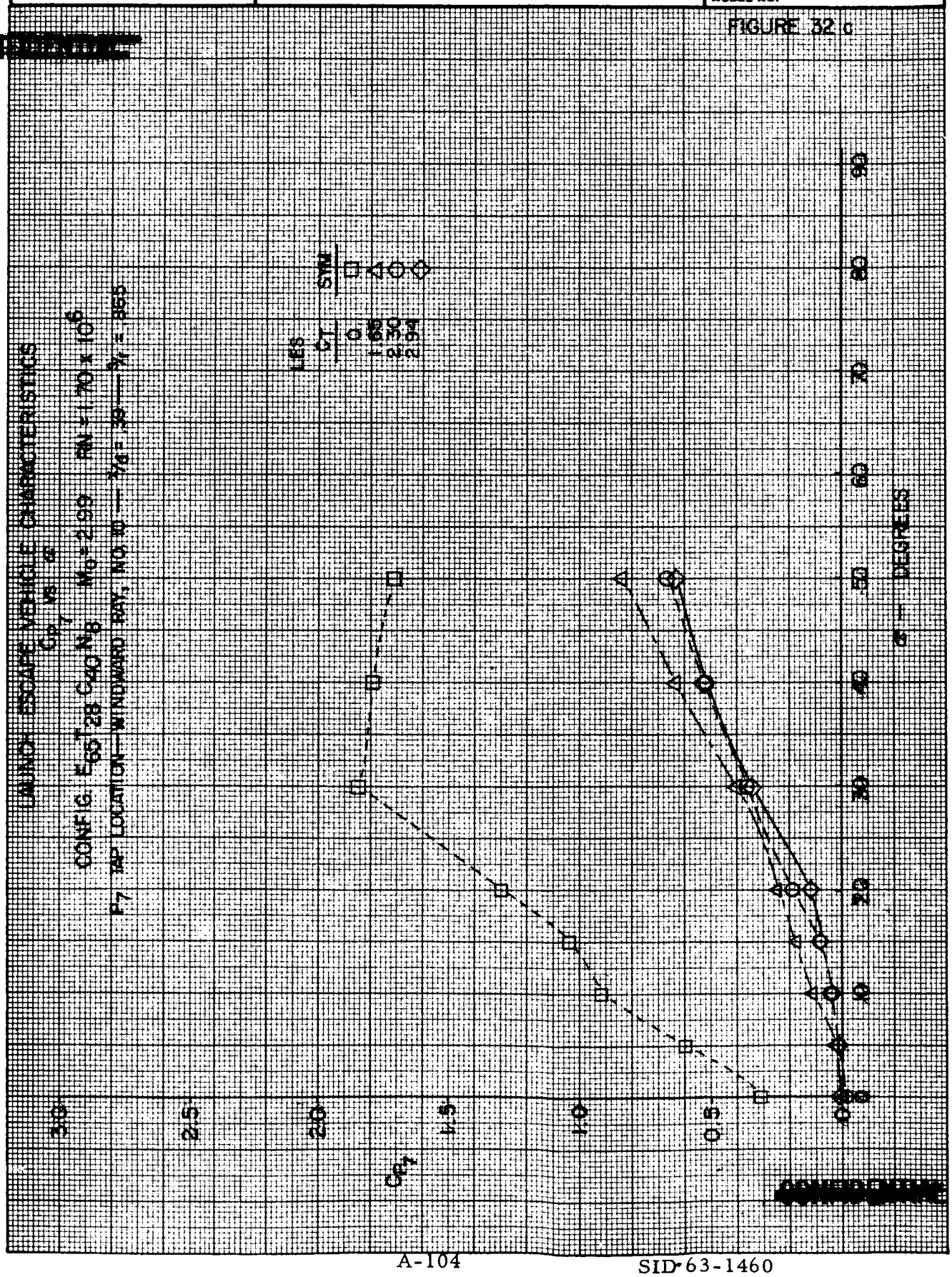

[redacted]

FORM M-113-N2- (REV. 3-61)

PREPARED BY:	NORTH AMERICAN AVIATION, INC. SPACE and INFORMATION SYSTEMS DIVISION	PAGE NO. OF
CHECKED BY:		REPORT NO.
DATE:		MODEL NO.

[redacted]

FIGURE 32.d

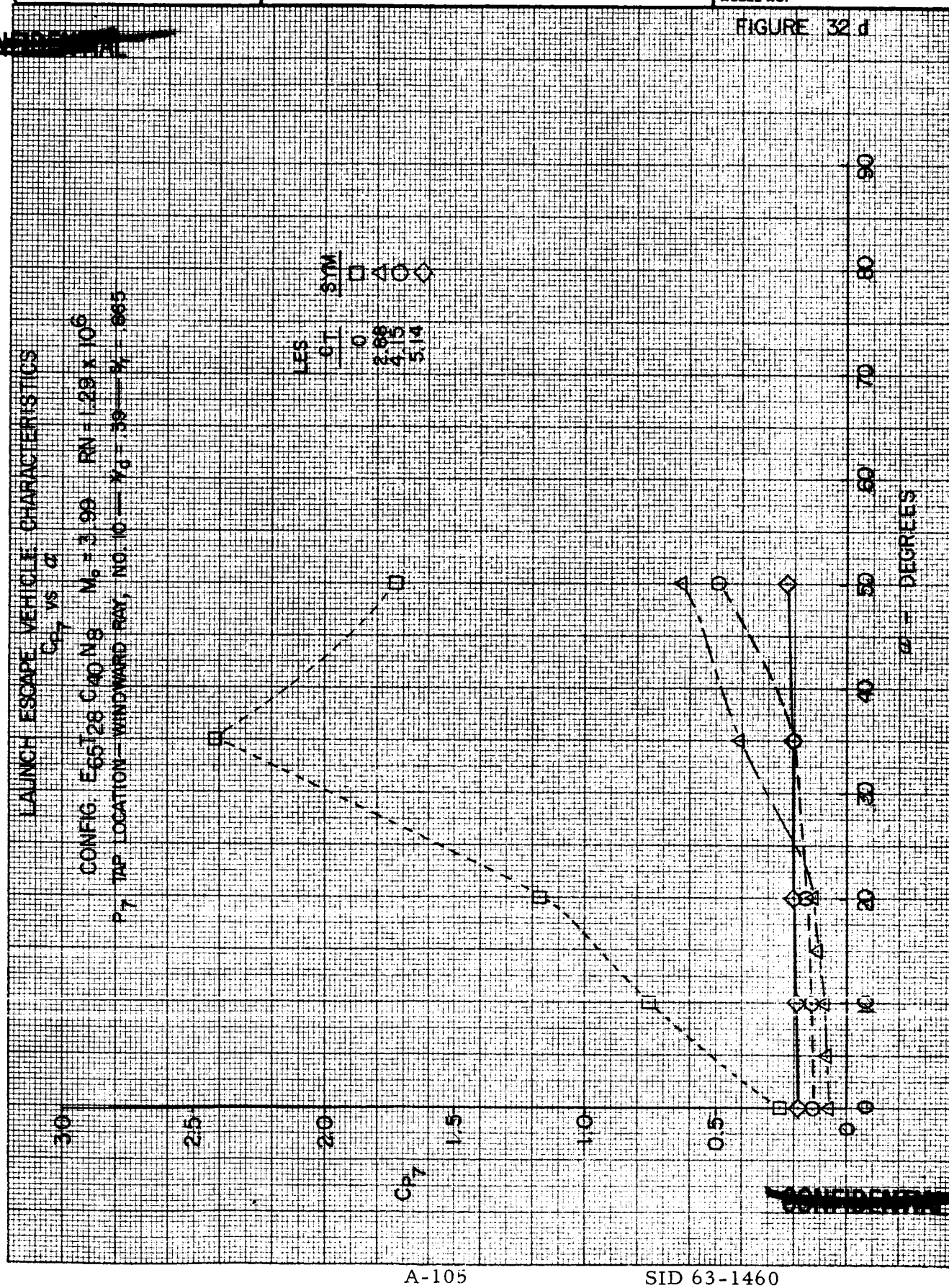

[redacted]

~~CONFIDENTIAL~~

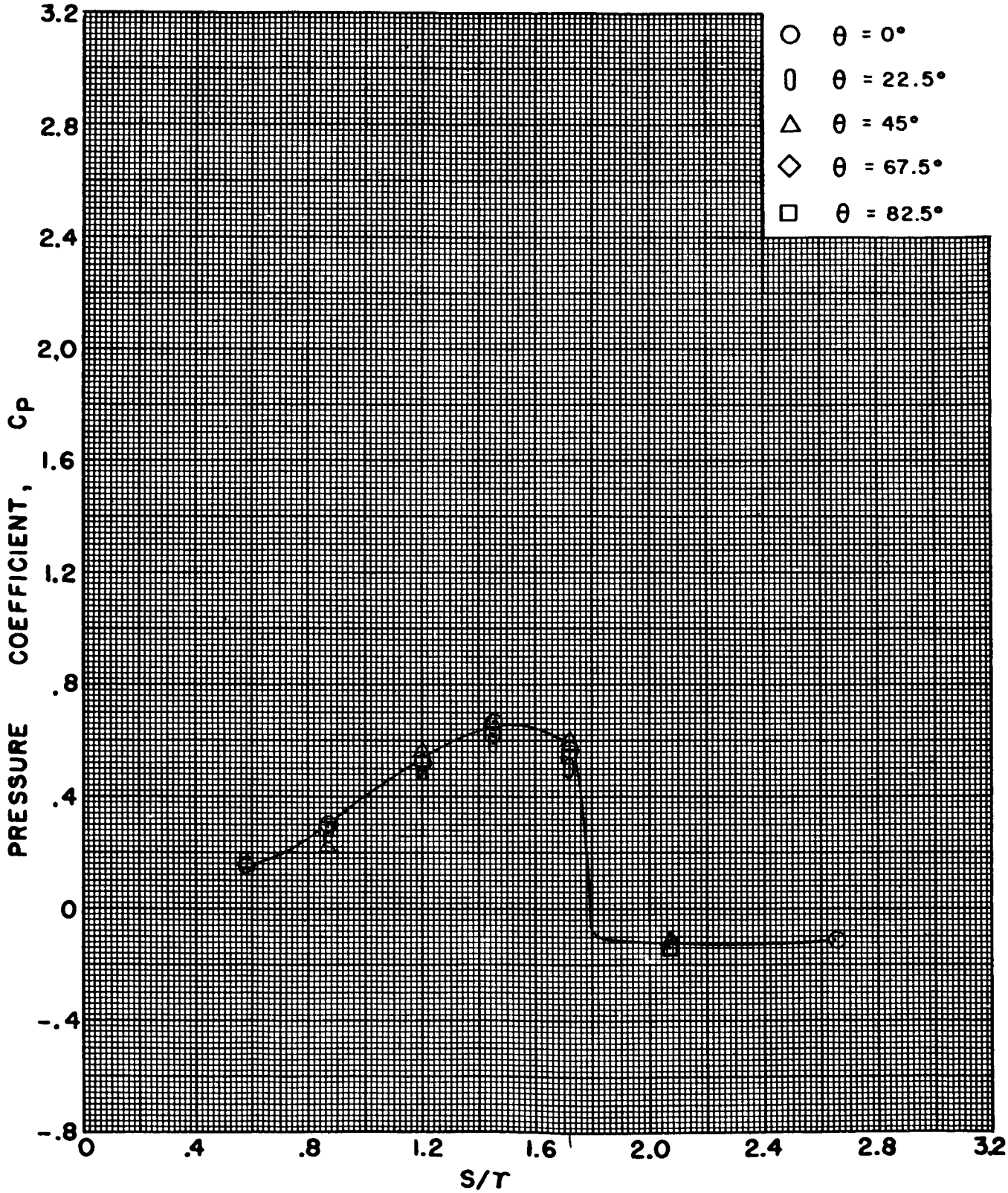

Figure 33a Configuration E[redacted]NT[redacted]C[redacted] 65 28 40

Mach No. = 1.98 $\alpha = 0°$ $C_T = 0$

~~CONFIDENTIAL~~

[redacted]

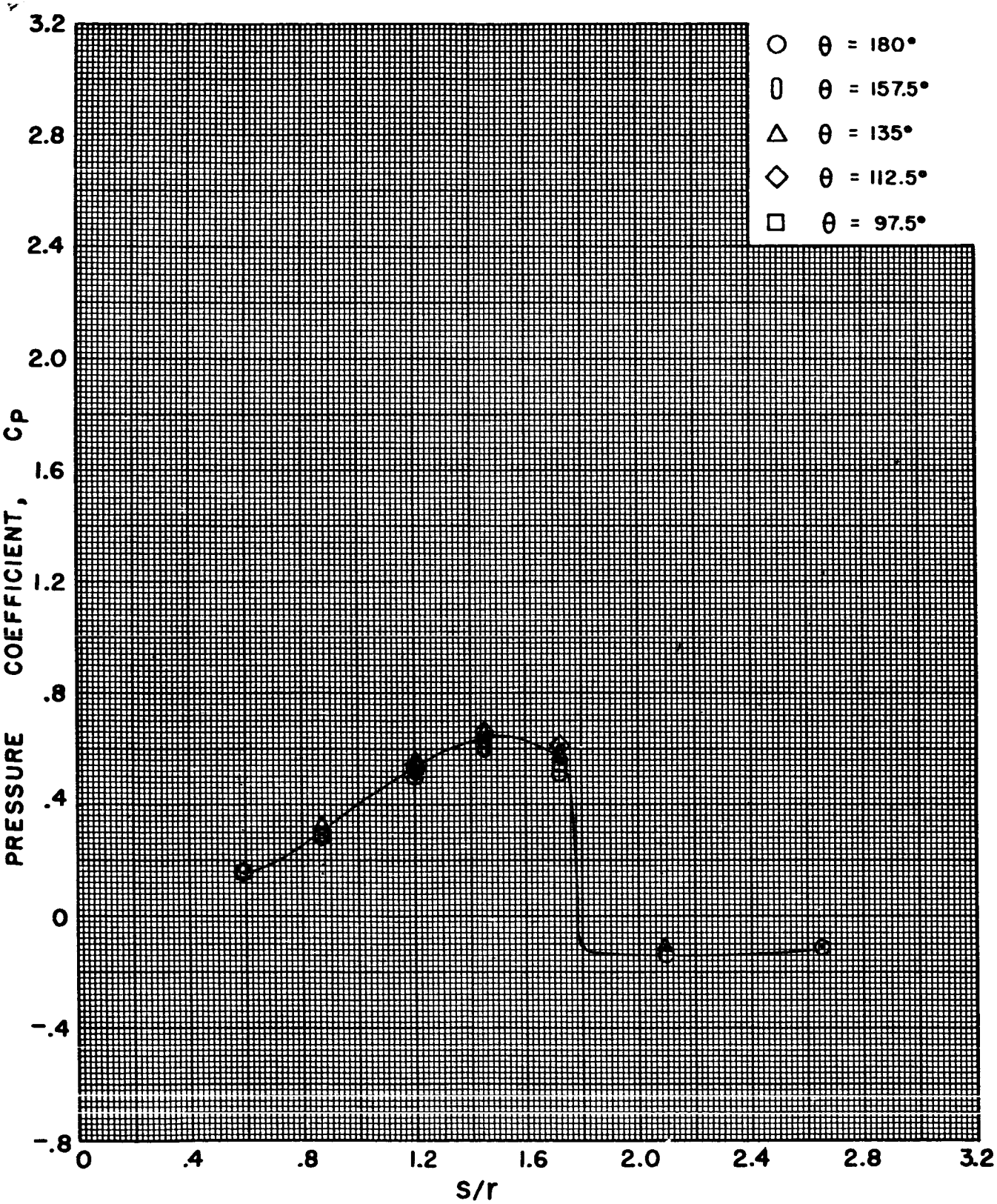

Figure 33b Configuration $E_{65}N_{8}T_{28}C_{40}$ Mach No. = 1.98 $\alpha = 0$ $C_T = 0$

[redacted]

~~CONFIDENTIAL~~

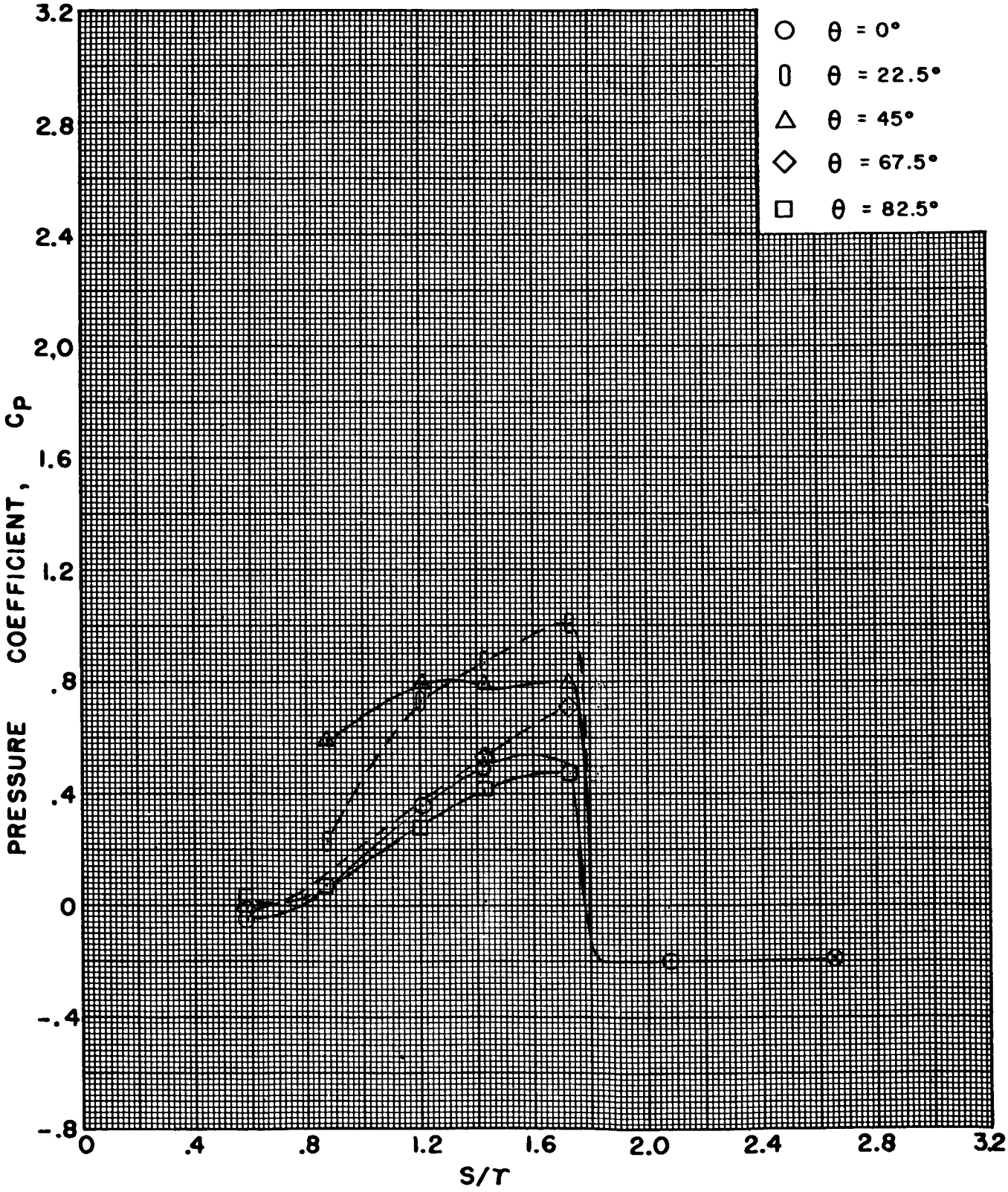

Figure 33c Configuration E[redacted]NT[redacted]C[redacted] 65 8 28 40

Mach No. = 1.98 α = 0° C_T = 1.14

~~CONFIDENTIAL~~

CONFI[redacted]

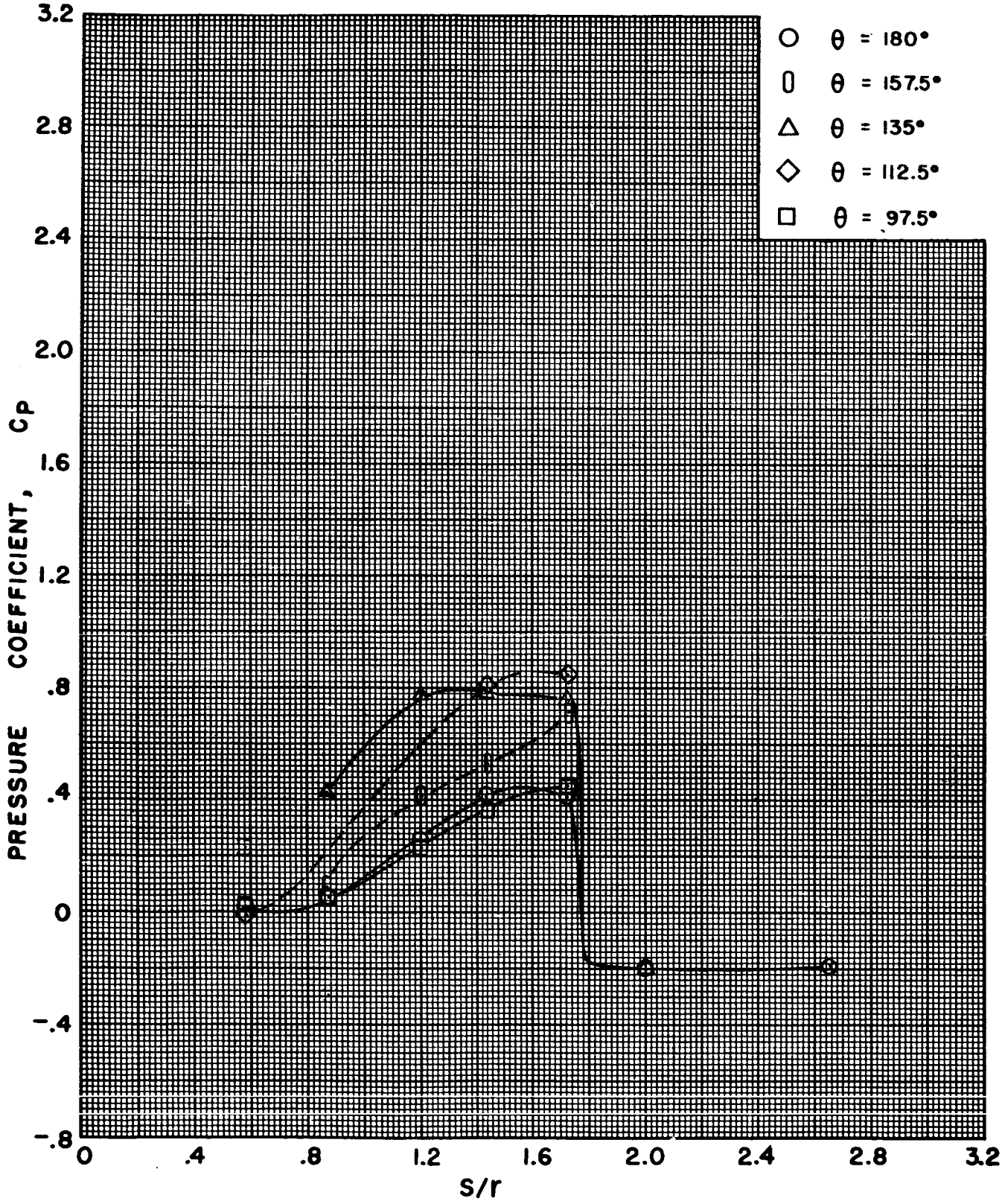

Figure 33d Configuration E[redacted]NT[redacted]C[redacted] (65 8 28 40) Mach No. = 1.98 α = 0° C_T = 1.14

[redacted]

[redacted]

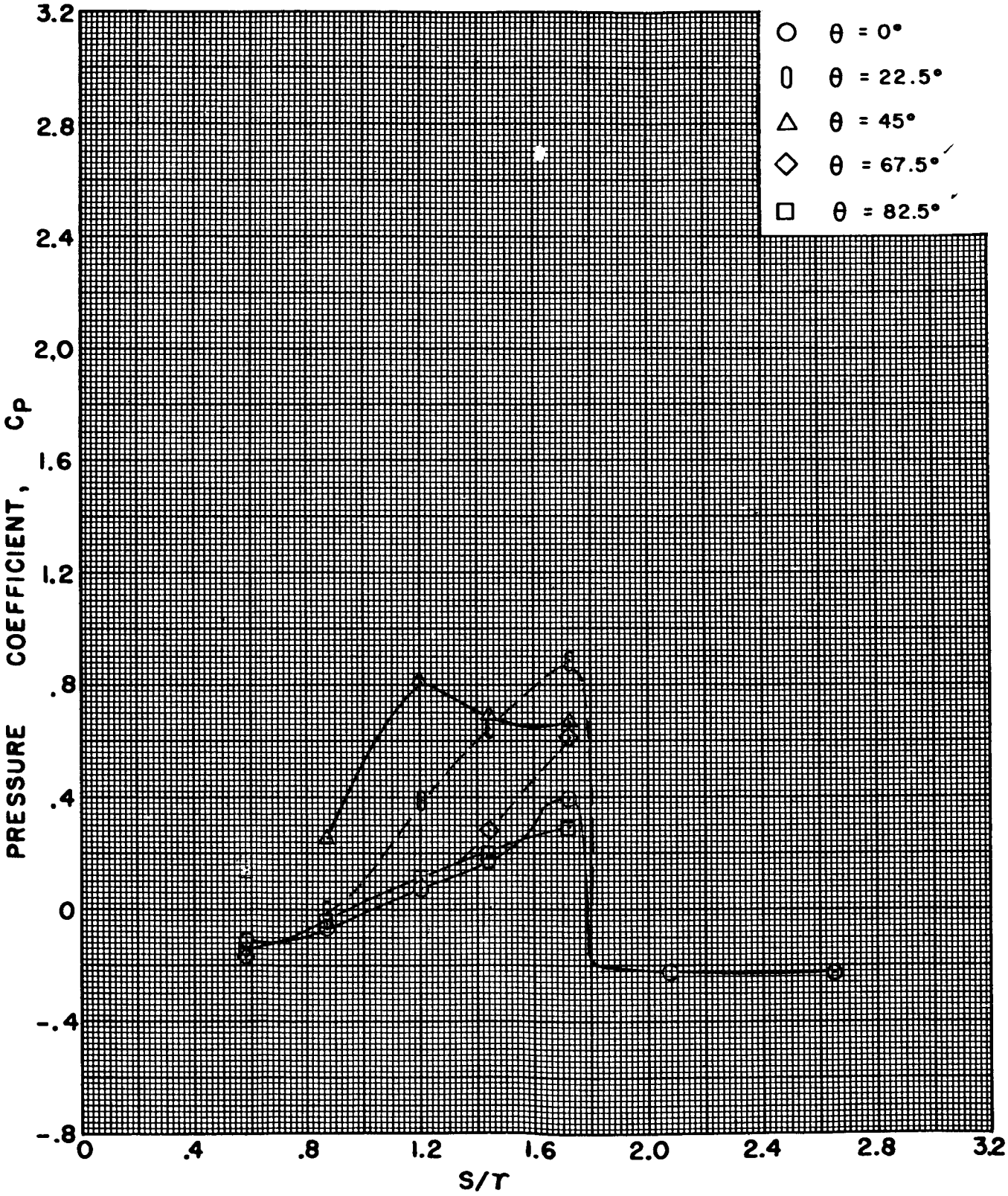

Figure 33e Configuration E[redacted]NT[redacted]C[redacted] 65 8 28 40

Mach No. = 1.98 $\alpha = 0°$ $C_T = 2.00$

[redacted]

~~CONFIDENTIAL~~

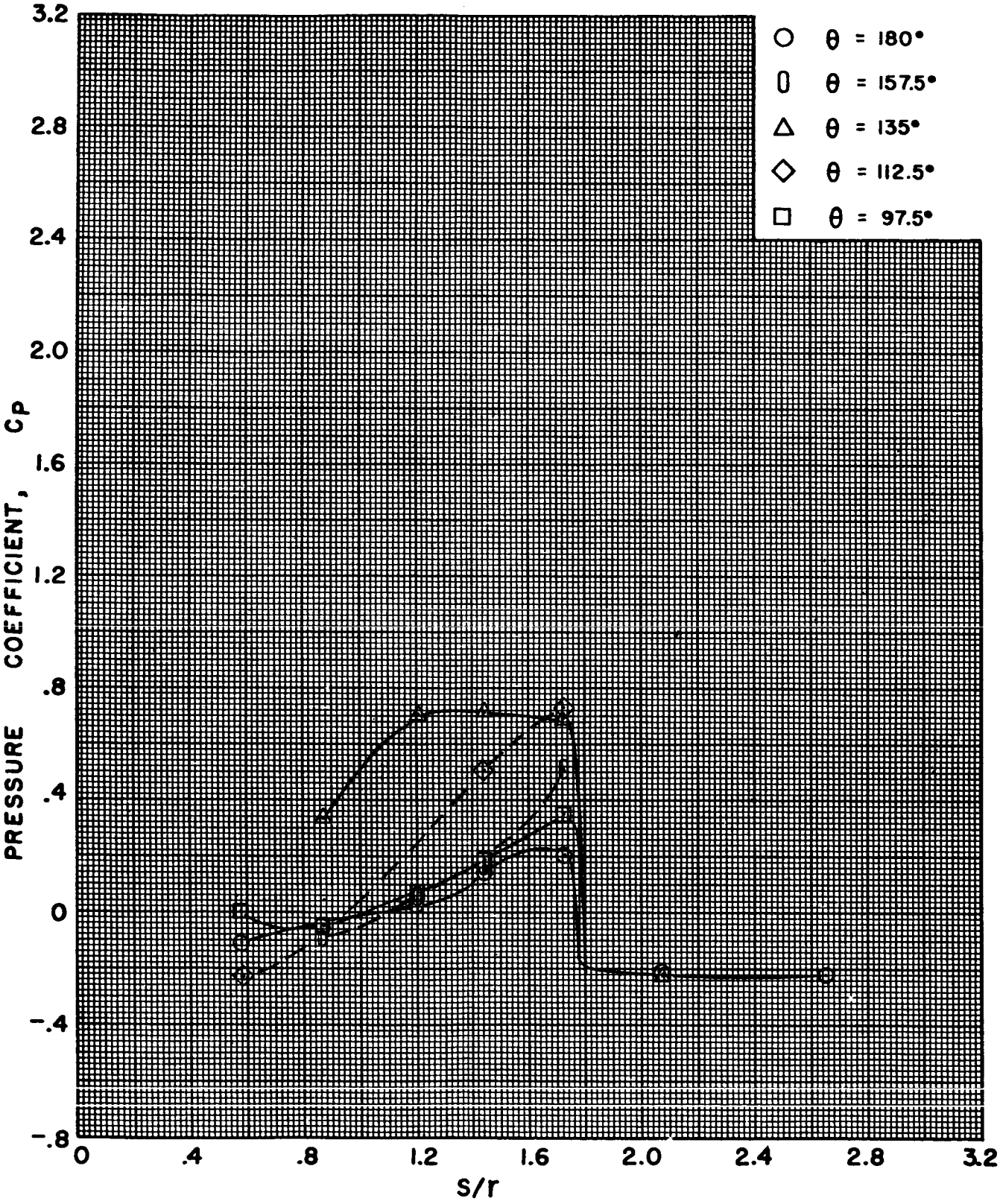

Figure 33f Configuration E[redacted]NT[redacted]C[redacted] 65 8 28 40

Mach No. = 1.98 $\alpha = 0°$ $C_f = 2.00$

~~CONFIDENTIAL~~

~~CONFIDENTIAL~~

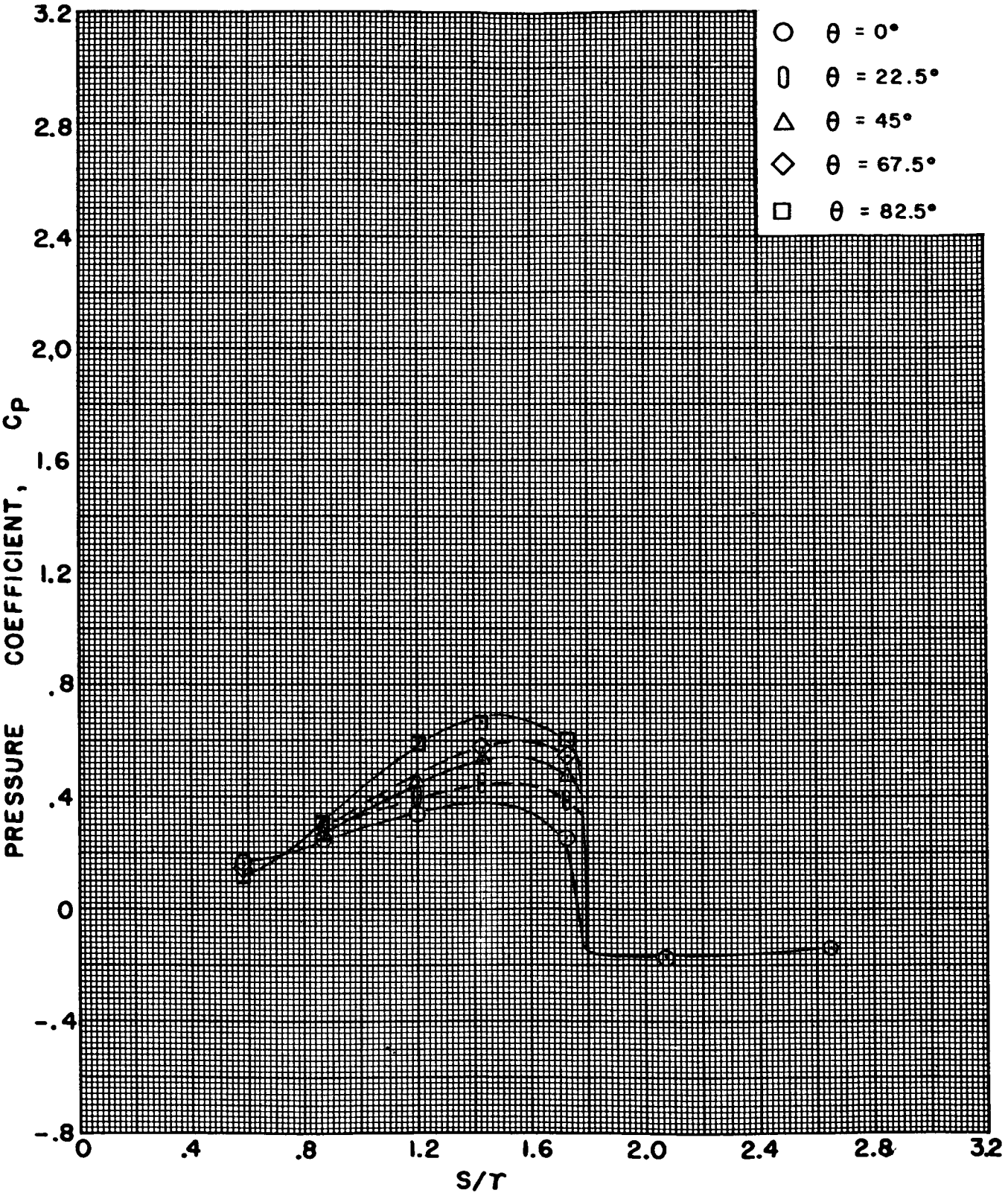

Figure 34a Configuration E[redacted]NT[redacted]C[redacted] 65 8 28 40

Mach No. = 1.98 $\alpha = 5°$ $C_T = 0$

~~CONFIDENTIAL~~

[redacted]

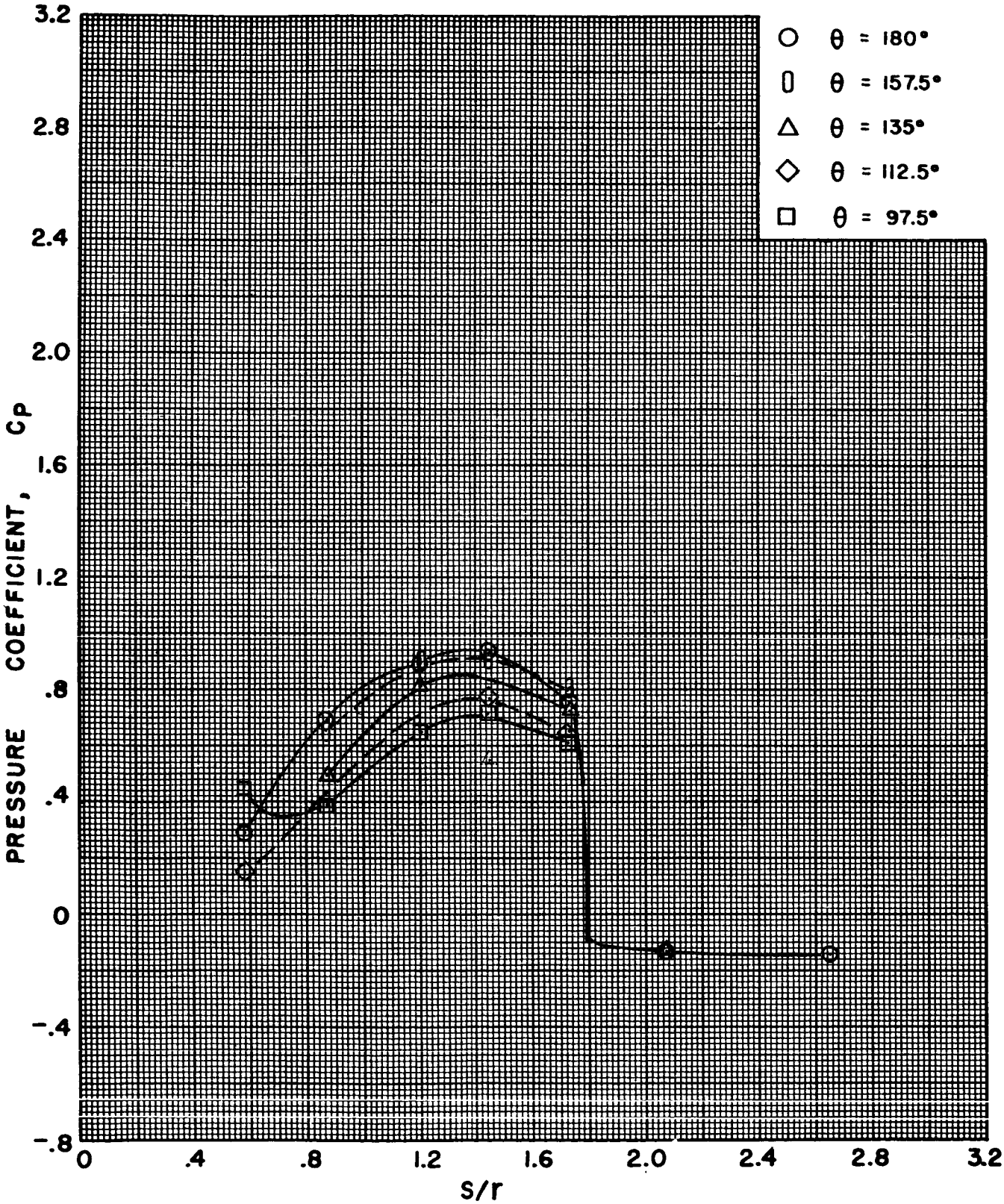

Figure 34b Configuration $E_{65}N_{8}T_{28}C_{40}$ Mach No. = 1.98 $\alpha = 5$ $C_T = 0$

[redacted]

~~CONFIDENTIAL~~

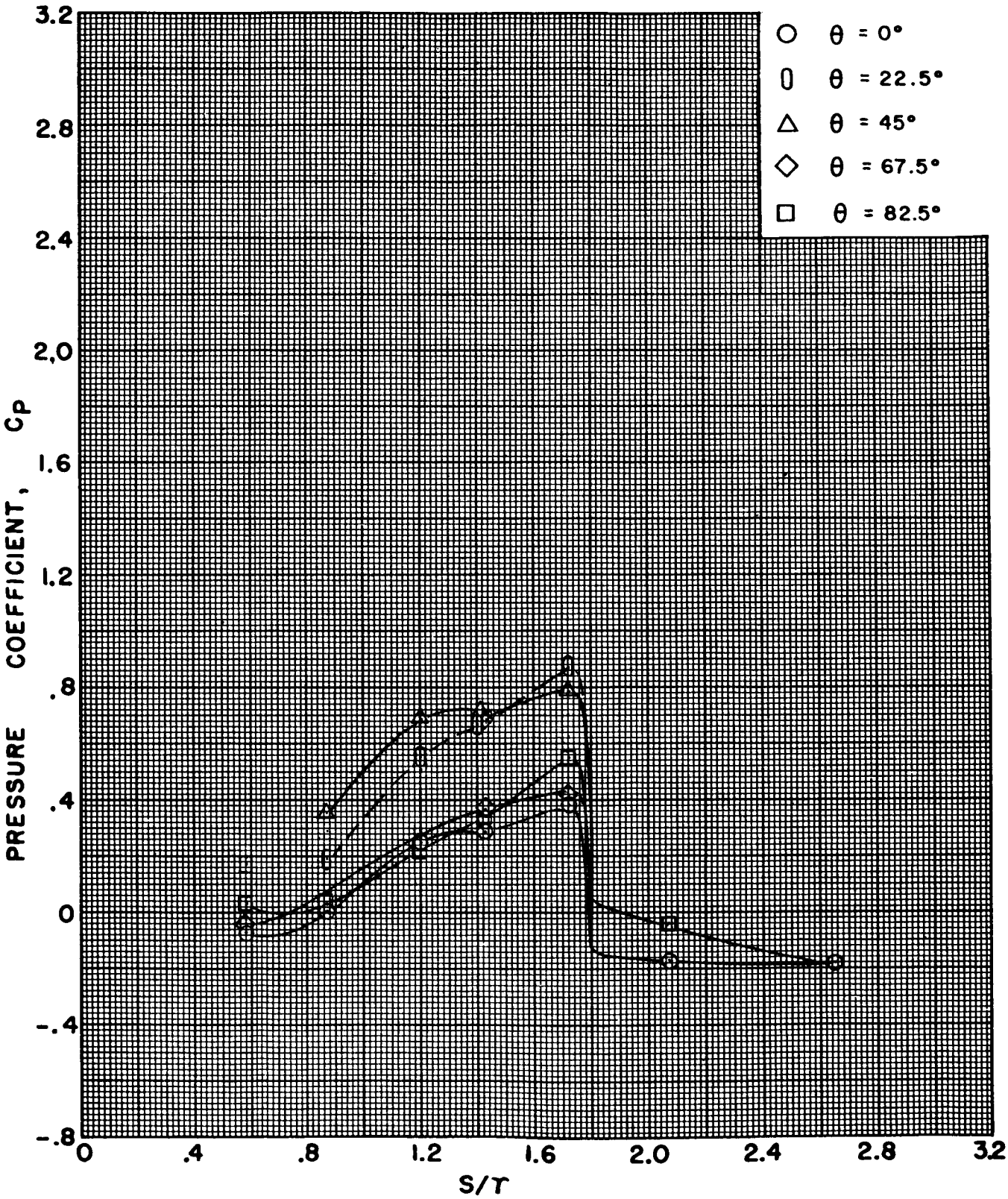

Figure 34c Configuration E[redacted]NT[redacted]C[redacted] 65 8 2B 40

Mach No. = 1.98 α = 5° C_T = 1.14

~~CONFIDENTIAL~~

~~CONFIDENTIAL~~

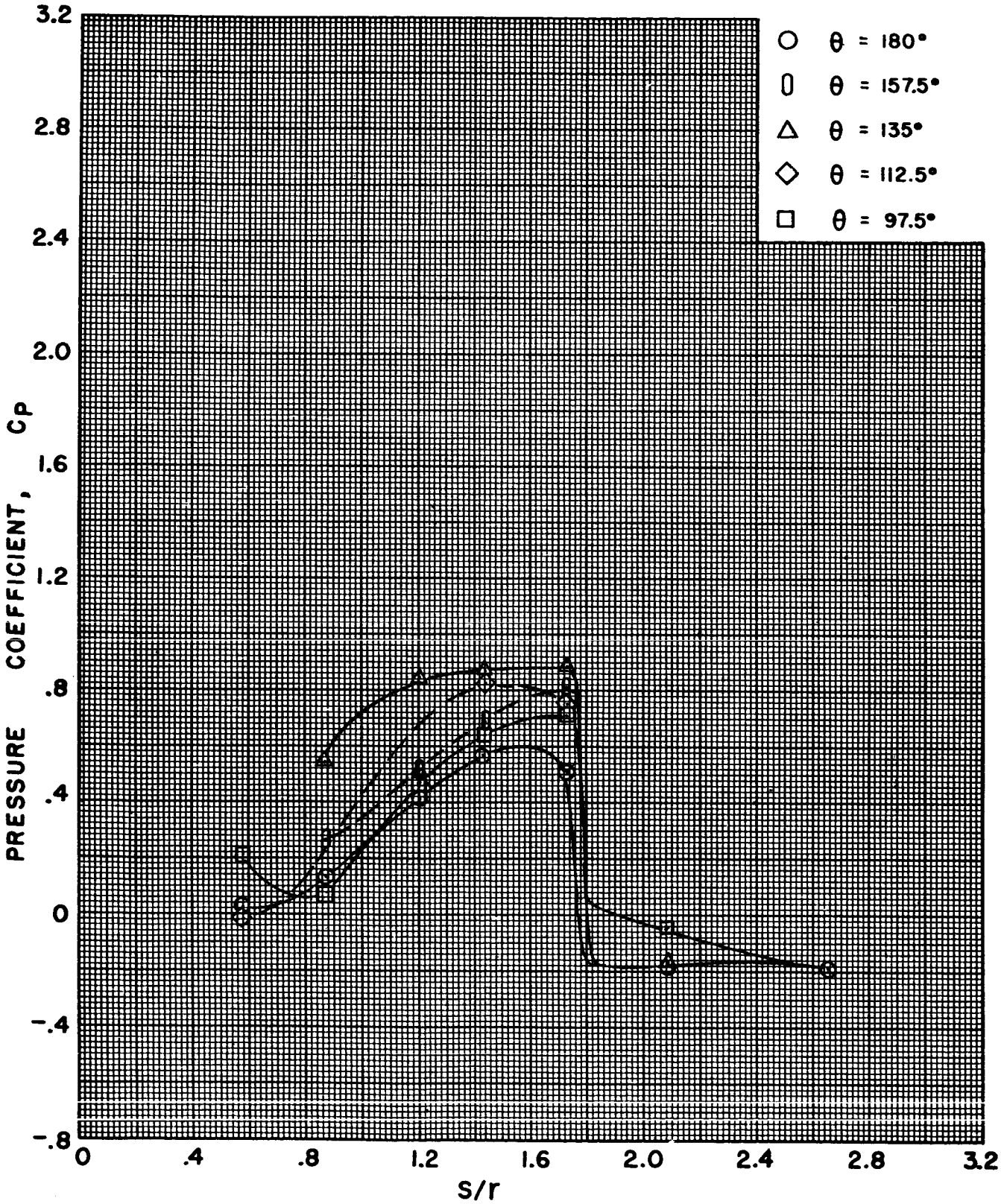

Figure 34d Configuration $E_{47}NT_{24}C_2$ Mach No. = 1.98 $\alpha = 5$ $C_T = 1.14$

~~CONFIDENTIAL~~

~~CONFIDENTIAL~~

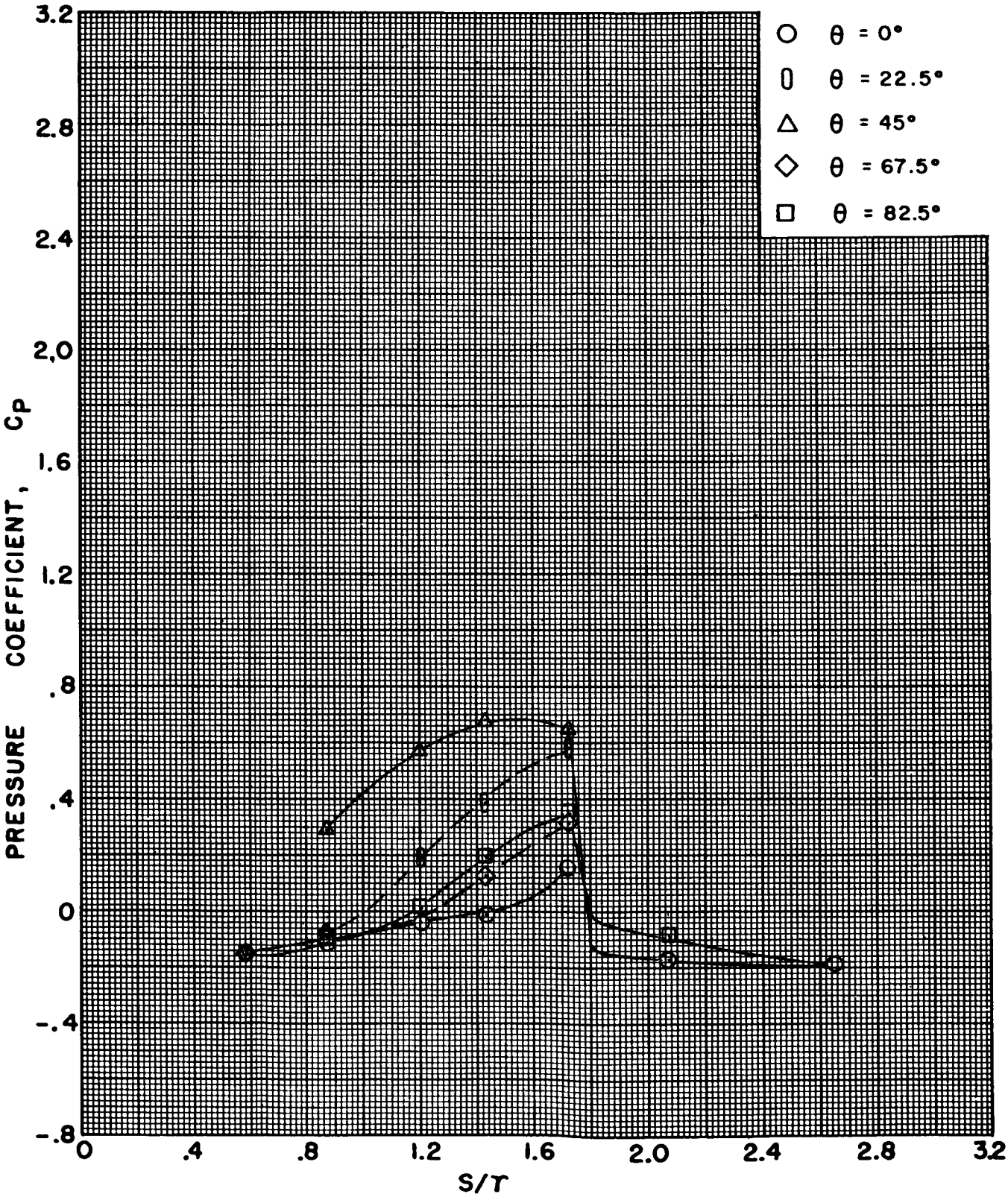

Figure 34e Configuration E[redacted]NT[redacted]C[redacted]
65 8 28 40

Mach No. = 1.98 α = 5° C_T = 2.00

~~CONFIDENTIAL~~

[redacted]

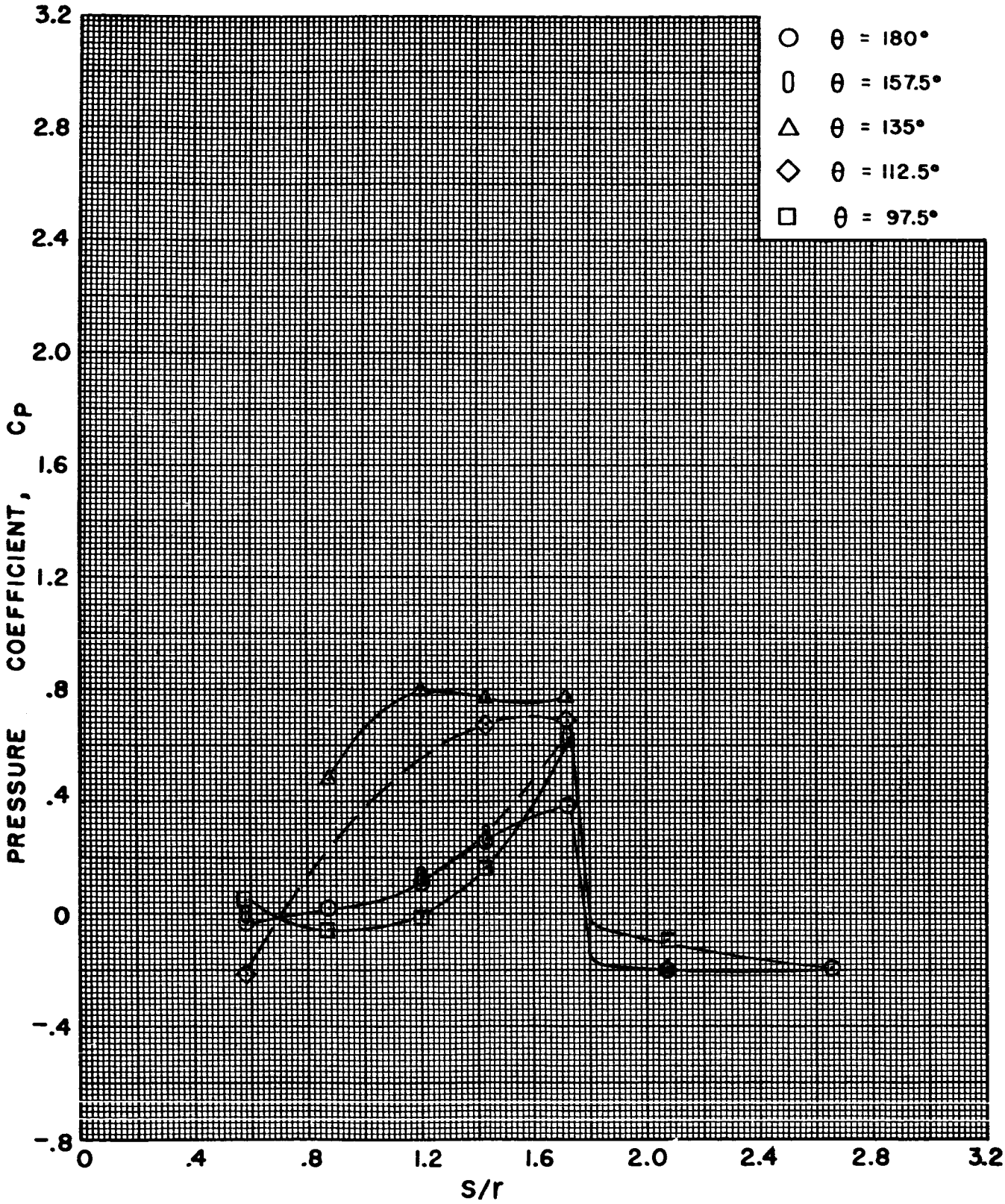

Figure 34f Configuration E[redacted]N[redacted]T[redacted]C[redacted]
65 8 28 40

Mach No. = 1.98 $\alpha = 5°$ $C_T = 2.00$

[redacted]

~~CONFIDENTIAL~~

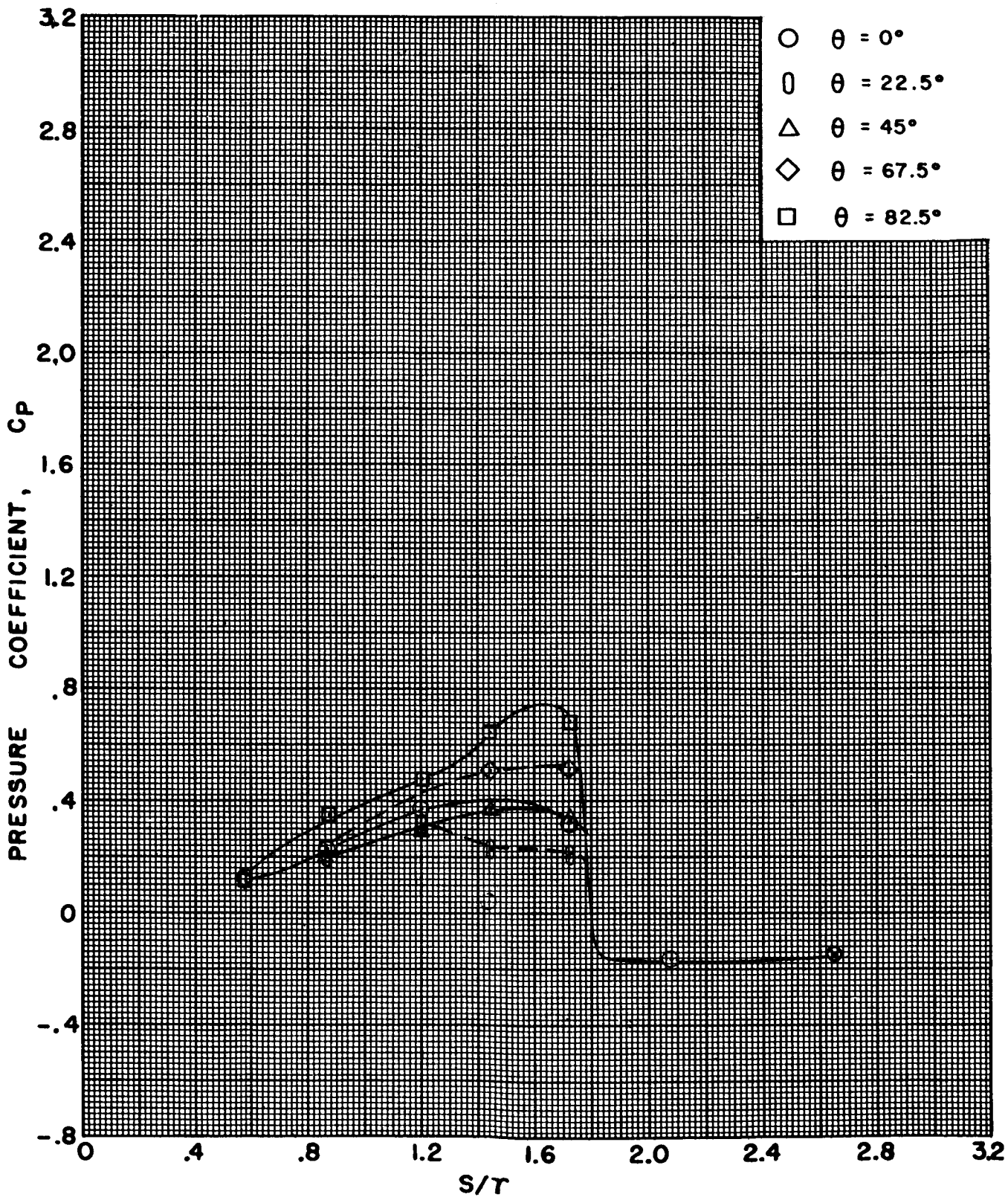

Figure 35a Configuration $E_{65}N_{8}T_{28}C_{40}$ Mach No. 1.98 $\alpha = 10°$ $C_T = 0$

~~CONFIDENTIAL~~

[redacted]

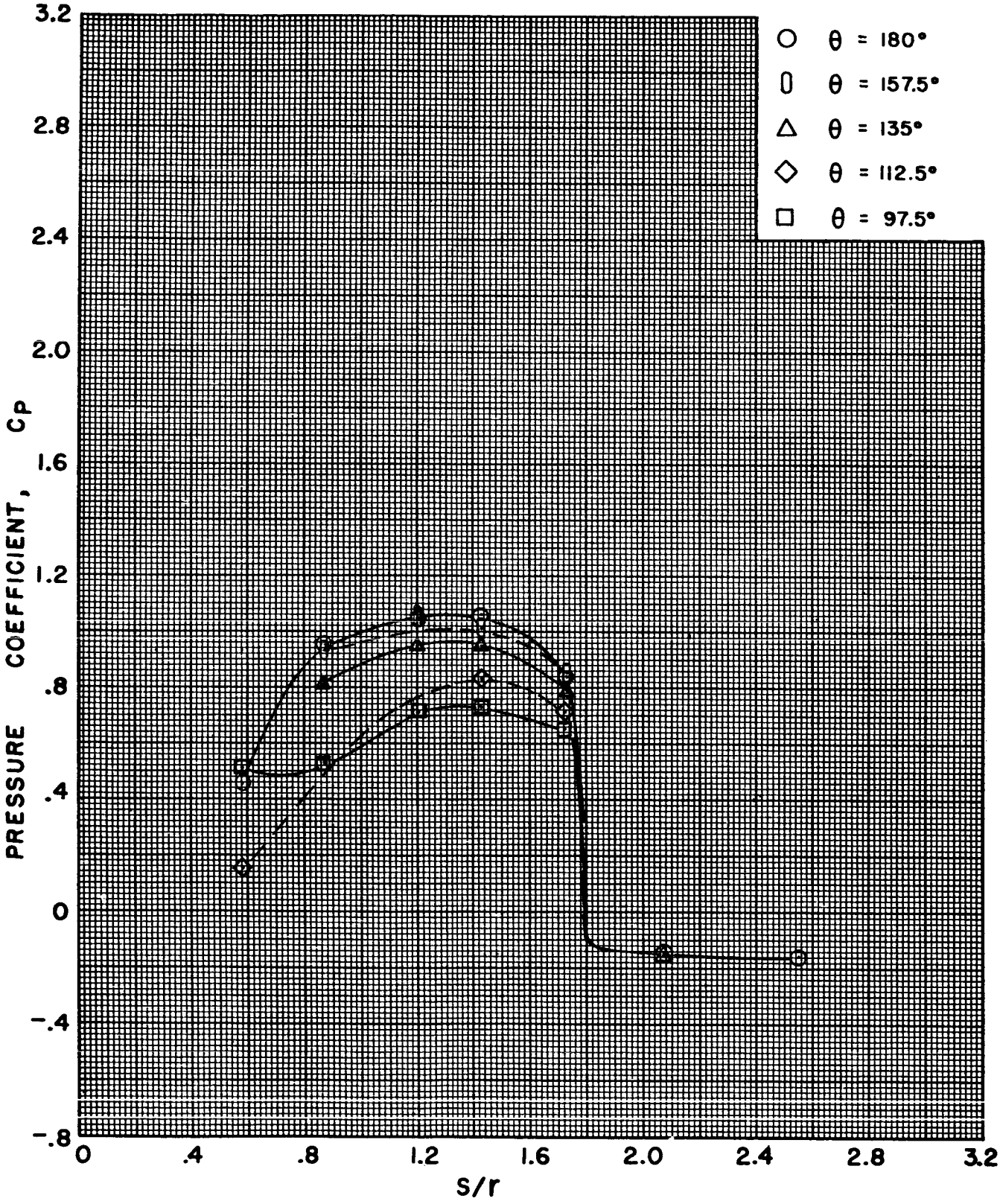

Figure 356 Configuration E[redacted]NT[redacted]C[redacted] 65 8 28 40 Mach No. = 1.98 α = 10 $C_T = 0$

[redacted]

~~CONFIDENTIAL~~

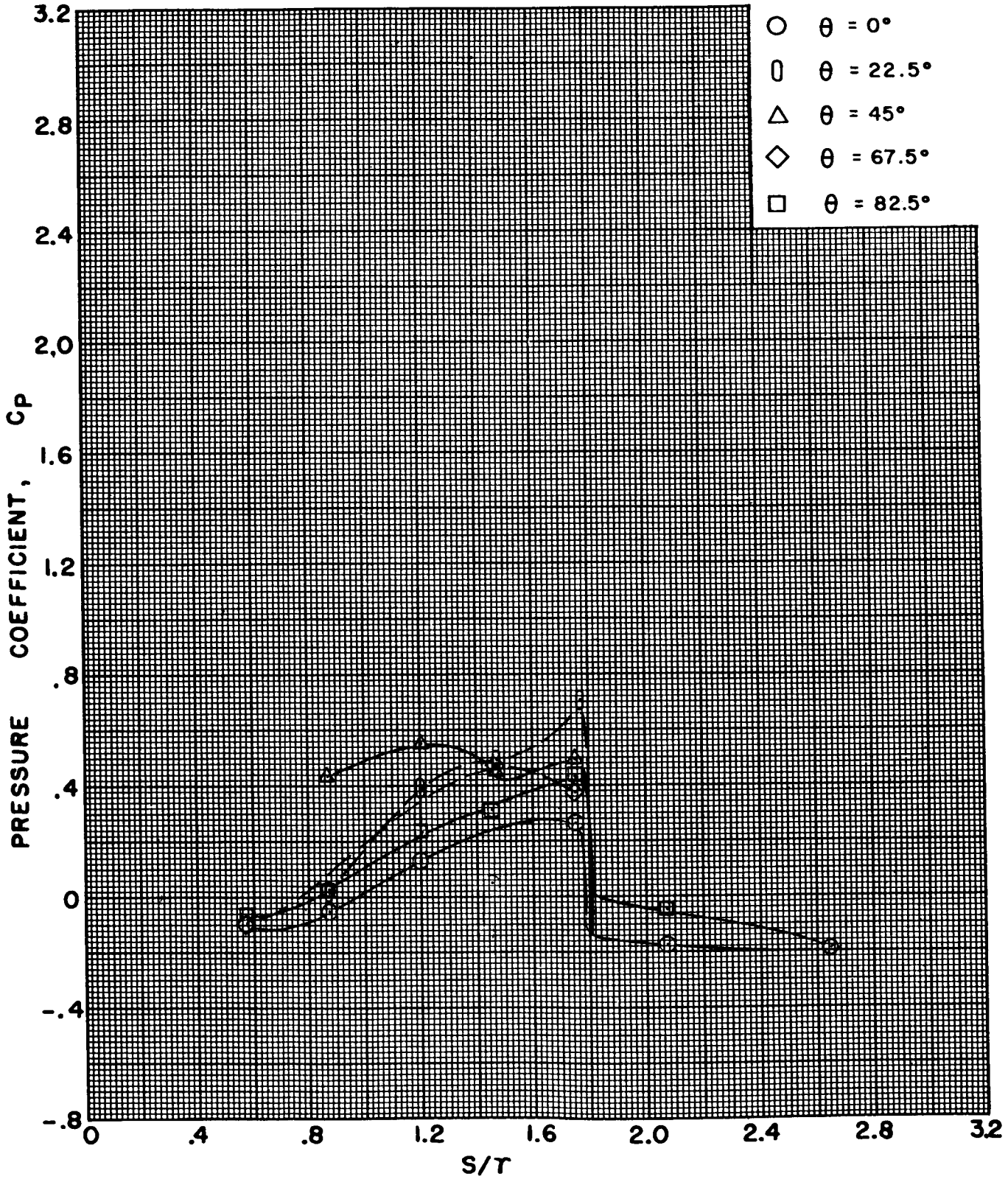

Figure 35c Configuration E[redacted]NT[redacted]C[redacted] 65 6 28 40

Mach No. 1.98 $\alpha = 10°$ $C_T = 1.14$

~~CONFIDENTIAL~~

[redacted]

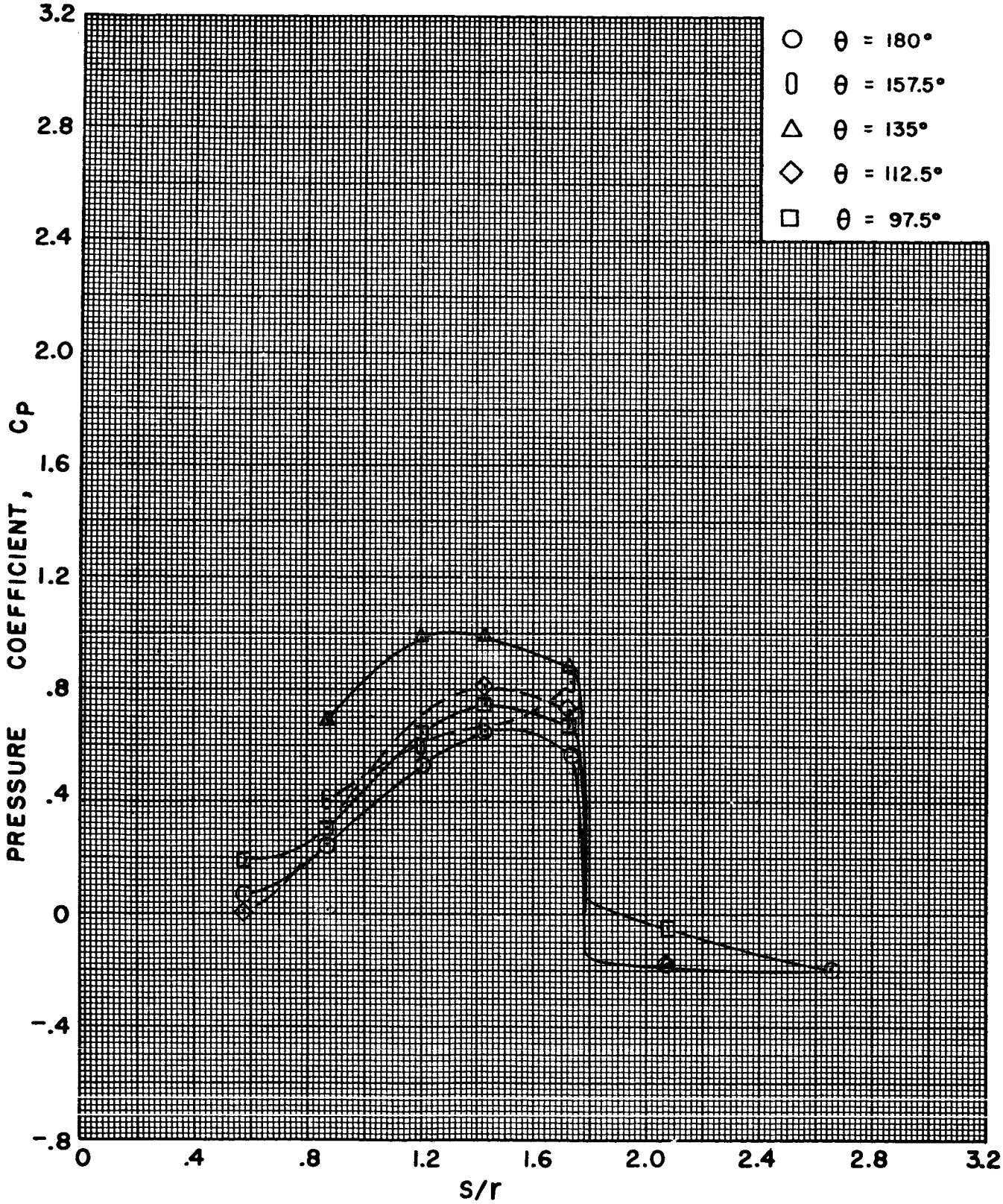

Figure 35d Configuration E[redacted]N[redacted]T[redacted]C[redacted]
65 8 28 40

Mach No. = 1.98 α = 10 C_T = 1.14

[redacted]

~~CONFIDENTIAL~~

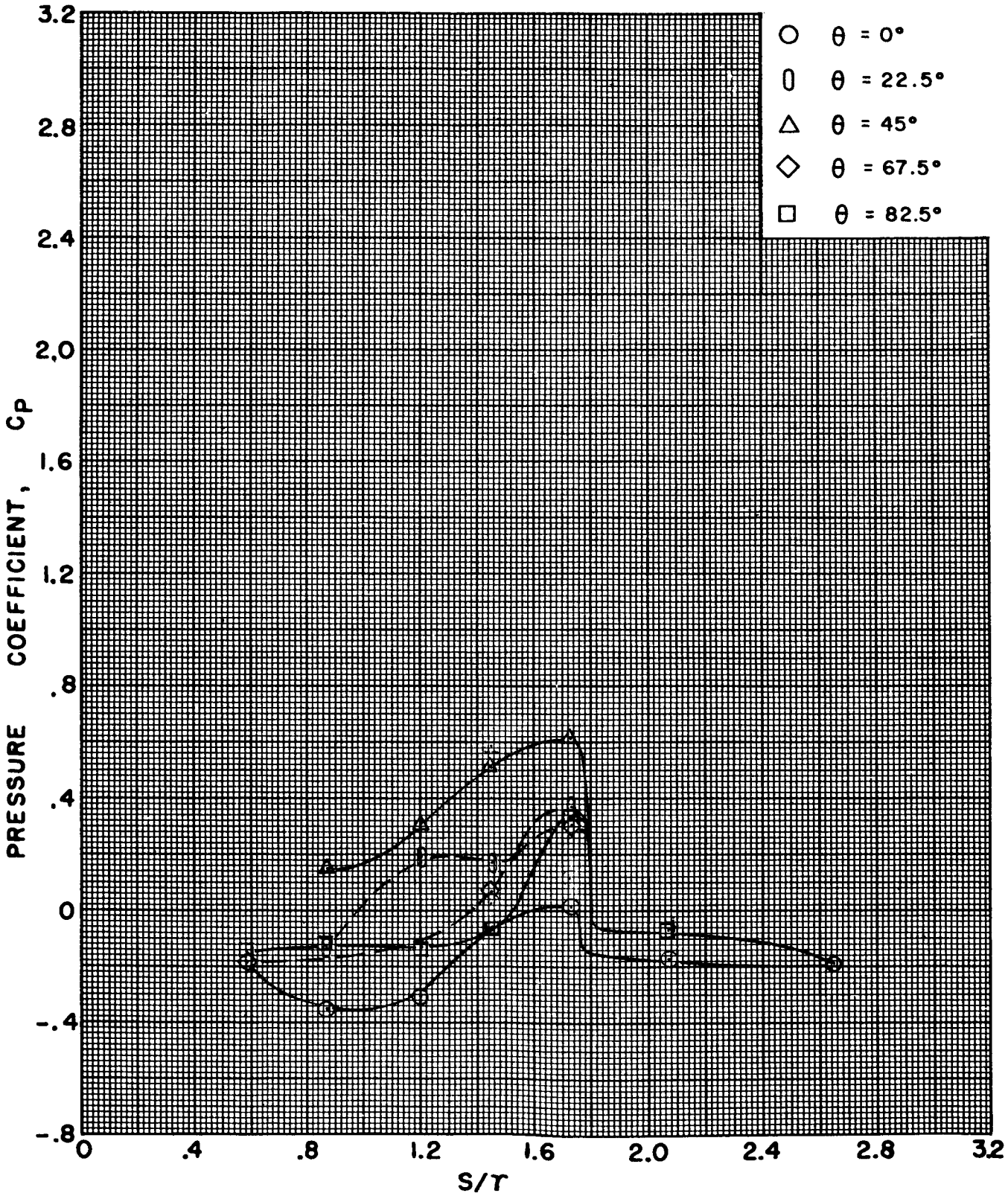

Figure 35e Configuration $E_{65}NT_{8}{}_{28}C_{40}$

Mach No. = 1.98 α = 10 C_T = 2.00

~~CONFIDENTIAL~~

[redacted]

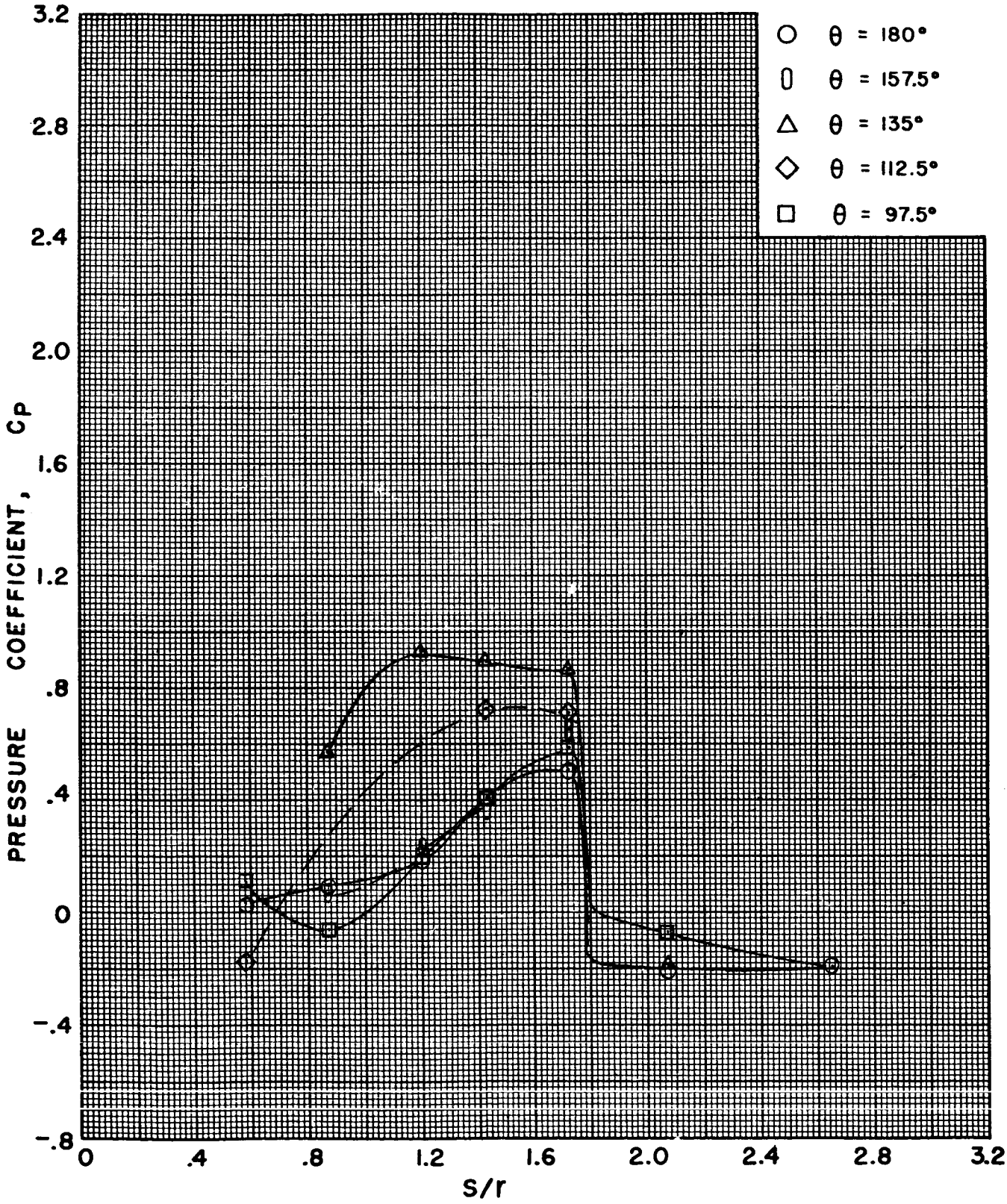

Figure 35f Configuration E[redacted]NT[redacted]C[redacted] 65 8 28 40

Mach No. = 1.98 $\alpha = 10°$ $C_T = 2.00$

[redacted]

[redacted]

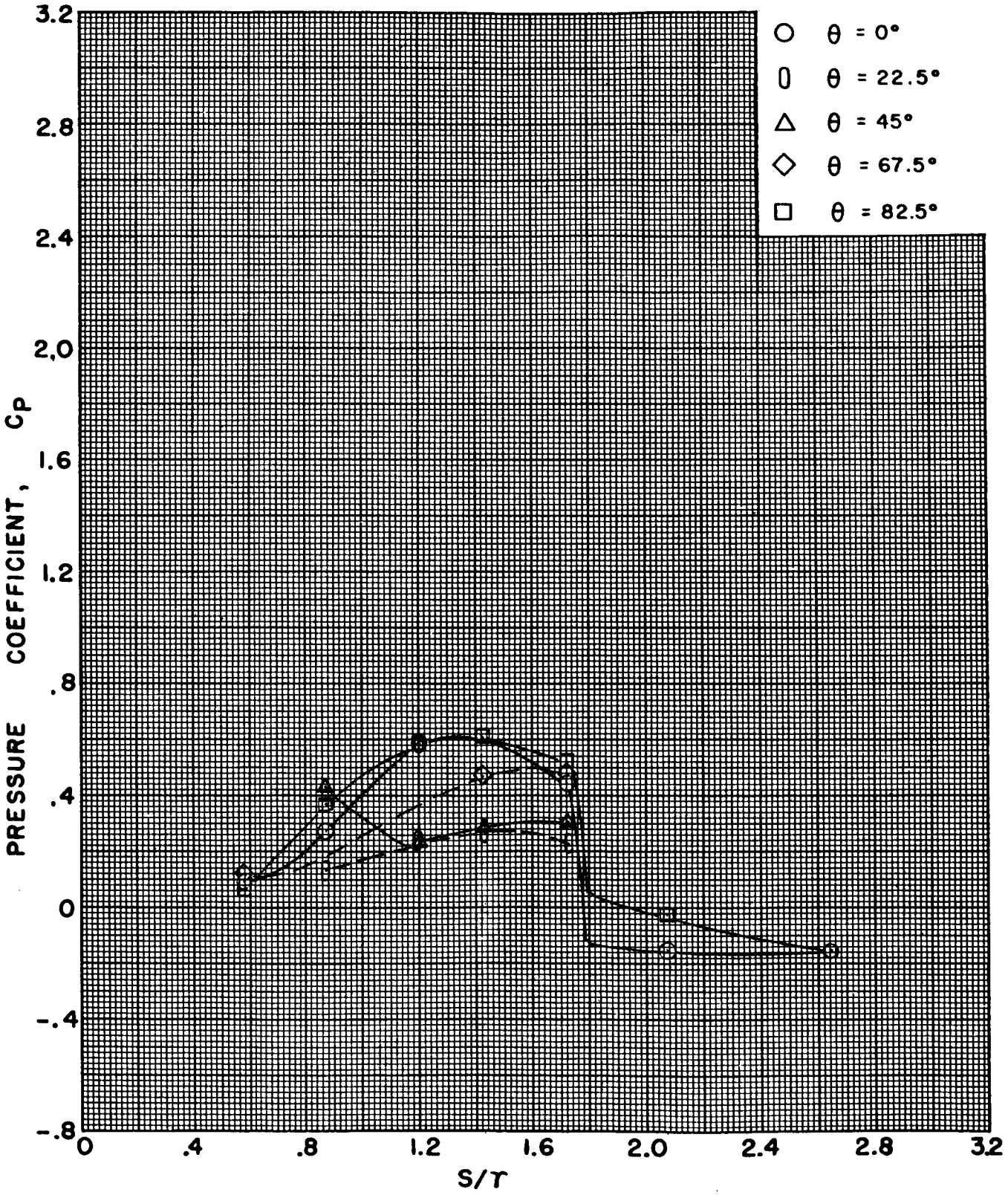

Figure 36a Configuration E[redacted]NT[redacted]C[redacted] 65 8 28 40

Mach No. = 1.98 α = 15° C_T = 0

[redacted]

~~CONFIDENTIAL~~

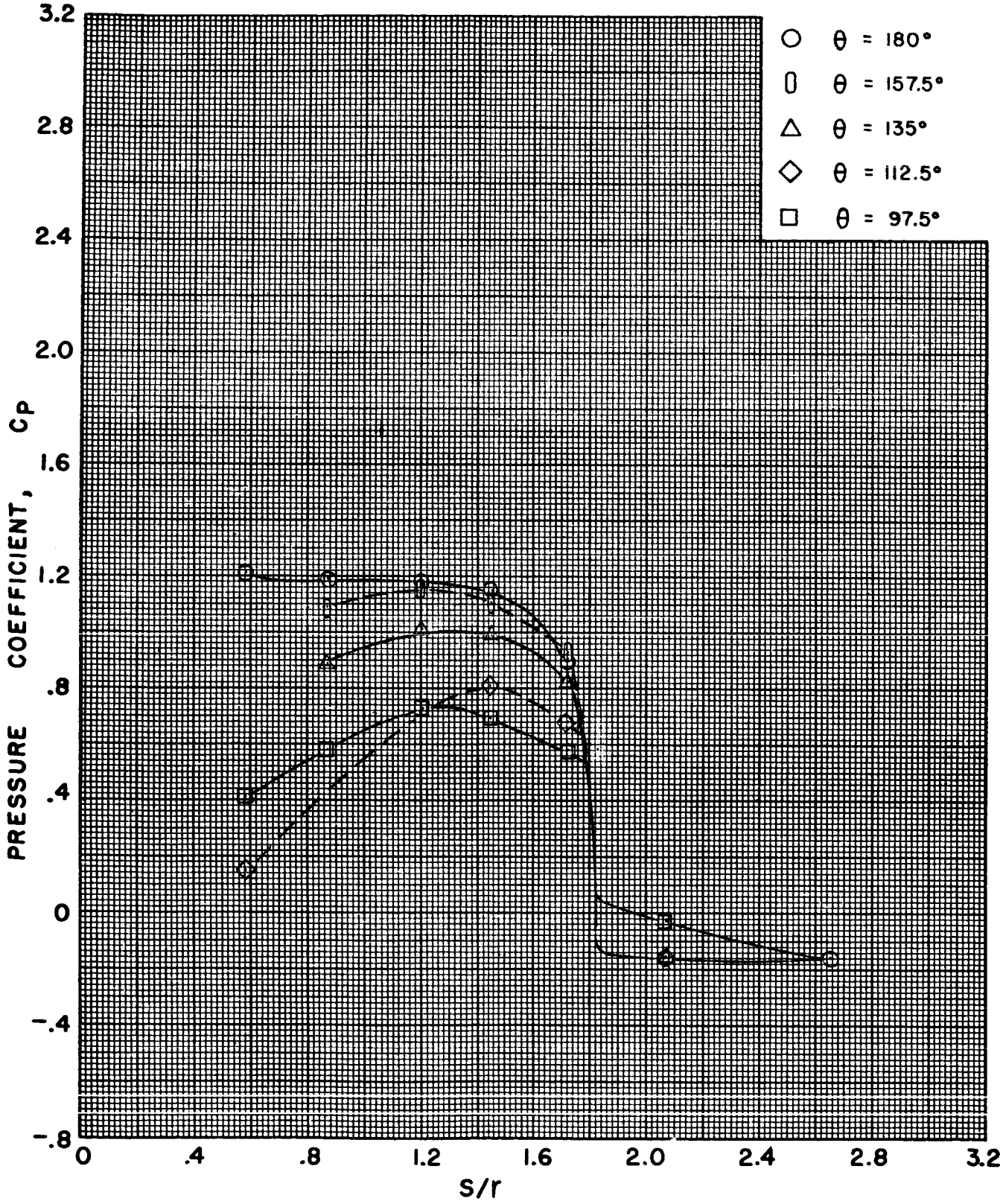

Figure 36 b Configuration $E_{47}NT_{24}C_2$

Mach No. = 1.98 $\alpha = 15°$ $C_T = 0$

~~CONFIDENTIAL~~

~~CONFIDENTIAL~~

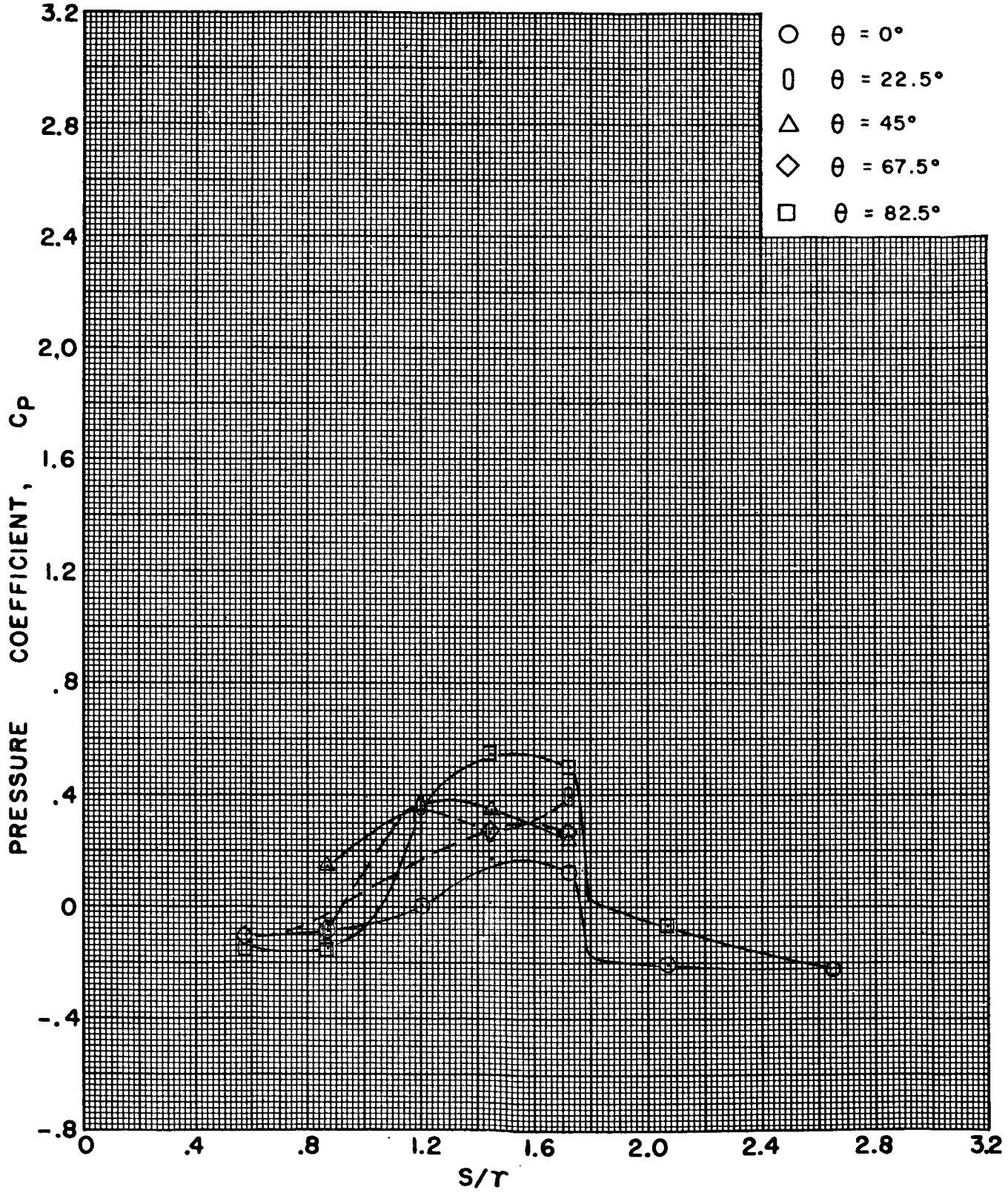

Figure 36c Configuration E[redacted]NT[redacted]Ca
65 6 28 40

Mach No. = 1.98 α = 15° C_T = 1.14

~~CONFIDENTIAL~~

[redacted]

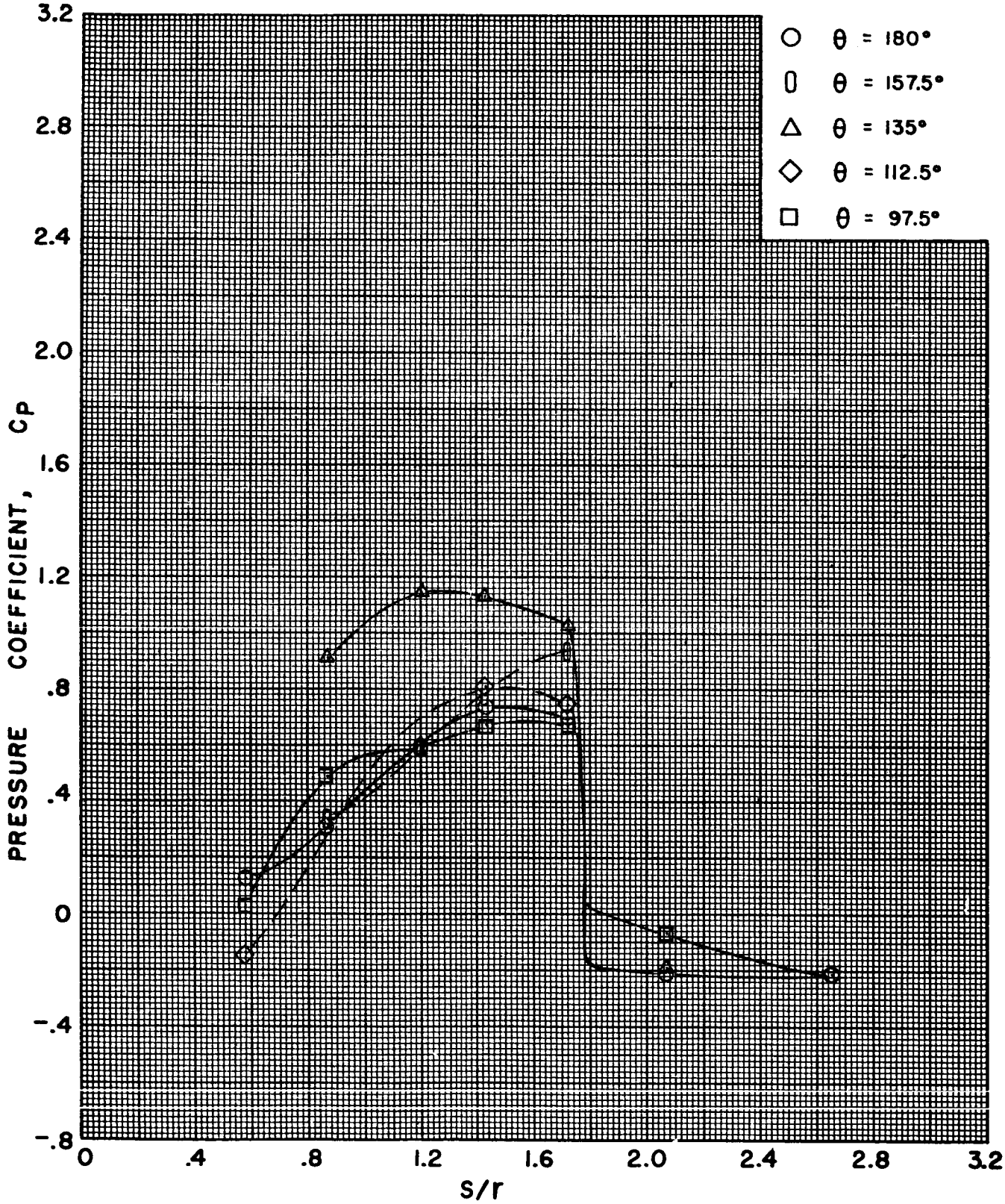

Figure 36d Configuration E[redacted]NT[redacted]C[redacted] 65 8 28 40

Mach No. = 1.98 $\alpha = 15°$ $C_T = 1.14$

[redacted]

~~CONFIDENTIAL~~

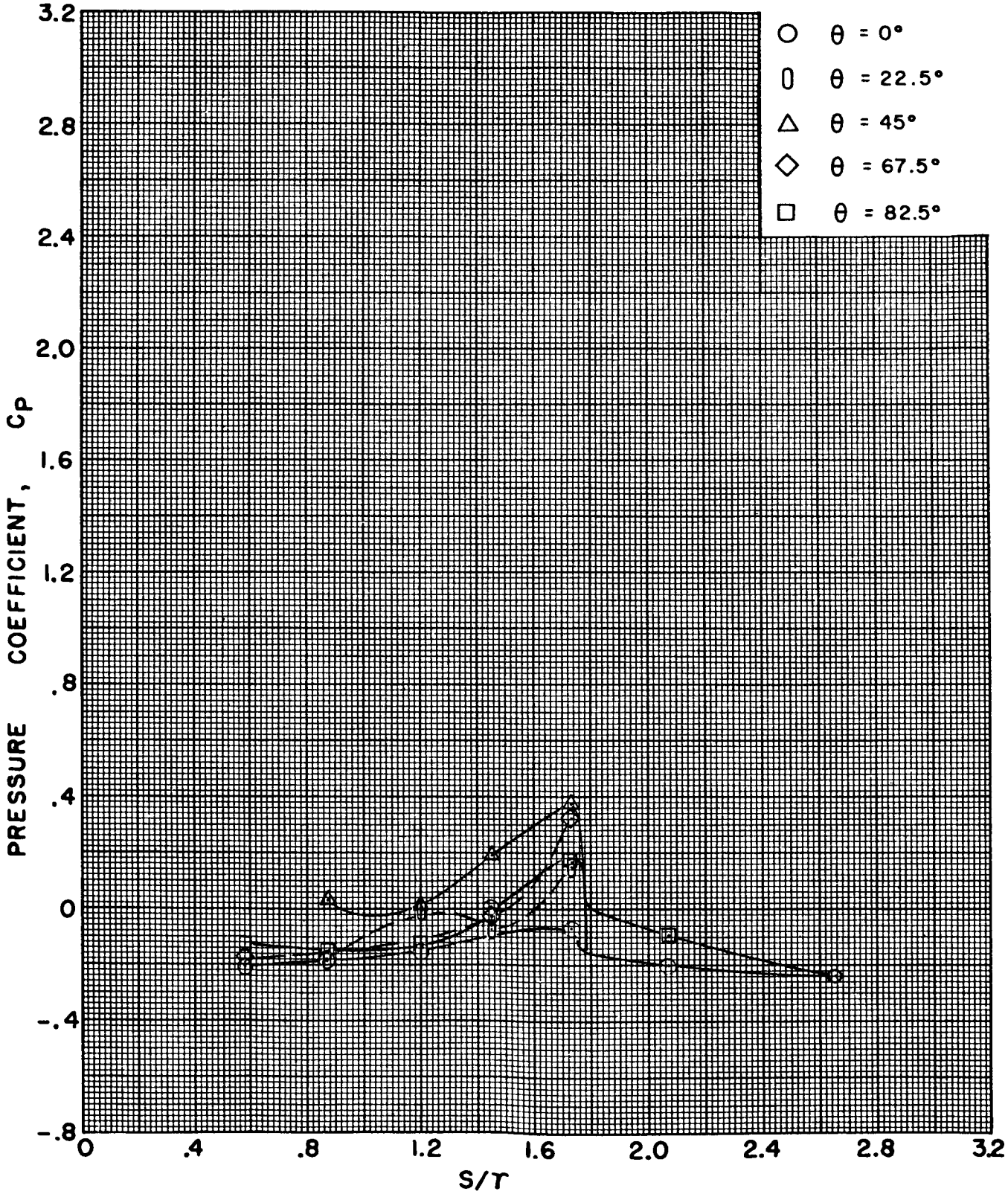

Figure 36e Configuration E[redacted]NT[redacted]C[redacted] 65 8 28 40

Mach No. = 1.98 α = 15° C_T = 2.00

~~CONFIDENTIAL~~

~~CONFIDENTIAL~~

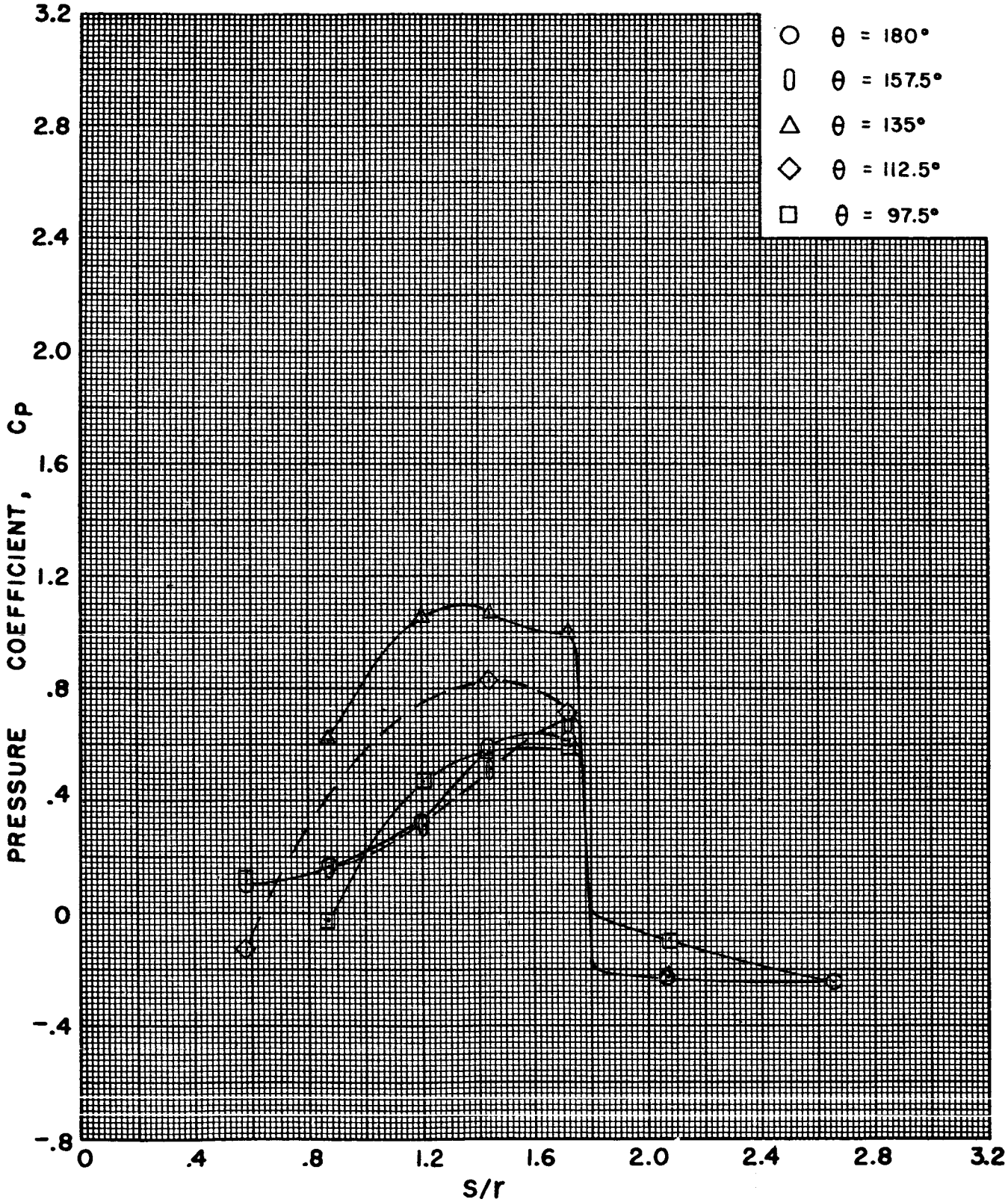

Figure 36f Configuration E[redacted]NT[redacted]C[redacted] 65 8 28 40

Mach No. = 1.98 $\alpha = 15°$ $C_T = 2.00$

~~CONFIDENTIAL~~

~~CONFIDENTIAL~~

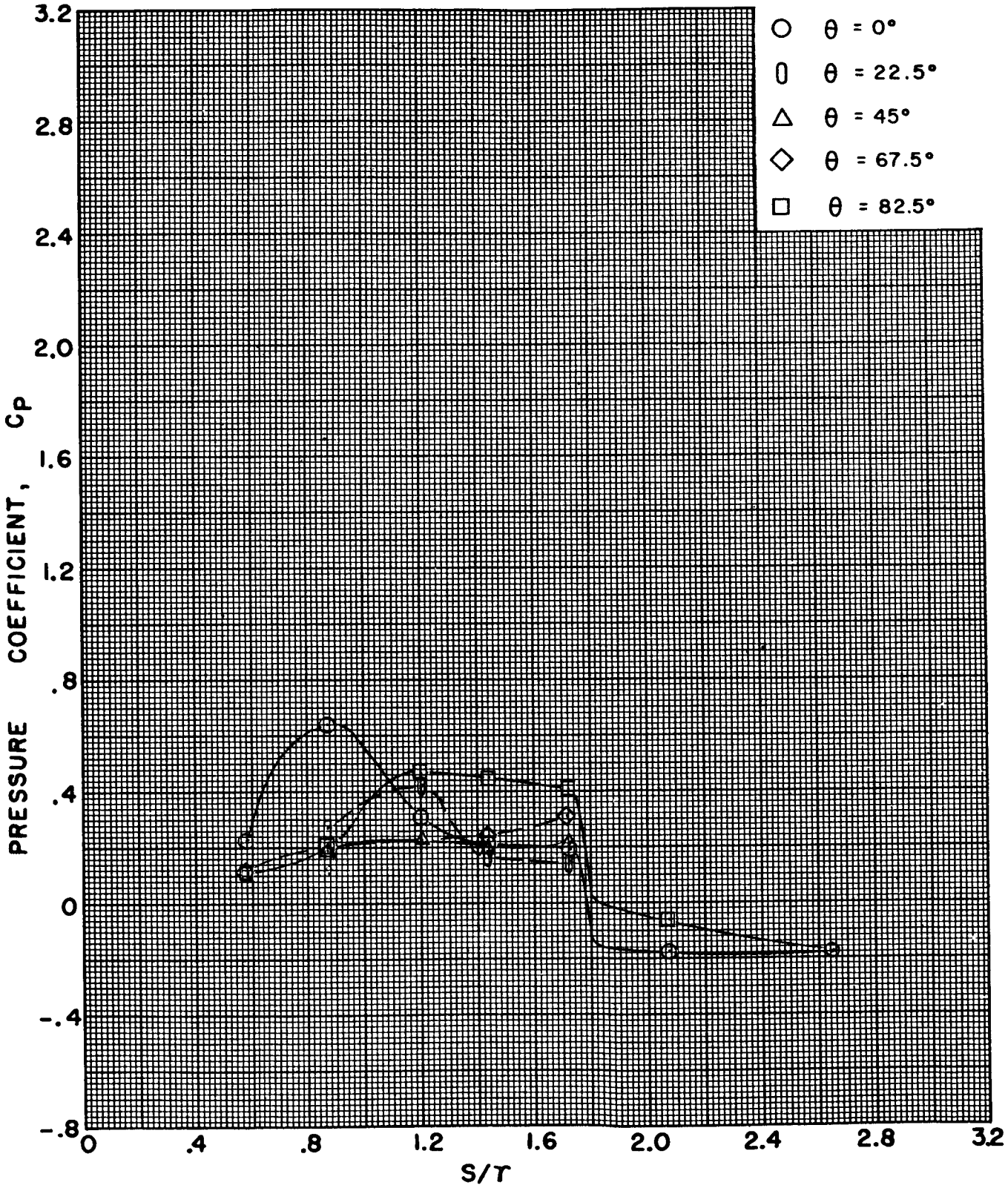

Figure 37a Configuration E 65 NT 8 28 C 40 Mach No. = 1.98 $\alpha = 20°$ $C_T = 0$

~~CONFIDENTIAL~~

[redacted]

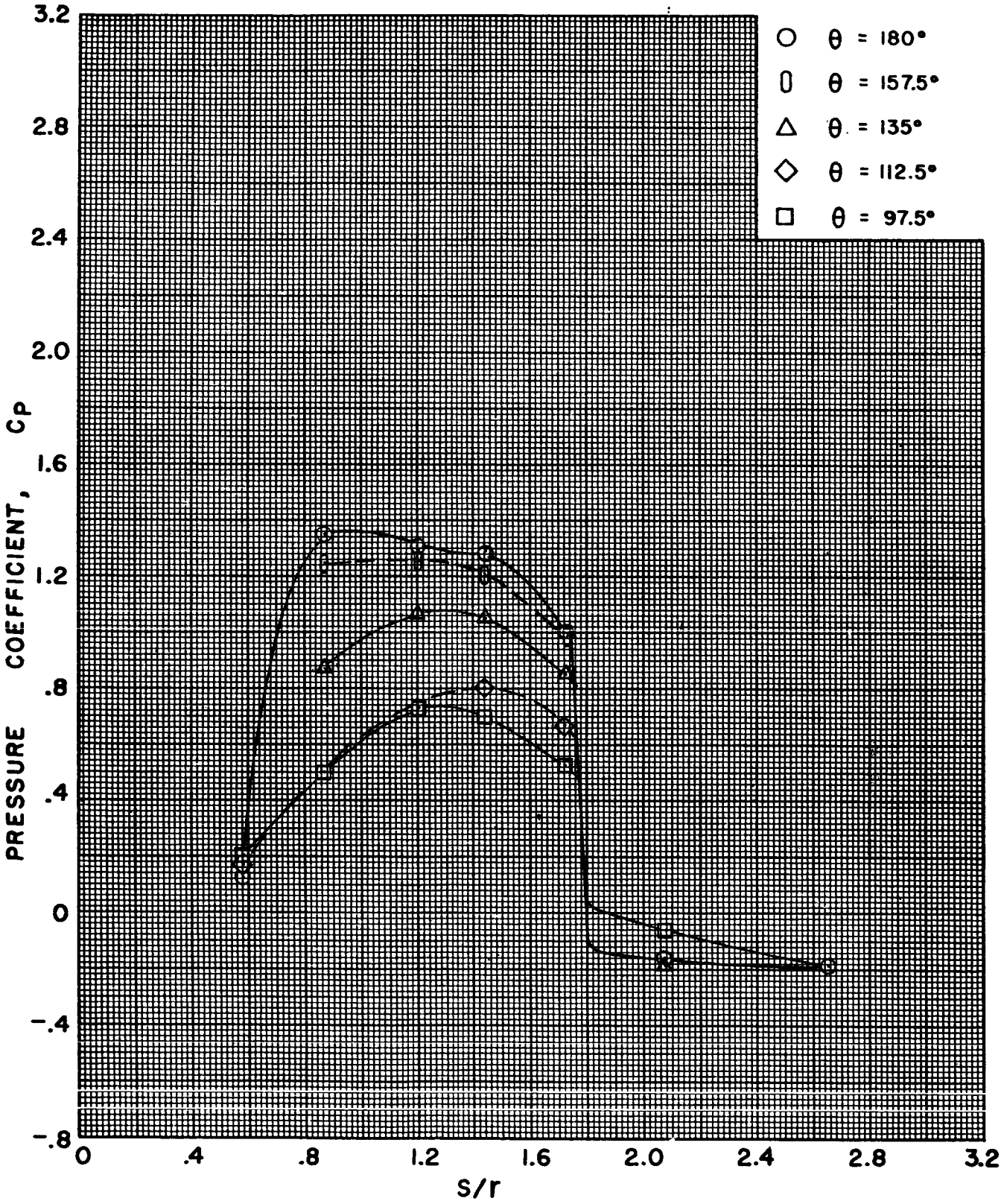

Figure 37b Configuration $E_{65}N_8T_{28}C_{40}$ Mach No. = 1.98 $\alpha = 20°$ $C_T = 0$

[redacted]

~~CONFIDENTIAL~~

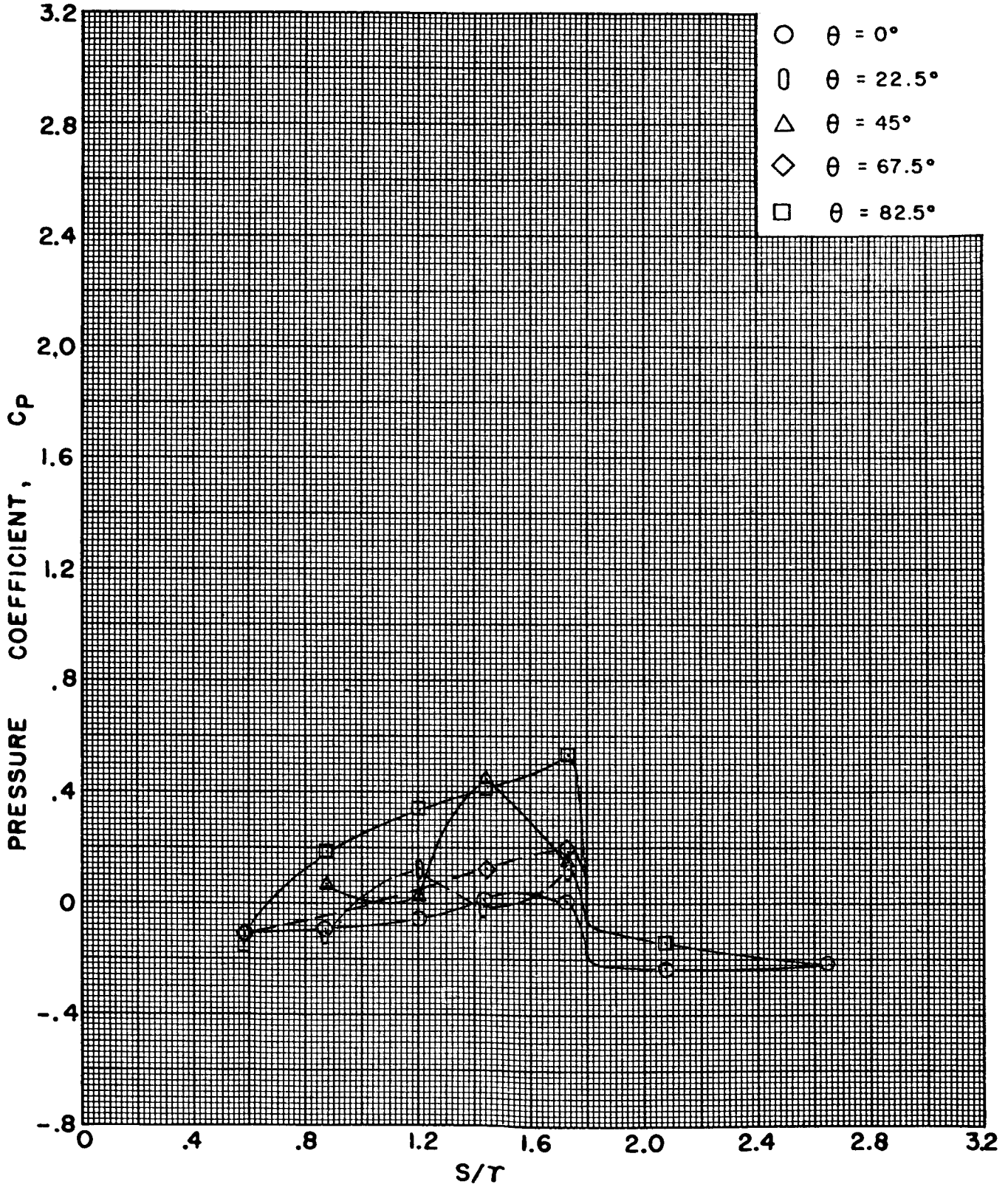

Figure 37c Configuration E[redacted]NT[redacted]C[redacted]
65 8 28 40

Mach No. = 1.98 $\alpha = 20°$ $C_T = 1.14$

~~CONFIDENTIAL~~

[redacted]

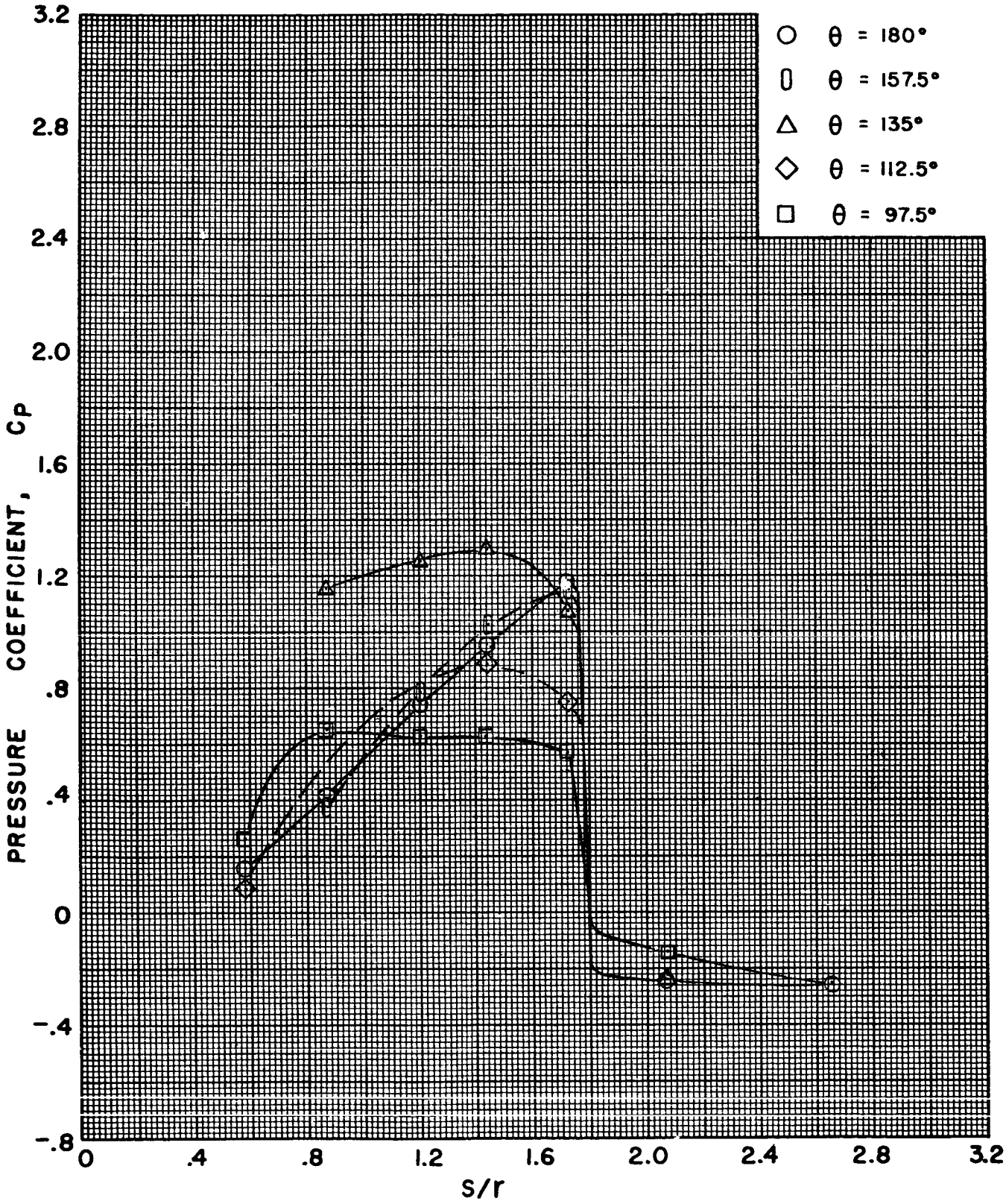

Figure 37d Configuration E[redacted]NT[redacted]C[redacted] 65 8 28 40

Mach No. = 1.98 α = 20° C_T = 1.14

[redacted]

~~CONFIDENTIAL~~

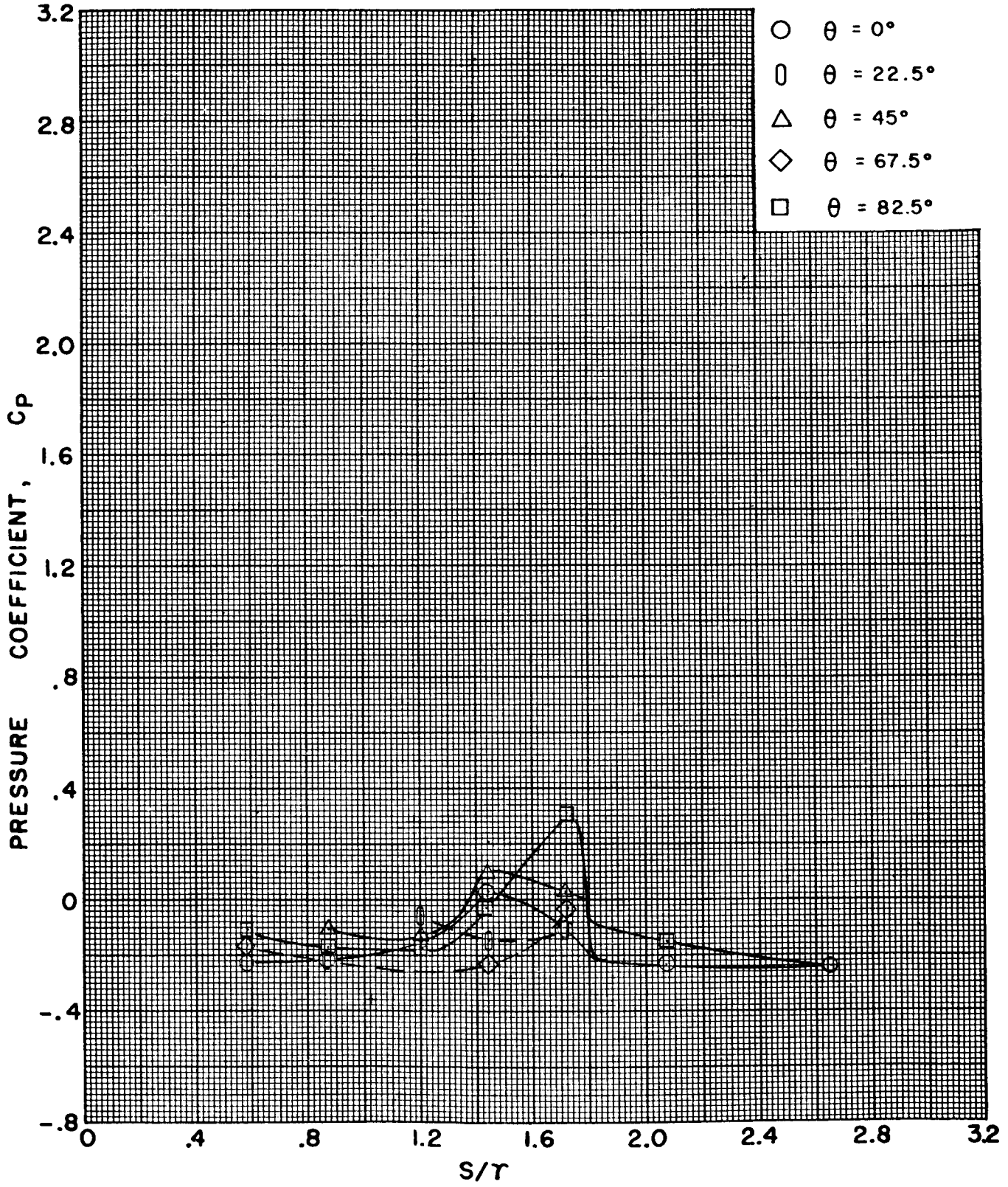

Figure 37e Configuration E[redacted]NT[redacted]C[redacted] 65 8 28 40

Mach No. = 1.98 α = 20° C_T = 2.00

~~CONFIDENTIAL~~

~~CONFIDENTIAL~~

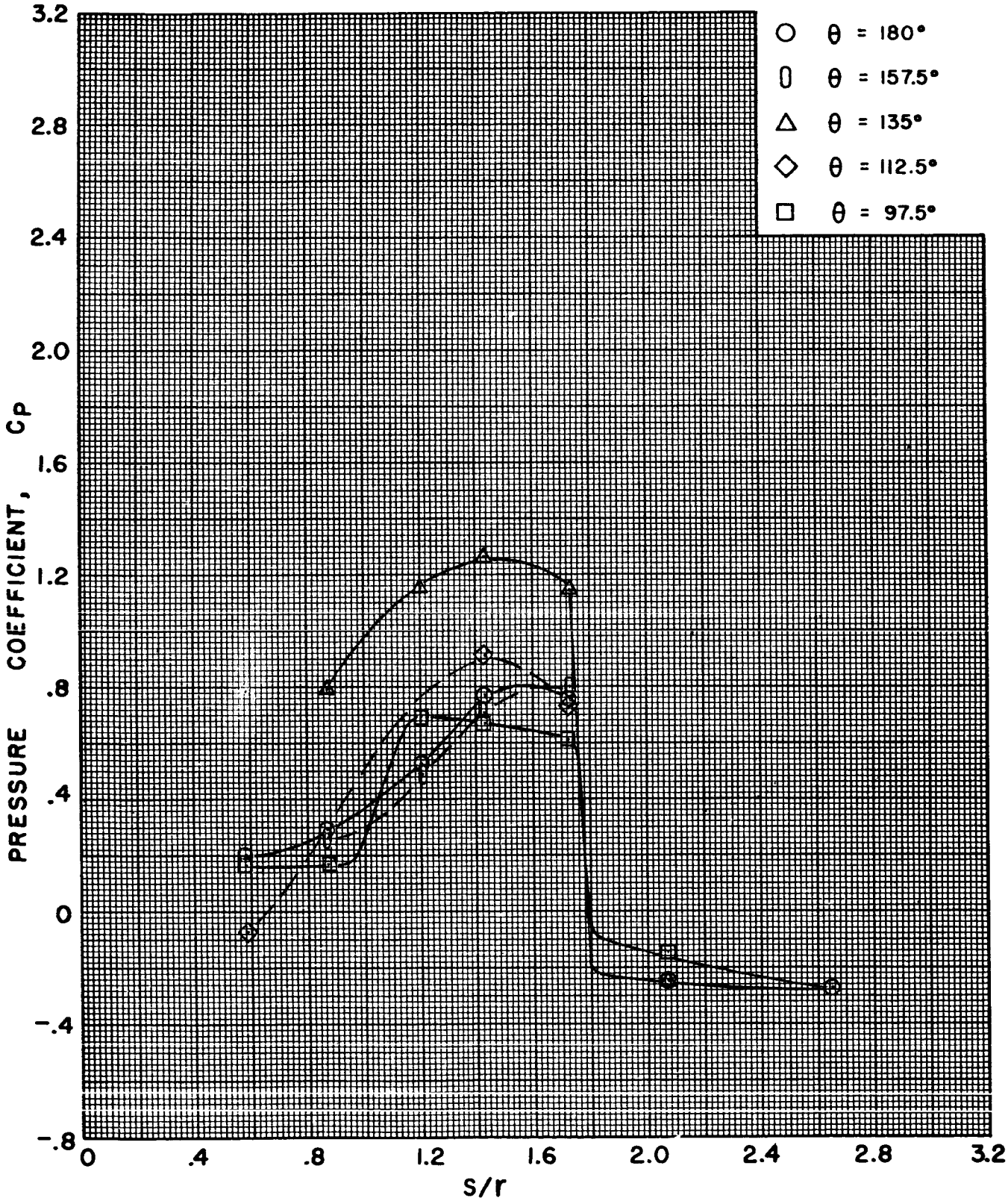

Figure 37f Configuration E[redacted]NT[redacted]C[redacted] 65 8 28 40

Mach No. = 1.98 $\alpha = 20°$ $C_T = 2.00$

~~CONFIDENTIAL~~

~~CONFIDENTIAL~~

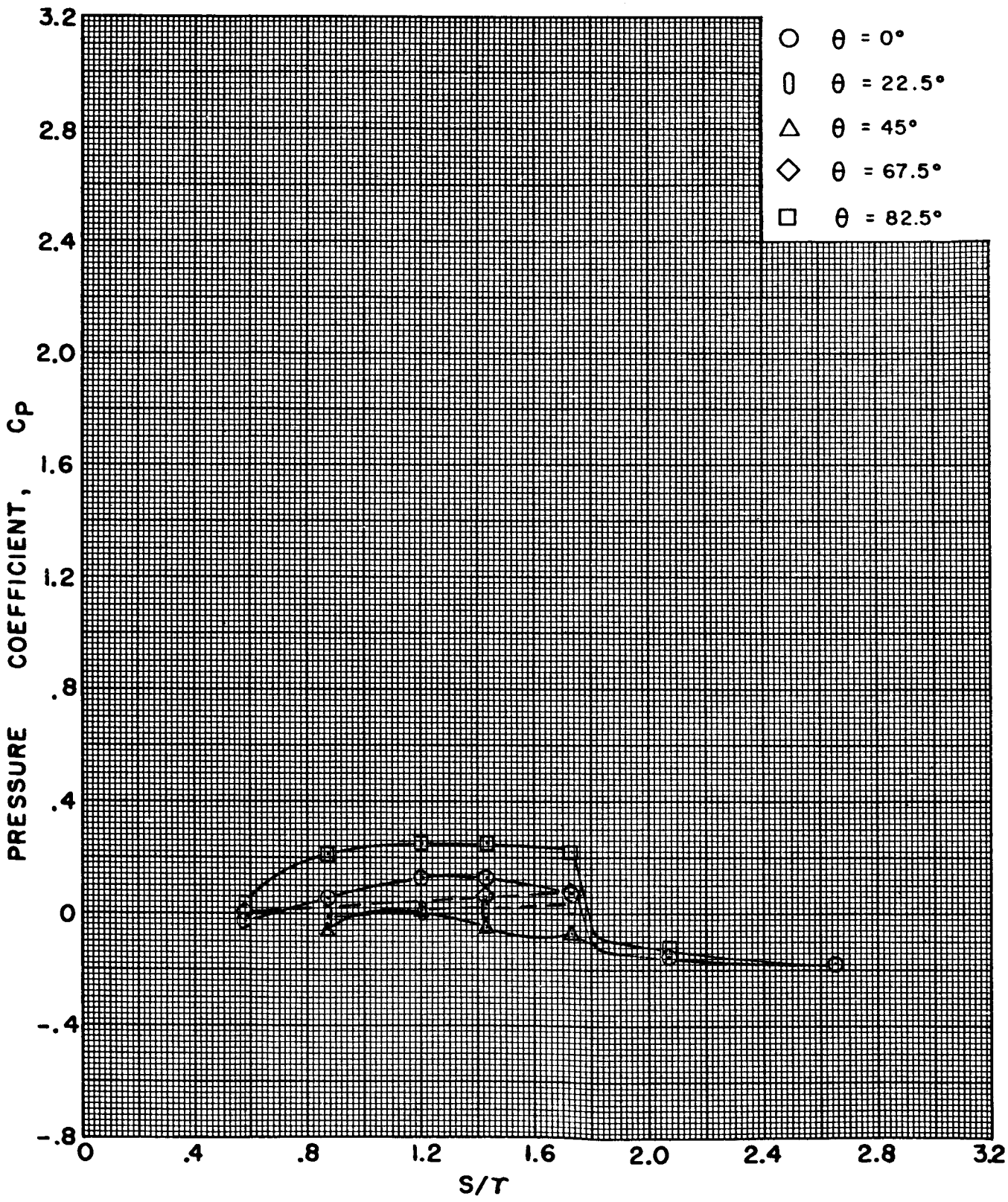

Figure 38a Configuration E[redacted]NT[redacted]C[redacted] 65 8 28 40

Mach No. = 1.98 $\alpha = 30°$ $C_T = 0$

~~CONFIDENTIAL~~

CONFIDENTIAL

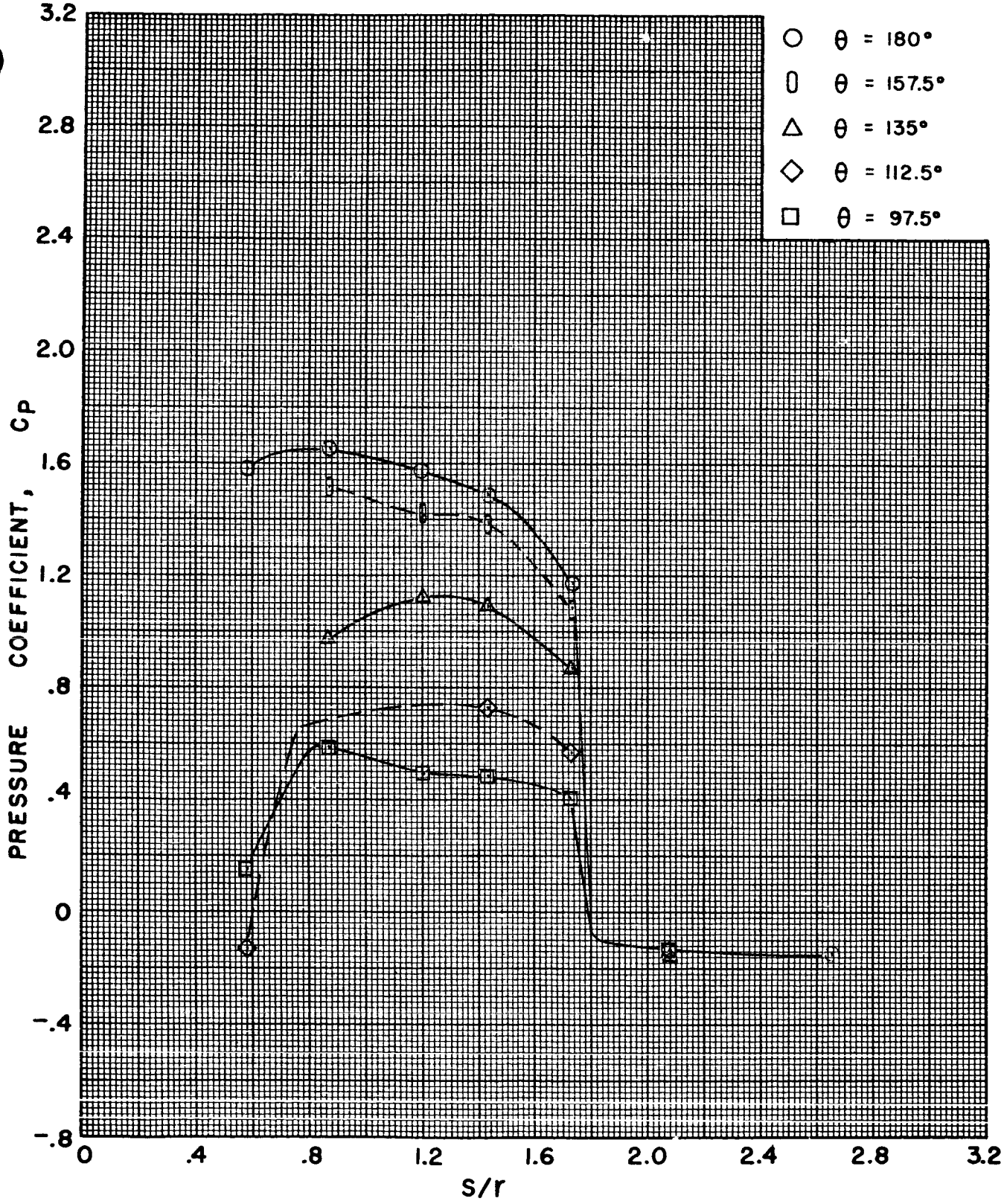

Figure 38b Configuration E65 NT8 28 C40

Mach No. = 1.98 $\alpha = 30°$ $C_T = 0$

CONFIDENTIAL

~~CONFIDENTIAL~~

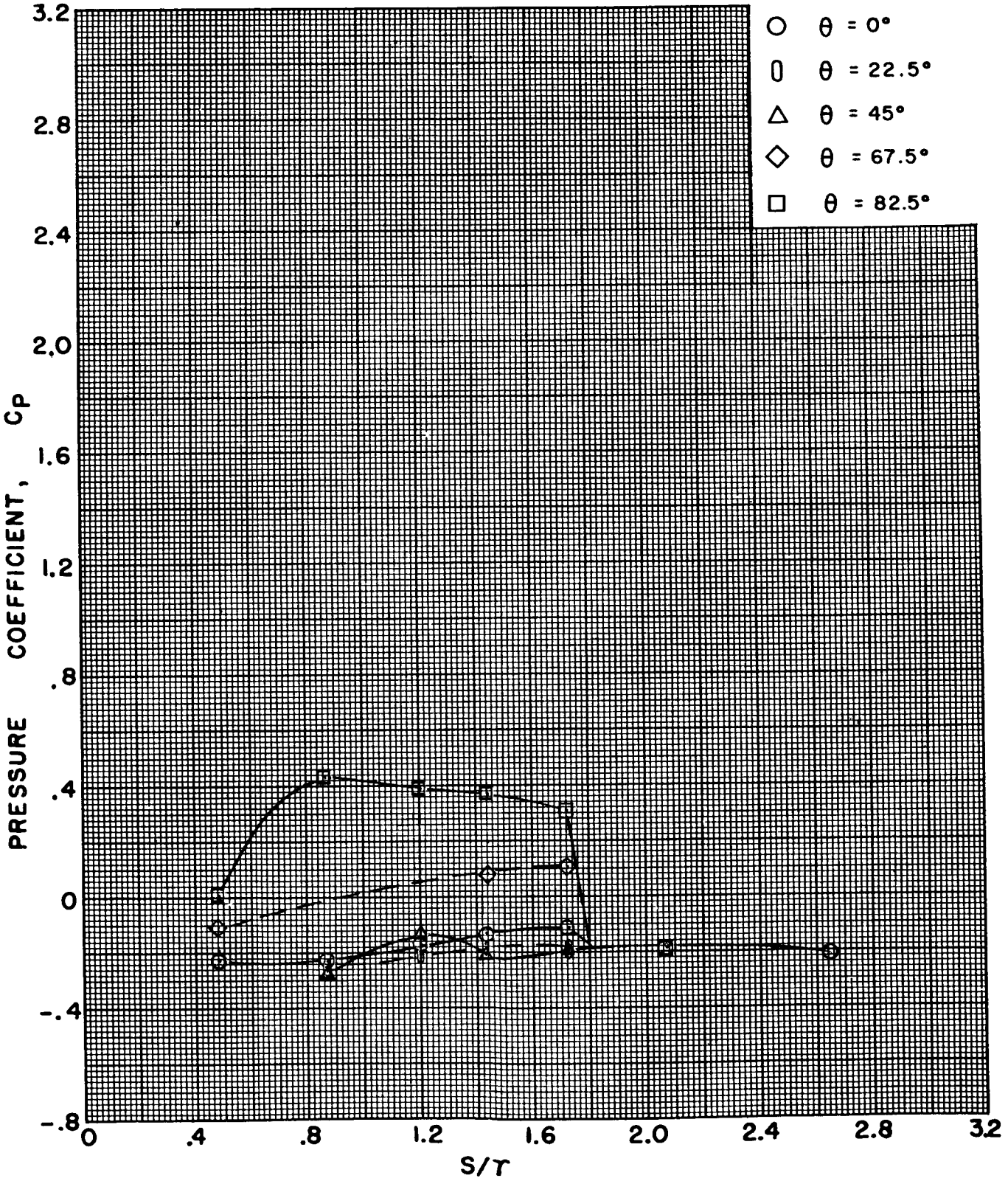

Figure 38c Configuration E[redacted]NT[redacted]C[redacted] 65 8 28 40

Mach No. = 1.98 α = 30° C_T = 1.14

~~CONFIDENTIAL~~

CONFI[redacted]

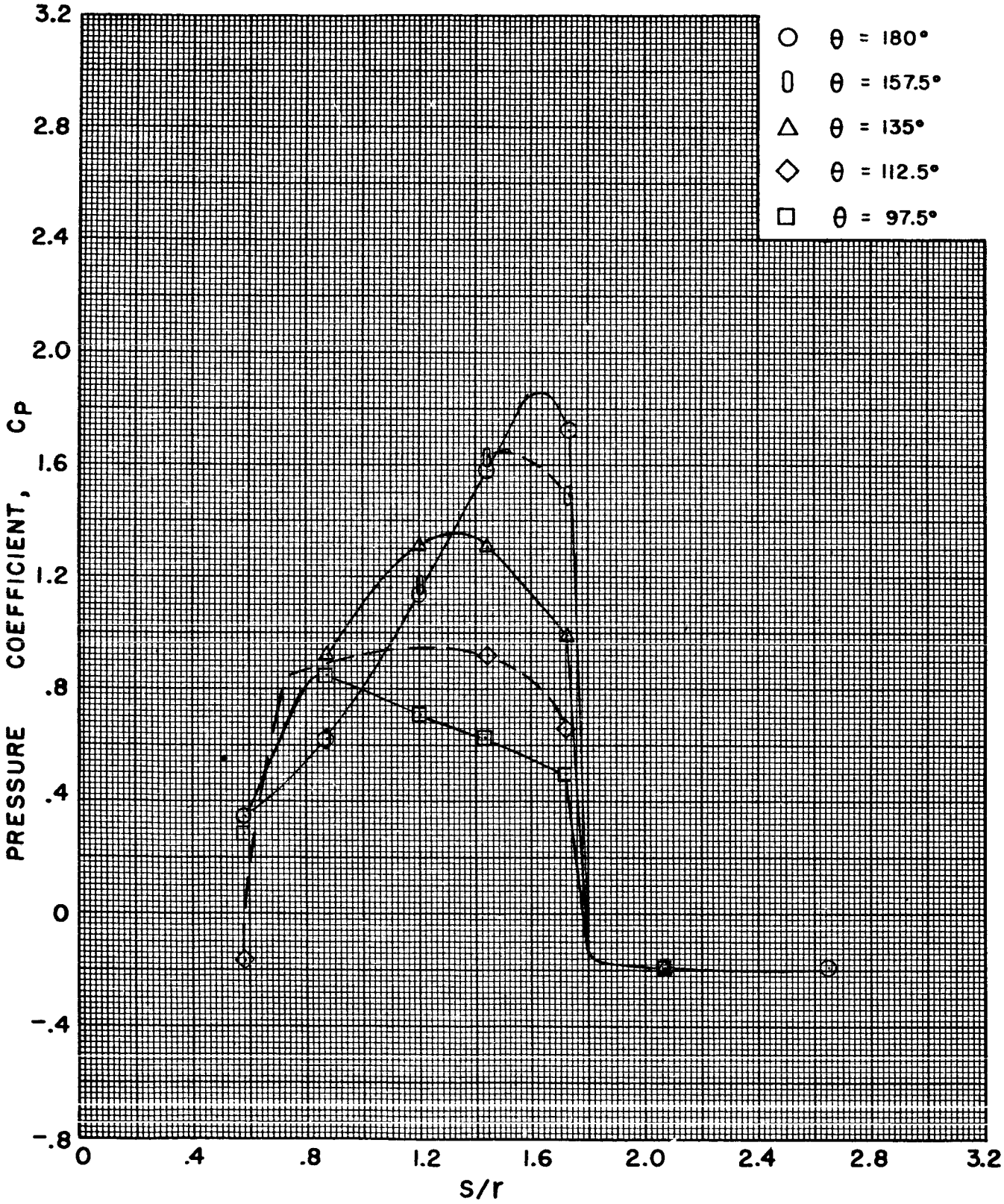

Figure 38 d Configuration E[redacted]NT[redacted]C[redacted]
65 8 28 40

Mach No. = 1.98 $\alpha = 30°$ $C_T = 1.14$

[redacted]

~~CONFIDENTIAL~~

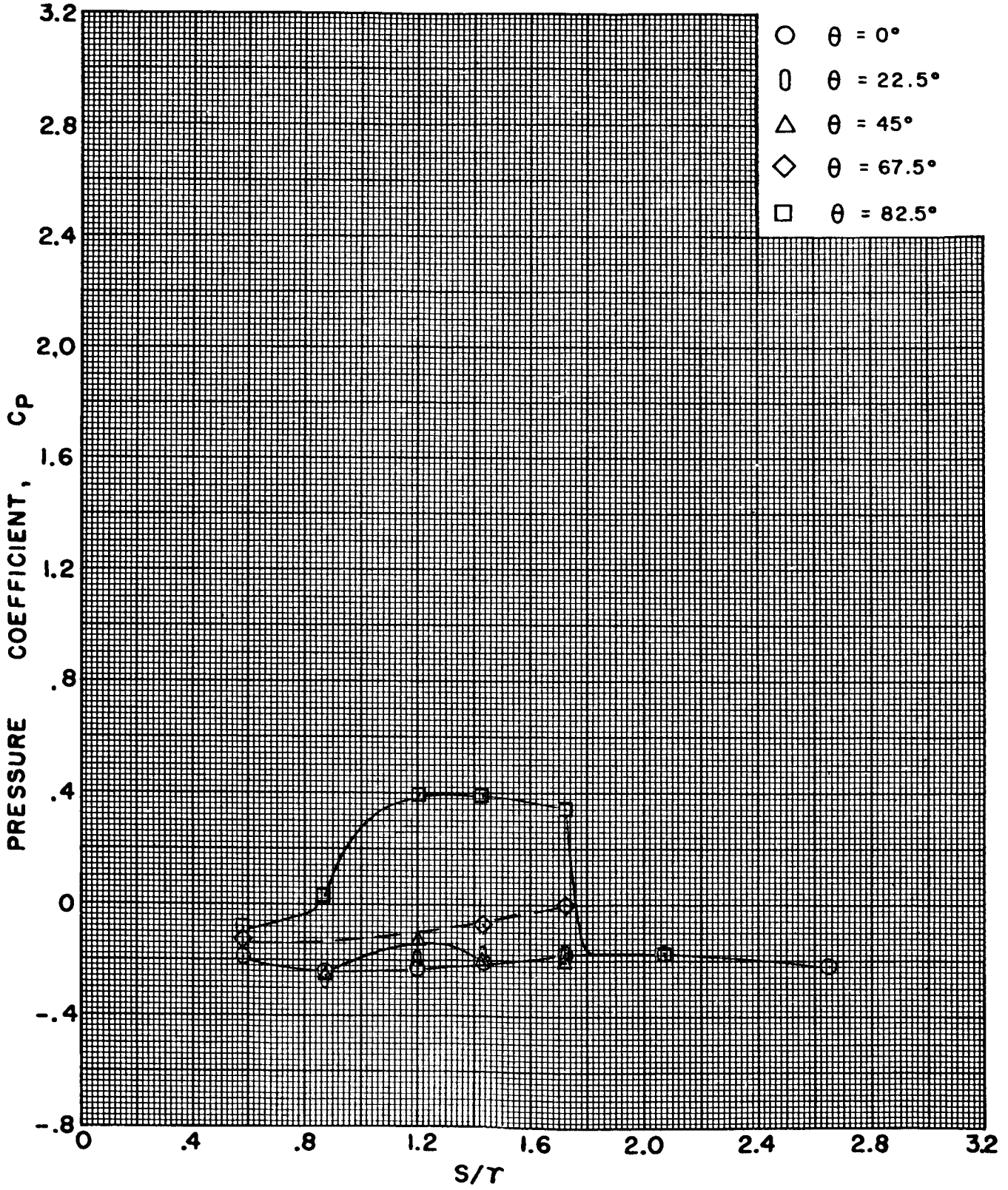

Figure 38e Configuration E[redacted]NT[redacted]C[redacted] 65 8 28 40 Mach No. = 1.98 $\alpha = 30°$ $C_T = 2.00$

~~CONFIDENTIAL~~

CO[redacted]

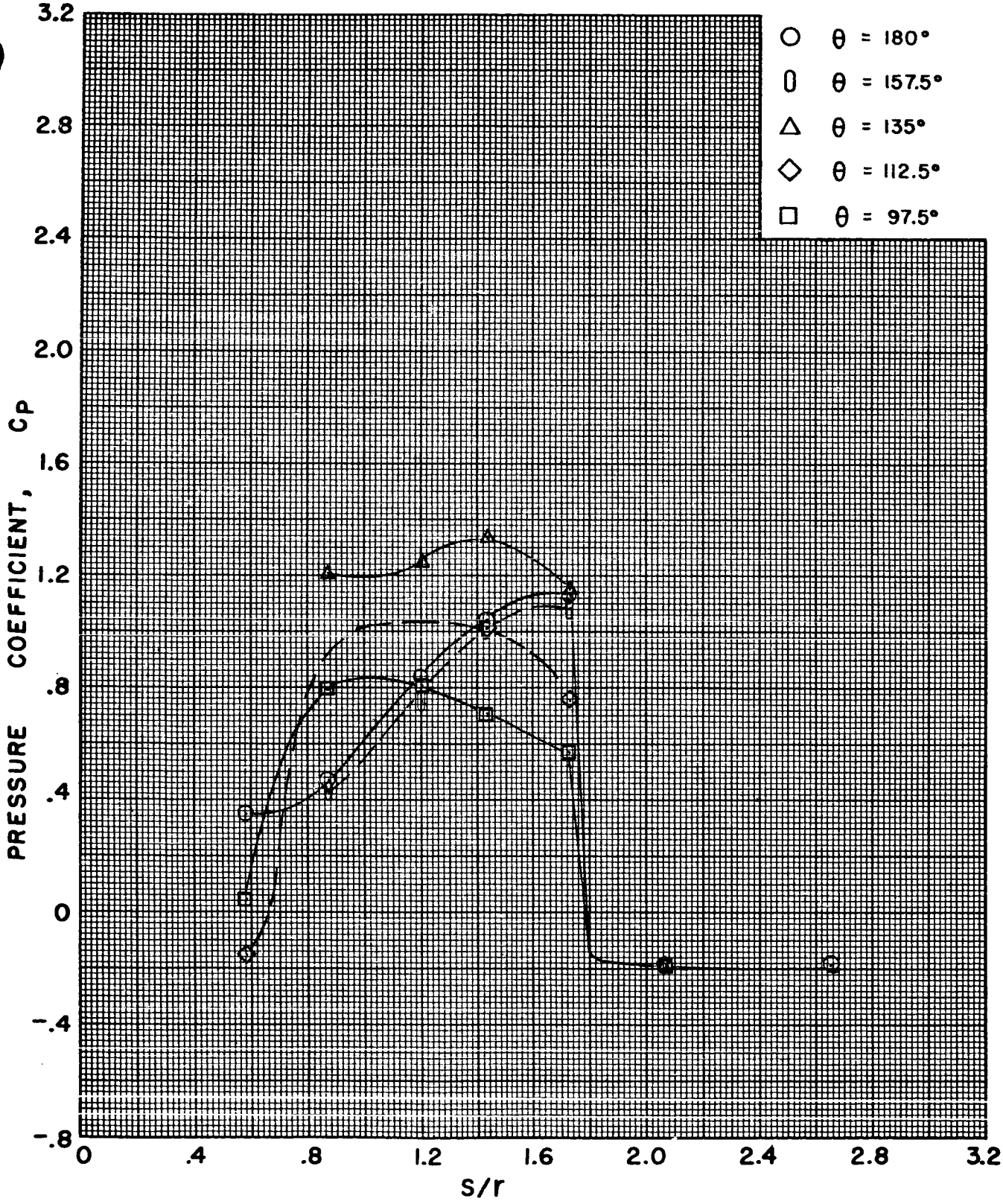

Figure 38f Configuration E[redacted]N[redacted]T[redacted]C[redacted]
65 8 28 40

Mach No. = 1.98 $\alpha = 30°$ $C_T = 2.00$

[redacted]

~~CONFIDENTIAL~~

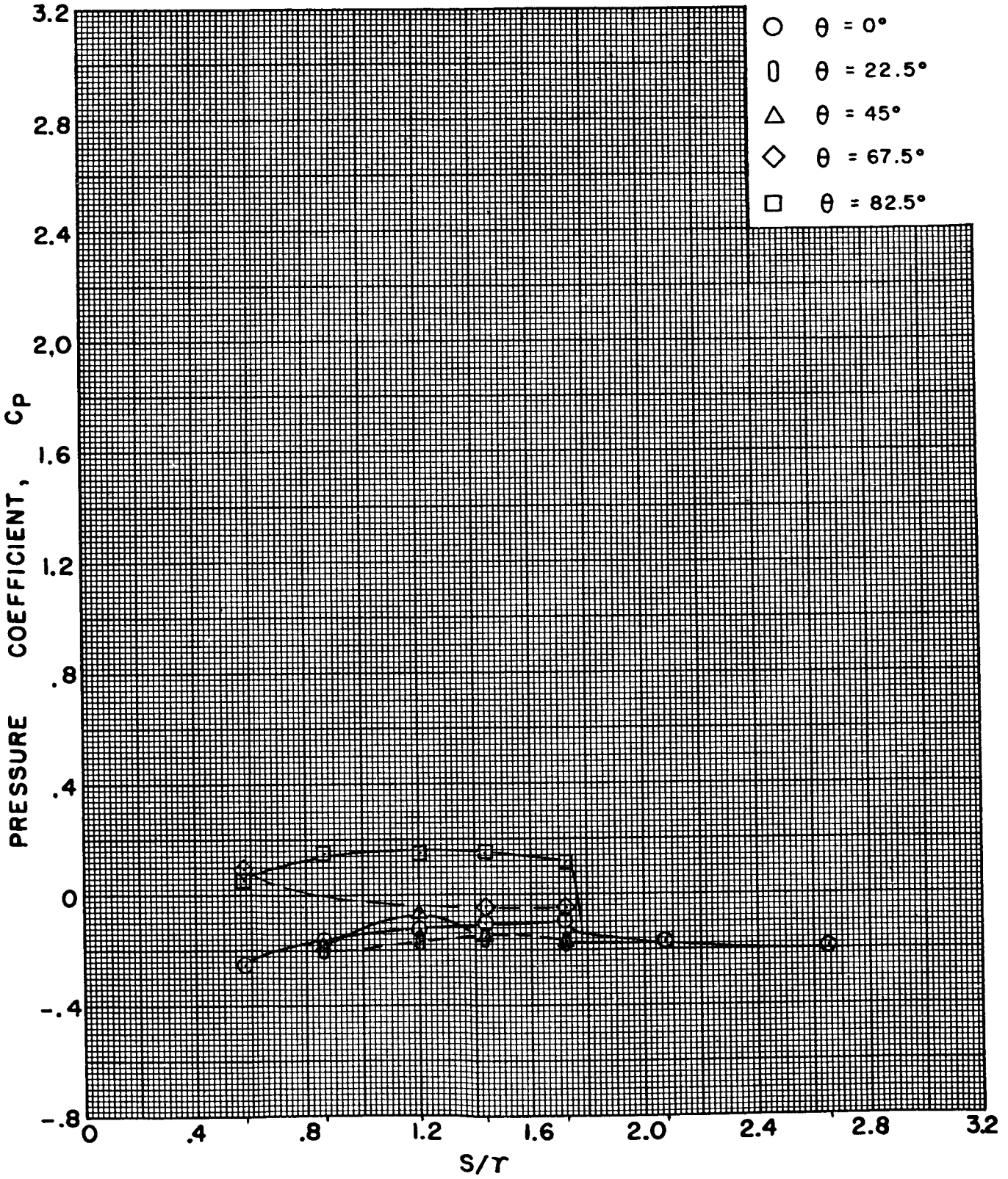

Figure 39a Configuration E[redacted]NT[redacted]C[redacted]
65 8 28 40

Mach No. = 1.98 $\alpha = 40°$ $C_T = 0$

~~CONFIDENTIAL~~

CO[redacted]DEN[redacted]AL

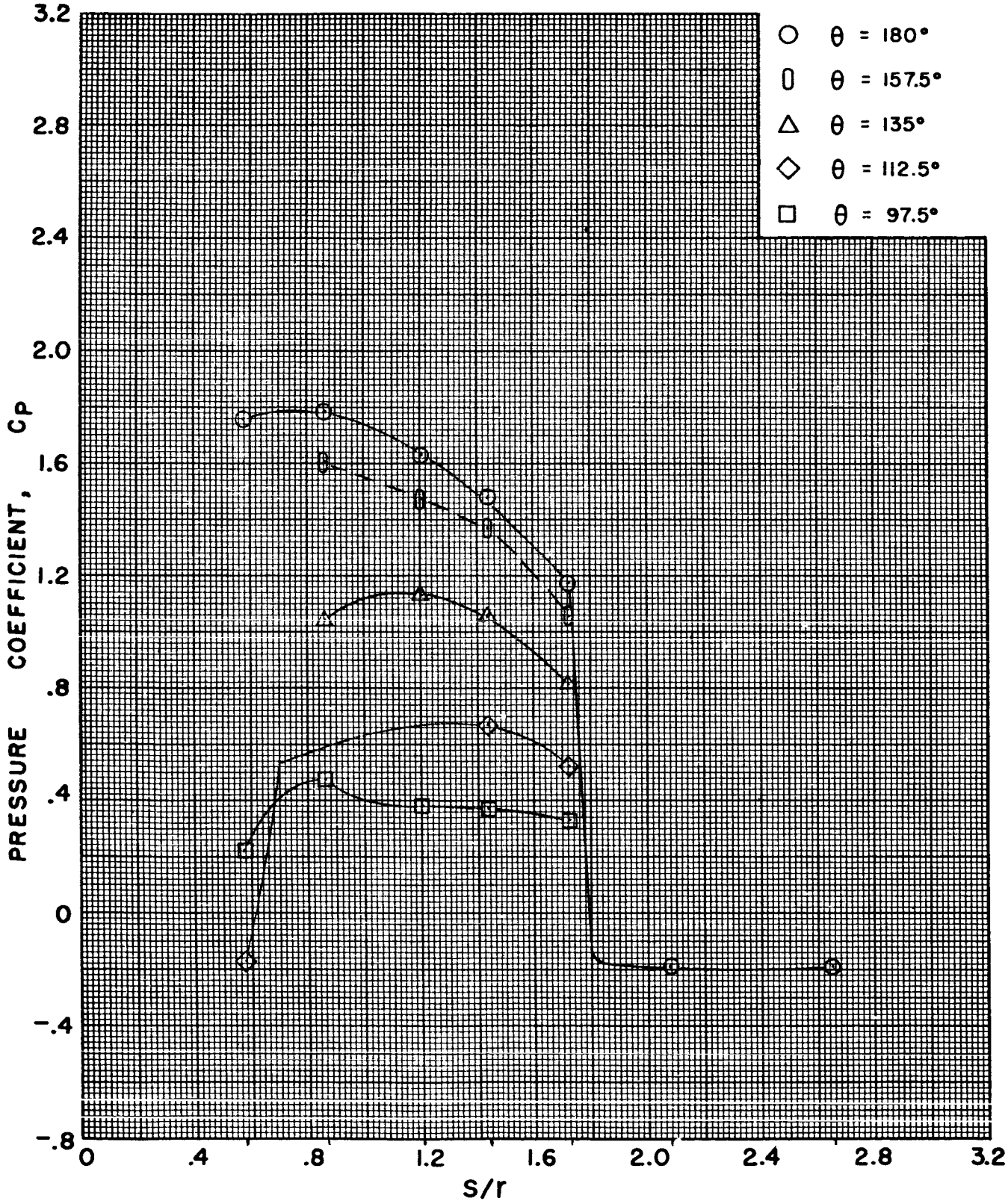

Figure 39b Configuration E[redacted]NT[redacted]C[redacted] 65 8 28 #0

Mach No. = 1.98 $\alpha = 40°$ $C_T = 0$

[redacted]

~~CONFIDENTIAL~~

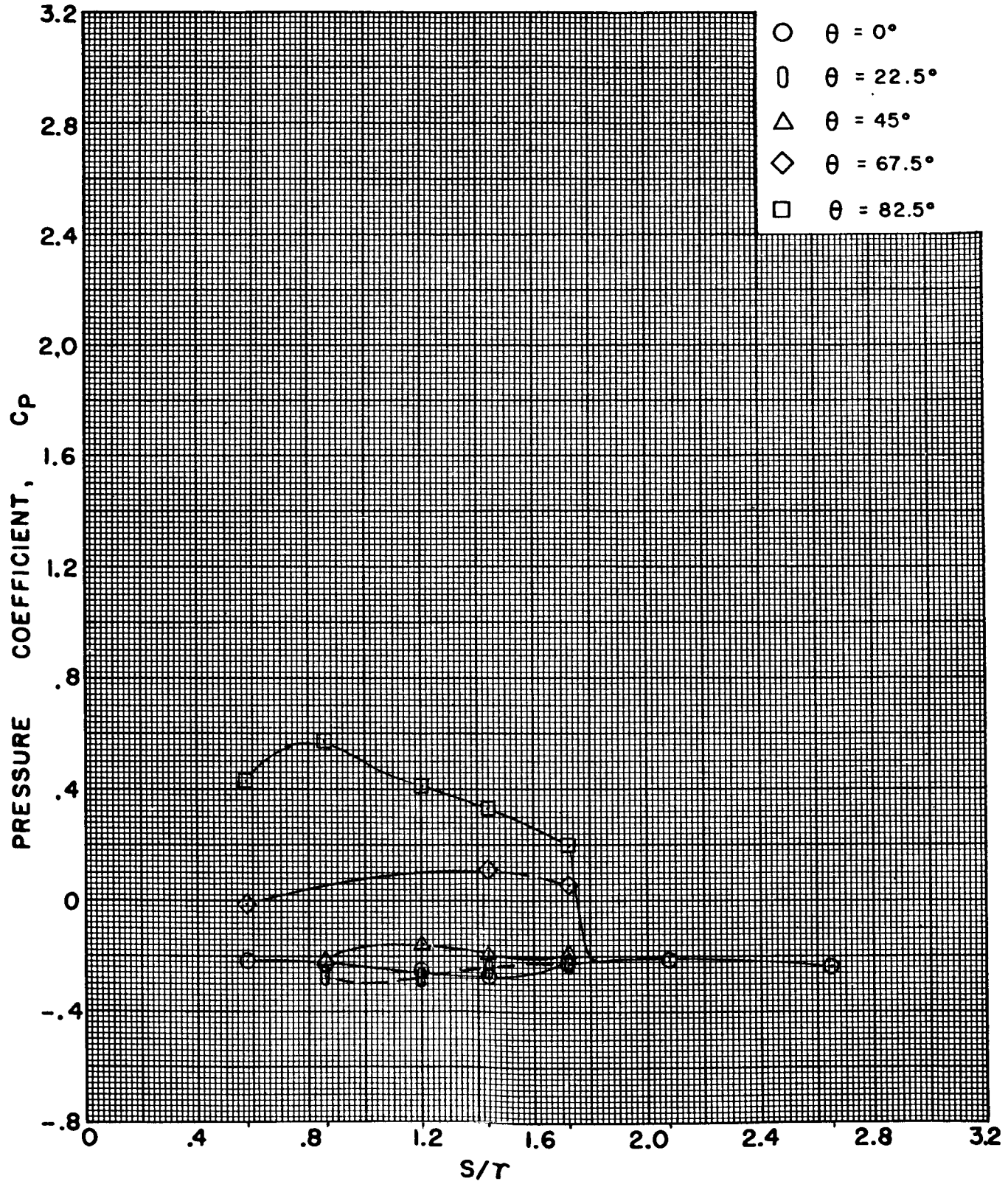

Figure 39c Configuration $E_{65}N_8T_{28}C_{40}$ Mach No. = 1.98 $\alpha = 40°$ $C_T = 1.14$

~~CONFIDENTIAL~~

CONFIDENTIAL

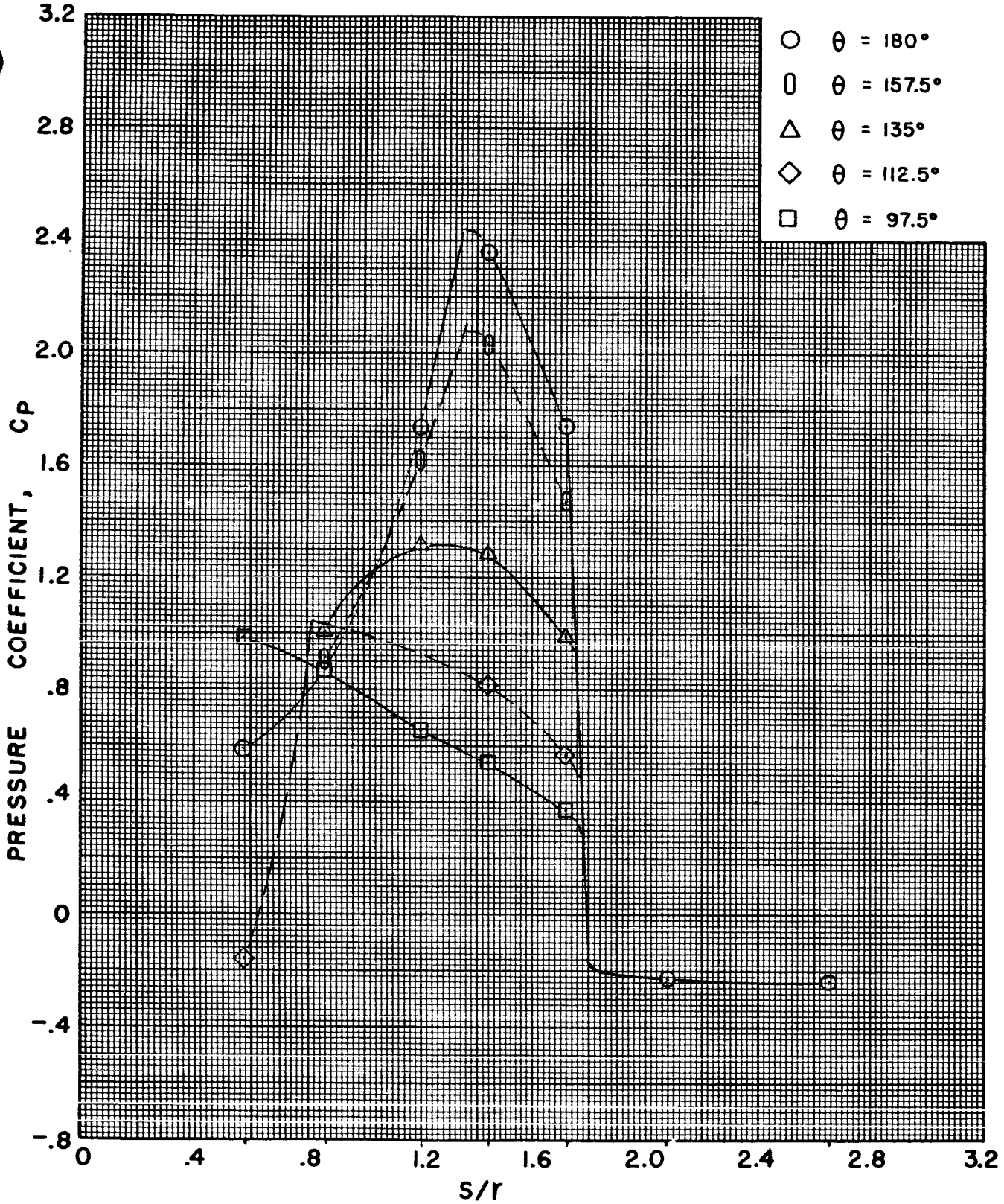

Figure 39d Configuration E[redacted]N[redacted]T[redacted]C[redacted]
65 8 28 40

Mach No. = 1.98 $\alpha = 40°$ $C_T = 1.14$

CONFIDENTIAL

~~CONFIDENTIAL~~

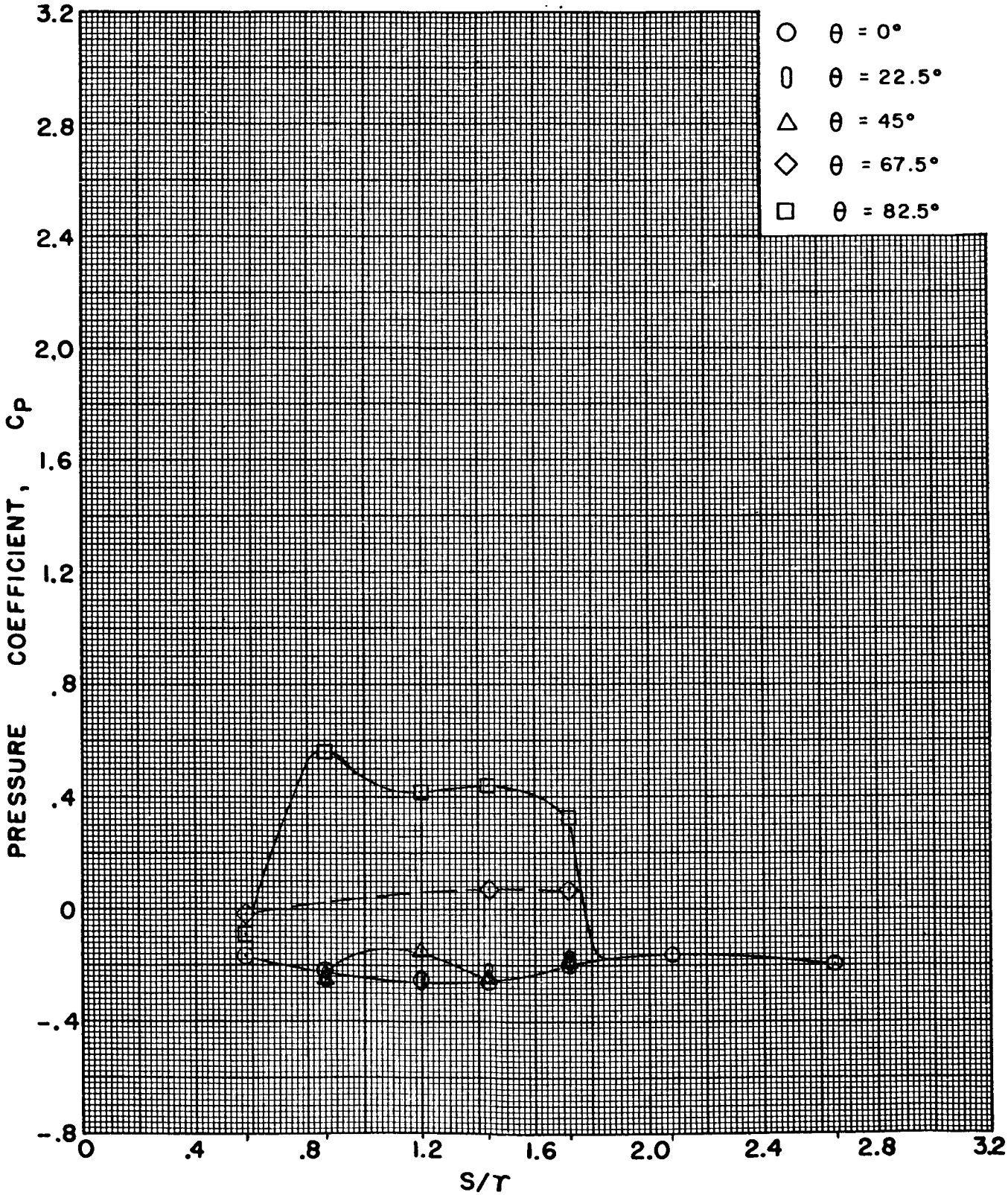

Figure 39e Configuration E[redacted]NT[redacted]C[redacted] 65 B 28 40

Mach No. = 1.98 α = 40° C_T = 2.00

~~CONFIDENTIAL~~

CONFIDENTIAL

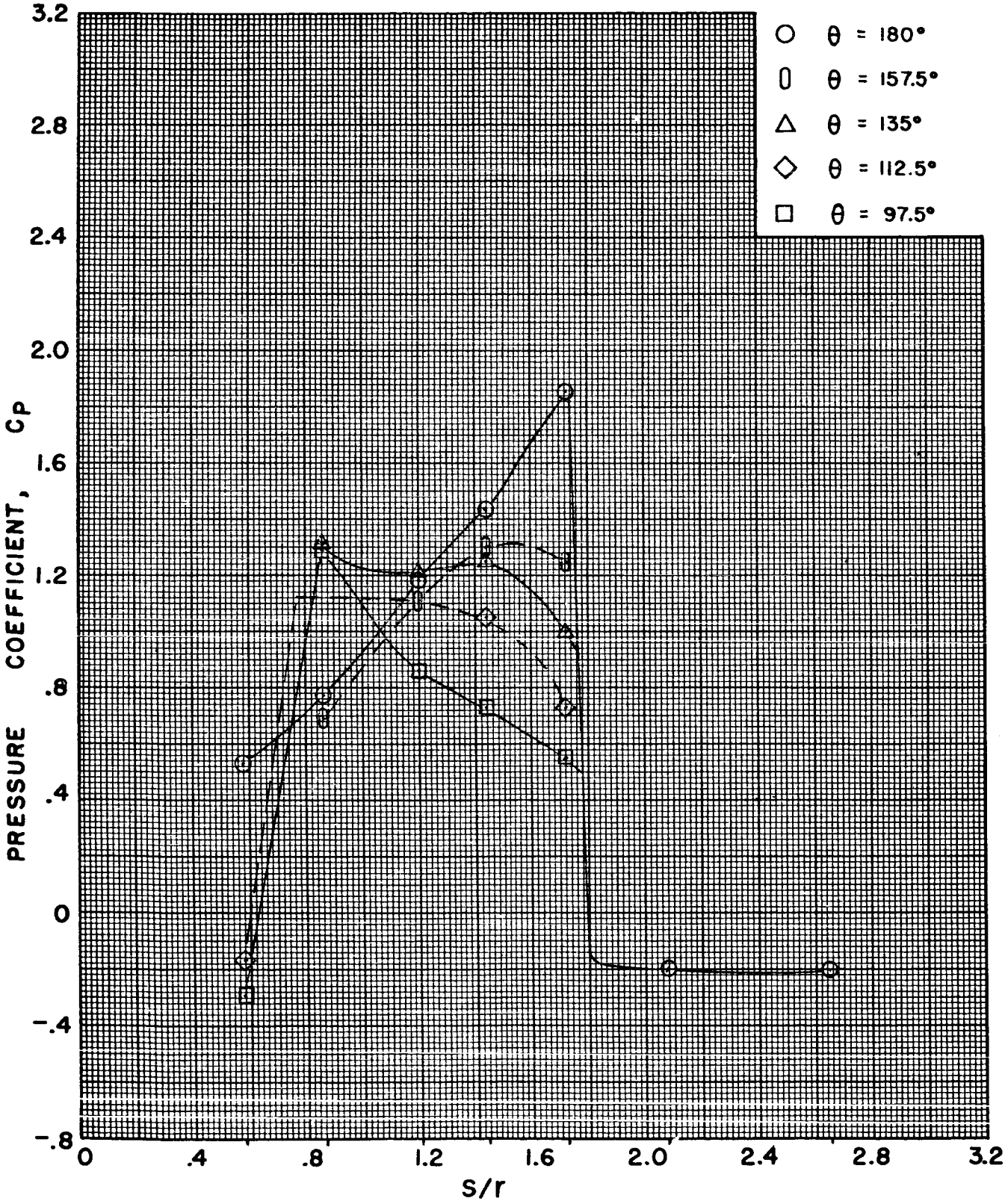

Figure 39f Configuration E[redacted]NT[redacted]C[redacted] 65 8 28 40

Mach No. = 1.98 $\alpha = 40°$ $C_T = 2.00$

CONFIDENTIAL

~~CONFIDENTIAL~~

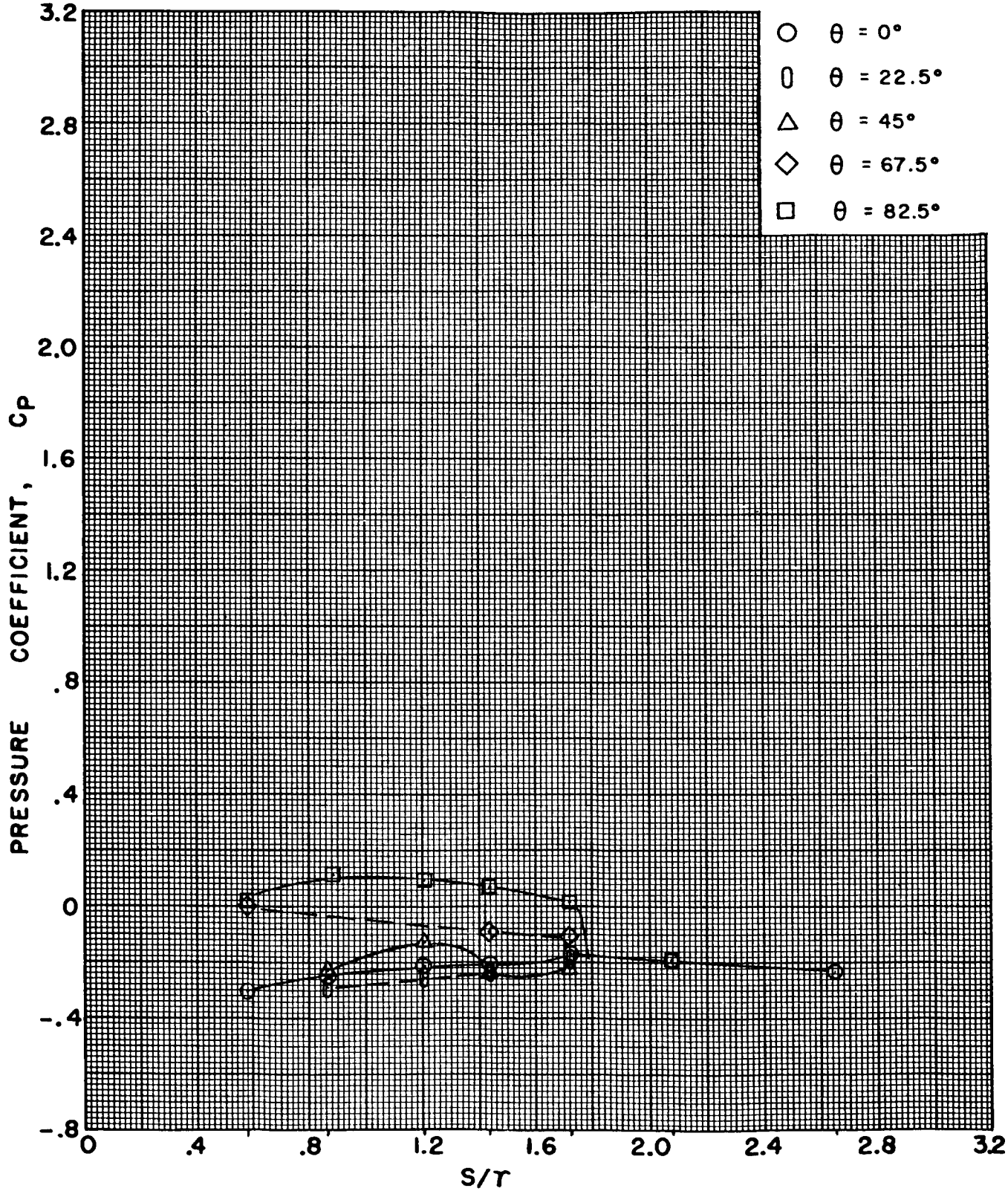

Figure 40a Configuration E[redacted]NT[redacted]C[redacted]
65 8 28 40

Mach No. = 1.98 $\alpha = 50°$ $C_T = 0$

~~CONFIDENTIAL~~

CON[redacted]

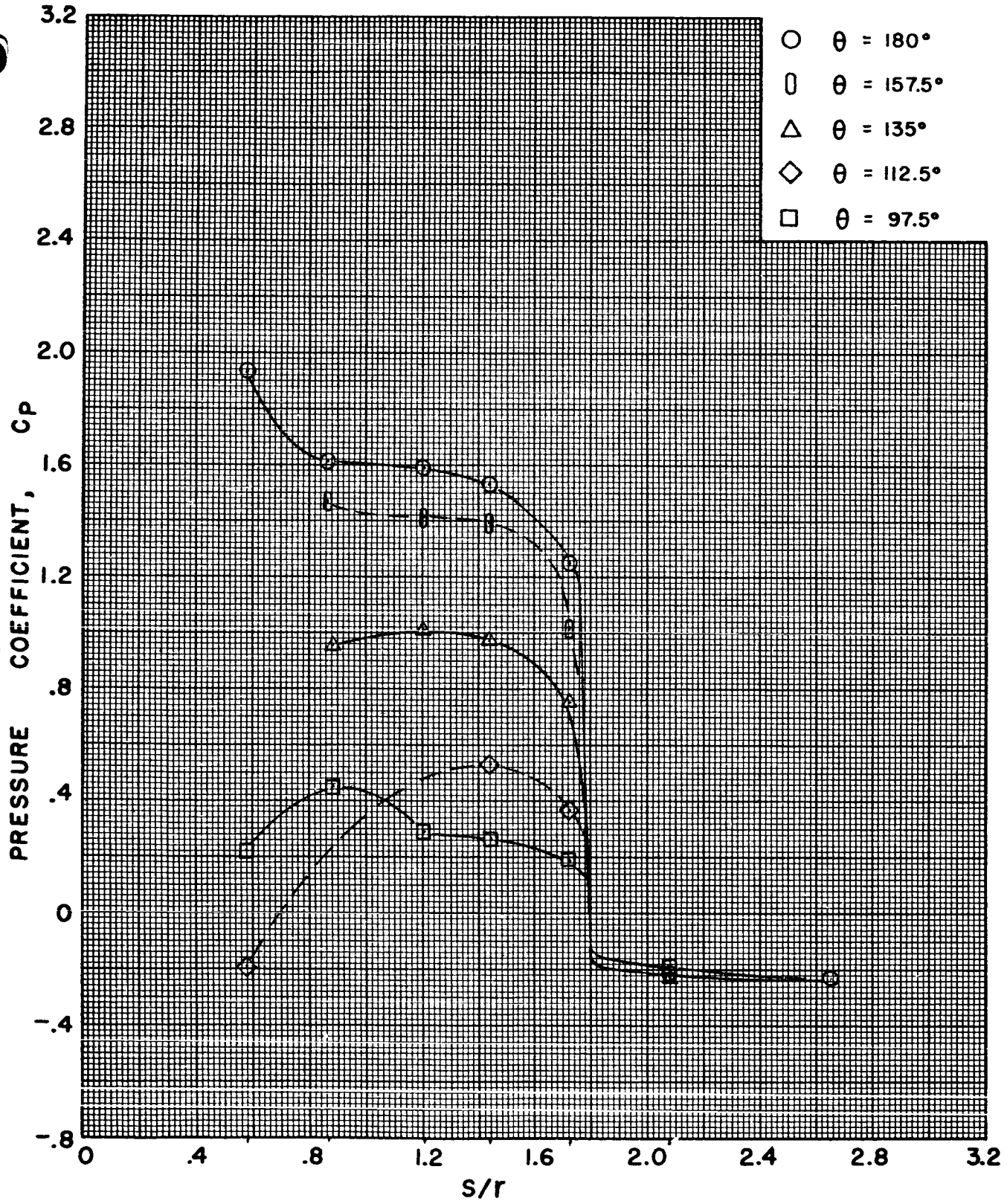

Figure 40b Configuration $E_{65}NT_{8}C_{28}$ Mach No. = 1.98 $\alpha = 50°$ $C_T = 0$

[redacted]

~~CONFIDENTIAL~~

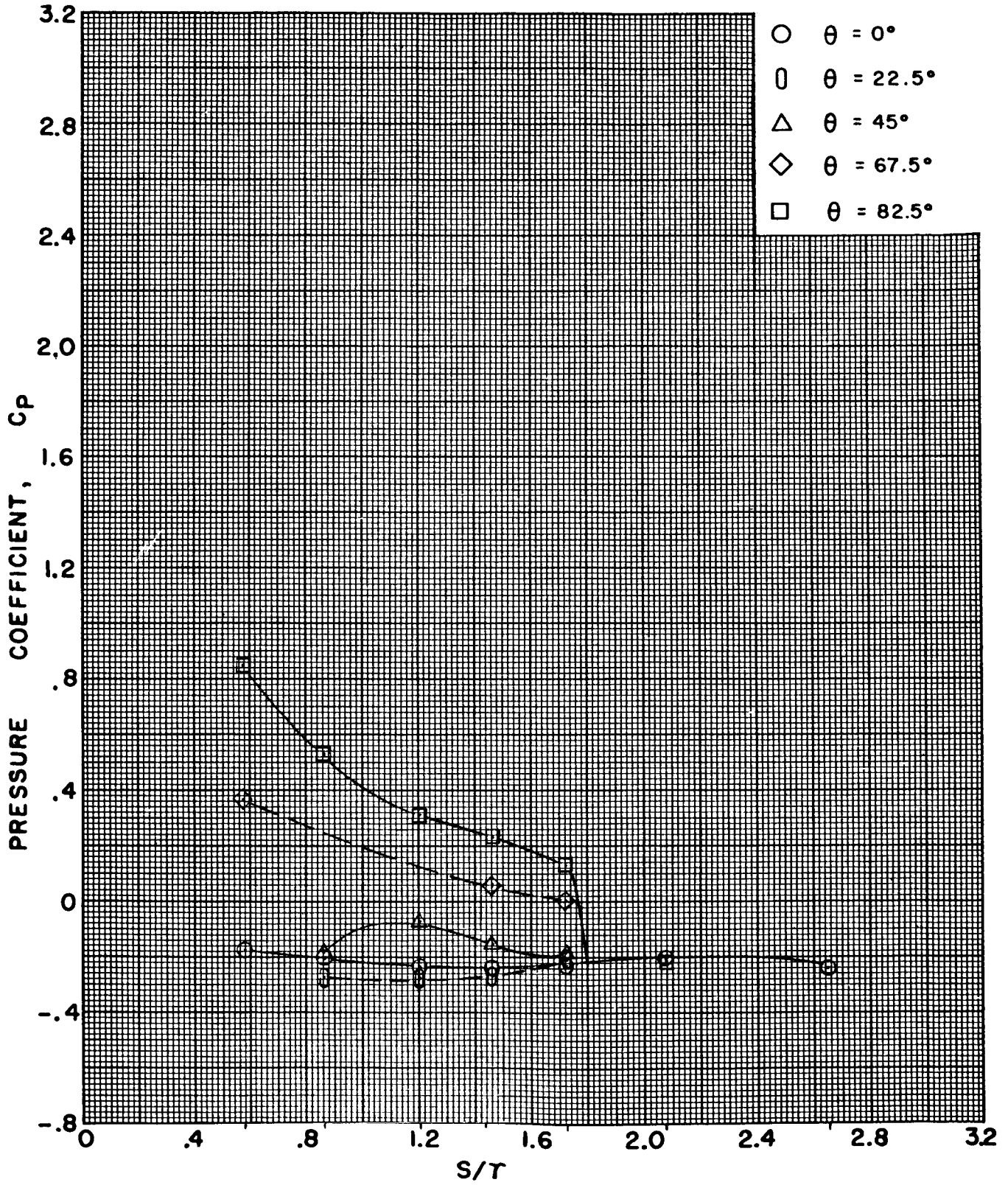

Figure 40c Configuration E[redacted]NT[redacted]C[redacted]
65 8 28 40

Mach No. = 1.98 $\alpha = 50°$ $C_T = 1.14$

~~CONFIDENTIAL~~

CON[redacted]

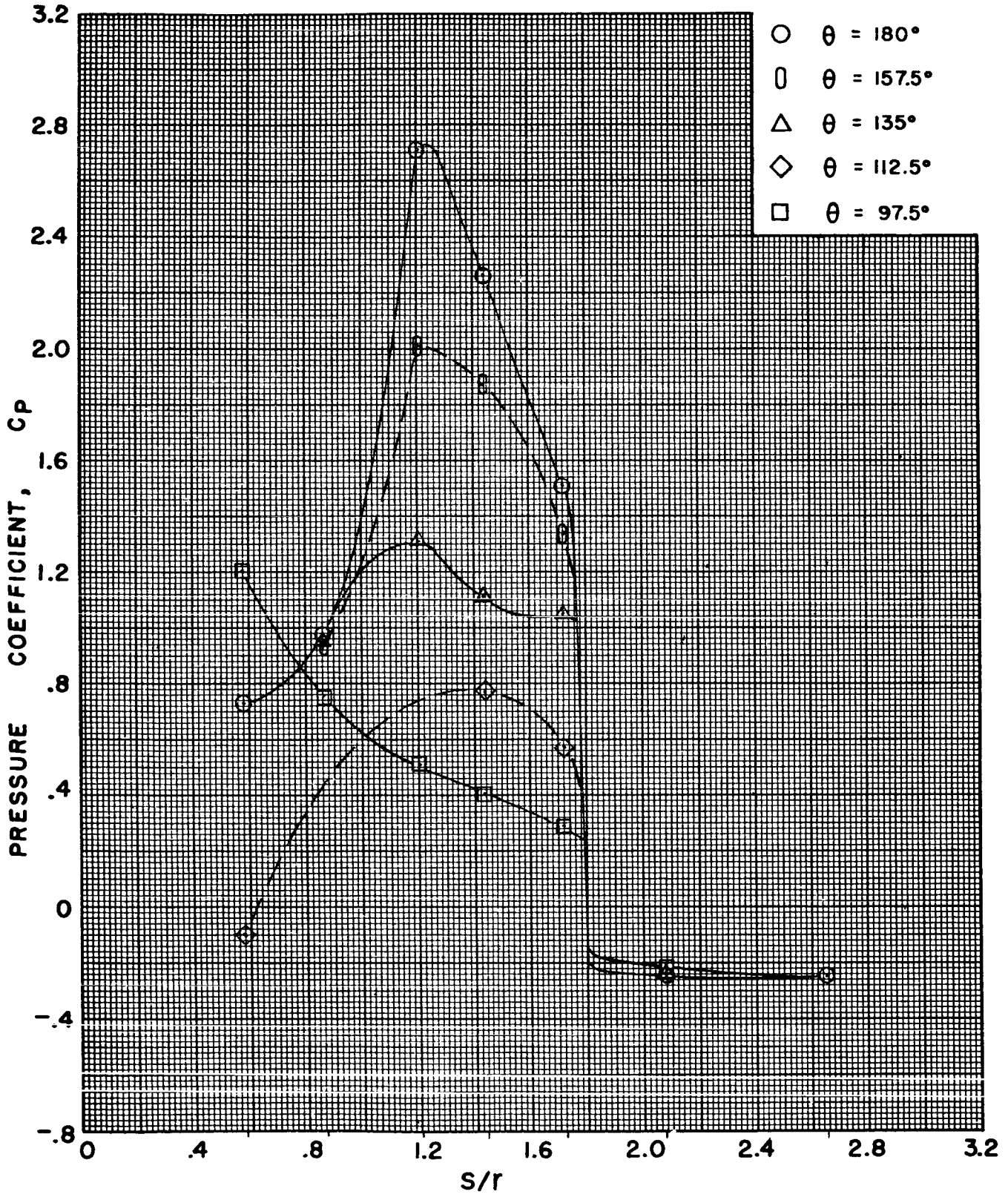

Figure 40d Configuration E[redacted]NT[redacted]C[redacted] 65 8 28 40

Mach No. 1.98 $\alpha = 50°$ $C_T = 1.14$

[redacted]

~~CONFIDENTIAL~~

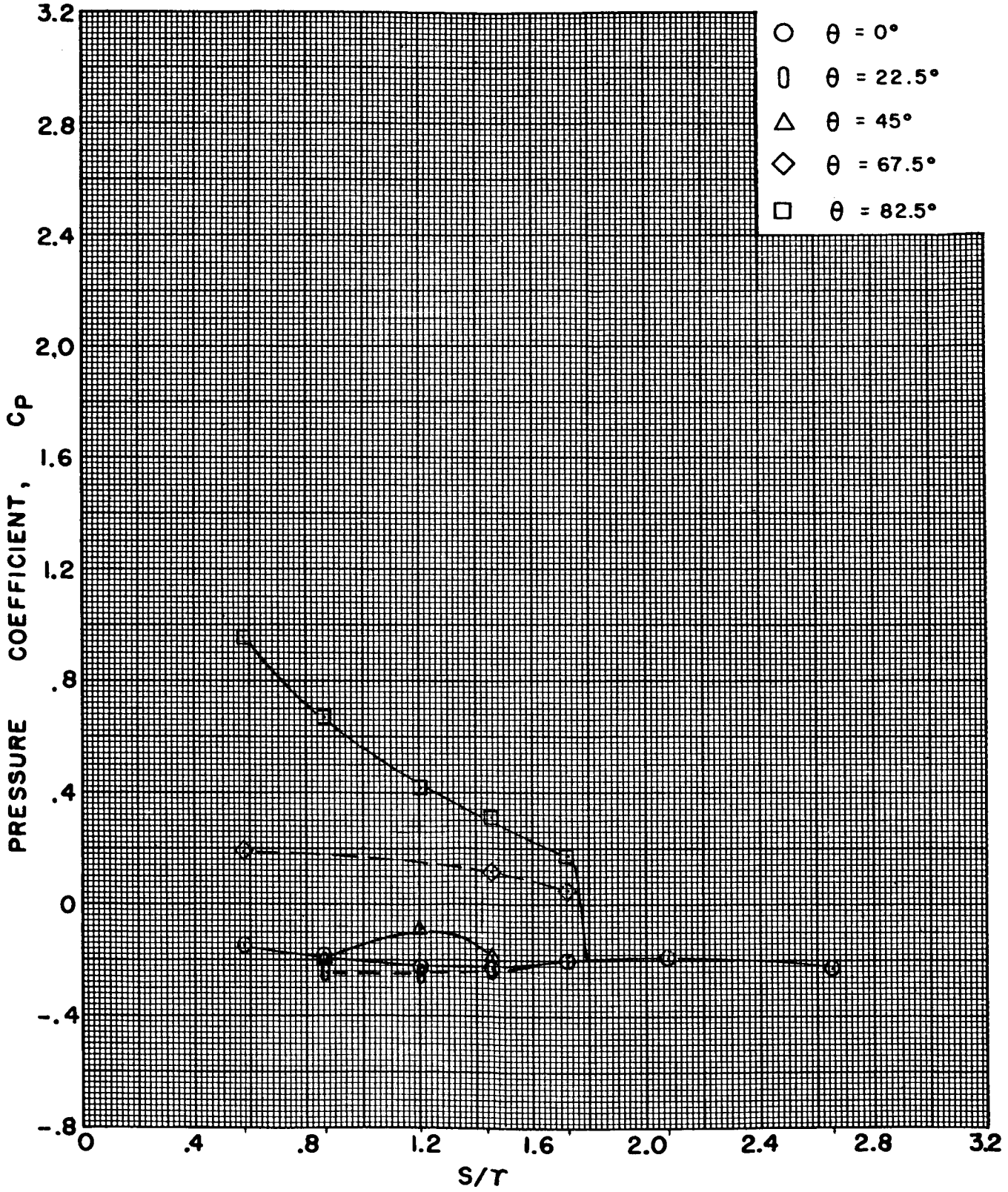

Figure 40e Configuration E[redacted]NT[redacted]C[redacted] 65 8 28 40

Mach No. = 1.98 $\alpha = 50°$ $C_T = 2.00$

~~CONFIDENTIAL~~

CONFIDENTIAL

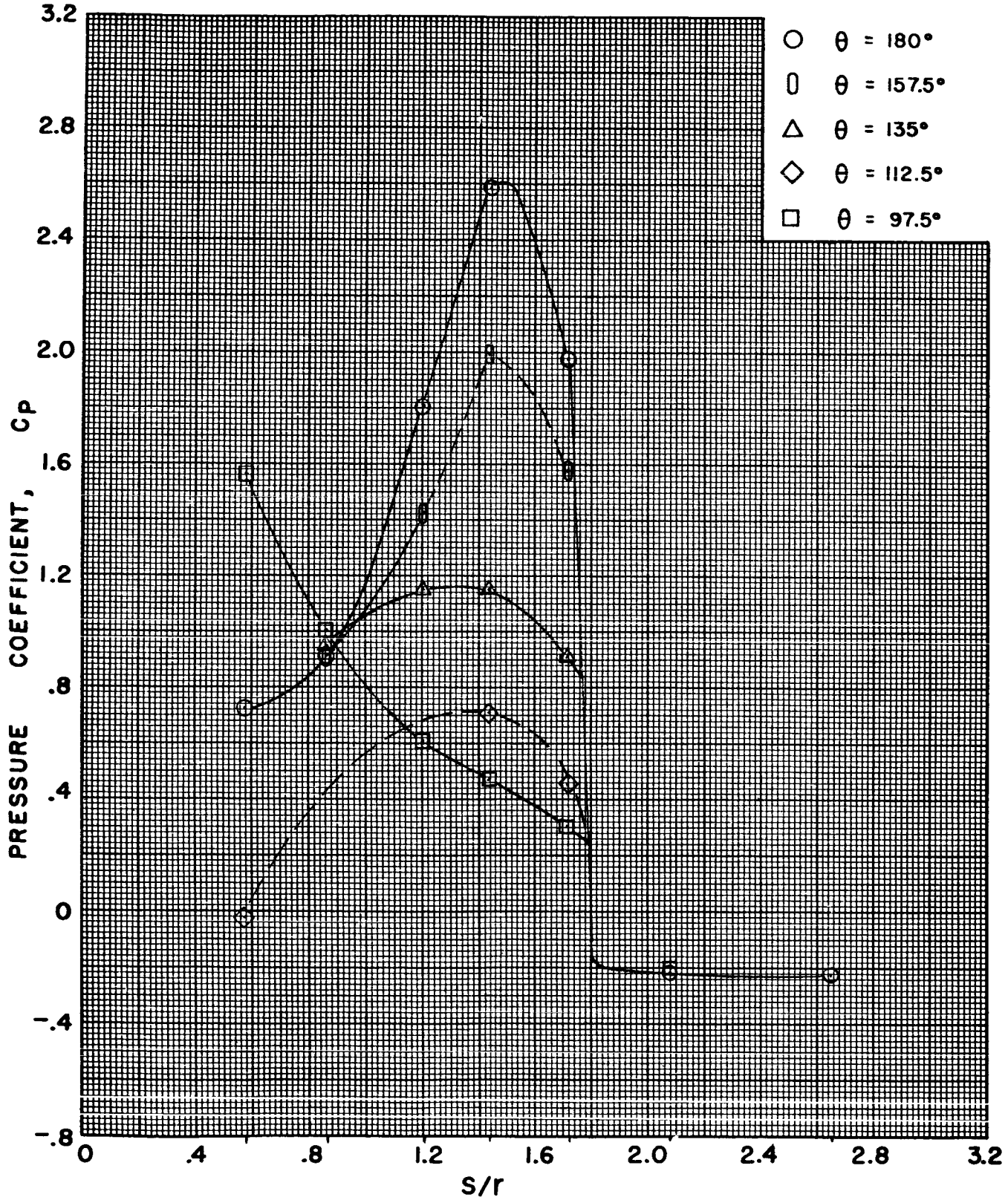

Figure 40f Configuration E65 NT8 C28 40

Mach No. = 1.98 $\alpha = 50°$ $C_T = 2.00$

CONFIDENTIAL

DISTRIBUTION FOR TEST REPORTS*
(PARAGRAPH 5.5)

Address	Copies
National Aeronautics and Space Administration Atlantic Missile Range Operations Port Canaveral, Florida Attn: Mr. B.P. Brown	5
NASA Headquarters 1520 H Street Washington, D. C. Attn: Mr. G.M. Low, MD(P)	6
Grumman Aircraft Engineering Corporation Bethpage, Long Island, New York Attn: P. Gardiner	1
MIT Instrumentation Laboratory 75 Cambridge Parkway Cambridge 39, Massachusetts	1
NASA Resident Apollo Spacecraft Project Officer Grumman Aircraft Engineering Corporation Bethpage, Long Island, New York Attn: Mr. Jack Small	1
National Aeronautics and Space Administration Post Office Drawer D White Sands Missile Range White Sands, New Mexico	2
National Aeronautics and Space Administration Manned Spacecraft Center Transportation Officer Elington Building 381 Houston, Texas Attn: Apollo Document Control Center Elington 336 - TO BE OPENED BY ADDRESSEE ONLY	25

*The distribution for this report has been accomplished in compliance with paragraph 1.2 of Exhibit I of contract NAS9-150 and the NASA Apollo Documentation Distribution List (NASA-MSC letter SP-63-478, dated 2 October 1963).

Address	Copies
National Aeronautics and Space Administration Headquarters NASA Plant Officer P.O. Box 2500 Daytona Beach, Florida Attn: Administrative Contracting Officer	2
National Aeronautics and Space Administration Manned Spacecraft Center Resident Apollo Spacecraft Project Office NAA 12214 Lakewood Boulevard Downey, California	2
National Aeronautics and Space Administration Ames Research Center Moffett Field, California Attn: Library	2
National Aeronautics and Space Administration Lewis Research Center Cleveland, Ohio Attn: Library	2
National Aeronautics and Space Administration Flight Research Center Edwards AFB, California Attn: Research Library	2
National Aeronautics and Space Administration Jet Propulsion Laboratory Pasadena, California Attn: Library	2
National Aeronautics and Space Administration Langley Research Center Langley AFB, Virginia Attn: Mr. A.T. Mattson	2
National Aeronautics and Space Administration Goddard Space Flight Center Greenbelt, Maryland Attn: Manned Flight Support Office, Code 512	2
National Aeronautics and Space Administration George C. Marshall Space Flight Center Huntsville, Alabama Attn: M-SAT-AP	2
National Aeronautics and Space Administration Resident Apollo Spacecraft Project Office MIT Instrumentation Laboratory 75 Cambridge Parkway Cambridge 39, Massachusetts	1